Novel Modifiers of $A\beta_{42}$ Toxicity in *Drosophila*

Yifan Yu

A dissertation submitted in partial fulfilment of the requirements for

Doctor of Philosophy

of

University College London.

Department of Genetics, Evolution and Environment

University College London

February 27, 2018

Declaration

I, Yifan Yu, confirm that the work presented in this thesis is my own. Where information has been derived from other sources, I confirm that this has been indicated in the thesis.

Abstract

Background: Alzheimer's disease (AD) is a progressive neurodegenerative disease that is characterized by two neuropathological hallmarks: neurofibrillary tangles composed of hyperphosphorylated tau protein and extracellular plaques composed of amyloid-β peptides (Aβ). Recent GWAS have linked PICALM and BIN1 to AD risk, and several studies have implicated PICALM and BIN1 in Aβ production and clearance. However, so far their roles in modulating $A\beta_{42}$ toxicity remain unclear.

Aims: This study aimed 1.) to test whether the fly orthologues of PICALM and BIN1, *lap* and *Amph*, suppress $A\beta_{42}$ toxicity and to elucidate the molecular mechanisms at work. 2.) to identify novel suppressors of $A\beta_{42}$ toxicity by genetic screens.

Results: 1.) I showed that over-expression of the *Drosophila* PICALM orthologue, *lap*, ameliorated $A\beta_{42}$ toxicity in an adult onset AD model without affecting Aβ levels. I then performed a small-scale targeted genetic screen of endocytic-exocytic genes and identified *Rab5* as a suppressor of $A\beta_{42}$ toxicity. Aβ in flies led to the accumulation of pre-synaptic vesicular glutamate transporter (VGlut). Lap directly interacted with VGlut and reduced its accumulation back to control levels. Consistent with this, Aβ caused an increase in extracellular glutamate levels, while *lap* expression reduced the Aβ-induced increase in extracellular glutamate levels, suggesting *lap* might play a role in modulating glutamatergic transmission. *Amph*, the homologue of another AD risk factor, BIN1, modulated post-synaptic glutamate receptor (GluRII) localization. Amph localisation was disrupted upon Aβ expression and restored upon *lap* over-expression. 2.) The rough eye phenotype (REP) of *Drosophila* allows for high-throughput screening of enhancers and suppressors of therapeutic targets in neurodegenerative diseases. Using the REP, my collaborators and I performed a genome-wide genetic screen to identify novel modifiers of Aβ toxicity. The primary hits were further validated using negative geotaxis and lifespan assays. I found 4 gene-knockdown suppressors of $A\beta_{42}$ toxicity. 3 of these suppressors did not reduce $A\beta_{42}$ levels.

Conclusions: 1.) I propose a model where *lap* and *Amph* collaborate to modulate glutamatergic transmission and so affect disease development. 2.) I find *Rab5*, *EndoA* and *Snap25* are potential gene-overexpression suppressors of $A\beta_{42}$ toxicity, and *CG15011*, *Larp*, *Pxn*, and *Sodh2* are potent gene-knockdown suppressors of $A\beta_{42}$ toxicity.

Acknowledgements

This work was conducted at the Department of Genetics, Evolution and Environment, University College London, United Kingdom and the Institute of Healthy Ageing, University College London, United Kingdom headed by Professor Linda Partridge.

At first, I would like to express my gratitude to Professor Linda Partridge for giving me the opportunity to work in her laboratory, being my supervisor and giving me intellectual and professional support during conduction of my thesis. I would also like to thank Professor David Gems for being my secondary supervisor and for his intellectual input accompanying the process of my promotion. I would like to thank Dr Teresa Niccoli for introducing me into the topics, invaluable help, technical assistance and support in the experimental procedures during my practical work and for her brilliant inspiration and ideas, intriguing questions and in-depth discussions about science during the development, realization and completion of the project and constructive criticism during reviewing of the manuscript and her patience with me. I am very grateful to my dear colleagues for creating a rich atmosphere that allows me to focus on work and provides joyful lives.

I owe a great deal to my friends and members of my family, especially my parents, grandparents, Tiandi Yang and Carina Kern who have helped extend my involvement in scientific research, and whose comments and questions have encouraged, supported and enlightened me.

Additionally, I would like to thank the Bloomington *Drosophila* Stock Center and Vienna *Drosophila* RNAi Center for providing the transgenic flies that I have used extensively.

Finally, I would like to thank China Scholarship Council for financing my study.

Impact statement

My work has validated that two GWAS hits, PICALM and BIN1, reduced $A\beta_{42}$ toxicity in a *Drosophila* model. My work also discovered that $A\beta_{42}$ led to abnormal glutamate transmission. PICALM and BIN1 were involved in regulating glutamate transmission and therefore affected disease development.

In addition to this, my work has identified several novel suppressors of $A\beta_{42}$ toxicity. These included gene overexpressing suppressors (e.g. *Rab5*, *EndoA*, *Snap25*) and gene knockdown suppressors (e.g. *CG15011*, *Larp*, *Pxn* and *Sodh2*).

In the future, it will be interesting to investigate whether these suppressors also reduce $A\beta_{42}$ toxicity in a mammalian model. If they do, these genes will be promising therapeutic targets for AD treatments.

Finally, this work was presented at the 13th international conference on Alzheimer's disease and Parkinson's disease using a poster. A research paper based on this work will be submitted to Nature Communications for publication.

Contents

List of figures

1. Introduction

1.1 Pathogenesis of Alzheimer's disease

In 1906, the first example of dementia was reported by Alois Alzheimer at the 37th conference of south-west German psychiatrists in Tubingen. Subsequently, this disease was named after the lecturer and became known as Alzheimer's disease (AD). AD is characterized by progressive memory loss, cognitive impairment and gradual neurodegeneration. In the severely impaired stage, AD patients show behavioral symptoms, major language dysfunction, difficulties in abstract reasoning, decision making, complete social dependence, and commonly die early (Graeber et al., 1997; Maurer et al., 1997). Through detailed examinations, Alzheimer described two histopathological characteristics of this disease: first, neuritic plaques (military foci), consistent with Redlich's prior findings (1898); second, neurofibrillary tangles, which were first described by Alzheimer. These typical plaques and tangles are extensively distributed in the hippocampus, limbic cortex and neocortex of brains and result in progressive neuronal lesions. It is now clear that they are the respective results of extracellular deposition of amyloid protein and intracellular accumulation of tau proteins.

After Alzheimer's report on Auguste's case, doctors subsequently diagnosed more AD cases that were significantly different from it. The majority of patients suffered from the disease after the age of 65. The predominant view now is that only 1% of AD cases are like Auguste's, which is defined as presenile or familial AD (with an age of onset < 65 years). The vast majority of other cases are termed senile or sporadic AD (onset of > 65 years). Sporadic AD is the most common, irreversible, progressive type of dementia. It is estimated that only ~13% of people aged 65 years suffer from AD but ~45% after the age of 85 (Goedert and Spillantini, 2006; Hardy, 2006).

With the development of biochemical and genetic techniques, the understanding of AD has steadily advanced. In the 1980s, the component of amyloid deposits, Aβ peptide, was first isolated and described by George Glenner (Glenner and Wong, 1984a, b). At the same time,

the subunit protein of neurofibrillary tangles, tau, was also identified (Goedert et al., 1989b; Goedert et al., 1988). Aβ and tau proteins are regarded as two diagnostic hallmarks of AD that induce cytotoxicity. Although both Aβ and tau induce neuronal toxicity, several specific neurons are more vulnerable to this toxicity. They are the cortical cholinergic and glutamatergic neurons (Bowen et al., 1976; Davies and Maloney, 1976; Perry et al., 1977; Whitehouse et al., 1982; Hsieh et al., 2006; Shankar et al., 2007; Snyder et al., 2005; Zhao et al., 2010). As cholinergic and glutamatergic transmission are important for memory formation in the cortex, this could explain why memory is severely impaired in AD cases (Bartus, 1979; Davis et al., 1978).

Although AD research has been so fruitful since the first description of AD by Alois Alzheimer, its treatment is still not effective. The main reason is that we still lack sufficient knowledge on the disease aetiology, which emphasizes the necessity of elucidating the molecular mechanisms underlying AD pathogenesis and so facilitating the discovery of targets for pharmacological intervention.

1.1.1 Amyloid hypothesis

In the 1980s, Aβ peptide was first identified from amyloid deposits in brain tissue from AD patients (Glenner and Wong, 1984a, b). Based on these findings, an amyloid hypothesis by which the neurodegeneration in AD resulted from deposition of Aβ peptide was proposed (Hardy, 2006; Hardy and Selkoe, 2002; Selkoe and Podlisny, 2002; Singleton and Hardy, 2016). This hypothesis was supported by the discovery of APP mutations in FAD patients in the following studies.

In the 1990s, the advent of genetic technology has revolutionized AD research. The application of linkage analysis and positional cloning has allowed scientists to establish the relationships between genes and diseases. This uncovered a number of mutations linked to aggressive, early onset forms of familial AD. The first mutant gene in familial AD patients is the amyloid precursor protein (APP) gene on chromosome 21 (Goate et al., 1991). Given that APP processing give rise to production of Aβ, this finding provides a link between APP mutations,

amyloid plaques in brain tissue and AD pathogenesis. The first APP mutation was identified at the position 22 of the Aβ sequence in a Dutch family (Levy et al., 1990). This missense mutation in APP leads to a several-fold increase in the toxic Aβ species, and lead these patients to develop AD earlier than the age of 65 [early-onset AD (EAOD)]. Following the discovery of the first APP mutation, another 12 mutations have subsequently been identified, including Austrian, Iranian, French, German, London, Swedish and Florida mutations. These mutations affect APP processing in different behaviors. For instance, several mutations such as the Swedish mutation elevate production of longer Aβ species ($A\beta_{42}$) (Citron et al., 1992; Saito et al., 2014), while others such as the Beyreuther/Iberian mutation increase the $A\beta_{42}/A\beta_{40}$ ratio (Guardia-Laguarta et al., 2010; Lichtenthaler et al., 1999). In addition to this, some mutations such as the Arctic mutation facilitate Aβ fibrillogenesis, while others such as the Dutch, Flemish and Italian mutations make Aβ resistant to proteolytic degradation (Nilsberth et al., 2001; Tsubuki et al., 2003). Until now, all of the known mutations are found at or near the α-, β-, γ-secretase cleavage sites or in the middle of the Aβ region and none of them are found outside this region. This evidence strongly supports the point that familial AD is a genetically inherited disease (Hardy, 2006; Hardy and Selkoe, 2002; Selkoe and Podlisny, 2002; Singleton and Hardy, 2016). However, further investigations have revealed that such familial AD only accounts for 1~2 % of AD cases and that the most are instead sporadic. Sporadic AD also shows increased levels of Aβ, which is not ascribed to genetic mutations in the APP gene but the disturbance of Aβ clearance (Mawuenyega et al., 2010).

Through research over the past decades, it is becoming increasingly clear how APP processing produces Aβ peptides. APP is processed along 2 pathways: the non-amyloidogenic and amyloidogenic pathways. Only the amyloidogenic pathway leads to production of Aβ. APP is a 695-770 amino acid long transmembrane protein (Koo, 2002) that functions in neurite outgrowth, axonal transport and apoptotic cell death (Baumkotter et al., 2014; Choi et al., 2013; Cousins et al., 2009; Cousins et al., 2013; Deyts et al., 2016; Deyts et al., 2012; Hoe et al., 2009; Koo, 2002; Osterhout et al., 2015; Wang et al., 2009b). Knockout of APP causes impairment in synaptic function, learning and memory only in aged mice (Corrigan et al., 2012; Dawson et al., 1999; Hefter et al., 2016; Lee et al., 2010b; Li et al., 1996; Ring et

al., 2007; Seabrook et al., 1999; Steinbach et al., 1998; Zheng et al., 1995; Zou et al., 2016). APP is composed of a short intracellular C-terminal domain linked to a longer extracellular N-terminal domain by a membrane-spanning domain. Alternative cleavage of APP can generate a series of heterogeneous polypeptides (Kang et al., 1987). Several lines of evidence have revealed that neurons predominantly express the APP695 isoform (Hick et al., 2015; Wang et al., 2014). In the healthy brain, APP fragments are usually released from the cellular membrane through α-endoproteolytic cleavages and then enter the nucleus to regulate transcription (Cao and Sudhof, 2001; Kimberly et al., 2001). This constitutive scission is most frequently mediated by α-secretase and APP is cut at the residue 687 between amino acid 16 and 17 of the Aβ region. This action enables the APP to secret the large, soluble ectodomain (APP-α) into the extracellular matrix and retain the 83-residue C-terminal fragments (CTF) (C83) on the cell surface (Sisodia, 1992). APP-α is neuroprotective and limits the activity of β-secretase (Kundu et al., 2016; Obregon et al., 2012).

In AD patients, APP proteins are cleaved at residue 671 by β-secretase to create slightly truncated APP derivatives (APP-β) and membrane-maintained 99-residue CTFs (C99). APP-β is released into the extracellular space (Haass et al., 1992). A recent study confirms that this fragment can also trigger neuronal death through binding to death receptor 6 (DR6) and thus gives rise to neurodegeneration (Nikolaev et al., 2009). APP on the cell surface prefers non-amyloidogenic processing, whereas APP internalization triggers amyloidogenic processing. Both C83 and C99 are further cleaved by γ-secretase to release the APP intracellular domain (AICD). AICD is a transcription factor to repress WAVE1 transcription. In turn, downregulation of WAVE1 activity prevents the APP trafficking and Aβ generation (Ceglia et al., 2015). This γ-secretase-mediated cleavage of C83 also produces the nontoxic p3 peptides (Seubert et al., 1992). C99 undergoes multiple γ-secretase-mediated cleavages. The first endopeptidase cleavage yields two products: $A\beta_{49}/_{50}$-residue AICD and $A\beta_{48}/_{49}$-residue AICD. $A\beta_{49}$ is sequentially cleaved by γ-secretase through its carboxypeptidase activity to remove 6 or 9 C-terminal amino acids to produce $A\beta_{43}$ or $A\beta_{40}$ respectively. $A\beta_{48}$ is also clipped by γ-secretase to yield 42 amino acid peptides designated $A\beta_{42}$ (Fernandez et al., 2014; Okochi et al., 2013). APP proteolysis occurs at the trans-Golgi network, endoplasmic reticulum

(ER) and early endosome where the β-secretase and γ-secretase are localized (Busciglio et al., 1993; Kinoshita et al., 2003; Koo and Squazzo, 1994; Wertkin et al., 1993; Xu et al., 1995a). The localization of APP is vital for production of different Aβ peptides. For instance, $Aβ_{42}$ is produced in the ER, while $Aβ_{40}$ is produced in the trans-Golgi network (Cook et al., 1997; Hartmann et al., 1997; Lee et al., 1998; Skovronsky et al., 1998; Wild-Bode et al., 1997).

Longer Aβ species (e.g. $Aβ_{42}$ and $Aβ_{43}$) are prone to self-aggregation to form dimers, oligomers, fibrils and plaques (Kim et al., 2007a). The formation of amyloid plaques starts from Aβ oligomerization. Then Aβ oligomers convert to nucleus (Lee et al., 2011). Amyloid nucleation requires three or four amyloid molecules, which is a stochastic and rare event (Nelson et al., 2005). Therefore, amyloid nucleation is a slow phase. Once the nucleus is formed or seeded, the nucleus grows fast to form fibrils (Eisenberg and Jucker, 2012). Aβ fibrillogenesis is stabilized by cross-seeding of Aβ fibrils and formation of cross-β sheets (Kajava et al., 2010). This process promotes maturation of amyloid plaques (Knowles et al., 2014). The prevalent view suggests that amyloid plaques give rise to neurotoxicity because they are found to be deposited in the brains of AD patients. However, this opinion is disputed as amyloid loads do not match AD progression. Growing evidence has shown that soluble $Aβ_{42}$ oligomers are the main toxic species whose levels correlate best with disease status (Walsh and Selkoe, 2007; Wang et al., 1999).

Recently, APP has been found to undergo a new form of proteolytic processing. This included the η-secretase pathway, where η-secretase snips at the 540 residue of APP and produces APP-η. The remaining CTFs are subsequently clipped by α- or β-secretases to release Aη-α or Aη-β respectively. Aη-α is the main neuronal toxic species (Willem et al., 2015). A potential η-secretase is matrix metalloproteinase 5 (MMP5) (Barganer et al., 2015) (Figure 1.1).

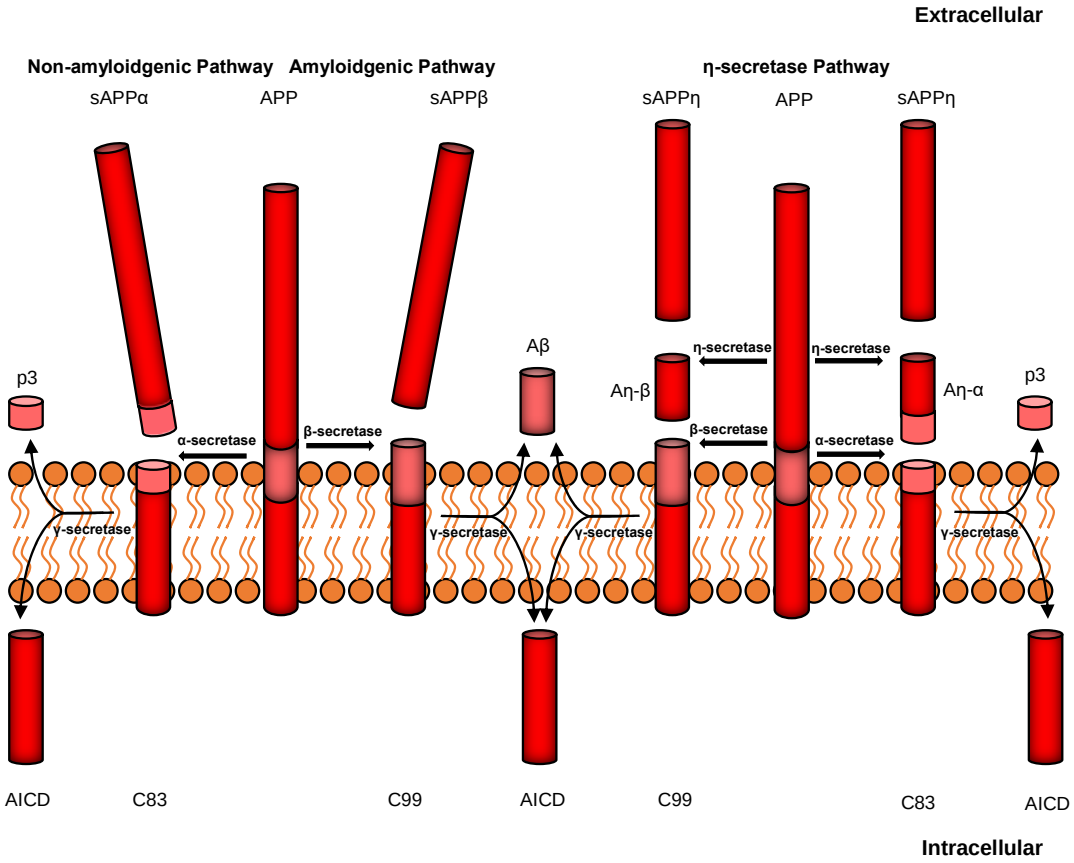

Figure 1.1 APP proteolysis. The non-amyloidogenic pathway includes APP cleavages by α- and γ-secretases and thus the generation of the sAPPα, C-terminal fragments (CTF83/AICD) and p3. α-secretases include ADAM9, ADAM10 and ADAM17. γ-secretases contain presenilin 1 and 2. The amyloid-β (Aβ) peptides are derived from an amyloidogenic pathway, including $Aβ_{40}$, $Aβ_{42}$, $Aβ_{43}$. APP undergoes proteolytic processing by β- and γ-secretases and generates the sAPPβ, C-terminal fragments (CTF99/AICD) and Aβ peptides. sAPPβ activates DR6. Aβ peptides oligomerise and fibrillise to from amyloid plaques. A typical β-secretase is BACE1. APP is also cleaved by η-secretases to release sAPPη (e.g. ADAM5). The remaining CTFs are subsequently cleaved by α- or β-secretases resulting in Aη-α or Aη-β respectively. Aη-α causes toxicity.

1.1.2 Presenilins in amyloidogenic pathway

As stated earlier, the amyloid hypothesis asserts that production of Aβ in the brain is the primary influence driving AD pathogenesis. Therefore, the activation of the amyloidogenic pathway might facilitate production of Aβ and affect AD progression. The amyloidogenic pathway is mediated by γ-secretase which has several subunits. However, only presenilins are found to have mutations linked to familial AD. Mutations in presenilins were first discovered in

familial AD (early onset AD, EOAD) patients by genetic linkage analysis and positional cloning. After an initial finding, mutations in another highly homologous gene were identified in EOAD. These two genes are named presenilin 1 (PS1) and presenilin 2 (PS2) respectively (Levy-Lahad et al., 1995a; Levy-Lahad et al., 1995b; Sherrington et al., 1995). Following the discovery of the first PSEN mutation, many missense mutations in PSEN are observed in EOAD cases. Most of them are speculated to lead to an increase in $A\beta_{42}$ production (Bentahir et al., 2006; Houlden et al., 2001; Kim et al., 2012; Kretner et al., 2011; Piccini et al., 2007; Uttner et al., 2010).

Presenilins harbor six to eight transmembrane (TM) segments. *In vivo*, the active PS protein is hard to detect. Usually its N-terminal and C-terminal fragments exist separately because when these two fragments are assembled into active PS (Capell et al., 1998; Nishimura et al., 1999; Thinakaran et al., 1997; Thinakaran et al., 1998), this PS form is unstable and rapidly degraded by proteases (Kim et al., 1997). The missense mutations cause PS to escape the proteolytic system (Jacobsen et al., 1999; Steiner et al., 1999a; Steiner et al., 1999b). Consequently, the mutated PS cannot be degraded, so its endoproteolytic activity is maintained.

Next, an open question is how the PS biological function correlates with the loss-of-function toxicity in AD. Recent evidence demonstrates that several missense mutations actually inhibit PS activity. For instance, exon 9 in PSEN encodes the TM6 and TM7 domains that contain two unusual intramembranous aspartates and form the active regions of PS. Missense mutation in exon 9 causes loss of endoproteolytic activity and a reduction in $A\beta_{42}$ level (Kim et al., 2005; Kim et al., 2001; Wolfe et al., 1999a). However, this mutation also leads to an incomplete digestion of long Aβ peptides and therefore enhances the $A\beta_{42}/A\beta_{40}$ ratio (Crook et al., 1998; Ishii et al., 1997; Wolfe et al., 1999b).

PS serves as an aspartyl protease and its proteolytic function stimulates APP cleavage. PS1 mutant mice show normal levels of APP substrates processed by α-and β-secretase but accumulate the γ-secretase-mediated APP substrates C83 and C99, suggesting that PS

serves as a subunit of γ-secretase (De Strooper et al., 1998). Moreover, PS immunoprecipitates with full-length APP protein. PS and APP colocalize to the same subcellular region suggesting that PS directly interacts with APP (Xia et al., 2000). However, the conflicting evidence argues that PS mediates $A\beta_{42}$ production through direct cleavage. This controversy has arisen from the fact that PS is distributed in the ER and early Golgi apparatus (Annaert et al., 1999; De Strooper et al., 1997; Kovacs et al., 1996; Walter et al., 1996) in contrast that the activity of γ-secretase is restricted to the late Golgi apparatus (Hartmann et al., 1997; Koo and Squazzo, 1994). The increasing findings suggest other 'nonproteolytic' functions of PS. Therefore, it is not surprising that PS is widely distributed in subcellular components although it is a γ-secretase (Esselens et al., 2004; Nelson et al., 2007; Tu et al., 2006).

1.1.3 Tauopathies

According to the amyloid hypothesis, formation of neurofibrillary tangles (NFTs) is caused by an imbalance between Aβ production and Aβ clearance. Neurofibrillary tangles are composed of tau proteins. Compared with amyloid plaques, NFTs correlate well with AD. However, tau mutations are never found in AD patients, but in other disorders, such as frontotemporal dementia and parkinsonism linked to chromosome 17 (FTDP-17), which are monogenic disorders caused by a dominant mutation (Hong et al., 1998). This suggests that tau itself is able to cause neurodegeneration.

Tau protein is encoded by the microtubule-associated proteins (*MAPT*) gene and enriched in both CNS and PNS neurons (Binder et al., 1985; Cleveland et al., 1977a, b; Couchie et al., 1992; LoPresti et al., 1995; Shin et al., 1991a; Shin et al., 1991b). The tau gene is composed of 16 exons that have been identified on chromosome 17. Of these, 11 tau exons are expressed in the CNS giving six isoforms through alternative mRNA splicing (Andreadis et al., 1992; Goedert et al., 1988; Neve et al., 1986). The differences between these six isoforms are dependent on the presence or absence of carboxy-terminal repeat domain (R2 encoded by exon (E) 10) or near-amino-terminal inserts (1N and 2N encoded by E2 and E3 respectively)

(Figure 1.2). Tau containing R2 is termed 4R-tau, otherwise it is called 3R-tau (Goedert et al., 1989a; Goedert et al., 1989b). In a healthy human brain, the ratio of the 3R-tau to the 4R-tau isoform is ~1. Tau has a biological function in healthy individuals (Cleveland et al., 1977a, b; Weingarten et al., 1975). Tau binds to microtubules (MTs), which is mediated by the MT binding sites and regions flanking MT binding sites (Gustke et al., 1994). The MT-binding domains comprise a positively charged proline-rich region, while other domains form a negatively charged acidic amino-terminal region known as the projection domain (Selkoe, 2002; Tanzi and Bertram, 2005). Under normal physiological conditions, the MT-binding domains are tightly attached to β-tubulin at the inner surface of the MTs, while the projection domain binds to the outer surface of the MTs, and so the projection domain is repulsed away from the MT-surface (Ballatore et al., 2007). As 4R-tau possesses a unique sequence flanking R2 repeats with twice the binding affinity compared with other MT binding regions, 4R-tau shows stronger MT binding affinity than 3R-tau (Butner and Kirschner, 1991; Goedert and Jakes, 1990).

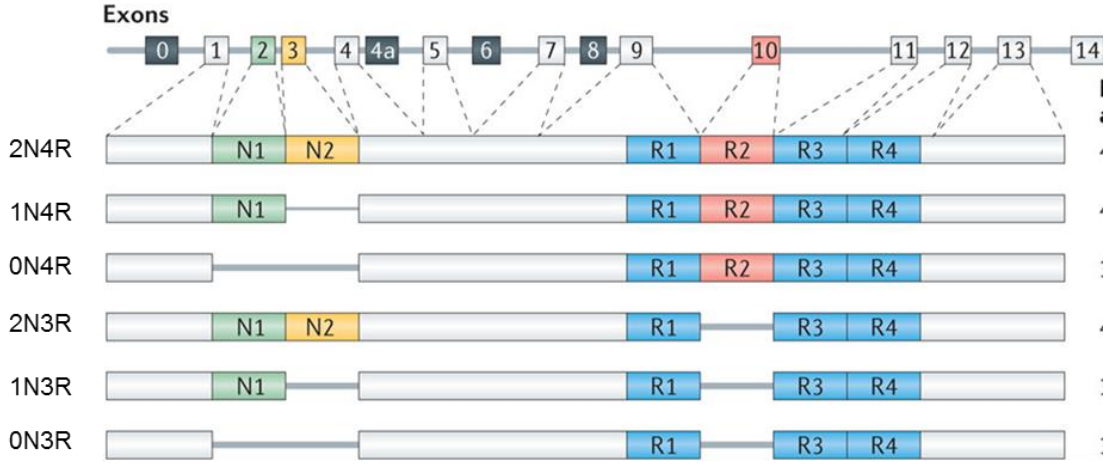

Figure 1.2 Schematic representation of the expression and splicing of the human tau gene in adult brain. The human tau gene consists of 16 exons (E). Among these, only E1, E2, E3, E4, E5, E7, E9, E10, E11, E12 and E13 are expressed in adult brain. Notably, E1, E4, E5, E7, E9, E11, E12 and E13 are constitutively spliced, whereas E2 (green), E3 (yellow) and E10 (red) are alternatively spliced to give rise to the six tau isoforms. The tau isoforms differ according to the presence of 0, 1 or 2 N (yielding 0N, 1N and 2N tau isoforms, respectively) and the presence of repeat R2 (yielding 3R or 4R tau isoforms, respectively). In the adult human brain, levels of the 3R and 4R isoforms are roughly equal, but the expression of 0N, 1N and 2N isoforms are quiet different: the 0N, 1N and 2N tau isoforms comprise ~37%, ~54% and ~9% of total tau, respectively. This diagram is adapted from (Wang and Mandelkow, 2016)

There are about 79 potential phosphorylation sites that are mostly clustered in the MT binding neighbor regions (Billingsley and Kincaid, 1997; Buee et al., 2000). These sites are usually hyperphosphorylated at the embryonic stage (Bramblett et al., 1993; Goedert et al., 1993; Kanemaru et al., 1992; Watanabe et al., 1993), but their phosphorylation levels decrease with age and only half of sites are phosphorylated in the adult healthy brain (Mawal-Dewan et al., 1994). However, in AD, tau is hyperphosphorylated. Hyperphosphorylated tau detaches from MT (Baumann et al., 1993; Bramblett et al., 1993; Drechsel et al., 1992; Yoshida and Ihara, 1993). This detachment possibly accounts for the compromise of MT-mediated axonal transport (Vossel et al., 2010). In addition to the loss-of-function toxicity, tau hyperphosphorylation also leads to gain-of-function toxicity of tau. Tau hyperphosphorylation accelerates tau assembly and neurofibrillary tangles (NFTs) formation (Alonso et al., 2001; Braak et al., 1994). The NFTs eventually give rise to synaptic dysfunction and neurodegeneration (DuBoff et al., 2012; Tracy et al., 2016). Although little is known about how phosphorylated tau assembles the paired helical filaments (PHFs) and straight filaments that are main components of NFT, a growing body of experimental evidence suggests that both PHFs and straight filaments are constituted of hyperphosphorylated tau (Lee et al., 2001). By stimulating a number of protein kinases, it has been seen that *in vitro* expressed tau is phosphorylated to generate typical pathological filaments (Baumann et al., 1993; Drewes et al., 1997; Hanger et al., 1992). It is interesting to note that not all phosphorylated sites are necessary for regulating tau assembly. Until now, the leading theory suggests that the free tau proteins are prone to aggregate and form intracellular NFTs following the extracellular accumulation of amyloid-β. This process is divided into five steps. First, as tau is disengaged from MTs, the cytosolic concentration of unbound tau rises. Then, unbound tau is prone to misfolding, which forms the early deposits lacking typical β-sheet structures. After that, pleated β-sheets gradually become visible pretangles and pretangles are transferred to PHFs. Finally, PHFs develop to more complex NFTs (Brion et al., 1993; Gotz et al., 1995; Maas et al., 2000; Santacruz et al., 2005). More recently, Liu et al. have reported that tau is also modified by O-glycosylation, which negatively regulates tau phosphorylation (Liu et al., 2004). It is still unknown whether tau dephosphorylation contributes to alleviating AD symptoms.

The detrimental role of tau species is a matter of debate. Recent 'amyloid cascade hypothesis' asserts that soluble oligomers are toxic species. In line with this hypothesis, tau oligomers lead to toxicity in cultured neurons (Flach et al., 2012; Tian et al., 2013a). In addition to this, switching off tau expression ameliorates memory deficiency in a mouse model of tauopathy although NFTs remains. This suggests that NFT formation is not the causative agent of AD (Alonso Adel et al., 2006; Santacruz et al., 2005; Sydow et al., 2011; Van der Jeugd et al., 2012). Remarkably the concept that tau does not propagate is also challenged. Tau aggregates are found to be released into the extracellular matrix (ECM) (Kfoury et al., 2012). The secreted tau is then taken up by the neighbor neurons (Frost et al., 2009; Wu et al., 2013). This neuron-neuron protein transmission is reminiscent of the behavior of amyloid-β. Tau seeding and transmission accelerate AD pathology.

1.1.4 Linking amyloid-β to tau

Amyloid-β and tau are two hallmark proteins of AD that have been extensively studied. However, their links have remained elusive. Based on the fact that enhanced hyperphosphorylation of tau is observed in APP transgenic animal models, while there is no obvious formation of amyloid-β in tau transgenic models, it seems that tau is a downstream target of amyloid-β toxicity (Gotz et al., 2004). This opinion is further supported by *in vivo* and *in vitro* evidence. In double transgenic mice expressing both APP and tau variants, the neurofibrillary tangles pathology, rather than amyloid-β pathology, is exacerbated (Gotz et al., 2001; Lewis et al., 2001; Oddo et al., 2004; Terwel et al., 2008). In iPSC-derived neurons, increased APP gene dosage is found to specifically increase tau protein levels (Moore et al., 2015; Muratore et al., 2014). Apart from this, the predominant view asserts that tau phosphorylation is also increased upon amyloid-β expression possibly by activating kinases such as PKA or GSK3 (Terwel et al., 2008). However, in tau$^{-/-}$ cells and tau deficient animals, the amyloid-induced toxicity is alleviated but not fully reversed, which suggests that tau may not be the unique target of amyloid-β (Rapoport et al., 2002; Vossel et al., 2010). Tau hyperphosphorylation is also activated by other amyloidogenic proteins, for example, NFT formation is induced by deposits of integral membrane protein 2B in familial British or Danish

dementia (Coomaraswamy et al., 2010). Several conflicting studies imply that amyloid-β and tau compromise different organelles, which does not support the idea that tau is a secondary effector of amyloid-β. For instance, amyloid-β contributes to defects in complex I of mitochondria while tau targets complex IV (Rhein et al., 2009) Moreover, tau post-translational modification is not altered in APP mice, changeling the idea that tau is a second messenger of amyloid-β (Lill et al., 2015). Taken together, an alternative point suggests that tau is a mediator of amyloid-β toxicity. For example, the interaction between tau and the tyrosine protein kinase (FYN) facilitates the dendritic transport of the NMDAR subunit 2B (NR2B) to postsynaptic sites, which gives rises to neuronal dysfunction. This hypothesis explains why knockout of tau ameliorates amyloid-β toxicity (Fuhrmann et al., 2010). In addition to this, given that tau negatively regulates axonal transport, tau reduction also protects from Aβ-induced defects in axonal transport (Vossel et al., 2010).

1.2 AD risk factors

Variants in the APP gene are associated with AD. Its discovery relied on unbiased linkage analysis and positional cloning. Genetic linkage analysis successfully mapped a number of genes underlying monogenic Mendelian diseases such as presenilins in EOAD as described earlier, but it cannot be applied to non-mendelian disease. As sporadic AD (late onset AD, LOAD) is a non-mendelian disease, traditional genetic linkage analysis is useless to uncover genetic risk factors. In 2005, genome-wide association studies (GWAS) were first developed and applied to AD research. This provides a method to find common variants of quite small effect sizes (Harold et al., 2009; Hollingworth et al., 2011; Lambert et al., 2009; Lambert et al., 2013; Naj et al., 2011; Seshadri et al., 2010). A variation in a single nucleotide is termed single nucleotide polymorphism (SNP). SNPs are used as markers to compare the frequency of alleles between disease cases and controls. The latest SNP chip allows for genotyping 1,000,000 SNPs and capturing > 80% of the variation in 90% the genome. Significant SNPs are then aligned to genotypes to identify possible causative genes (Kruglyak, 2008; McCarthy et al., 2008; Vilhjalmsson and Nordborg, 2013; Wray et al., 2013).

So far, more than 1000 GWAS studies have been published to identify 695 susceptibility genes for AD. These genes include APOE4, CR1, BIN1, CD2AP, EPHA1, CLU, MS4A6A, PICALM and ABCA7 (Harold et al., 2009; Hollingworth et al., 2011; Lambert et al., 2009; Lambert et al., 2013; Naj et al., 2011; Seshadri et al., 2010). These genes are mainly categorized into protein transport, intracellular signaling pathways and protein clearance. PICALM, BIN1 and CD2AP are all involved in clathrin-mediated endocytosis (CME) (Koo et al., 2015; Koo et al., 2011; Moreau et al., 2014; Zhao et al., 2015b; Cormont et al., 2003; Leprince et al., 2003; Leprince et al., 1997; Lynch et al., 2003; Micheva et al., 1997; Pant et al., 2009; Ramjaun and McPherson, 1998; Slepnev et al., 2000; Tebar et al., 1999; Wigge et al., 1997). CR1, CLU and ABCA7 are responsible for clearance of toxic proteins (Fuhrmann et al., 2010) Bell et al., 2007; (Fu et al., 2016; Kim et al., 2013b; Li et al., 2016; Sakae et al., 2016; Satoh et al., 2015). APOE4, EPHA1 and MS4A6A could mediate downstream cascades of amyloid-β (Bell et al., 2012; Deane et al., 2008).

Although GWAS have provided numerous hit for AD risk, they bear several limitations. Firstly, GWAS cannot identify rare variants in a disease, and so a novel approach is required. The revolution of whole genome sequencing provided such a method, which discovered that rare variants in TREM2 are strongly associated with LOAD (Guerreiro et al., 2013; Jonsson et al., 2013). Secondly, GWAS cannot elucidate the biological function of GWAS hits in AD pathology. As such, the following experiments are required to achieve functional characterization of disease linked genetic variability. Thirdly, GWAS cannot detect the influences of protein modification on AD progression. Therefore, the functional experiments are still inevitable to understanding the molecular mechanisms underlying disease.

1.2.1 ApoE4 in LOAD

The first identified risk factor for AD is the allele of apolipoprotein E (ApoE4). It was first discovered in a biochemical screen (Strittmatter et al., 1993), confirmed by subsequent GWAS (Corder et al., 1993) and remains the strongest AD risk factor to date. ApoE4 is one of three isoforms of the ApoE protein, conferring the most susceptibility for LOAD compared with other

AD risk genes (Namba et al., 1991; Rebeck et al., 1993; Schmechel et al., 1993). Mutations in ApoE4 are estimated to increase the frequency of AD and reduce the age of onset for AD (Corder et al., 1993; Farrer et al., 1997). Moreover, ApoE4 carriers show more severe cognitive defects and memory impairments compared to non-carriers (Cosentino et al., 2008; Dik et al., 2000; Elias-Sonnenschein et al., 2011; Farlow et al., 2004; Fleisher et al., 2007; Petersen et al., 1995; Ramakers et al., 2008; Smith et al., 1998; Whitehair et al., 2010).

ApoE is an apolipoprotein that binds to low density lipoprotein receptor (LDLR) (Beisiegel et al., 1989; Innerarity and Mahley, 1978; Kim et al., 1996; Kowal et al., 1989). It is polymorphic and is characterized by three isoforms: ApoE2, ApoE3 and ApoE4. The differences between these isoforms come from different amino acid residues at positions 112 and 158 (Rall et al., 1982; Weisgraber et al., 1981). These differences lead to ApoE4 having stronger affinity with LDLR, including LDLR-related protein 1 (LRP1) (Dong et al., 1994; Hatters et al., 2006). Although the molecular mechanism by which apoE4 elevates AD risk remains elusive, there are two possible genetic pathways to explain the detrimental effects of ApoE4: the Aβ-dependent and the Aβ-independent pathway.

With regard to the Aβ-dependent pathway, first, ApoE4 enhances Aβ aggregation, fibril and amyloid plaque formation (Biere et al., 1995; Evans et al., 1995; Ma et al., 1994). Both *in vitro* and *in vivo* experiments have demonstrated that ApoE4 accelerates Aβ aggregation and firbillogenesis (Buttini et al., 1999; Cerf et al., 2011; Hamanaka et al., 2000; Nathan et al., 1994; Veinbergs et al., 1999) and ApoE4 mice have more Aβ oligomers and plaques (Bales et al., 2009; Fryer et al., 2005; Oakley et al., 2006; Youmans et al., 2012). In contrast, the expression of ApoE2 and E3 alleles lower the risk for AD. Mice expressing human ApoE2 or E3 have significantly reduced Aβ fibrils and deposition (Holtzman et al., 2000; Holtzman et al., 1999). More recently, evidence has demonstrated that ApoE4 has a direct effect on Aβ production through promoting APP transcription (Huang et al., 2017). In addition to this, ApoE4 interacts with LRP1 which slows the $A\beta_{42}$ uptake by neurons or blood brain barriers (Kanekiyo et al., 2013) Zhao et al., 2015b). ApoE4 expression also inhibits autophagy which might further interfere with Aβ clearance (Parcon et al., 2017).

With respect to the Aβ-independent pathway, ApoE4 expression suppresses neurite growth and mitochondrial function in primary neuronal cultures and confers spatial learning and memory deficits in mice, which is rescued by ApoE3 (Mauch et al., 2001; Pfrieger, 2003). This is possibly attributed to abnormal glucose and lipid metabolism (Hamanaka et al., 2000; Rapp et al., 2006). A recent study reveals that ApoE4 impairs neuronal insulin signaling (Zhao et al., 2017). Moreover, ApoE4 substantially reduces lipid transports from neurons to glia and therefore causes neuronal dysfunction (Liu et al., 2017). Apart from this, ApoE4 is reported to reduce anti-inflammatory responses (Lynch et al., 2003). Therefore, it markedly confers neuroinflammation and neurodegeneration in a model of tauopathy (Shi et al., 2017)

1.2.2 BIN1 in LOAD

The BIN1 gene is the second strongest susceptibility gene for LOAD. At least 11 single-nucleotide polymorphisms (SNPs) in BIN1 are linked to the AD risk. These include the most significant SNPs rs744373 and rs7561528 (Carrasquillo et al., 2011; Kamboh et al., 2012; Lambert et al., 2011; Wijsman et al., 2011). These SNPs elevate or lower AD risk, which depends on how they mediate the expression of BIN1 (Chapuis et al., 2013; Glennon et al., 2013).

Since whether the change of BIN1 expression in AD is still controversial (Chapuis et al., 2013; Glennon et al., 2013), BIN1's role in AD pathology remains explored. Given that it binds to dynamin and plays a crucial role in endocytosis and endosomal trafficking (Takei et al., 1999), BIN1 and PICALM are predicted to act on a common pathway. Lack of BIN1 displays learning deficits (Di Paolo et al., 2002).

BIN1 has been implicated in tau pathology, although its role is a matter of debate, with some studies suggesting that upregulation blocks the uptake and spread of tau (Calafate et al., 2016) while others suggesting that downregulation ameliorates tau hyperphosphorylation (Chapuis et al., 2013).

BIN1 is also recently reported to contribute to Aβ production. For instance, BIN1 is found to regulate vesicular scission, so its depletion decreases BACE1 recycling to the plasma membrane and BACE1 lysosomal degradation, therefore increasing Aβ production (Miyagawa et al., 2016; Ubelmann et al., 2017). The contribution of BIN1 to Aβ clearance and pathology remains unknown. Given that BIN1 functions in apoptosis and inflammation (Chang et al., 2007; Elliott et al., 2000; Galderisi et al., 1999; Wechsler-Reya et al., 1997), it might have many impacts on AD pathology.

1.2.3 PICALM in LOAD

The PICALM gene is an important risk locus for LOAD after APOE4 and BIN1. Until now, more than ten AD-associated SNPs in PICALM have been identified (Carrasquillo et al., 2015; Harold et al., 2009; Hollingworth et al., 2011; Lambert et al., 2013). Among them, several SNPs such as rs3851179 are neuroprotective, while the others are associated with a higher risk of AD (Harold et al., 2009; Lambert et al., 2013). These SNPs affect AD risk through their influence on PICALM expression (Zhao et al., 2015b; (Raj et al., 2012).

PICALM is ubiquitously expressed in neurons, glial and endothelial cells, and is involved in clathrin-mediated endocytosis (Tian et al., 2013). It physically binds to soluble NSF attachment protein receptors (SNAREs) such as VAMP2, VAMP8 and RAB5, RAB11 and promotes vesicular formation (Koo et al., 2015; Koo et al., 2011; Moreau et al., 2014; Zhao et al., 2015b).

The association between PICALM and tau pathology is not fully understood. One potential pathway underpinning the role of PICALM in tau pathology is that down-regulation of PICALM leads to elevated autophagy and therefore promotes tau degradation (Moreau et al., 2014). Apart from this, it is unclear whether lack of PICALM prevents tau transmission.

PICALM expression is decreased in brain samples of AD patients (Ando et al., 2013; Parikh et al., 2014). However, the role of PICALM in Alzheimer's disease remains controversial. On one hand, knockdown of PICALM limits APP or γ-secretase internalization and therefore inhibits

$A\beta_{42}$ production (Kanatsu et al., 2014; Moreau et al., 2014; Xiao et al., 2012; Yu et al., 2010). On the other hand, PICALM over-expression promotes APP degradation including APP-CTF and $A\beta_{42}$ clearance (Tian et al., 2013b; Zhao et al., 2015b). Although PICALM in endothelial cells is implicated in transportation of $A\beta_{42}$ across the blood-brain barrier and removal of $A\beta_{42}$ (Zhao et al., 2015b), little is known about the contribution of PICALM in neurons to modulating Aβ pathology: on one hand, uptake of Aβ might enhance Aβ elimination (Kanekiyo et al., 2013); on the other hand, abundant Aβ accumulation in neurons might lead to lysosomal dysfunction (Hu et al., 2009b). In addition to this, as PICALM is involved in synaptic function and immunity (Harel et al., 2008; Scotland et al., 2012), this suggests that PICALM might affect AD progression independent of Aβ or tau pathology.

1.2.4 Ageing as a risk factor for LOAD

Ageing is characterized by a gradual functional decline of all organ systems, accompanied by a wide range of physiological challenge, loss of ability, decline in function and death. It is estimated that by 2050, 2 billion people worldwide will be over the age of 60 years (Bloom et al., 2011). Increased population ageing raises vulnerability to diseases like cancer, diabetes, cardiovascular disorders and neurodegenerative diseases. It is anticipated that human health will become society's big burden in the next ten years (Bloom et al., 2011). In the past decades, scientists made great efforts to understand a connection between ageing and neurodegenerative disease. Slowly, the genetic basis underlying ageing and neurodegenerative disease is becoming clearer.

Ageing and neurodegenerative disease share basic cellular pathways such as DNA repair, histone methylation, ubiquitin-proteasome degradation, autophagy and NAD production. These pathways are lost with age and impaired with neurodegenerative disease. For example, elevation of ubiquitin protein ligases or ATG proteins is able to increase life expectancy as well as attenuate neurodegenerative pathology (Carrano et al., 2014; Carrano et al., 2009; Heimbucher et al., 2015; Li et al., 2007; Liu et al., 2011; Vilchez et al., 2012; Gong et al., 2006; Harrison et al., 2009; Juhasz et al., 2007; Lee et al., 2010a; Matsumoto et al., 2011; Minnerly

et al., 2017; Mori et al., 1987; O'Rourke et al., 2013; Ryu et al., 2016; Soda et al., 2009). The lifespan and healthspan are increased by an improvement in DNA repair ability, an activation of histone methylation and a supplementation of NAD (Madabhushi et al., 2015; Suberbielle et al., 2013; Fang et al., 2016; Greer et al., 2010; Greer et al., 2011; Han et al., 2017; Li et al., 2013; Merkwirth et al., 2016; Zhang et al., 2016).

However, dozens of studies have demonstrated that some of the molecular mechanisms of the ageing process and neurodegeneration are opposite. For instance, it is well known that glutamate receptors are critical in memory formation and are reduced in AD brains. However, their silencing delays ageing of *Drosophila* (Verma et al., 2015). Another example to elucidate the odds between ageing and neurodegeneration is protection of mitochondrial function. A modest restriction of mitochondrial function improves the survival rate in C. *elegans and Drosophila* (Copeland et al., 2009; Ewbank et al., 1997; Felkai et al., 1999; Feng et al., 2001; Jonassen et al., 2001; Jonassen et al., 1998; Rea et al., 2007; Stenmark et al., 2001; Vajo et al., 1999; Wong et al., 1995), but mitochondrial function is impaired in AD or PD patients, so an improvement of mitochondrial dysfunction delays progression of AD and PD (Anandatheerthavarada et al., 2003; Caspersen et al., 2005; Devi et al., 2006; Hirai et al., 2001; Wang et al., 2009a; Yao et al., 2009).

The contributions of several age-related genes in neurodegenerative disease also appear contradictory. For example, an inhibition of IIS pathway is able to partially alleviate paralysis of $A\beta_{42}$ worms, flies and APP/PS1 mice owing to an enhanced clearance of $A\beta_{42}$ (Chiang et al., 2010; Cohen et al., 2006; Cohen et al., 2009), while a restoration of IIS pathway is reported to protect against $A\beta_{42}$ toxicity in mammalian models (Carro et al., 2006; Carro et al., 2002; Craft et al., 2012; Dudek et al., 1997). This alleviation is attributed to a promotion in memory formation. Also, suppression of mTOR by rapamycin has been proven to eliminate $A\beta_{42}$ toxicity through an elevation of autophagy (Ravikumar et al., 2004; Spilman et al., 2010), whereas a block of mTOR gives rise to memory loss (Fortress et al., 2013; Jobim et al., 2012a; Jobim et al., 2012b; Mac Callum et al., 2014; Parsons et al., 2006; Schicknick et al., 2008). This opposite action resembles different roles of RAS and SIRT in ageing and neurodegeneration

as well. On one hand, activation of SIRT1 by resveratrol abolishes neurotoxicity in HD and AD (Parker et al., 2005); on the other hand, inhibition of SIRT1 is also indicated in neuroprotection (Li et al., 2008). Moreover, a reduction of SIRT2 expression by AKT1 facilitates neuronal survival in HD and PD (Luthi-Carter et al., 2010). This discrepancy is also seen in the role of the UPR in AD. Either a reduction of the UPR repressor Bip or elevation of UPR activator Xbp-1 is sufficient to increase longevity of $A\beta_{42}$-expressing flies (Casas-Tinto et al., 2011; Niccoli et al., 2016), but suppression UPR through knockout of eIF2α rescues memory deficits of AD mice models (Ma et al., 2013b) and upregulation of UPR^{mt} through overexpression of JNK3 aggravates amyloid-β toxicity (Yoon et al., 2012).

This evidence suggests that although the cellular pathways involved in ageing and AD are overlapped, ageing might not to be the causative of AD. Ageing merely increases vulnerability to AD (Niccoli and Partridge, 2012; Rogers et al., 2012). Therefore, anti-ageing strategy might be an effective avenue to delay onset of age-related diseases, although it may not be a treatment for AD.

1.3 Glutamategeric transmission with Alzheimer's disease

1.3.1 Glutamate release and uptake

The main symptom experienced by AD patients is memory impairment. This is something essential for everyday life, allowing an individual to store and retrieve acquired knowledge and so beneficially affect subsequent behavior. During memory formation, glutamatergic transmission plays a crucial role.

Glutamate is the principal excitatory transmitter that is pumped into vesicles through vesicular glutamate transporter (VGLUT) and then vesicles are released into the extracellular matrix (Daniels et al., 2004; Rossano et al., 2017). VGLUT can be divided into three subtypes (VGLUT1-3) and consists of 8-10 putative transmembrane domains (El Mestikawy et al., 2011; Schafer et al., 2002). It is mainly distributed in neurons and glial cells. VGLUT takes up cytoplasmic glutamate and transports glutamate inside vesicles. These then fuse with the

plasma membrane so that glutamate is exocytosed and released. This loading of glutamate into vesicles is driven by an electrochemical H^+ gradient and mediated by Cl^-. Low concentrations of Cl^- facilitate glutamate uptake by VGLUT while high concentrations inhibit it (Fremeau et al., 2001; Kaneko et al., 2002; Li et al., 2003). Once released into the extracellular space excess extracellular glutamate is taken up by excitatory amino acid transporters (EAATs), mostly located on glia. EAATs are composed of three homomeric subunits. This trimer forms a bowl-shaped structure and the glutamate-binding sites are located towards the bottom of the structure (Tzingounis and Wadiche, 2007). When extracellular Na^+ or H^+ bind to the gates of EAAT, the glutamate-binding site is exposed to the extracellular matrix and the glutamate is translocated inside (Barbour et al., 1988; Bouvier et al., 1992; Erecinska et al., 1983; Kanai et al., 1995; Kanner and Bendahan, 1982; Kanner and Sharon, 1978; Klockner et al., 1993; Stallcup et al., 1979; Wadiche et al., 1995; Zerangue and Kavanaugh, 1996b). But when intracellular K^+ binds to the gates, the glutamate-binding site faces the cytoplasm and glutamate uptake is blocked (Levy et al., 1998; Owe et al., 2006; Zerangue and Kavanaugh, 1996a). Glutamate taken up by glia is converted into glutamine by glutamine synthetase in glia, which is exclusively expressed in astrocytes, and released into the extracellular space where it is taken up by neurons and used to generate glutamate. Therefore, glial cells are the source of glutamine for glutamate biosynthesis. Non-vesicular transporters such as xCT transporters are also located on glia cells. These transporters modulate glutamate release from glia (Augustin et al., 2007). Non-vesicular release of glutamate is regarded as a reversed glutamate uptake (Szatkowski et al., 1990).

An increase in extracellular glutamate is found in both *in vitro* and in *vivo* model of AD. This is usually attributed to Aβ-induced impairment of glutamate uptake by glial cells (Cummings et al., 2015; Hefendehl et al., 2016; Li et al., 2009; Talantova et al., 2013). However, one study suggests that neurons are directly involved in the elevated glutamate levels in the extracellular matrix (Cummings et al., 2015). Taken together, it is likely that glutamate excitotoxicity is linked to AD.

1.3.2 Glutamate excitotoxicity

Glutamate activates glutamate receptors. In turn, glutamate receptor alters glutamate release by a retrograde messenger. Glutamate receptors fall into three groups: NMDAR, AMPAR and mGluR. All three types are involved in memory formation and decay.

AMPARs are ionotropic GluRs (Benke et al., 1998; Derkach et al., 1999; Ehlers, 2000) and composed of four subunits (GluA1 – GluA4), formed by homomeric GluA1 subunits or heteromeric GluA1/GluA2 and GluA2/GluA3 subunits. GluA1 is a highly Ca^{2+}-permeable AMPAR (CP-AMPAR) that is necessary for memory acquisition. During memory acquisition, GluA1 is trafficked to spines. However, GluA1 is not involved in memory retrieval because the selective blockade of GluA1-containing CP-AMPARs has no effect on memory after it has been established. After memory is established, synaptic GluA1-containing CP-AMPARs gradually switch back to GluA2-containing Ca^{2+}-impermeable AMPARs (CI-AMPARs) by lateral diffusion. Memory loss is concomitant with GluA1 dephosphorylation and endocytosis. In addition to this, hippocalcin is transported to the plasma membrane and destabilizes GluA2 (Palmer et al., 2005). This initiates the GluA2 recycling. Moreover, PICK1 is activated during memory loss and facilitates the internalization of GluA2. (Emond et al., 2010; Hanley and Henley, 2005; Lin and Huganir, 2007; Oliet et al., 1997; Peineau et al., 2009; Terashima et al., 2008). Taken together, under basal conditions, the synapse is dominated by CI-AMPARs. During memory establishment, synaptic CI-AMPARs switch to CP-AMPARs. Next, synaptic CP-AMPARs gradually scale down synaptic strength via the replacement of synaptic CP-AMPARs with CI-AMPARs, while during memory decay, synaptic CP-AMPARs are internalized. After that, GluA2 is endocytosed and might scale up synaptic strength.

The *Drosophila* nervous system also expresses different types of glutamate receptors (GluRs). Like mammalian glutamate receptors, *Drosophila* GluRs are composed of many subunits. Due to distinct properties of subunits, GluRs are further divided into: metabotropic glutamate receptors (mGluRs) and ionotropic glutamate receptors (iGluRs). mGluRs are glutamate-activated G-protein coupled receptors and formed by heteromeric GluRA/XR

subunits (Andlauer et al., 2014; Bogdanik et al., 2004; Mitri et al., 2004; Parmentier et al., 1996). iGluRs are glutamate-gated ion channels and fall into four categories: NMDA, AMPA, kainate receptors and glutamate-gated chloride channels. NMDA receptors are formed by NR1/NR2 subunits (Ultsch et al., 1993; Xia et al., 2005). AMPA receptors are the main excitatory iGluRs and composed of two subtypes: A type and B type. Type A contains GluRIIA, C, D and E subunits (Schuster et al., 1991) while type B contains GluRIIB, C, D and E subunits (Petersen et al., 1997). Compared to AMPA receptors in mammalian neurons, *Drosophila* AMPA receptors require extremely high concentrations of glutamate for activation (Han et al., 2015; Heckmann et al., 1996). However, like mammalian AMPA receptors, *Drosophila* AMPA receptors are permeable to calcium (Chang et al., 1994; Han et al., 2015). Another type of excitatory iGluRs are kainate receptors and these are composed of GluRIA or GluRIB subunits. Kainate receptors are activated by kainate rather than glutamate (Ultsch et al., 1992; Volkner et al., 2000). In addition to this, *Drosophila* has inhibitory iGluRs, glutamate-gated chloride channels, which are formed by GluCl subunits (Delgado et al., 1989; Liu and Wilson, 2013). The function of glutamate receptors is conserved in invertebrates. *Drosophila*'s glutamate receptors are involved in memory consolidation (Wu et al., 2007; Xia et al., 2005).

In the past, glutamatergic transmission was found to be attenuated, concomitant with Aβ accumulation. For instance, either AMPARs or NMDARs is endocytosed upon Aβ exposure (500 nM) for 7 days (Hsieh et al., 2006; Shankar et al., 2007; Snyder et al., 2005; Zhao et al., 2010). However, this idea has been disputed. Firstly, NR2B subunits of NMDARs are reported to be activated by Aβ oligomers and inhibition of NR2B prevents Aβ-mediated neurotoxicity (Hu et al., 2009a; Li et al., 2009; Li et al., 2011; Talantova et al., 2013). Secondly, the lines of evidence have shown that although GluA2 subunits of AMPAR are removed from cell surfaces, GluA1 subunits accumulate with low levels of Aβ (5 nM) for 2h. This suggests that low doses of Aβ leads to excitotoxicity as a primary response, while high doses of Aβ scales down synaptic strength and results in synaptic loss (Liu et al., 2010; Whitcomb et al., 2015).

Recently the mechanism of how Aβ oligomers affect glutamate receptor has increasingly becoming clear. At least four interacting partners of Aβ oligomers have been identified. First,

Aβ oligomers physically interact with the α7 nicotinic acetylcholine receptor (α7 nAChR). The activation of α7 nAChR will induce CaMKII phosphorylation and therefore AMPAR activation, but this process is blocked by Aβ oligomer expression (Dineley et al., 2002a; Dineley et al., 2002b; Wang et al., 2000; Wang et al., 2003). Aβ oligomers also bind to cellular prion protein (PrP^C) and PrP^C interacts with NR2D or mGluR5. Either Aβ-PrP^C-NR2D or Aβ-PrP^C-mGluR5 complex triggers Fyn activation and then synaptic loss (Lauren et al., 2009; Um et al., 2013; Um et al., 2012). Moreover, Aβ oligomers bind to EphB2 and lead to EphB2 degradation. EphB2 depletion dramatically reduces NR1 subunits on the cell surface and thus impairs memory acquisition (Cisse et al., 2011). Aβ oligomers have a high affinity for LilrB2. Aβ oligomers act on LilrB2 to activate PP2A and PP2B, which leads to internalization of AMPARs and impairment in memory (Kim et al., 2013a).

1.4 Research progress in Alzheimer's disease

1.4.1 Mammalian models of AD

Given the scarcity of postmortem brain tissues of AD patients and the fact that disease brain tissue of living patients is difficult to obtain, there is limited experimental access to human disease relevant samples. Therefore, various animal models have been developed to recapitulate AD phenotypes. The first human APP cell model is derived from SH-SY5Y cells. APP-expressing SH-SY5Y cells do not recapitulate severe AD phenotypes such as cell death, but they facilitate the understanding of the APP processing (Jamsa et al., 2011; Matsumoto et al., 2006). Recently, several human APP neuronal models have been established. These neurons differentiate from embryonic stem cells, human neural progenitor cells (hNPCs), induced pluripotent stem cells (iPSCs) or are directly converted from somatic cells (Choi et al., 2014; Hu et al., 2015; Israel et al., 2012; Kondo et al., 2013). However, none of the APP mutations successfully recapitulated AD phenotypes except for increased $A\beta_{42}$ levels. Only models with over-expression of APP develop detectable AD pathology including synaptic degeneration. However, this unphysiologically high level of APP caused by the overexpression induces a number of undesirable side effects. For example, over-expression of APP interferes with intracellular transport, synaptic adhesion, synaptogenesis and increases NMDAR

expression (Baumkotter et al., 2014; Choi et al., 2013; Cousins et al., 2009; Cousins et al., 2013; Deyts et al., 2016; Deyts et al., 2012; Hoe et al., 2009; Koo, 2002; Osterhout et al., 2015; Wang et al., 2009b). In addition to APP over-expression, three-dimensional culture or extension of culture time might be an alternative way to promote toxicity (Choi et al., 2013; Shi et al., 2012). Primary neurons from APP fetal mice have also been used for AD studies for decades. These cells display cell death and decreased synaptic transmission (Baldassarro et al., 2017; Katsurabayashi et al., 2016). Administration of > 500 nM of $A\beta_{42}$ to primary cultures also induces synaptic loss and cell death (Lauren et al., 2009; Um et al., 2013; Um et al., 2012). However, this model is considered very artefactual since it neglects the APP processing and uses extremely high, non-physiological concentrations of $A\beta_{42}$.

Mice models have also been instrumental for AD research, with numerous murine models having been developed. A typical example is APPSw transgenic mice that over-express the Swedish double mutant APP (e.g. APP23 and Tg2576) (Games et al., 1995; Hsiao et al., 1996; Saydoff et al., 2013). These mice are characterized by the increased $A\beta_{42}$ production, amyloid plaques at 9 months, and synaptic and memory deficits at 6 months. However, they do not display neurofibrillary tangles (NFTs) and neuronal loss. APP/PS1 transgenic mice (e.g. PSAPP and 5XFAD) are the other commonly used mouse models that carry mutations in PS1. They display more severe AD phenotypes such as the enhanced $A\beta_{42}$ production and $A\beta_{42}$/ $A\beta_{40}$ ratio at 2 month of age and amyloid plaques at 2-3 month of age (Girard et al., 2014; Holcomb et al., 1998; Oakley et al., 2006). These two models have been used to investigate FAD pathology. However, they suffer from over-expression artifacts derived from mutations of APP and PS1. In order to overcome this problem, several knock-in (KI) murine models have been recently generated. APP KI mice (APP^{NL-F}) lead to an increase in both β-cleavage and γ-cleavage of APP, which elevates the $A\beta_{42}$ levels and $A\beta_{42}/A\beta_{40}$ ratio. These mice display accumulation of amyloid plaques and therefore impaired memory at 18 months, whereas the other APP KI mice with Arctic mutations (APP^{NL-G-F}) show Aβ pathology earlier from 2 months and memory problems at 6 months (Saito et al., 2014). BACE1 KI mice also display the elevated levels of $A\beta_{42}$ and cognitive deficits (Plucinska et al., 2014). However, PSEN1 KI mice show a decrease in the $A\beta_{42}$ levels but a significant increase in $A\beta_{42}/A\beta_{40}$ ratio. These mice

have Aβ deposition and memory impairment (Xia et al., 2015).

Although numerous murine models have been established to study FAD pathology, no models successfully recapitulate SAD pathology. It is well established that overproduction of $A\beta_{42}$ has failed to produce significant neurodegeneration in mice (Hsiao et al., 1996; Mucke et al., 2000). Therefore, the Aβ injected mouse model is developed. However, 100 uM of $A\beta_{42}$ is unphysiologically high to induce Aβ toxicity. Therefore, this model is not widely used by researchers to study disease progression (Gotz et al., 2001; Roberson et al., 2007). With respect to the ApoE4 transgenic mice, the endogenous ApoE is replaced by human ApoE4. These mice have cognitive impairment without amyloid plaques deposits (Osorio et al., 2007).

1.4.2 *Drosophila* model of AD

A number of non-mammalian models have also been developed. Amongst these, *Drosophila melanogaster* serves as a model organism for genetic analysis mainly because it provides a compromise between experimental ease and evolutionary conservation. It has a hundred year history in genetic research and is still used as a favorite model organism for laboratory studies of embryonic development. It is a useful model in biological research due to its small size and low care requirements. It is cheap and easy to breed in big numbers. Its major advantage for the study of neurodegenerative diseases is its relatively short development time and lifespan, ~10 days and ~3 months, respectively, and its relatively complex behaviors ranging from simple avoidance to learning and memory (Guo et al., 2000; Guo and Zhong, 2006; Shuai et al., 2010).

Drosophila has complex and highly differentiated central (CNS) and peripheral nervous systems (PNS). For example, *Drosophila* has compound eyes, which give them sharp vision. Their eyes consist of 760 ommatidia and each ommatidium contains eight photoreceptor cells and pigment cells. Pigment cells are responsible for absorbing light and transducing light signals to photoreceptors. Subsequently, photoreceptors convert optical signals to chemical information and then send this information to optical lobes of brains. Under the normal

physiological condition, *Drosophila* compound eyes have highly organized arrangements of retinal neurons and a smooth surface. However, when neurons degenerate, their eyes gradually lose photoreceptors, which gives rise to a roughened surface. This phenotype is termed rough eye phenotype (REP). As REP is easily observed under light microscopy, it provides a convenient tool for genetic modifier screens (Armakola et al., 2012; Gitler et al., 2009; Treusch et al., 2011; Chung et al., 2013; Kim et al., 2014; Tardiff et al., 2013). In addition to this, *Drosophila* motor systems are well developed. The most notable motor systems are the giant fiber (GF) system that controls locomotion, flight, and an escape response. The GF system comprises of a pair of interneurons whose cell bodies reside in the brains, with axons descending along the midline into the thoracic ganglion. The ventral ganglion in the thorax is connected to two muscle fibers: the dorsal longitudinal muscle (DLM) via chemical (cholinergic) synapses and tergotrochanteral muscle (TTM) via electric (glutamatergic) synapse (Allen and Godenschwege, 2010; Augustin et al., 2011). In *Drosophila* models of neurodegenerative diseases, the function of *Drosophila* nervous systems can be measured by locomotion and flight assays. Therefore, *Drosophila* behavioral deficiency is an important phenotype of neuronal dysfunction (Lasagna-Reeves et al., 2016; Park et al., 2013; Rousseaux et al., 2016). To coordinate sensory input and motor output, a delicate CNS, the mushroom body (MB), is developed in *Drosophila*. The mushroom body neurons (MBNs) are comprised of two classes: Kenyon cells (KCs) and output neurons (MBONs) (Aso et al., 2014; Campbell et al., 2013; Lin et al., 2014; Owald et al., 2015; Perisse et al., 2013; Turner et al., 2008). KCs receive information through their dendrites in the calyx, while MBONs convey information to downstream motor neurons (Pai et al., 2013; Placais et al., 2013). This learning process is also modulated by dopamine neurons (Boto et al., 2014; Claridge-Chang et al., 2009; Kim et al., 2007b; Mao and Davis, 2009; Qin et al., 2012; Riemensperger et al., 2005; Schroll et al., 2006; Schwaerzel et al., 2003) The learned information is stored in the mushroom body that is also involved in memory acquisition, consolidation, forgetting and retrieval. Similar to mammalian memory, *Drosophila* memory is classified into: short-term memory (STM) (0–1 h), intermediate-term memory (ITM) (0.5-3 h), early-phase long-term memory (LTM) (9-24 h) and late-phase long-term memory (LP-LTM) (18-48 h). The formation of LTM and LP-LTM is dependent on protein synthesis (Akalal et al., 2010; Pascual and Preat, 2001; Tully et al., 1994;

Yu et al., 2006). In order to organize and store different forms of memory traces, the KCs differentiate into three highly organized subtypes: α/β, α'/β' and γ MBNs. The γ MBNs are the primary site for STM formation (Akalal et al., 2006; Blum et al., 2009; Cervantes-Sandoval et al., 2013; Xie et al., 2013; Zars et al., 2000; Zhang and Roman, 2013). The γ MBNs then convey information to the α'/β' MBNs for ITM formation (Cervantes-Sandoval et al., 2013; Davis, 2011; Krashes et al., 2007; Wang et al., 2008). The α/β MBNs are required for acquisition of all forms of memory, especially LTM (Akalal et al., 2010; Cervantes-Sandoval et al., 2013; Dubnau et al., 2001; Huang et al., 2013; Huang et al., 2012; McGuire et al., 2001; Perisse et al., 2013; Xie et al., 2013; Yu et al., 2006). In addition to this, a specific subtype of the γ MBNs plays an important role in LP-LTM acquisition (Akalal et al., 2010; Yu et al., 2004). The processes of STM, ITM and LTM are also modulated by the anterior paired lateral neuron (APLn) (Lin et al., 2014; Liu and Davis, 2009; Liu et al., 2007; Pitman et al., 2011), dorsal paired medial neurons (DPMn) (Keene et al., 2004; Krashes et al., 2007; Waddell et al., 2000; Yu et al., 2005) and dorsal anterior lateral DAL neurons (DALn) (Chen et al., 2012), respectively. In AD models, *Drosophila* memory is severely impaired, consistent with the fact that its mushroom body is degenerated (Chiang et al., 2010; Wang et al., 2012).

Another advantage of the fly is the numerous well-established molecular tools and genetic database developed during its long history as an animal model in research. It was one of the first organisms with a fully sequenced genome. There are roughly 13600 genes, located on four chromosomes. Nearly 70% of human disease-causing genes have homologs in the fly. The fly also benefits from well-established binary expression systems such as the GAL4/UAS (upstream activation sequence) system. The GAL4/UAS system was first developed by Brand and Perrimon and is based on transcription factor (TF) enhancer sequences from yeast *Saccharomyces cerevisiae* (Brand and Perrimon, 1993). The relevant proteins are not present in *Drosophila* and their expression does not interfere with normal biological processes in the cell. GAL4 is cloned under the control of a tissue specific promoter, thus restricting its expression to a particular tissue of interest. The target gene is cloned under the control of the UAS promoter. GAL4 binds to the UAS enhancer sequence driving the expression of the gene of interest. Usually Gal4 lines and reporter lines expressing UAS-regulated transgenes are

separated. When required, two lines will be crossed with each other to drive the expression of the target gene in those tissues where GAL4 is expressed.

However, the GAL4/UAS system is limited to spatial regulation because once the GAL4 and UAS-linked transgene coexist in the fly genome, this transgene will be immediately expressed. The development of the gene-switch (GS) system has extended the application of the GAL4/UAS system, allowing activation of genes only in the presence of steroid hormones or chemically related compounds, thus allowing temporal regulation (Ford et al., 2007; Osterwalder et al., 2001). In the GS system, GAL4 is fused with the regulatory domain of the human progesterone receptor, which is recognized and activated by the activator mifepristone (RU486) (Osterwalder et al., 2001; Poirier et al., 2008). In the absence of RU486, the GAL4 loses its activity. Only when flies with the GS driver and the UAS component are fed a RU486 dose, the GS system becomes transcriptionally active and induces gene expression.

At least three *Drosophila* models have been widely used as Alzheimer's disease models. *Drosophila* has the conserved γ-secretase (Takasugi et al., 2003) and APP-like protein (APPL), but not β-secretase. Therefore, $A\beta_{42}$ is not detected in flies. Overexpression of human APP and BACE1 genes in fly brains recapitulates several AD phenotypes such as shortened lifespan, synaptic loss, locomotor and memory deficits (Chakraborty et al., 2011). Flies expressing $A\beta_{arc}$ display similar neurodegenerative phenotypes (Crowther et al., 2005), while flies expressing single copy of $A\beta_{42}$ merely exhibit the rough eye phenotype, synaptic degeneration and impairment in memory performance (Finelli et al., 2004). Like the murine model, the *Drosophila* model of $A\beta_{42}$ displays amyloid deposits (Chiang et al., 2010; Iijima et al., 2004).

Our *Drosophila* AD model is gifted from Dr. P. Fernandez-Funez that expresses two copies of $A\beta_{42}$ (Casas-Tinto et al., 2011). UAS-$A\beta_{42}$x2 is fused with an extracellular export signal that is driven by different Gal4 including elavGS, D42-Gal4 and Mef2-Gal2. ElavGS is a GS driver linked to the promoter of Elav. Elav encodes a neuronal specific protein, so this driver is only expressed in *Drosophila* neurons. Flies expressing two copies of $A\beta_{42}$ in neurons recapitulate

some AD symptoms such as shortened lifespan, locomotor deficits and eye degenerative phenotypes (Figure 1.3). Moreover, this Aβ-expressing model develops amyloid plaques (Casas-Tinto et al., 2011). D42-Gal4 is restricted to expression in motor neurons and Mef2-Gal4 is limited to expression in muscles. Larvae expressing $A\beta_{42}$ in either motor neurons or muscles display severe morphological defects in motor neurons (Mhatre et al., 2014). As single neurons are distinguishable in larvae muscles, *Drosophila* larvae are the alternative choice for unraveling neurodegeneration during AD progression.

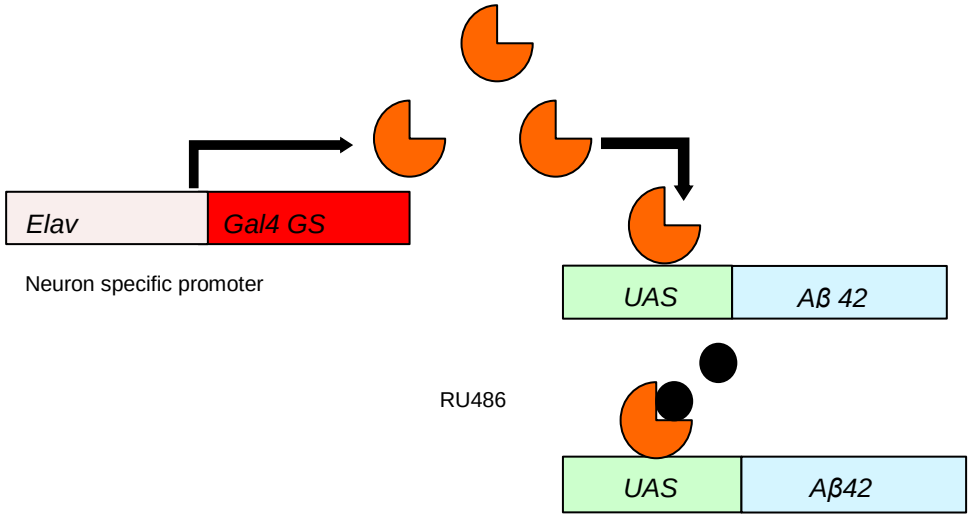

Figure 1.3 Schematic of the Gal4/UAS binary expression system. In the absence of the chemical RU486, the transcription factor, Gal4, is inactive. When the chemical RU486 is present in neurons, Gal4 binds to UAS and activates expression of $A\beta_{42}$.

Recently, a novel repressible binary system has been developed, which is utilized by the *Neurospora crassa* for the catabolism of quinic acid, and so named the Q system. It is constituted of two genes (QF and QS). QF is a transcriptional activator that binds to an enhancer termed QUAS. QF activity is repressed by a repressor, QS. This block is removed by quinic acid (Potter et al., 2010).

The first *Drosophila* model of neurodegenerative diseases using the Q system is established by Pearce and colleagues (Pearce et al., 2015). In this model, the constitutive Q system is used to express the huntingtin protein. Subsequent work established the *Drosophila* model of AD using the inducible Q system. This model displays shortened lifespan (Niccoli et al., 2016). In my study, I used this inducible AD model. Briefly, QUAS was fused with $A\beta_{arc}$ and expressed

in neurons under the control of syt-QF (Syt-QF is a pan-neuronal driver), while modifier genes are expressed in glia by a glial specific driver GSG3285-GS. The combination of the Q system and the Gal4/UAS system makes it possible to investigate the communication between neurons and glia. These two systems also allow for the restricting of $A\beta_{arc}$ expression in neurons and the expression of modifiers in glial cells.

Aside from these widely used models of AD, several novel AD models have emerged such as zebrafish, *C. elegans* and yeast (Boyd-Kimball et al., 2006; Treusch et al., 2011). Each model has significant strengths and weaknesses. For example, yeast is easy to perform genetic screens on. However, yeast does not have neurons and therefore lacks most AD phenotypes. Zebrafish is a vertebrate model which is easy to track protein localization in due to its transparency. However, the current zebrafish model does not recapitulate AD phenotypes. In summary, a combination of different animal models will be the best approach for AD research.

1.4.3 Genetic screens in neurodegenerative diseases

Due to the limited availability of human samples and the need for experimental analysis of mechanisms, animal models are indispensable for disease research. The success of model organisms such as *Drosophila* is in part linked to the power of its genetic screens. Genetic screens were first applied to identify dozens of molecular pathways during *Drosophila* development. This allows genetic screens to become a powerful tool to elucidate gene function and gene networks in various organisms, from human cells to mice.

Forward genetic screens are used to determine the gene responsible for a phenotype. These screens are conducted using mutagens such as UV radiation to induce mutations. However, UV radiation has a disadvantage of deleting multiple loci, and it is hence difficult to map the resulting mutations. Many mutagenesis programmes have instead been conducted with chemicals such as EMS (Nusslein-Volhard and Wieschaus, 1980; Nusslein-Volhard et al., 1984). EMS has many merits. First, this method is the most efficient. It induces mutations every 1 to 2 Mb. Second, it induces point mutations. Finally, EMS targets spermatogonial stem

cells, allowing mutations to be passed onto offspring. However, it is still very laborious to map and identify the mutations resulting from chemical mutagenesis (Berger et al., 2001; Martin et al., 2001). To overcome this problem, insertional mutagenesis has become a favored method. Insertional mutagenesis induces mutations by insertion of mobile genetic elements into the genome, and often is carried out using a P-element as the mutagen. The P-element inserts into its hotspots to disrupt gene function, and the mutated gene is rapidly and easily identified by inverse PCR methods. Although P-element insertion is much less efficient than EMS-induced mutagenesis, it is still widely used because it is economical and time-saving (Perrimon et al., 1996; Spradling et al., 1999). Unlike forward genetic screens, reverse genetic screens are the strategy to discover the phenotype caused by genetic manipulation. They are also categorized into gain-of-function and loss-of-function screens. In *Drosophila*, gain-of-function screens use P-element to insert a UAS element into the genome. When genes are in proximity of the UAS element, their expression will be affected by UAS activation (Rogge et al., 1991; Rorth et al., 1998). Loss-of-function screens begin with the knockout or knockdown of genes (Olivier et al., 1993; Duchek and Rorth, 2001; Duchek et al., 2001). Because the knockout of essential genes is lethal, the large-scale knockdown of genes by RNAi is the most frequently used type of reverse genetic screens (Fraser et al., 2000; Gonczy et al., 2000).

RNA interference emerges as a potent, specific and ubiquitous means of gene silencing, which is characterized by base-pairing to target mRNA and thus post-transcriptionally regulating protein synthesis. In general, RNAi includes microRNAs (miRNAs), small interfering RNAs (siRNAs) and PIWI-interacting RNAs (piRNAs) pathways (Lee et al., 1993; Reinhart et al., 2000). Among them, miRNA pathways rely on two principal regulations: miRNA-mediated repression of translation (Olsen and Ambros, 1999; Seggerson et al., 2002) and mRNA deadenylation that leads to mRNA decay (Behm-Ansmant et al., 2006; Eulalio et al., 2009; Eulalio et al., 2007; Giraldez et al., 2006; Piao et al., 2010; Rehwinkel et al., 2005; Wu et al., 2006), while siRNA pathways cause transcript degradation (Fire et al., 1998).

With respect to screen measurements, genetic screens can also be categorised into simple

screens, modifier screens, complementation screens and clonal screens (synthetic lethal screens). Simple screens aim to identify genes involved with a given phenotype, while in modifier screens, a phenotype is defined by genetic defects, and the modifier screen aims at finding second-site mutations that either enhance or suppress that phenotype (Olivier et al., 1993; Rogge et al., 1991). Notably, Cao's work is a typical modifier screen, which identifies enhancers and suppressors of $A\beta_{42}$ toxicity (Cao et al., 2008). Similar to modifier screens, complementation screens are designed to reveal genes to restore phenotypical defects. In order to detect function of essential genes, clonal screens were developed by Tian and Rubin (1993). The principle of clonal screen is to use the Flp/FRT system to generate site-specific recombination in a given tissue. Flp is a recombinase from the yeast that targets the FRT sites. In the Flp/FRT screen, Flp and FRT are integrated into *Drosophila* genome. When Flp is placed under the control of a tissue-specific promoter, its mediated recombination is restricted to a specific tissue, thus potentially circumventing the lethality caused by constitutive knock-out in the whole body (Golic and Lindquist, 1989; Xu et al., 1995b).

In neuroscience research, *Drosophila* genetic screens are commonly dependent on morphological screens and behavioral screens. As flies have small bodies, morphological changes are usually not visible to the naked eye. Therefore, a microscope is required to observe subtle phenotypes, such as the REP of *Drosophila*. In some cases, phenotypes like larval brain size are not clearly detectable under a dissecting microscope, but they are easily detected with the help of fluorescence reporters. Green fluorescence protein (GFP) is the most commonly used fluorescence reporter that is fused to a protein. Changes in GFP intensity or localization of a specific protein serve as readout (Brenman et al., 2001; Gao et al., 1999; Gao et al., 2000). This method is also useful in screens using transparent animal models like cells, worms and zebrafish. Behavioral analysis is the main method to dissect genetic pathways underlying animal behaviors. They are usually facilitated by video recording, like the sleep/wake activities of zebrafish, the locomotion and flight of flies and the resistant movements of worms (Burchell et al., 2013; Denzel et al., 2014; Rihel et al., 2010; Tufi et al., 2014). In summary, genetic screens are an efficient method to discover unknown genes and their functions.

In terms of research on neurodegenerative diseases, *Drosophila* is a powerful model for high-throughput screening for an abundance of causative or therapeutic targets. Both forward and reverse methods are easily applied to *Drosophila* screens. The rough eye phenotype (REP) of *Drosophila* is a detectable phenotype during neurodegeneration, which is widely used to identify unappreciated modifiers of neurodegenerative diseases such as Huntington's disease (HD), AD, Amyotrophic lateral sclerosis (ALS) and Spinocerrebellar ataxia (SCA) (Kim et al., 2014; Lasagna-Reeves et al., 2016; Lu et al., 2013; Park et al., 2013). However, the novel identified genetic targets for disease intervention in *Drosophila* are required to be confirmed by subsequent mammalian studies (Yamamoto et al., 2014). *Drosophila* eye screening was first applied to seek modifiers of $A\beta_{42}$ toxicity in 2008 (Cao et al., 2008). However, in this study, firstly, the authors used constitutive knockout flies, which cannot limit gene silencing in eyes and led to numerous lethality. Secondly, they only screened about 2000 mutants, which covered a small amount of the *Drosophila* genome. Thirdly, they did not use other measurements to confirm the reliability of their screens. Therefore, my collaborators and I intended to screen 7593 strains corresponding to 7025 genes using a RNAi library of flies and validated the efficiency of *Drosophila* eye screening in identification of modifiers of $A\beta_{42}$ toxicity.

1.4.3 Aims of work

The aim of this work is to investigate candidate modifiers of Aβ toxicity from GWAS and from a *Drosophila* screen.

In terms of chapter 3 and 4, although GWAS studies have implicated PICALM and BIN1 in AD pathology, little is known about their contributions to Aβ pathology *in vivo*. My work aimed to uncover the roles of the *Drosophila* homologues of PICALM and BIN1, *lap* and *Amph* respectively, in Aβ pathology. Furthermore, my work explored the molecular mechanisms underlying the contributions of *lap* and *Amph* to Aβ pathogenesis.

With regard to chapter 5, *Drosophila* is a powerful model system for rapidly screening therapeutic targets in neurodegenerative diseases. However, only one prior study applied this to AD research. As this study has several disadvantages, my collaborators and I performed a

genome-wide screen using a *Drosophila* model of AD and aimed to identify novel genetic targets for AD treatment.

2. Methods

2.1 Fly strains

The following fly strains were obtained from the Bloomington *Drosophila* Stock Center: w^{1118}, w^{Dah}, all UAS-Rab stocks, all UAS lines, unless otherwise stated, UAS-Amph, lap RNAi line (TRiP.HMS01939), nSyb-QF2, tubulin-QS (tub-QS), D42-Gal4, Mef2-Gal4 and GSG3285-GS. Other stains: Elav-GS was derived from the original elavGS 301.2 line (Osterwalder et al., 2001) that was kindly given by Dr. H. Tricoire (CNRS); the UAS-$A\beta_{42}$ stock was gifted from Dr. P. Fernandez-Funez (University of Minnesota, Twin Cities, USA); the UAS-cindr line was gifted from Dr. H. Stenmark (University of Oslo, Oslo, Norway). The UAS-lap line was generated by me. The QUAS-$A\beta_{arc}$ line was generated by Dr. T. Niccoli. The UAS-Rab8-HA and UAS-Rab11-HA were obtained from the FlyORF. The Amph RNAi (v9264) line and all RNAi lines in chapter 5 were obtained from the Vienna *Drosophila* RNAi Center.

As flies with different genetic backgrounds exhibit nonspecific mutations, all transgenic flies are required to backcross with the w^{Dah} stock to guarantee that all transgenic lines have uniform genetic backgrounds unless stated. The wild-type white Dahomey (w^{Dah}) has been captured and maintained in the laboratory since 1970 in population cages with overlapping generations. This method of culture keeps the flies outbred and avoids the large reductions in lifespan that happens with the methods of fly culture generally used in laboratories. Backcrossing ensures that any difference between the mutant and control flies are only attributable to the expression of the transgene alone rather than any mutation present in the genetic background (Partridge and Gems, 2007). In order to attain this goal, all stocks are necessarily backcrossed at least six generations.

2.2 Fly husbandry and culture

All stocks were maintained at 18˚C while experimental flies were grown at 25˚C and 65% humidity. They were all raised on a 12:12 light: dark cycle and on a standard sugar/yeast (SY) medium. The standard SY medium was made by dissolving 15 g agar in 700 ml distilled water

and heating the medium until boiling. Then 100 g of autolysed yeast powder and 50 g of sugar were added and the medium was boiled again. After this additional 170 ml of distilled water were added into the medium that was left to cool down. When temperature of the medium reached under 60 ˚C, 30 ml of nipagin (100 g/L) and 3 ml propionic acid (both were anti-fungal preservatives) were added. Finally, the medium was dispensed (4 ml per vial) into plastic vials and allowed to be left at room temperature overnight before storing at 4 ˚C (Bass et al., 2007; Burnett et al., 2011).

For induction with mifepristone (RU486), 24–48 hr after eclosion, female flies carrying a heterozygous copy of elavGS and at least one UAS construct were fed SYA medium supplemented with 200 mM mifepristone (RU486) to induce transgene expression. For induction with quinic acid (QA), flies were put on food containing 7.5 g of QA per liter. This allows for $A\beta_{arc}$ expression.

2.3 Lifespan analysis

It is necessary for a lifespan analysis to ensure that all flies are born at the same time. For this reason, a prevalent lifespan analysis was to allow parental flies to lay eggs less than 24 hours on grape juice plates with yeast paste. The grape juice plates are made as follows: 25 g agar was dissolved in 500 ml distilled water and boiled. Next 300 ml of red grape juice were added and the mixture was heated again. After adding additional 50 ml of distilled water, the medium was cooled to below 60 ˚C. To avoid bacterial infection, 21 ml of nipagin (100g/L) were added. Eventually, the medium was dispensed into plastic petri dishes and allowed to set at room temperature before storing at 4 ˚C.

The eggs collected from the plates were washed with phosphate buffered saline (PBS) solution and transferred into falcon tubes. The eggs were washed for several times and then 20 µl of egg suspension was dispensed into 200 ml glass bottles containing 70 ml SY food (~300 eggs per bottle). After eclosion, adults were allowed to mate for 24–48 h. Finally, these flies were separated into 10 vials (15 flies per vial). For each genotype and/or experimental condition, 10 vials were set up, equaling to 150 flies per genotype/condition. Importantly, flies

were tipped to fresh vials of SY food three times a week throughout life. The number of dead flies found during each tipping was recorded and accidental escapees were censored from the experiment. Data were presented as cumulative survival curves using the Kaplan-Meier method, and survival rates were compared between different genotypes or experimental conditions using log-rank tests.

2.4 Negative geotaxis assay

The locomotor age-related decline is a hallmark of the dysfunctional capacity of flies (Gargano et al., 2005; Jones et al., 2009). It was assessed with a negative geotaxis assay. As described in a previous article (Niccoli et al., 2016), 45 flies were placed in a glass walled chamber 25 cm tall (at least 3 replicates per genotype and/or experimental condition). The chamber was divided into the top 5 cm, center 15 cm, and bottom 5 cm. After a recovery of flies for 20 min, the chamber was disposed vertically and flies were gently tapped down to the bottom. Then flies were free to climb up and their numbers at the top, middle or bottom were scored after 20 sec. Data were presented as a cumulative graph and a performance index (PI) was calculated for each time point and plotted using a formula below. Statistical analysis was evaluated by two-ways ANOVA followed by Tukey *post-hoc* test.

$$\mathrm{PI} = \frac{0.5 * [\mathrm{Number(top)} + \mathrm{Number(middle)} + \mathrm{Number(bottom)} + \mathrm{Number(top)} - \mathrm{Number(bottom)}]}{\mathrm{Number(top)} + \mathrm{Number(middle)} + \mathrm{Number(bottom)}}$$

2.5 Generation of transgenic line

To generate a UAS-lap transgenic line, a 1.4 kb DNA fragment containing the lap A isoform was amplified by PCR using primers CACCATGACCATGGCAGGG and TTACTGTGCGGCGCCG, gateway cloned into an entry vector and transferred into a pUAST vector that was achieved. The UAS-lap construct was transformed into the w^{1118} background. This transgene was inserted on chromosome 2 in the attP40 site. The expression of lap was confirmed by qPCR and western blotting. To ensure a homogeneous genetic background between transgenic lines, UAS-lap was backcrossed to the W^{Dah} stock for six generations. All experiments were carried out on mated females, unless otherwise stated.

2.6 Quantitative PCR

Total RNA was extracted from 20-25 fly heads per sample using TRIzol (GIBCO) according to the manufacturer's instructions. The concentration of total RNA purified for each sample was measured using an Eppendorf biophotometer. One microgram of total RNA was then subjected to DNA digestion using DNase I (Ambion), immediately followed by reverse transcription using the SuperScript II system (Invitrogen) with oligo(dT) primers. Quantitative PCR was performed using the PRISM 7000 sequence-detection system (Applied Biosystems) and SYBR Green (Molecular Probes) by following the manufacturer's instructions. Each sample was analyzed in duplicate and values were presented as the mean of three-four independent biological repeats ± SEM. Primers used were:

lap GCACTTGGACTATTTGGTGCAC + GCATAAATCGCTCTTGCCATATG

eIF1A ATCAGCTCCGAGGATGACGC + GCCGAGACAGACGTTCCAGA

2.7 Co-immunoprecipitation

Adult fly heads were isolated from W^{Dah} flies. 40 fly heads were cut off with scissors. The heads were transferred to a 1.5-mL Eppendorf tube and homogenized in 600 µL of lysis buffer [50 mM Tris (pH 7.5), 150 mM NaCl, 0.5% NP-40 (v/v), 0.1 mM $MgCl_2$, 0.1 mM Na_3VO_4, 5 mM NEM, 1:10 dilution of protease inhibitor cocktail (Roche, P8340), 1:100 dilution of phosphatase inhibitor cocktail 2 (Sigma) and 1 mM phenylmethylsulfonyl fluoride (PMSF)] and spun at 13000 rpm (17,949 × g) for 15 min at 4°C. 50 µL of the supernatant was taken for input, while 200 uL of the remaining supernatant was subjected to IP. The lysates were precleared with 10 uL of protein G dynabeads (Life Technologies, 10004D) for 10 min at 4°C. 50 uL of the same beads were crosslinked with anti-PICALM antibody by 20 mM DMP (dissolved in 0.2 M triethanolamine) followed by incubation with the precleared lysates for 1h at 4°C. Anti-PICALM beads were collected by a magnetic stand and 200 µL of supernatant was removed with a narrow-end pipette. The beads were washed for five times with 1 mL PBS with 0.5% BSA (PBSB). Elution of the immuneprecipitated proteins were performed by heating beads at 70°C for 5 min with 20 uL 2x SDS sample buffer and 200 mM DTT. The immunoprecipitated proteins and beads were magnetically separated and the IP fraction was saved. Input and supernatant

were diluted in 2x SDS sample buffer to a 1× final concentration with 200 mM DTT.

2.8 Western blotting

15 fly heads were flash frozen in liquid nitrogen, vortexed and separated through a small sieve (no. 25, 710 µm, Precision Eforming, LLC). Protein samples were prepared by homogenizing in 2x SDS Laemmli sample buffer [4% SDS, 20% glycerol, 120 mM Tris-HCl (pH 6.8), 200 mM DTT with bromophenol blue] and boiled at 95°C for 10 min. Samples were separated on pre-cast 4%–12% Invitrogen Bis-Tris gels (NP0322) or customized 10% Bis-Tris gels. Then samples were blotted onto PVDF (for Atg8 and Grp78) or nitrocellulose membrane (for PICALM and VGlut) in Tris-glycine buffer supplemented with 20% methanol. Membranes were blocked in 5% milk in TBST (Tris-buffered saline with 0.1% Tween-20) for 1 hr at room temperature (RT) and then incubated with primary antibodies overnight at 4°C or 1 hr at RT (for Grp78). Primary antibody dilutions used were as follows: anti-PICALM, 1:3,000 (Abcam, ab127551); anti-Actin, 1:10,000 (Abcam, ab1801); anti-Atg8, 1:1,000 and anti-VGlut, 1:10,000 (a gift from Dr A. DiAntonio, Washington University, St. Louis). Secondary antibodies used were anti-rabbit and anti-mouse HRP (Abcam, ab6789 and ab6721) at 1:10,000 dilutions for 1 hr at RT. Bands were visualized with Luminata Forte (Millipore) and imaged with ImageQuant LAS4000 (GE Healthcare Life Sciences). Quantification was carried out with ImageQuant software.

2.9 $A\beta_{42}$ ELISA

Five fly heads were homogenized in 50 ml GnHCl extraction buffer [5 M guanidinium HCl, 50 mM HEPES (pH 7.3), 1:10 dilution of protease inhibitor cocktail (Roche, P8340), and 5 mM EDTA) and centrifuged at 21,000 x g for 5 min at 4 °C. The cleared supernatant was retained as the total fly $A\beta_{42}$ sample. $A\beta_{42}$ levels were measured with an ELISA kit (Thermal Fisher, KHB3441), according to the manufacturer's instructions, and total protein levels were measured with a Bradford assay (Bio-Rad protein assay reagent). The amount of $A\beta_{42}$ in each sample was expressed as a ratio of the total protein content (pictograms per microgram of total protein). Data are expressed as the mean ± SEM obtained from three biological repeats for

each genotype.

2.10 Immunohistochemistry

Wandering third-instar larvae were dissected in HL3 solution and fixed in Bouin's fixative (for VGlut and GluRII) or 4% PFA (for Amph) for 20 min. Larvae were then rinsed in PBS with 0.2% Triton-100 (PBST) and blocked in 5% BSA in PBST for 1 hr at RT. Larvae were then incubated with primary antibodies overnight at 4°C and washed in PBST three times. Primary antibody dilutions used were as follows: anti-GluRIIA, 1:100 (8B4D2 obtained from the Developmental Studies Hybridoma Bank, University of Lowa, Lowa City, IA); anti-VGlut, 1:10,000; anti-GluRIIB, 1:2500; anti-GluRIIC, 1: 1000 (a gift from Dr A. DiAntonio, Washington University, St. Louis) and anti-Amph, 1: 2500 (a gift from Dr A. Zelhof, Indiana University, Bloomington). Secondary antibodies were anti-HRP, 1:200 (Jackson ImmunoResearch, West Grove, PA); anti-rabbit Alexa Fluor 568, 1:1000 (Thermal Fisher, A11036) and anti-mouse Alexa Fluor 568, 1:1000 (Thermal Fisher, A11019), which were incubated for 1 hr at RT. After washing, larvae were mounted in Vectashield (Vector Laboratories, Burlingame, CA).

All images were acquired using a Zeiss LSM700 inverted confocal microscope, with the 63x objective. The images were shown as maximum intensity projections of the complete Z-stack. The 10 µm of stacks were taken from muscles 7 and 6 of segments A2-A4. All images for one experiment were taken at the same microscopy settings. The mean fluorescence intensity of each slice of the NMJ was measured with ImageJ. Values shown were the averages for 5–10 NMJ ± SEM. Samples were compared by one-way ANOVA followed by Tukey's *post hoc* test.

2.11 Live imaging

Heterozygous D42-Gal4 > UAS-iGluSnFR L2 larvae were prepared for live imaging essentially as described and imaged on a Zeiss LSM880 airyscan confocal microscope, with the 40x objective. We immobilized larvae by gently squeezing them under a cover glass in halocarbon oil. Images were collected at a rate of 1 frame/s. A single plane was taken from the ventral nerve cord (VNC). All images for one experiment were taken at the same microscopy settings.

Imaged iGluSnFR fluorescence intensity was used to calculate spontaneous activity as the fractional change in fluorescence intensity and reported as % $\Delta F/F_0$. F_0 is the minimum fluorescence intensity. For each animal only one trial was collected. We imaged one plane of focus per animal and drew one ROI to quantify the magnitude of signal fluctuation at each pixel over time. Each ROI displayed a local and transient increase in the fluorescence intensity. The same size of ROI was analyzed in each field of view. We set the baseline of measurements to 0. All images for one experiment were taken at the same microscopy settings. Values shown were the averages for 5 VNC ± SEM. Samples were compared by one-way ANOVA followed by Tukey's *post hoc* test.

2.12 Statistical analysis

Data were presented as means +SEM. Comparisons were performed using Student's t-test (for two groups), one-way ANOVA followed by Turkey *post-hoc* test (for more than two groups), or two-way ANOVA followed by Turkey *post-hoc* test (for groups across two variables, with multiple comparisons between individual groups). All comparison tests were two-tailed. Results with $p < 0.05$ were considered significant.

3. PICALM reduces $A\beta_{42}$ toxicity by modulating glutamate transmission

3.1 Background

Genome-wide association studies (GWAS) are a powerful tool to identify numerous unknown genetic variants to AD. One of these mutations has been linked to PICALM (phosphatidylinositol-binding clathrin assembly protein), which is involved in clathrin-dependent endocytosis (Harold et al., 2009; Lambert et al., 2013). PICALM is a brain-specific adaptor in humans, and is involved in cargo selection (Tian et al., 2013). It physically binds to soluble NSF (N-ethylmaleimide-sensitive factor) attachment protein receptors (SNAREs) like VAMP2, VAMP8, RAB5, RAB11 to guide synaptic vesicles (SV) from the plasma membrane into endosomes (Koo et al., 2015; Koo et al., 2011; Moreau et al., 2014; Zhao et al., 2015b). PICALM expression is decreased in brain samples of AD patients (Ando et al., 2013; Parikh et al., 2014). However, the role of PICALM in Alzheimer's disease remains controversial. On one hand, PICALM knockdown reduces $A\beta_{42}$ generation by limiting APP or γ-secretase internalization and promotes tau degradation by triggering autophagy (Kanatsu et al., 2014; Moreau et al., 2014; Xiao et al., 2012; Yu et al., 2010). On the other hand, PICALM over-expression modulates APP degradation via elevated autophagy and $A\beta_{42}$ clearance through transcytosis (Tian et al., 2013b; Zhao et al., 2015b). Although several studies have implicated PICALM in $A\beta_{42}$ production and turn-over (Xiao et al., 2012), little is known about its contribution to the development of AD pathology downstream of Aβ production.

PICALM-mediated endocytosis regulates the cell surface expression of proteins and controls protein internalization. Its cargos include the vesicular glutamate transporters (VGlut). Glutamate excitotoxicity has long been speculated to play an important role in AD development (Abramov et al., 2009; Hynd et al., 2004). Glutamate uptake and release are changed in Alzheimer's disease, giving rise to excess extracellular glutamate (Cummings et al., 2015; Hefendehl et al., 2016; Li et al., 2009; Talantova et al., 2013).

Here I demonstrated that overexpression of the *Drosophila* PICALM orthologue, *lap*, alleviated $A\beta_{42}$-induced shortened lifespan and locomotor defects in a *Drosophila* AD model without affecting $A\beta_{42}$ levels. I then demonstrated that Aβ expression led to the accumulation of vesicular glutamate transporters (VGlut) near the presynaptic active zone. *Lap* directly interacted with VGlut and reduced its accumulation back to control levels. Aβ expression also elevated glutamate release, while *lap* expression reduced this excessive glutamate release. Therefore, I identified a novel mechanism by which *lap* could modulate aberrant glutamatergic transmission in Alzheimer's disease, and possibly affect disease development.

3.2 Results

3.2.1 *Lap* reduces $A\beta_{42}$ toxicity

To explore the role of *PICALM in vivo*, I looked at the role that the *Drosophila* homologue, *lap*, played in the development of Aβ pathology in *Drosophila.* I used an adult onset model of Aβ toxicity expressing two copies of wild type $A\beta_{42}$ (Casas-Tinto et al., 2011) under the control of an inducible pan-neuronal driver (elav-GS). Elav-GS is only induced in the presence of the drug RU486 (Osterwalder et al., 2001), which I fed to the flies only after eclosion. This restricted expression of Aβ to adult, post-mitotic neurons (Figure 1.2). In all cases these $A\beta_{42}$-expressing flies have a shortened lifespan (compared to the Aβ RU0 condition, the Aβ RU200 condition had 42% mean lifespan) and display locomotor deficits from day 14 onwards (Figure 3.1), suggesting that wild type $A\beta_{42}$ is toxic to adult neurons. Moreover, I generated the UAS-lap line and this line showed a marked increase in *lap* expression (Figure 3.1A, relative to eIF1A; elavGS > lap RU0: 100 $\pm$ 13.59 %, n = 3; elavGS > lap RU200: 256.8 $\pm$ 7.14 %, n = 3. $p < 0.01$, Student's *t-test*). eIF1A is used as a reference gene for our experiments since it showed the least fluctuation in our Aβ expressing flies when tested together with a panel of reference genes (Ling and Salvaterra, 2011; Niccoli et al., 2016). I found that co-overexpression of *lap* attenuated $A\beta_{42}$ toxicity. Comparing to $A\beta_{42}$ expression, co-expression of $A\beta_{42}$ and *lap* led to lifespan extension of 12% (Figure 3.1B, mean lifespan, Aβ RU0: 100 %; Aβ RU200: 42 %; Aβ lap RU0: 100 %; Aβ lap RU200: 47 %, n > 120 per condition. p was shown in Figure 3.1B, log-rank test) and a small but significant improvement in

locomotor performance (Figure 3.1C and Table 3.1, PI, day 7, Aβ RU0: 89.67 ± 0.36 %; Aβ RU200: 94.13 ± 1.26 %; Aβ lap RU0: 93.8 ± 0.56 %; Aβ lap RU200: 89.01 ± 0.77 %; day 10, Aβ RU0: 84.27 ± 0.47 %; Aβ RU200: 87.05 ± 0.95 %; Aβ lap RU0: 89.31 ± 2.12 %; Aβ lap RU200: 82.71 ± 0.89 %; day 14, Aβ RU0: 90.77 ± 1.96 %; Aβ RU200: 72.71 ± 0.69 %; Aβ lap RU0: 85.38 ± 3.26 %; Aβ lap RU200: 83.56 ± 2.60 %; day 18, Aβ RU0: 91.07 ± 1.13 %; Aβ RU200: 54.40 ± 2.20 %; Aβ lap RU0: 83.21 ± 0.98 %; Aβ lap RU200: 70.79 ± 3.23 %; day 21, Aβ RU0: 82.20 ± 1.78 %; Aβ RU200: 35.29 ± 4.49 %; Aβ lap RU0: 78.09 ± 4.58 %; Aβ lap RU200: 52.54 ± 2.90 %; day 25, Aβ RU0: 84.80 ± 1.77 %; Aβ RU200: 18.92 ± 0.71 %; Aβ lap RU0: 80.92 ± 1.76 %; Aβ lap RU200: 30.56 ± 1.43 %, n = 3 per condition. Interaction of time and genotype, $p < 0.0001$; time, $p < 0.0001$, genotype, $p < 0.0001$, two-ways ANOVA), without affecting $A\beta_{42}$ levels (Figure 3.1F, Aβ RU0: 4.02 ± 0.01 pg/ug protein; Aβ RU200: 58.54 ± 8.14 pg/ug protein; Aβ lap RU0: 3.01 ± 0.66 pg/ug protein; Aβ lap RU200: 59.57 ± 7.25 pg/ug protein, n = 3 per condition. $p < 0.0001$; one-way ANOVA). In contrast, inhibition of *lap*, using *lap* RNAi, enhanced $A\beta_{42}$ toxicity leading to worsening of the mean lifespan from 43% to 38% (Figure 3.1D, mean lifespan, Aβ RU0: 100 %; Aβ RU200: 42 %; Aβ lap RNAi RU0: 100 %; Aβ lap RNAi RU200: 47 %, n > 120 per condition. p was shown in Figure 3.1D, log-rank test). In this case, I backcrossed the *lap* RNAi line with the $w^{+}v^{-}$ W^{Dah} stock for six generations and then crossed it with the $w^{-}v^{+}$ W^{Dah} stock to remove different genetic backgrounds. However, I still see a difference in lifespan between the uninduced control of Aβ and that of Aβ and *lap* RNAi. As the attP insertion site of Trip lines has no effect on the expression of endogenous genes, I supposed the most likely explanation for the difference between the Aβ RU0 and Aβ lap RU0 condition is therefore RNAi leakage. The RNAi leakage is often observed in the Trip lines and this leakage might lead to that Aβ lap RNAi RU0 group had longer lifespan. Additionally, the effect of RNAi leakage was seen in locomotion because the Aβ RU0 group had better locomotor performance than the Aβ lap RNAi RU0 group. Therefore, although the co-expression of Aβ and *lap* RNAi worsened climbing defects, it is unclear whether inhibition of *lap* affected climbing defects of Aβ-expressing flies (Figure 3.1E and Table 3.2, PI, day 7, Aβ RU0: 89.67 ± 0.36 %; Aβ RU200: 94.13 ± 1.26 %; Aβ lap RNAi RU0: 63.88 ± 4.3 %; Aβ lap RNAi RU200: 44.17 ± 9.1 %; day 10, Aβ RU0: 84.27 ± 0.47 %; Aβ RU200: 87.05 ± 0.95 %; Aβ lap RNAi RU0: 50.56 ± 0.74 %; Aβ lap RNAi RU200: 41.67 ± 0.48 %; day 14, Aβ RU0: 90.77 ±

1.96 %; Aβ RU200: 72.71 ± 0.69 %; Aβ lap RNAi RU0: 50.29 ± 0.74 %; Aβ lap RNAi RU200: 21.94 ± 2 %; day 18, Aβ RU0: 91.07 ± 1.13 %; Aβ RU200: 54.40 ± 2.20 %; Aβ lap RNAi RU0: 43.78 ± 2.79 %; Aβ lap RNAi RU200: 0 ± 0 %; day 21, Aβ RU0: 82.20 ± 1.78 %; Aβ RU200: 35.29 ± 4.49 %; Aβ lap RNAi RU0: 43.72 ± 1.51 %; Aβ lap RNAi RU200: 0 ± 0 %; day 25, Aβ RU0: 84.80 ± 1.77 %; Aβ RU200: 18.92 ± 0.71 %; Aβ lap RNAi RU0: 37.29 ± 3.39 %; Aβ lap RNAi RU200: 0 ± 0 %, n = 3 per condition. interaction of time and genotype, $p < 0.0001$; time, $p < 0.0001$, genotype, $p < 0.0001$, two-ways ANOVA).

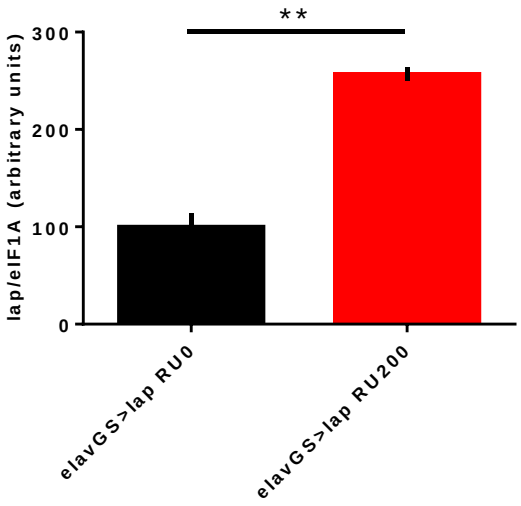

(A)

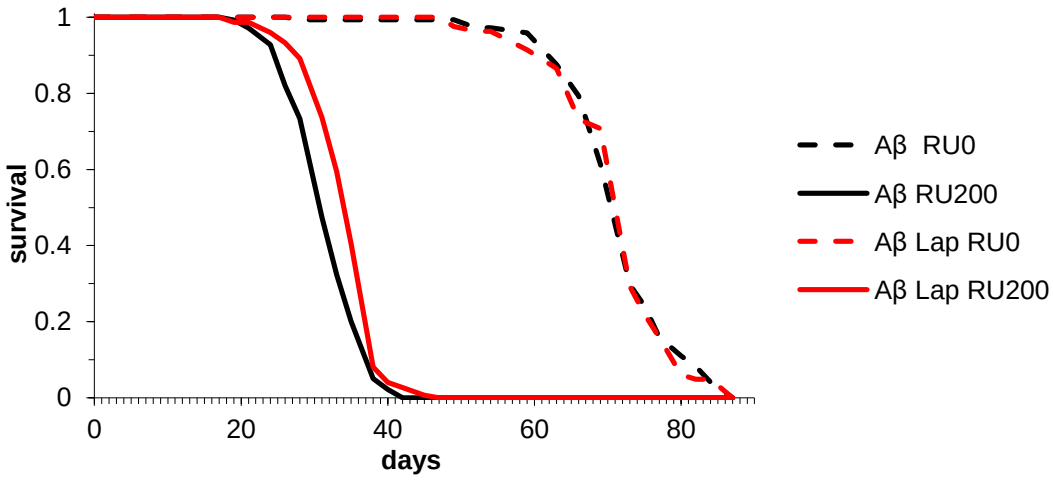

(B)

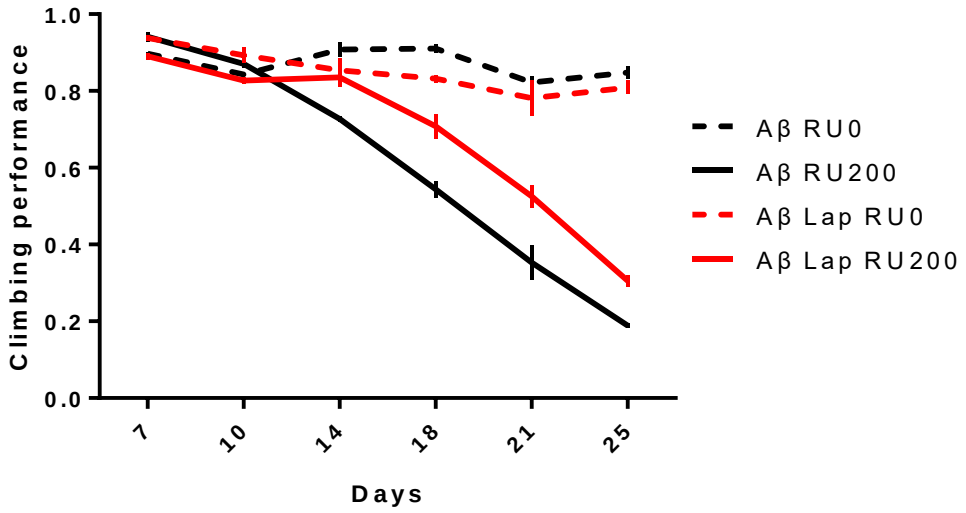
Climbing performance
1.0
0.8
0.6
0.4
0.2
0.0
7
10
14
18
21
25
Days
Aβ RU0
Aβ RU200
Aβ Lap RU0
Aβ Lap RU200

(C)

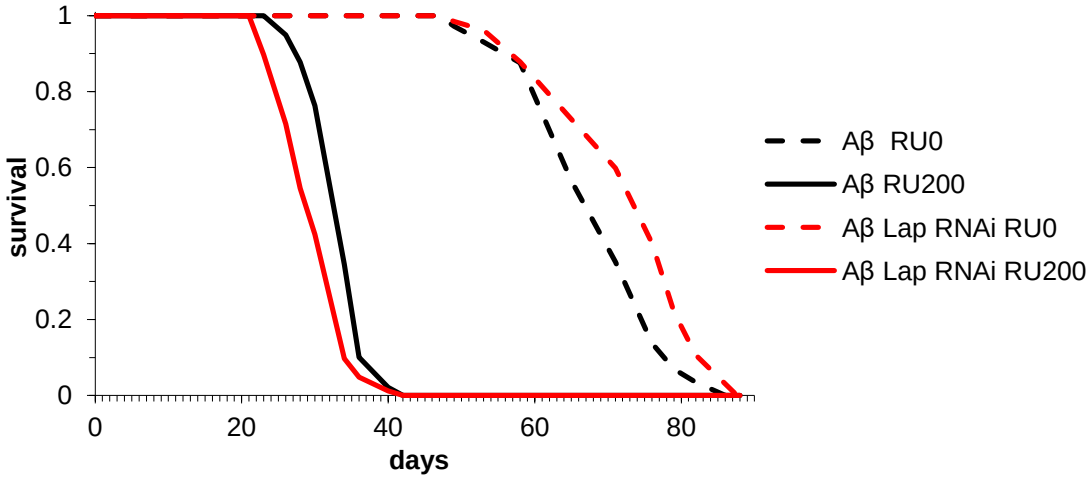
survival
1
0.8
0.6
0.4
0.2
0
0
20
40
60
80
days
Aβ RU0
Aβ RU200
Aβ Lap RNAi RU0
Aβ Lap RNAi RU200

(D)

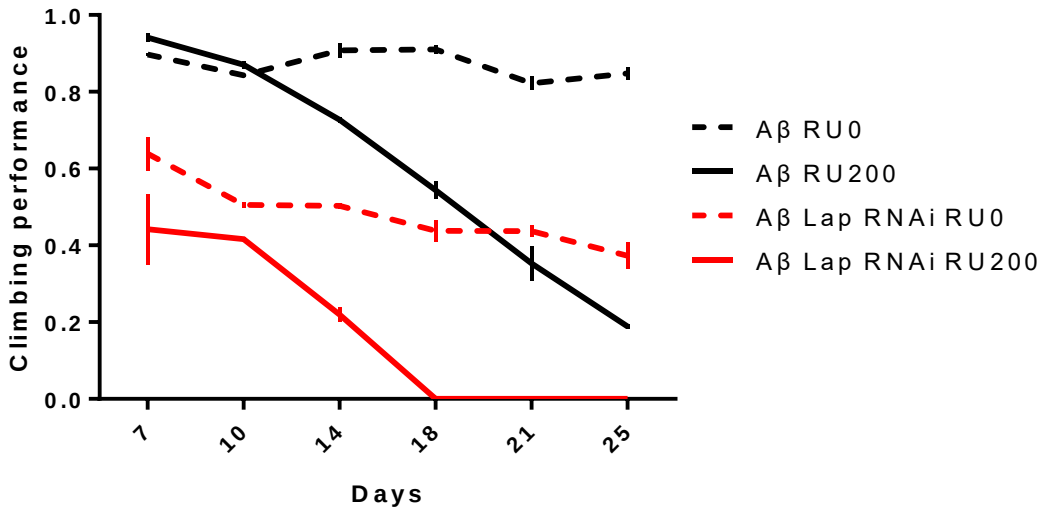
Climbing performance
1.0
0.8
0.6
0.4
0.2
0.0
7
10
14
18
21
25
Days
Aβ RU0
Aβ RU200
Aβ Lap RNAi RU0
Aβ Lap RNAi RU200

(E)

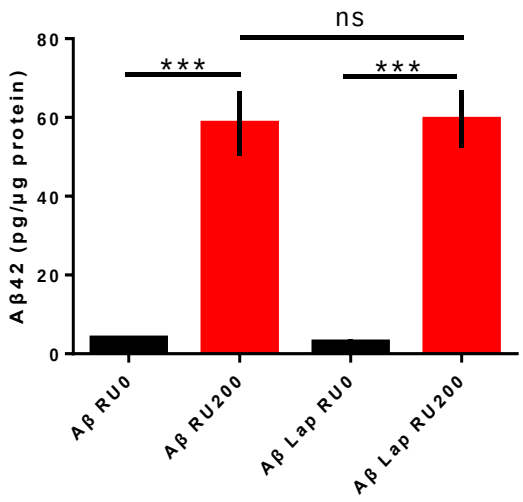

(F)

Figure 3.1 *Lap* alleviates $A\beta_{42}$ toxicity.

(A) *Lap* mRNA levels in heads of 7-day-old flies expressing *lap* (RU200) or not in neurons (RU0), measured by qPCR (relative to eIF1A), plotted as means ± SEM. Genotypes: UAS-lap; elavGS. Statistical significance was determined by Student's t-test, **p < 0.01.

(B) Survival curves of flies expressing Aβ with *lap* or not in adult neurons (RU200) and uninduced controls (RU0). Expression of Aβ in the neurons shortened lifespan, but *lap* expression extended lifespan, n > 120. Aβ RU0 vs Aβ RU200, p < 0.0001; Aβ RU0 vs Aβ lap RU0, n.s., not significant; Aβ lap RU0 vs Aβ lap RU200, p < 0.0001; Aβ RU200 vs Aβ lap RU200, p < 0.0001, determined by log-rank test.

(C) Locomotor performance index of flies of the same genotypes. Aβ caused climbing defects from day 14 onwards, but expression of *lap* resulted in a small but significant improvement in locomotor performance compared to Aβ alone (Aβ RU200 vs Aβ lap RU200), n = 3 (50 animals per condition). Interaction of time and genotype, p < 0.0001; time, p < 0.0001, genotype, p < 0.0001, determined by two-ways ANOVA followed by Tukey's *post-hoc* test. Statistical analyses were shown in Table 3.1

(D) Adult survival of flies harboring Aβ with or without *lap* RNAi in adult neurons (RU200) and uninduced controls (RU0). Inhibition of *lap* reduced longevity of Aβ-expressing flies, n > 120. Aβ RU0 vs Aβ RU200, p < 0.0001; Aβ RU0 vs Aβ lap RU0, p < 0.0001; Aβ lap RU0 vs Aβ lap RU200, p < 0.0001; Aβ RU200 vs Aβ lap RU200, p < 0.0001, determined by log-rank test.

(E) Climbing index of flies of the same genotypes, n = 3 (50 animals per condition). Interaction of time and genotype, p < 0.0001; time, p < 0.0001, genotype, p < 0.0001, determined by two-ways ANOVA followed by Tukey's *post-hoc* test.

Statistical analyses were shown in Table 3.2

(F) $A\beta_{42}$ protein levels, measured by ELISA, in the heads of 21-day-old flies expressing Aβ or Aβ and *lap* in neurons (RU200) and uninduced controls (RU0). Means ± SEM, n = 3. ****p < 0.0001, determined by one way ANOVA; Aβ RU0 vs Aβ RU200, ***p < 0.001; Aβ RU0 vs Aβ lap RU0, n.s., not significant; Aβ lap RU0 vs Aβ lap RU200, ***p < 0.001; Aβ RU200 vs Aβ lap RU200, n.s., not significant, comparison by Tukey's *post-hoc* test.

Table 3.1 Statistical summary of locomotor performance index of flies expressing Aβ with or without *lap*

Day 7	Aβ RU0	Aβ RU200	Aβ lap RU0	Aβ lap RU200
Aβ RU0		n.s.	n.s.	n.s.
Aβ RU200			n.s.	n.s.
Aβ lap RU0				n.s.
Aβ lap RU200				
Day 10	Aβ RU0	Aβ RU200	Aβ lap RU0	Aβ lap RU200
Aβ RU0		n.s.	n.s.	n.s.
Aβ RU200			n.s.	n.s.
Aβ lap RU0				n.s.
Aβ lap RU200				
Day 14	Aβ RU0	Aβ RU200	Aβ lap RU0	Aβ lap RU200
Aβ RU0		< 0.0001	n.s.	n.s.
Aβ RU200			< 0.001	n.s.
Aβ lap RU0				< 0.01
Aβ lap RU200				
Day 18	Aβ RU0	Aβ RU200	Aβ lap RU0	Aβ lap RU200
Aβ RU0		< 0.0001	n.s.	< 0.0001
Aβ RU200			< 0.0001	< 0.0001
Aβ lap RU0				< 0.001
Aβ lap RU200				
Day 21	Aβ RU0	Aβ RU200	Aβ lap RU0	Aβ lap RU200
Aβ RU0		< 0.0001	n.s.	< 0.0001

Aβ RU200			< 0.0001	< 0.0001
Aβ lap RU0				< 0.0001
Aβ lap RU200				
Day 25	Aβ RU0	Aβ RU200	Aβ lap RU0	Aβ lap RU200
Aβ RU0		< 0.0001	n.s.	< 0.0001
Aβ RU200			< 0.0001	< 0.01
Aβ lap RU0				< 0.0001
Aβ lap RU200				

Table 3.2 Statistical summary of locomotor performance index of flies expressing Aβ with or without *lap* RNAi

Day 7	Aβ RU0	Aβ RU200	Aβ lap RNAi RU0	Aβ lap RNAi RU200
Aβ RU0		n.s.	< 0.0001	< 0.0001
Aβ RU200			< 0.0001	< 0.0001
Aβ lap RNAi RU0				< 0.0001
Aβ lap RNAi RU200				
Day 10	Aβ RU0	Aβ RU200	Aβ lap RNAi RU0	Aβ lap RNAi RU200
Aβ RU0		n.s.	< 0.0001	< 0.0001
Aβ RU200			< 0.0001	< 0.0001
Aβ lap RNAi RU0				n.s.
Aβ lap RNAi RU200				
Day 14	Aβ RU0	Aβ RU200	Aβ lap RNAi RU0	Aβ lap RNAi RU200
Aβ RU0		< 0.0001	< 0.0001	< 0.0001
Aβ RU200			< 0.0001	< 0.0001
Aβ lap RNAi RU0				< 0.0001
Aβ lap RNAi RU200				
Day 18	Aβ RU0	Aβ RU200	Aβ lap RNAi RU0	Aβ lap RNAi RU200
Aβ RU0		< 0.0001	< 0.0001	< 0.0001
Aβ RU200			< 0.0001	< 0.0001
Aβ lap RNAi RU0				< 0.0001

Aβ lap RNAi RU200				
Day 21	Aβ RU0	Aβ RU200	Aβ lap RNAi RU0	Aβ lap RNAi RU200
Aβ RU0		< 0.0001	< 0.0001	< 0.0001
Aβ RU200			< 0.0001	< 0.0001
Aβ lap RNAi RU0				< 0.0001
Aβ lap RNAi RU200				
Day 25	Aβ RU0	Aβ RU200	Aβ lap RNAi RU0	Aβ lap RNAi RU200
Aβ RU0		< 0.0001	< 0.0001	< 0.0001
Aβ RU200			< 0.0001	< 0.0001
Aβ lap RNAi RU0				< 0.0001
Aβ lap RNAi RU200				

3.2.2 *Lap* regulates longevity

As PICALM has been suggested to influence ageing (Piaceri et al., 2011; Ponomareva et al., 2017), I analyzed the effect of *lap* on ageing, I over-expressed and down-regulated *lap* in *Drosophila* neurons through feeding RU486. Until now, addition of RU486 has not been found to affect lifespan in previous studies, but there is a possible concern. Here I found that *lap* over-expression shortened lifespan of 9% (Figure 3.2A, elavGS > lap RU0: 100 %; elavGS > lap RU200: 90 %, n > 120 per condition. $p < 0.0001$, log-rank test), while *lap* RNAi extended lifespan of 9%. This indicated that the inhibition of *lap* expression was neuroprotective in ageing (Figure 3.2B, elavGS > lap RNAi RU0: 100 %; elavGS > lap RNAi RU200: 110 %, n > 120 per condition. $p < 0.0001$, log-rank test). So the neuroprotective effect of *lap* over-expression was specific to Aβ toxicity and not due to a broader effect on ageing. As glutamate neurotransmission declines with age (Segovia et al., 2001), it is possible that increased glutamate transmission, probably associated with downregulation of *lap*, might be crucial in delaying ageing. I did not investigate the effect of *lap* alone on locomotor performance, so I merely concluded that, from lifespan analysis, the benefit of *lap* is dependent on modulating Aβ toxicity. Collectively, my data is in supports that *lap* over-expression attenuates Aβ-induced phenotypes observed.

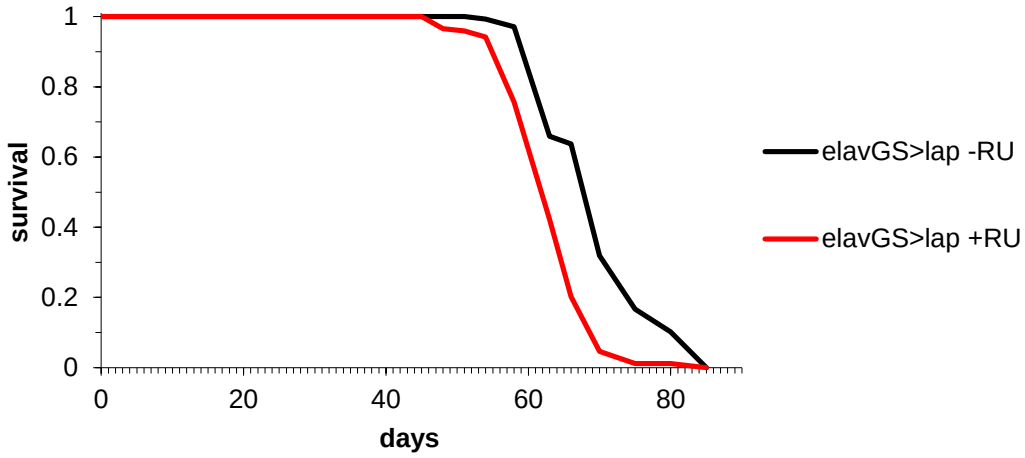

(A)

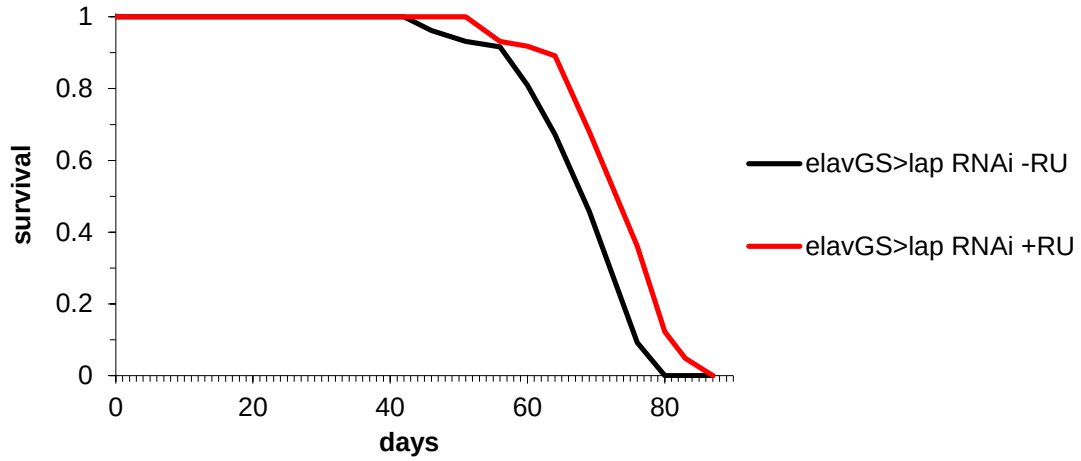

(B)

Figure 3.2 Inhibition of *lap* in neurons increases longevity. (A-B) Adult survival curves of *lap* over-expressing or *lap* RNAi flies in adult neurons (+RU) and uninduced controls (-RU), n > 120. p < 0.0001, by log-rank test.

3.2.3 *Lap* does not alter UPR and autophagy

I sought to uncover the molecular mechanism by which *lap* reduced $A\beta_{42}$ toxicity. Aβ has been reported to impair autophagy, UPR and proteostasis (Niccoli et al., 2016). I first investigated whether Aβ affected autophagy, as assayed by Atg8. Atg8 is the *Drosophila* homologue of LC3. There are two forms of Atg8: Atg8-I is a 13.6 kD protein and Atg8-II is a ~12 kD protein. During autophagosome formation, cytosolic Atg8-I is converted to membrane-bound Atg8-II. As Atg8-II is an active form of autophagy, an increase in the ratio of Atg8-II/Atg8-I is an indicator of

autophagic induction (Kabeya et al., 2000; Mizushima et al., 1998). The ratio of Atg8-II/Atg8-I was not altered upon Aβ expression, indicating that autophagy activity was not impaired in the $Aβ_{42}$-expressing flies (Figure 3.3A). In a previous study (Moreau et al., 2014), *lap* was shown to be a negative regulator of Atg8-II expression. However, I did not find that *lap* expression altered Atg8-II levels (Figure 3.3A, Aβ RU0: 100 ± 20.63 %; Aβ RU200: 83.58 ± 11.54 %; Aβ lap RU0: 98.11 ± 8.07 %; Aβ lap RU200: 101.5 ± 1.11 %, n = 3 per condition. $p > 0.05$, one-way ANOVA).

Next, I analyzed the influence of Aβ expression on the UPR. BiP (Grp78) is a negative regulator of the UPR. Its expression has been found to elevate upon Aβ expression, indicating UPR activity is increased upon Aβ expression (Ma et al., 2013b; (Niccoli et al., 2016). Unexpectedly, BiP levels were down-regulated in my $Aβ_{42}$-expressing flies and this was not reversed back upon *lap* expression (Figure 3.3B, Aβ RU0: 100 ± 13.93 %; Aβ RU200: 45.62 ± 5.74 %; Aβ lap RU0: 102.4 ± 23.74 %; Aβ lap RU200: 46.10 ± 6.13 %, n = 3 per condition. $p < 0.001$, one-way ANOVA). Therefore, my results found that Aβ expression inhibited BiP expression. However, a reduction in BiP protein could lift the block of UPR inhibition and therefore induce UPR activation through a negative feedback. So it is not a good marker of UPR activity. It is still unknown that UPR is activated or inhibited upon Aβ expression. My results merely showed that the neuroprotective effect of *lap* was independent of UPR activity.

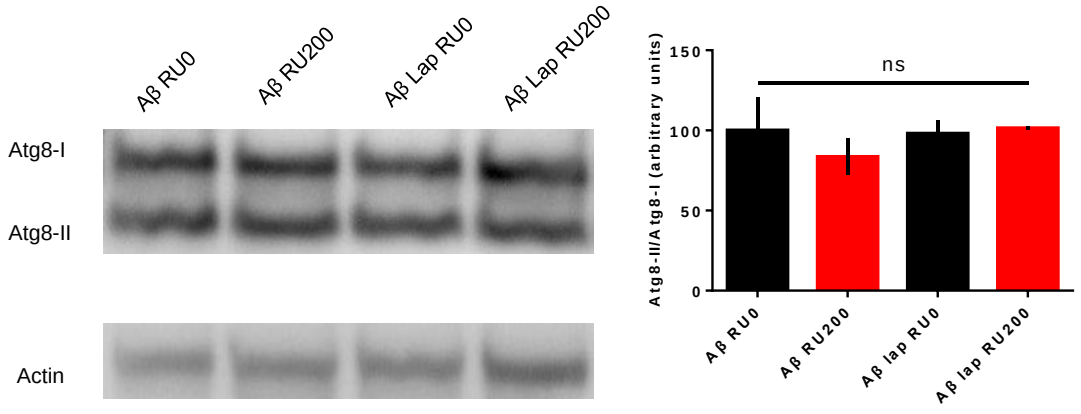

(A)

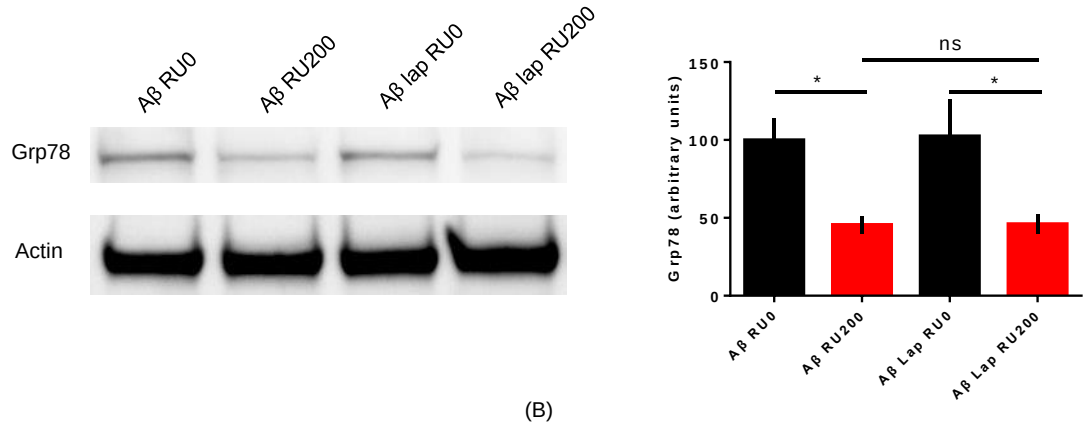

(B)

Figure 3.3 *Lap*'s neuroprotective effect is independent of autophagy and UPR.

(A) Western blot of Atg8 in 21-day-old flies of the same genotypes, plotted below as means ± SEM (n = 3). Aβ does not affect Atg8 levels. Genotypes: UAS-Aβ; elavGS, UAS-Aβ/UAS-lap; elavGS. n.s., not significant, determined by one-way ANOVA.

(B) Western blot of Grp78 in 21-day-old flies of the same genotypes, plotted below as means ± SEM (n = 3). The image is a representative gel of the same samples. Genotypes are above. ***p < 0.001, determined by one-way ANOVA; Aβ RU0 vs Aβ RU200, *p < 0.01; Aβ RU0 vs Aβ lap RU0, n.s., not significant; Aβ lap RU0 vs Aβ lap RU200, *p < 0.01; Aβ RU200 vs Aβ lap RU200, n.s., not significant, comparison by Tukey's *post-hoc* test.

3.2.4 *Lap* mediates VGlut localization

As noted above, PICALM is involved in clathrin-mediated endocytosis (Bao et al., 2005), which is disrupted by Aβ oligomers (Treusch et al., 2011). Clathrin-mediated endocytosis is crucial for either sending misfolded or toxic proteins for degradation or regulating the cell surface expression of proteins. Given that *lap* has been shown to bind to vesicular glutamate transporters (VGlut) (Vanlandingham et al., 2014), I next investigated whether *lap* affected the internalization of VGlut. I confirmed that *lap* directly interacted with VGlut by co-immunoprecipitation (Figure 3.4A). Then I measured the total expression of VGlut in *Drosophila*'s brains and its expression did not change. Given that the total expression of VGlut in brains might not reflect the expression of VGlut in neurons, it was difficult to conclude that *lap* did not regulate VGlut expression in neurons (Figure 3.4B, Aβ RU0: 100 $\pm$ 12.85 %; Aβ RU200: 98.44 $\pm$ 18.78 %; Aβ lap RU0: 96.88 $\pm$ 11.47 %; Aβ lap RU200: 111.16 $\pm$ 18.94 %, n = 3 per condition. $p > 0.05$, one-way ANOVA). I then examined whether this interaction mediated

VGlut distribution, because defects in endocytic trafficking have been shown to maintain receptors on the plasma membrane (Treusch et al., 2011). As *Drosophila* fly brains have a high density of neurons, it is difficult to monitor individual synapses. I therefore turned to larval neuromuscular junctions (NMJ), which provide an excellent model system for monitoring individual synapses, and are extensively used to analyze cellular and molecular mechanisms of protein localization and synaptic neurotransmission (Keshishian et al., 1996). Total number of synaptic boutons is markedly reduced at motor neurons upon expression of $A\beta_{42}$, indicating that expression of $A\beta_{42}$ leads to changes of the morphology of NMJ (Mhatre et al., 2014). I expressed $A\beta_{42}$ and *lap* in motor neurons using D42-Gal4, and found that VGlut was abnormally accumulated near the presynaptic active zone upon $A\beta_{42}$ expression and this accumulation was abrogated by *lap* over-expression (Figure 3.4C, D42: 100 $\pm$ 20.10 %, n = 10; D42 > Aβ: 181 $\pm$ 21.73 %, n = 10; D42 > lap: 113.2 $\pm$ 18.26 %, n = 10; D42 > Aβ lap: 93.36 $\pm$ 26.67, n = 8. $p < 0.05$; one-way ANOVA), suggesting that $A\beta_{42}$ expression affects glutamatergic synaptic transmission and this is modulated by *lap* over-expression.

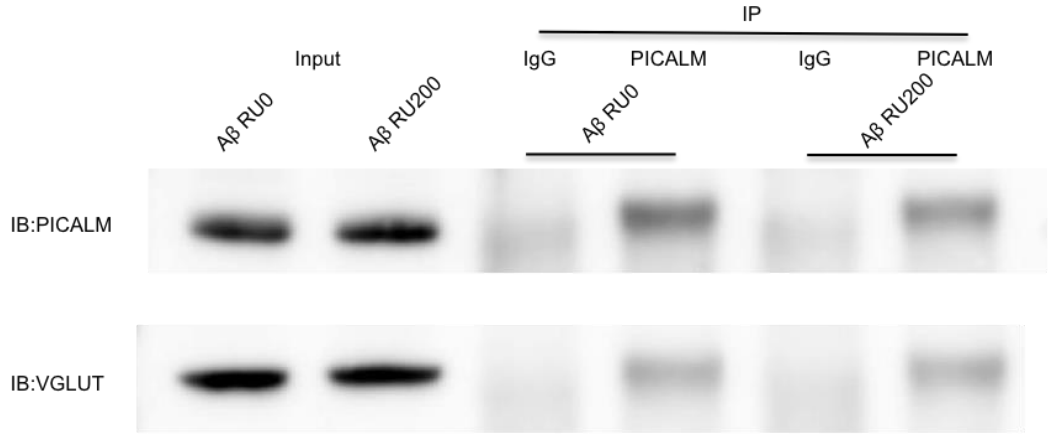

(A)

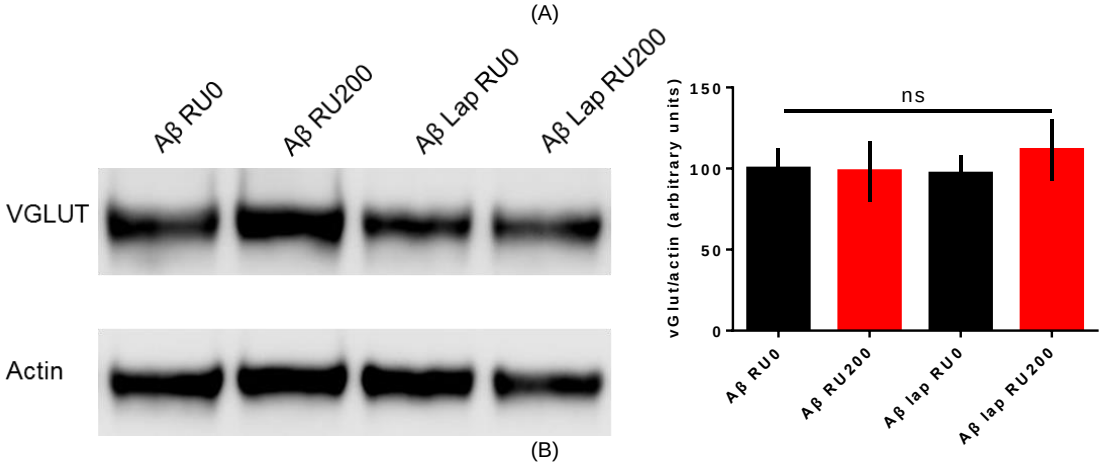

(B)

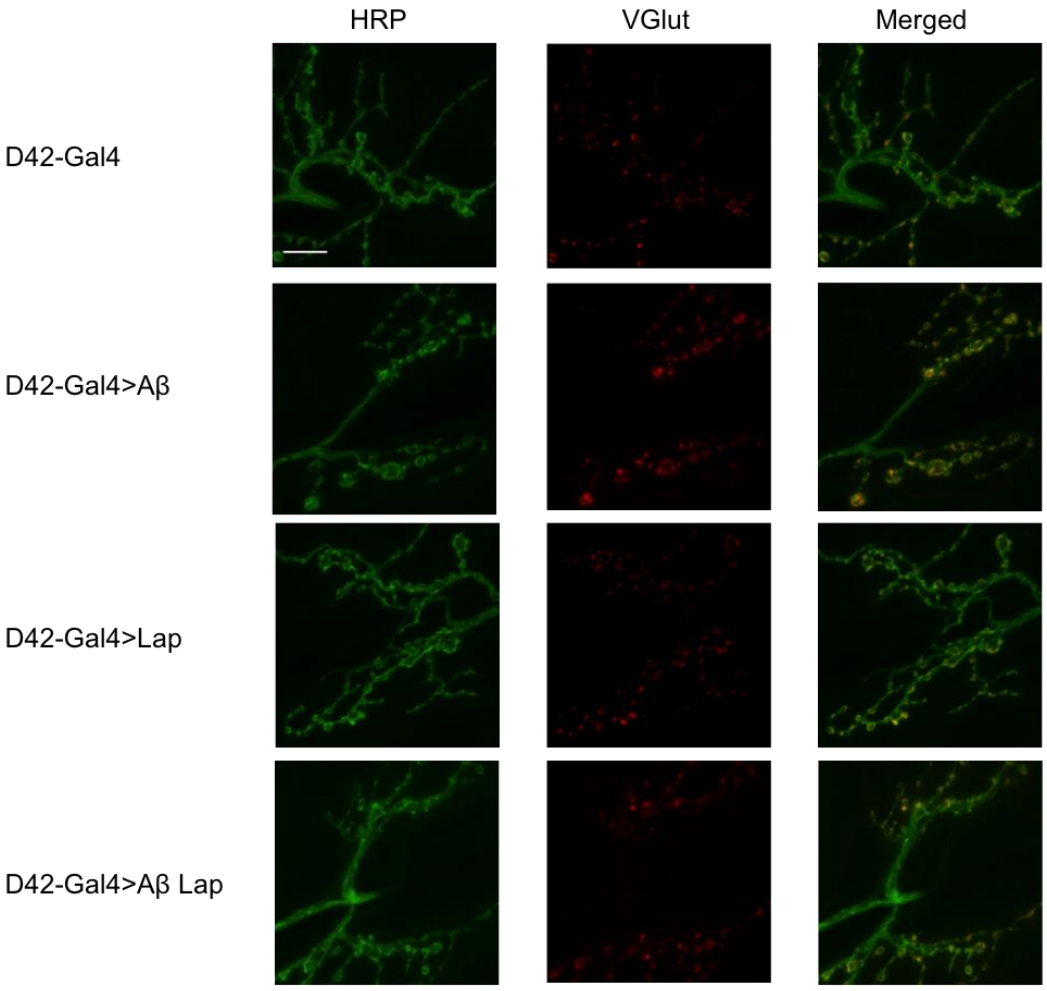

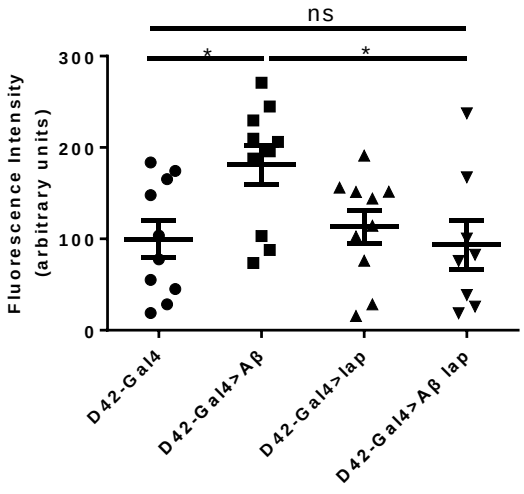

(C)

Figure 3.4 *Lap* reduces Aβ-induced accumulation of VGlut at the NMJ.

(A) Western blot of *lap* and VGlut on a PICALM pull-down showing co-IP of VGlut both in induced (RU200) and un-induced (RU0) flies. Inputs were samples before the IP and IgG control was a beads-only pull-down.

(B) Western blot of VGlut levels in heads of 21-day-old flies, plotted below as means ± SEM, n = 3. The image was a representative gel of the same samples. Genotypes: UAS-Aβ; elavGS, UAS-Aβ/UAS-lap; elavGS. n.s., not significant,

determined by one-way ANOVA.

(C) Confocal images of the NMJ of wandering third-instar larvae expressing Aβ, *lap* or Aβ and *lap*, driven by D42-Gal4. Fluorescence intensity scores were plotted as means ± SEM, n ≥ 8. Genotypes: D42-Gal4, UAS-Aβ; D42-Gal4, UAS-lap; D42-Gal4, UAS-Aβ/UAS-lap; D42-Gal4. *p < 0.05, determined by one-way ANOVA; control (D42-Gal4) vs Aβ, *p < 0.05; control vs lap, n.s., not significant; lap vs Aβ lap, n.s., not significant; Aβ vs Aβ lap, *p < 0.05, comparison by Tukey's *post-hoc* test. Scale bar, 10 μm.

3.2.5 *Lap* regulates glutamate release

Alzheimer's disease has been found to be associated with glutamate excitotoxicity (Abramov et al., 2009; Hynd et al., 2004; Ping et al., 2015). This was attributed to Aβ-induced impairment of glutamate uptake, giving rise to excess extracellular glutamate (Li et al., 2009; Talantova et al., 2013). Here I used the fluorescent extracellular glutamate reporter iGluSnFR to detect extracellular glutamate levels (Marvin et al., 2013; Stork et al., 2014). iGluSnFR is a genetically encoded glutamate indicator which composed of a *Escherichia coli* GltI protein and a circularly permutated (cp) GFP. When glutamate binds to the GltI protein, the GltI protein changes its conformation and therefore the coupled cpGFP produces a fluorescence increase. iGluSnFR can detect 4 uM of glutamate. I expressed UAS-iGluSnFR in motor neurons of intact L2 larvae using D42-Gal4 and observed spontaneous, local bursts of fluorescence in the neuropil, and coordinated waves of activity running along the anterior-posterior axis associated with larval crawling (Movie 1, Figure 3.5A, B, F, G, H and I). Co-expression of iGluSnFR and Aβ revealed an increase in glutamate responsive fluorescence and number of glutamate response in the neuropil, but not the duration of each glutamate response (Movie 2, Figure 3.5A, C, F, G, H and I, average response time, D42: 15.41 ± 1.22 s; D42 > Aβ: 12.97 ± 1.04 s; D42 > lap: 14.5 ± 0.89 s; D42 > Aβ lap: 11.92 ± 1.17 s, n = 5 per condition. p < 0.0001; one-way ANOVA), which was consistent with a murine study (Hefendehl et al., 2016). *Lap* expression reduced the increase in glutamate responsive fluorescence (Movie 3 and 4, Figure 3.5A, E and F, average response, D42: 12.34 ± 1.26 %; D42 > Aβ: 47.52 ± 3.23 %; D42 > lap: 19.82 ± 1.25 %; D42 > Aβ lap: 13.93 ± 1.81 %, n = 5 per condition. p < 0.0001; one-way ANOVA) and total area under the curve describing the glutamate response back to control levels (Figure 3.5A, E and G, total

areal under response, D42: 39.56 ± 4.23; D42 > Aβ: 172 ± 17.66; D42 > lap: 75.34 ± 6.01; D42 > Aβ lap: 76.66 ± 8.51, n = 5 per condition. $p < 0.0001$; one-way ANOVA). However, *lap* expression did not affect the increased number of glutamate release events upon Aβ expression (Movie 3 and 4, Figure 3.5A, E and H, average number of response, D42: 4.2 ± 0.58; D42 > Aβ: 30 ± 2.3; D42 > lap: 31.8 ± 1.86; D42 > Aβ lap: 26.6 ± 2.16, n = 5 per condition. $p < 0.0001$; one-way ANOVA). Collectively, my work suggested that Aβ might enhance glutamate release due to the increased accumulation of VGlut. *Lap* reduced glutamate release due to the decreased accumulation of VGlut.

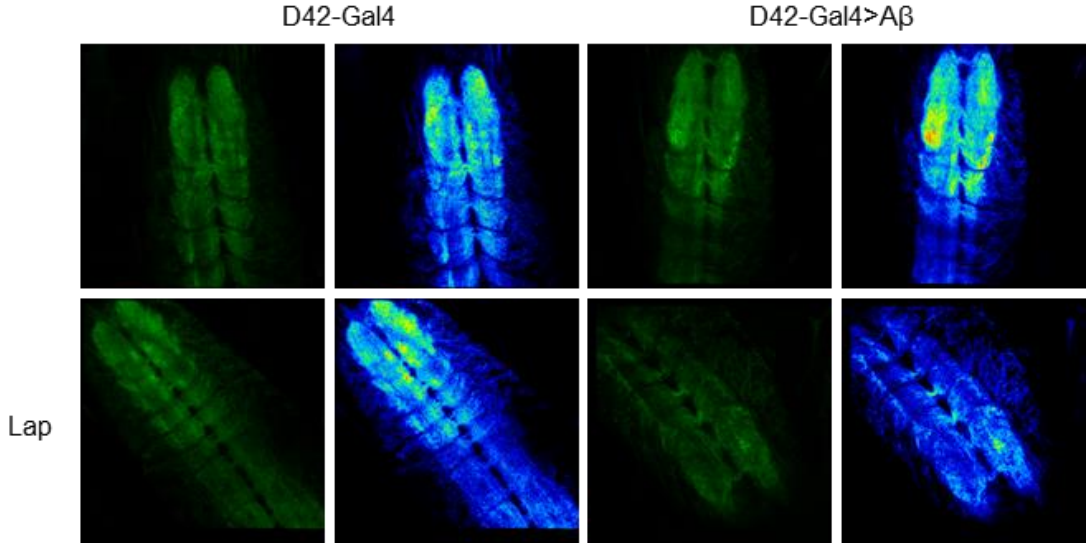

(A)

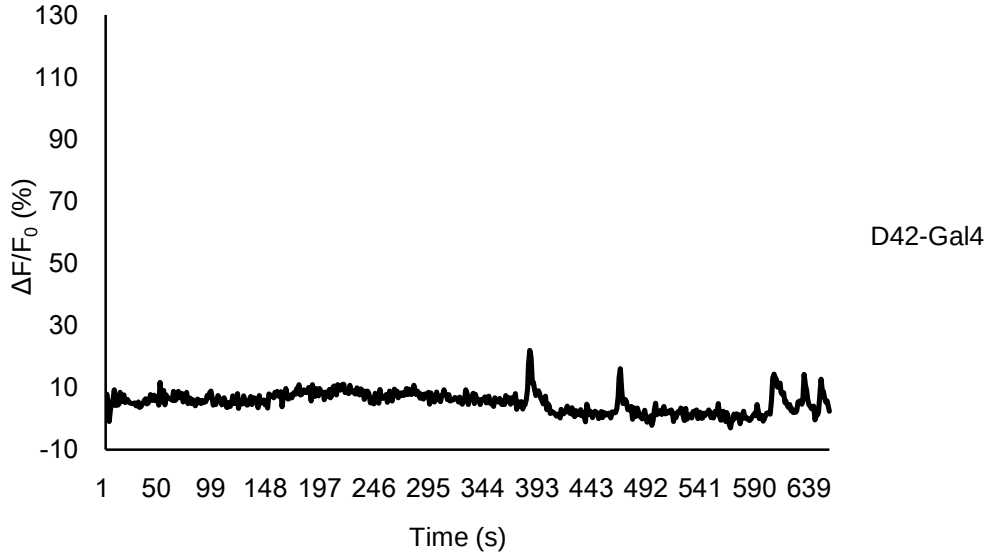

(B)

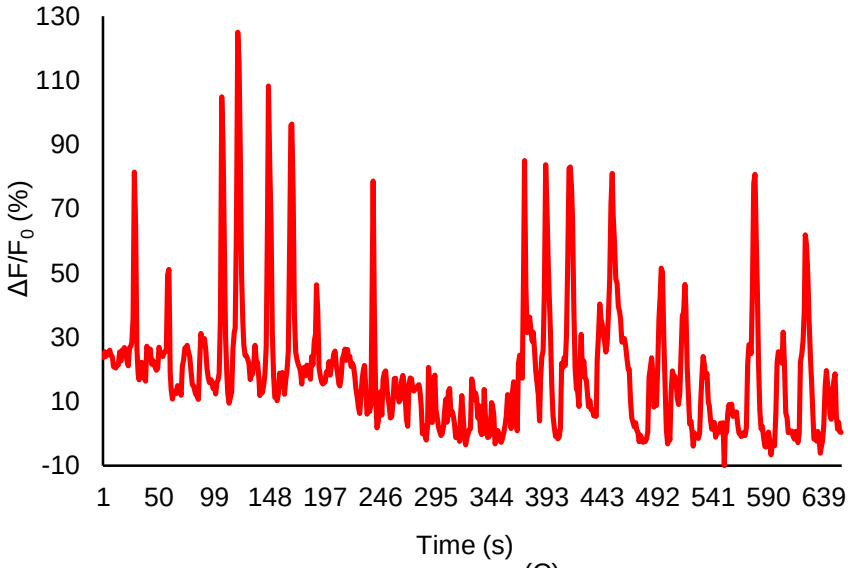
130
110
90
70
50
30
10
-10
ΔF/F0 (%)
1 50 99 148 197 246 295 344 393 443 492 541 590 639
Time (s)
D42-Gal4>Aβ

(C)

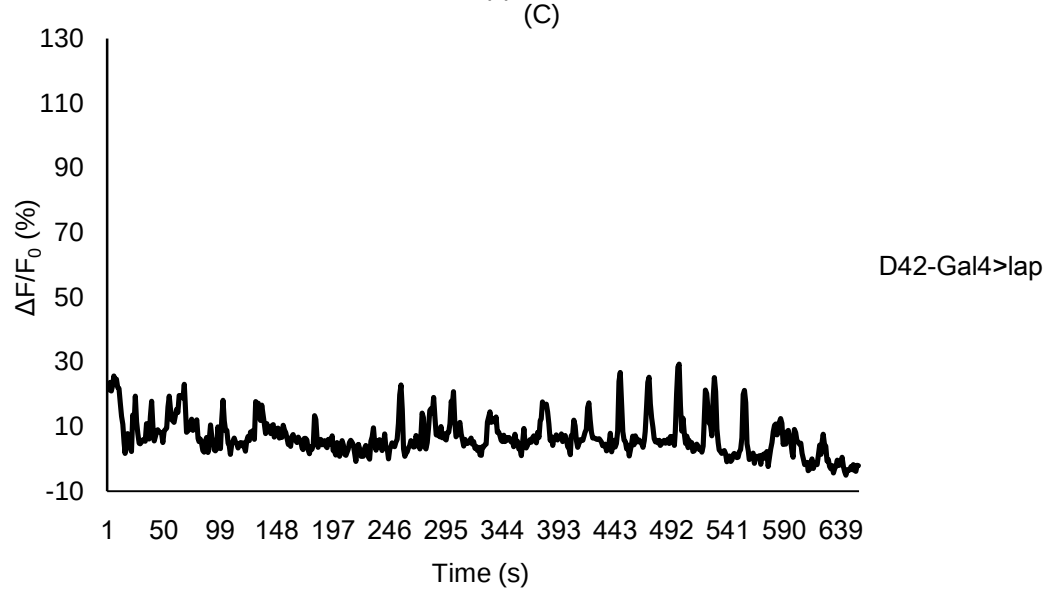
130
110
90
70
50
30
10
-10
ΔF/F0 (%)
1 50 99 148 197 246 295 344 393 443 492 541 590 639
Time (s)
D42-Gal4>lap

(D)

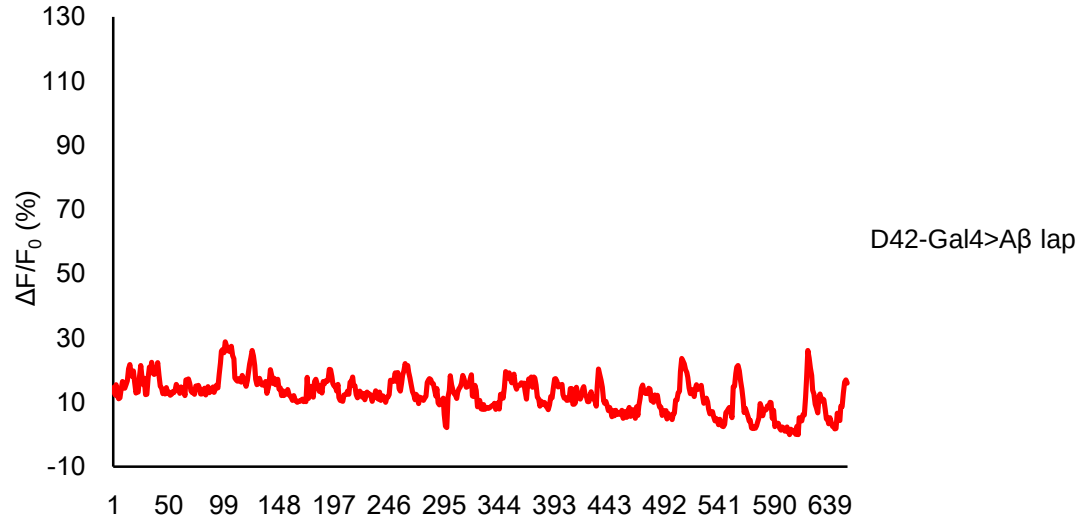
130
110
90
70
50
30
10
-10
ΔF/F0 (%)
1 50 99 148 197 246 295 344 393 443 492 541 590 639
Time (s)
D42-Gal4>Aβ lap

(E)

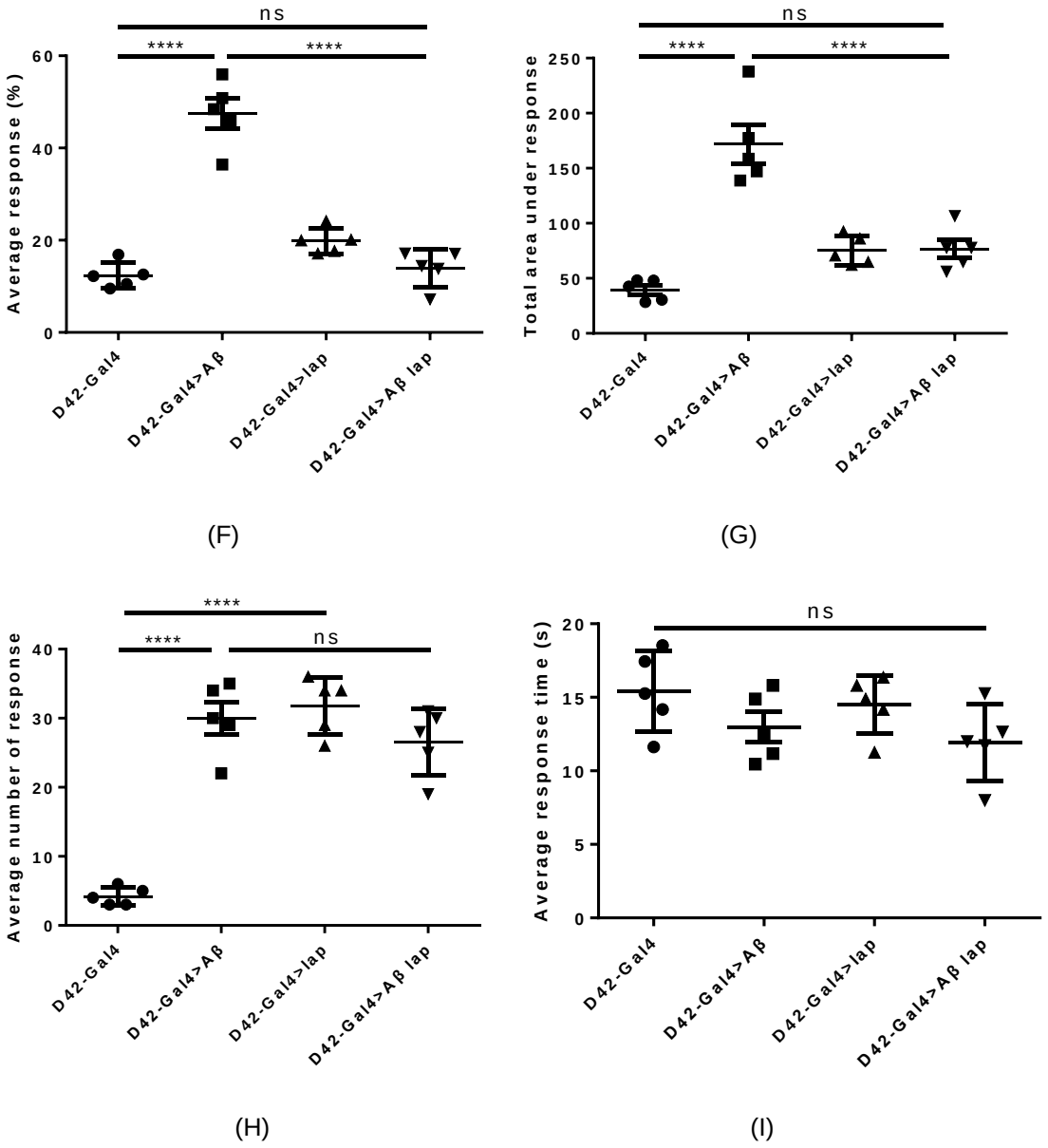

Figure 3.5 *Lap* decreases excess glutamate release upon Aβ expression.

(A) Confocal time-lapse analysis of intact L2 larvae. Neuronally expressed iGluSnFR shows local and transient increases in fluorescence reflecting the release of the neurotransmitter glutamate. The image is a representative burst of the movie. Genotypes: D42-Gal4/UAS-iGluSnFR, UAS-Aβ; D42-Gal4/UAS-iGluSnFR, UAS-lap; D42-Gal4/UAS-iGluSnFR, UAS-Aβ/UAS-lap; D42-Gal4/UAS-iGluSnFR. Scale bar, 20 μm.

(B-E) The respective trace of iGluSnFR fluorescence changes displays the spontaneous activity in the neuropil. Fluorescence signals are normalized to minimum fluorescence in each trace. Genotypes are as above.

(F) Quantification of the percent change of fluorescence in the neuropil of L2 larvae expressing Aβ, *lap* or Aβ and *lap*, driven by D42-Gal4, plotted as means ± SEM, n = 5. Genotypes are as above. ****$p < 0.0001$, determined by one-way ANOVA; control (D42-Gal4) vs Aβ, ****$p < 0.0001$; control vs lap, n.s., not significant; lap vs Aβ lap, n.s., not significant;

Aβ vs Aβ lap, ****p < 0.0001, comparison by Tukey's *post-hoc* test.

(G) Quantification of the area under the response in the neuropil of L2 larvae expressing Aβ, *lap* or Aβ and *lap*, driven by D42-Gal4, plotted as means ± SEM, n = 5. Genotypes are as above. ****p < 0.0001, determined by one-way ANOVA; control (D42-Gal4) vs Aβ, ****p < 0.0001; control vs lap, n.s., not significant; lap vs Aβ lap, n.s., not significant; Aβ vs Aβ lap, ****p < 0.0001, comparison by Tukey's *post-hoc* test.

(H) Quantification of the number of the response in the neuropil of L2 larvae expressing Aβ, *lap* or Aβ and *lap*, driven by D42-Gal4, plotted as means ± SEM, n = 5. Genotypes are as above. ****p < 0.0001, determined by one-way ANOVA; control (D42-Gal4) vs Aβ, ****p < 0.0001; control vs lap, ****p < 0.0001; lap vs Aβ lap, n.s., not significant; Aβ vs Aβ lap, n.s., not significant, comparison by Tukey's *post-hoc* test.

(I) Quantification of the duration of the glutamate response in the neuropil of L2 larvae expressing Aβ, *lap* or Aβ and *lap*, driven by D42-Gal4, plotted as means ± SEM, n = 5. Genotypes are as above. n.s., not significant, determined by one-way ANOVA.

3.2.6 *Lap* in glia is possibly involved in $A\beta_{42}$ pathology

Glial cells were previously reported to be abnormally activated in AD (Ando et al., 2013; Parikh et al., 2014). Moreover, PICALM is abundant in glial and endothelial cells (Baig et al., 2010). However, the role of *lap* in glial cells remains elusive. To this end, I used a model developed in the lab where $A\beta_{arc}$ was under the control of Q expression system. The Q expression system consists of two qa genes (QF and QS). QF is a transcriptional activator that binds to the promoter QUAS. QS is a repressor to QF. The repression of QF by QS is liberated by quinic acid (Potter et al., 2010). In our QUAS-$A\beta_{arc}$ line, QUAS is fused with $A\beta_{arc}$ and driven by a neuronal driver (Syn-QF2). Syn-QF2 is inhibited by QS expressed from a ubiquitous promoter (Tub-QS). QS is blocked by the chemical quinic acid thus relieving its inhibition and allowing activation of the QF2 driver. *Lap* expression, on the other hand, was regulated by a glial-specific geneswitch driver (GSG3285-GS) and activated by RU486. Therefore, this novel AD model allows $A\beta_{arc}$ expression in neurons and concomitant *lap* expression in glial cells (Figure 3.6A). $A\beta_{arc}$ carries a mutation associated with familial AD. This mutation is thought to enhance $A\beta_{42}$ fibrillation and toxicity. Therefore, although the Q system failed to induce a robust expression of $A\beta_{arc}$ (Figure 3.6D, Aβ -QA -RU: 11.64 $\pm$ 0.77 pg/ug protein; Aβ -QA +RU:

9.96 ± 0.24 pg/ug protein; Aβ lap -QA -RU: 10.6 ± 0.6 pg/ug protein; Aβ lap -QA +RU: 12.33 ± 0.61 pg/ug protein; Aβ +QA -RU: 13.37 ± 0.81 pg/ug protein; Aβ +QA +RU: 15.96 ± 0.22 pg/ug protein; Aβ lap +QA -RU: 15.19 ± 2.47 pg/ug protein; Aβ lap +QA +RU: 16.3 ± 1.06 pg/ug protein, n = 3 per condition; p < 0. 01; one-way ANOVA), the QUAS-$A\beta_{arc}$ flies still displayed reduced lifespan and progressive impairment in climbing performance (Aβ -QA -RU vs Aβ +QA -RU and Aβ -QA +RU vs Aβ +QA +RU) (Figure 3.6B and C). This confirmed that this model is useful to investigate the role of glial cells in AD pathogenesis. Notably, *lap* over-expression significantly increased longevity of $A\beta_{arc}$-expressing flies. However, the presence of the *lap* construct (Aβ lap +QA -RU) also increased longevity compared to expression of the glial-specific drive alone (Aβ +QA –RU and Aβ +QA +RU) (Figure 3.6B, mean lifespan, Aβ -QA -RU: 100 %; Aβ -QA +RU: 100 %; Aβ lap -QA -RU: 100 %; Aβ lap -QA +RU: 100 %; Aβ +QA -RU: 60 %; Aβ +QA +RU: 53 %; Aβ lap +QA -RU: 68 %; Aβ lap +QA +RU: 69 %, n > 120 per condition; p was shown in Figure 3.6B, log-rank test). Moreover, although *lap* over-expression attenuated locomotor defects of $A\beta_{arc}$-expressing flies, its corresponding uninduced control (Aβ lap -QA +RU) also improved age-related locomotor defects compared to other uninduced controls (Aβ-QA –RU; Aβ -QA +RU and Aβ lap -QA -RU) (Figure 3.6C, PI, day 7, Aβ -QA -RU: 93.46 ± 1.59 %; Aβ -QA +RU: 96.03 ± 0.73 %; Aβ lap -QA -RU: 92.16 ± 3.54 %; Aβ lap -QA +RU: 94.04 ± 1.99 %; Aβ +QA -RU: 96.81 ± 1.16 %; Aβ +QA +RU: 93.5 ± 0.52 %; Aβ lap +QA -RU: 93.49 ± 1.71 %; Aβ lap +QA +RU: 94.95 ± 1.43 %; day 10, Aβ -QA -RU: 91.52 ± 1.6 %; Aβ -QA +RU: 90.52 ± 0.5 %; Aβ lap -QA -RU: 96.08 ± 0.98 %; Aβ lap -QA +RU: 96.38 ± 1.92 %; Aβ +QA -RU: 78.22 ± 2.12 %; Aβ +QA +RU: 88.24 ± 1.14 %; Aβ lap +QA -RU: 88.87 ± 2.06 %; Aβ lap +QA +RU: 86.19 ± 2.26 %; day 14, Aβ -QA -RU: 87.04 ± 2.33 %; Aβ -QA +RU: 87.8 ± 1.66 %; Aβ lap -QA -RU: 97.06 ± 0 %; Aβ lap -QA +RU: 92.42 ± 0.76 %; Aβ +QA -RU: 79.21 ± 2.34 %; Aβ +QA +RU: 84.96 ± 1.5 %; Aβ lap +QA -RU: 85.42 ± 2.73 %; Aβ lap +QA +RU: 93.43 ± 0.51 %; day 18, Aβ -QA -RU: 80.86 ± 7.12 %; Aβ -QA +RU: 81.79 ± 4.29 %; Aβ lap -QA -RU: 82.35 ± 3.4 %; Aβ lap -QA +RU: 91.67 ± 3.33 %; Aβ +QA -RU: 71.54 ± 1.97 %; Aβ +QA +RU: 74.54 ± 1.04 %; Aβ lap +QA -RU: 84.06 ± 1.71 %; Aβ lap +QA +RU: 90.86 ± 2.85 %; day 21, Aβ -QA -RU: 70.99 ± 1.24 %; Aβ -QA +RU: 73.4 ± 1.6 %; Aβ lap -QA -RU: 71.88 ± 3.13 %; Aβ lap -QA +RU: 89.17 ± 2.21 %; Aβ +QA -RU: 53.78 ± 2.92 %; Aβ +QA +RU: 55.86 ± 2.27 %; Aβ lap +QA -RU: 55.09 ± 2.02 %; Aβ lap +QA +RU: 73.89 ± 1.86 %; day 25, Aβ -QA

-RU: 67.31 ± 5.88 %; Aβ -QA +RU: 66.67 ± 3.7 %; Aβ lap -QA -RU: 66.67 ± 2.08 %; Aβ lap -QA +RU: 78.33 ± 1.67 %; Aβ +QA -RU: 30.21 ± 2.13 %; Aβ +QA +RU: 46 ± 4.32 %; Aβ lap +QA -RU: 50.98 ± 5.12 %; Aβ lap +QA +RU: 68.18 ± 1.31 %; day 28, Aβ -QA -RU: 62.83 ± 0.59 %; Aβ -QA +RU: 60.21 ± 1.44 %; Aβ lap -QA -RU: 59.38 ± 5.41 %; Aβ lap -QA +RU: 65.83 ± 5.47 %; Aβ +QA -RU: 19.17 ± 2.73 %; Aβ +QA +RU: 28.97 ± 4.68 %; Aβ lap +QA -RU: 29.17 ± 3.65 %; Aβ lap +QA +RU: 43.33 ± 3.63 %; day 31, Aβ -QA -RU: 60.33 ± 2.85 %; Aβ -QA +RU: 55.69 ± 0.86 %; Aβ lap -QA -RU: 64.58 ± 2.76 %; Aβ lap -QA +RU: 65 ± 2.89 %; Aβ +QA -RU: 22.99 ± 3.04 %; Aβ +QA +RU: 31.07 ± 2.33 %; Aβ lap +QA -RU: 26.67 ± 2.55 %; Aβ lap +QA +RU: 40.15 ± 4.61 %; day 36, Aβ -QA -RU: 41.28 ± 1.48 %; Aβ -QA +RU: 36.32 ± 1.34 %; Aβ lap -QA -RU: 27.78 ± 5.56 %; Aβ lap -QA +RU: 47.5 ± 2.89 %; Aβ +QA -RU: 8.33 ± 2.73 %; Aβ +QA +RU: 15.15 ± 2 %; Aβ lap +QA -RU: 11.54 ± 5.09 %; Aβ lap +QA +RU: 12.5 ± 6.37 %, n = 3 per condition. Interaction of time and genotype, $p < 0.0001$; time, $p < 0.0001$, genotype, $p < 0.0001$, two-ways ANOVA). Therefore, I cannot conclude that *lap* in glial cells diminished $A\beta_{42}$ toxicity. It is still unclear the contribution of glial *lap* to AD progression.

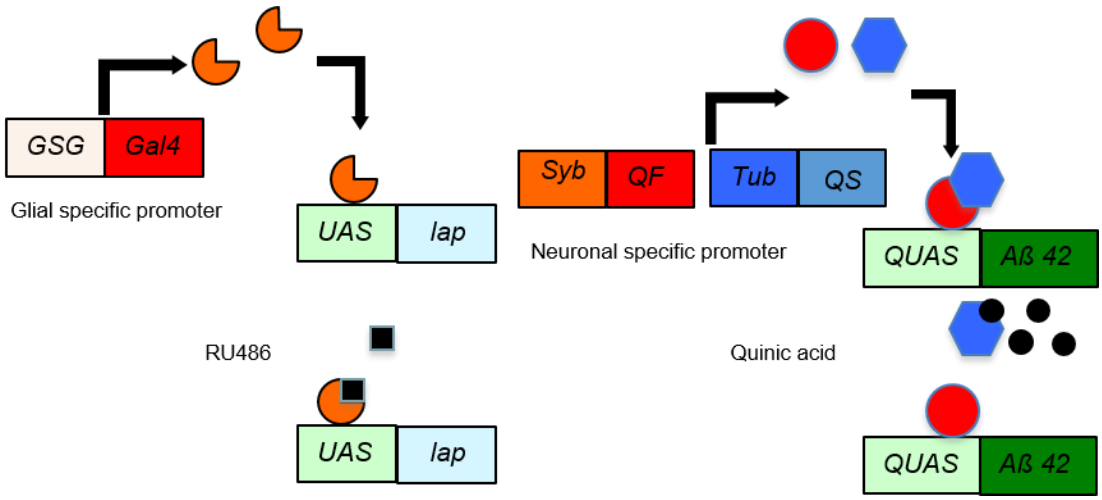

(A)

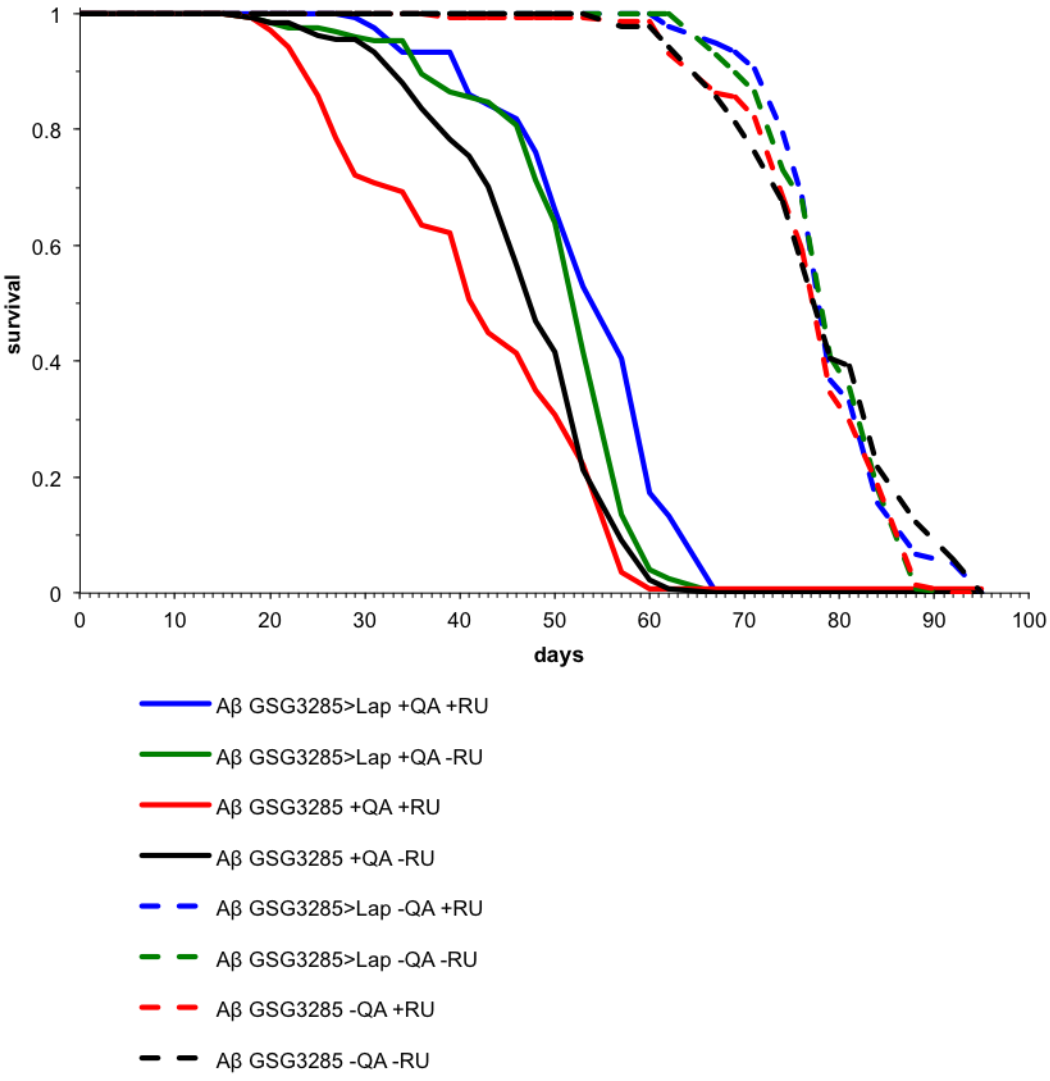
survival
days
Aβ GSG3285>Lap +QA +RU
Aβ GSG3285>Lap +QA -RU
Aβ GSG3285 +QA +RU
Aβ GSG3285 +QA -RU
Aβ GSG3285>Lap -QA +RU
Aβ GSG3285>Lap -QA -RU
Aβ GSG3285 -QA +RU
Aβ GSG3285 -QA -RU

(B)

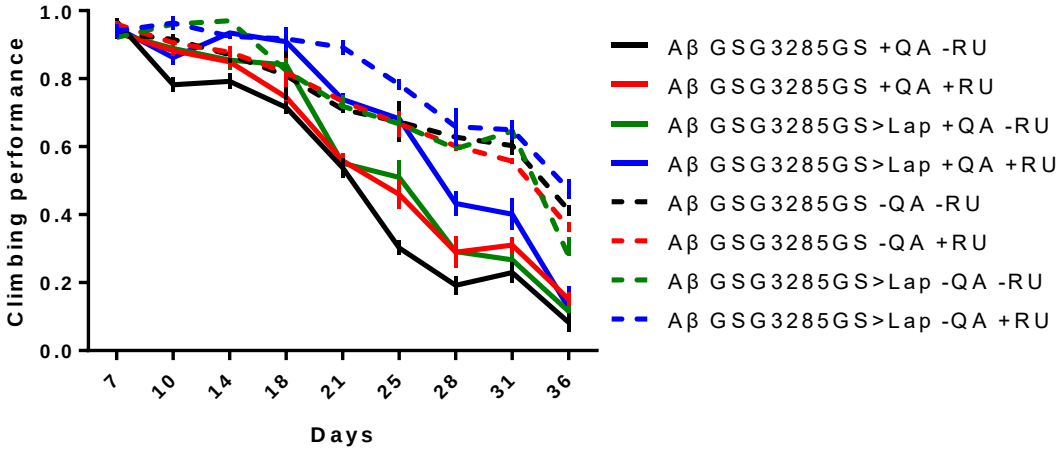
Climbing performance
Days
Aβ GSG3285GS +QA -RU
Aβ GSG3285GS +QA +RU
Aβ GSG3285GS>Lap +QA -RU
Aβ GSG3285GS>Lap +QA +RU
Aβ GSG3285GS -QA -RU
Aβ GSG3285GS -QA +RU
Aβ GSG3285GS>Lap -QA -RU
Aβ GSG3285GS>Lap -QA +RU

(C)

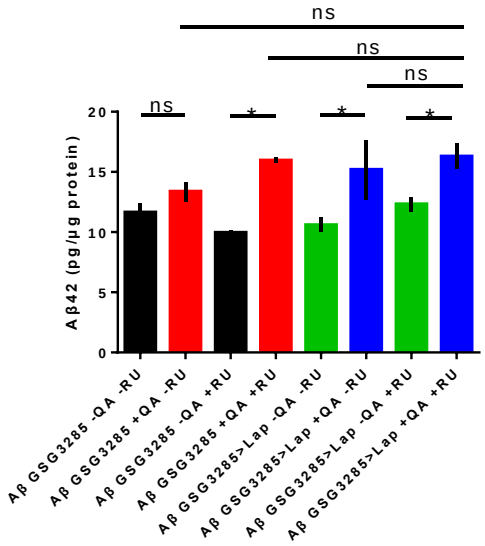

(D)

Figure 3.6 *Lap* in glia possibly suppresses $A\beta_{arc}$ toxicity.

(A) Schematic of the Q repressible binary expression system. In the absence of the transcription factor, Syn-QF, the QUAS-$A\beta_{arc}$ does not express. When Syn-QF and QUAS-$A\beta_{arc}$ transgenes are present in neurons where QF is expressed, QF binds to QUAS and activates expression of $A\beta_{arc}$. When Tub-QS, Syn-QF, and QUAS-$A\beta_{arc}$ transgenes are present in neurons and both QF and QS are active, QS represses QF and $A\beta_{arc}$ is not expressed. When flies are fed quinic acid, QS is repressed and QF is activated. Again, $A\beta_{arc}$ is expressed.

(B) Survival curves of flies expressing *lap* in glia under the control of the GSG3285 promoter, while $A\beta_{arc}$ was induced by feeding flies QA, n > 120. Genotypes: QUAS-Aβ; GSG3285/nSybQF2 tubQS, QUAS-Aβ/UAS-lap; GSG3285/nSybQF2 tubQS. Statistical analyses were determined by log-rank test and shown in Table 3.3.

(C) Climbing performance index of flies of the same genotypes. The climbing performance of Aβ lap (+RU) was significantly better than those of other groups, n = 3 (50 animals per condition). Interaction of time and genotype, $p < 0.0001$; time, $p < 0.0001$, genotype, $p < 0.0001$, determined by two ways ANOVA followed by Tukey's *post-hoc* test. Statistical analyses were shown in Table 3.4.

(D) $A\beta_{42}$ protein levels, measured by ELISA, in the heads of 28-day-old flies expressing Aβ (+QA), Aβ and *lap* (+QA) and uninduced controls (-QA). Means ± SEM, n = 3. **$p < 0.01$, determined by one way ANOVA; Aβ -QA -RU vs Aβ +QA -RU, n.s., not significant; Aβ -QA +RU vs Aβ +QA +RU, *$p < 0.05$; Aβ lap -QA -RU vs Aβ lap +QA -RU, ****$p < 0.0001$; Aβ lap -QA +RU vs Aβ lap +QA +RU, ****$p < 0.0001$; Aβ +QA -RU vs Aβ lap +QA +RU, n.s., not significant; Aβ +QA +RU vs Aβ lap +QA +RU, n.s., not significant; Aβ lap +QA -RU vs Aβ lap +QA +RU, n.s., not significant, comparison by Tukey's *post-hoc* test.

Table 3.3 Statistical summary of survival curves of flies expressing Aβ with or without *lap* in glia

	Aβ +QA -RU	Aβ +QA +RU	Aβ lap +QA -RU	Aβ lap +QA +RU	Aβ -QA -RU	Aβ -QA +RU	Aβ lap -QA -RU	Aβ lap -QA +RU
Aβ +QA -RU		< 0.0001	< 0.0001	< 0.0001	< 0.0001	< 0.0001	< 0.0001	< 0.0001
Aβ +QA +RU			< 0.0001	< 0.0001	< 0.0001	< 0.0001	< 0.0001	< 0.0001
Aβ lap +QA -RU				< 0.0001	< 0.0001	< 0.0001	< 0.0001	< 0.0001
Aβ lap +QA +RU					< 0.0001	< 0.0001	< 0.0001	< 0.0001
Aβ -QA -RU						n.s.	n.s.	n.s.
Aβ -QA +RU							n.s.	n.s.
Aβ lap -QA -RU								n.s.
Aβ lap -QA +RU								

Table 3.4 Statistical summary of locomotor performance index of flies expressing Aβ with or without *lap* in glia

Day 7	Aβ +QA -RU	Aβ +QA +RU	Aβ lap +QA -RU	Aβ lap +QA +RU	Aβ -QA -RU	Aβ -QA +RU	Aβ lap -QA -RU	Aβ lap -QA +RU
Aβ +QA -RU		n.s.	n.s.	n.s.	n.s.	n.s.	n.s.	n.s.
Aβ +QA +RU			n.s.	n.s.	n.s.	n.s.	n.s.	n.s.
Aβ lap +QA -RU				n.s.	n.s.	n.s.	n.s.	n.s.

Aβ lap +QA +RU					n.s.	n.s.	n.s.	n.s.
Aβ -QA -RU						n.s.	n.s.	n.s.
Aβ -QA +RU							n.s.	n.s.
Aβ lap -QA -RU								n.s.
Aβ lap -QA +RU								
Day 10	Aβ +QA -RU	Aβ +QA +RU	Aβ lap +QA -RU	Aβ lap +QA +RU	Aβ -QA -RU	Aβ -QA +RU	Aβ lap -QA -RU	Aβ lap -QA +RU
Aβ +QA -RU		n.s.	n.s.	n.s.	< 0.05	n.s.	< 0.001	< 0.001
Aβ +QA +RU			n.s.	n.s.	n.s.	n.s.	n.s.	n.s.
Aβ lap +QA -RU				n.s.	n.s.	n.s.	n.s.	n.s.
Aβ lap +QA +RU					n.s.	n.s.	n.s.	n.s.
Aβ -QA -RU						n.s.	n.s.	n.s.
Aβ -QA +RU							n.s.	n.s.
Aβ lap -QA -RU								n.s.
Aβ lap -QA +RU								
Day 14	Aβ +QA	Aβ +QA	Aβ lap	Aβ lap	Aβ -QA	Aβ -QA	Aβ lap	Aβ lap

	-RU	+RU	+QA -RU	+QA +RU	-RU	+RU	-QA -RU	-QA +RU
Aβ +QA -RU		n.s.	n.s.	n.s.	<0.05	n.s.	<0.001	<0.5
Aβ +QA +RU			n.s.	n.s.	n.s.	n.s.	n.s.	n.s.
Aβ lap +QA -RU				n.s.	n.s.	n.s.	n.s.	n.s.
Aβ lap +QA +RU					n.s.	n.s.	n.s.	n.s.
Aβ -QA -RU						n.s.	n.s.	n.s.
Aβ -QA +RU							n.s.	n.s.
Aβ lap -QA -RU								n.s.
Aβ lap -QA +RU								

Day 18	Aβ +QA -RU	Aβ +QA +RU	Aβ lap +QA -RU	Aβ lap +QA +RU	Aβ -QA -RU	Aβ -QA +RU	Aβ lap -QA -RU	Aβ lap -QA +RU
Aβ +QA -RU		n.s.	n.s.	< 0.001	n.s.	n.s.	n.s.	< 0.001
Aβ +QA +RU			n.s.	< 0.01	n.s.	n.s.	n.s.	< 0.01
Aβ lap +QA -RU				n.s.	n.s.	n.s.	n.s.	n.s.
Aβ lap +QA +RU					n.s.	n.s.	n.s.	n.s.
Aβ -QA -RU						n.s.	n.s.	n.s.

Aβ -QA +RU							n.s.	n.s.
Aβ lap -QA -RU								n.s.
Aβ lap -QA +RU								
Day 21	Aβ +QA -RU	Aβ +QA +RU	Aβ lap +QA -RU	Aβ lap +QA +RU	Aβ -QA -RU	Aβ -QA +RU	Aβ lap -QA -RU	Aβ lap -QA +RU
Aβ +QA -RU		n.s.	n.s.	< 0.001	< 0.01	< 0.001	< 0.001	< 0.0001
Aβ +QA +RU			n.s.	< 0.001	< 0.01	< 0.01	< 0.01	< 0.0001
Aβ lap +QA -RU				< 0.001	< 0.01	< 0.001	< 0.01	< 0.0001
Aβ lap +QA +RU					n.s.	n.s.	n.s.	< 0.01
Aβ -QA -RU						n.s.	n.s.	< 0.001
Aβ -QA +RU							n.s.	< 0.01
Aβ lap -QA -RU								< 0.01
Aβ lap -QA +RU								
Day 25	Aβ +QA -RU	Aβ +QA +RU	Aβ lap +QA -RU	Aβ lap +QA +RU	Aβ -QA -RU	Aβ -QA +RU	Aβ lap -QA -RU	Aβ lap -QA +RU
Aβ +QA -RU		< 0.01	< 0.0001	< 0.0001	< 0.0001	< 0.0001	< 0.0001	< 0.0001
Aβ +QA			n.s.	< 0.0001	< 0.0001	< 0.0001	< 0.0001	< 0.001

+RU								
Aβ lap +QA -RU				< 0.01	< 0.01	< 0.01	< 0.01	< 0.001
Aβ lap +QA +RU					n.s.	n.s.	n.s.	n.s.
Aβ -QA -RU						n.s.	n.s.	n.s.
Aβ -QA +RU							n.s.	n.s.
Aβ lap -QA -RU								n.s.
Aβ lap -QA +RU								
Day 28	Aβ +QA -RU	Aβ +QA +RU	Aβ lap +QA -RU	Aβ lap +QA +RU	Aβ -QA -RU	Aβ -QA +RU	Aβ lap -QA -RU	Aβ lap -QA +RU
Aβ +QA -RU		n.s.	n.s.	< 0.0001	< 0.0001	< 0.0001	< 0.0001	< 0.0001
Aβ +QA +RU			n.s.	< 0.05	< 0.0001	< 0.0001	< 0.0001	< 0.0001
Aβ lap +QA -RU				< 0.05	< 0.0001	< 0.0001	< 0.0001	< 0.0001
Aβ lap +QA +RU					< 0.001	< 0.01	< 0.01	< 0.0001
Aβ -QA -RU						n.s.	n.s.	n.s.
Aβ -QA +RU							n.s.	n.s.
Aβ lap -QA -RU								n.s.

Aβ lap -QA +RU								
Day 31	Aβ +QA -RU	Aβ +QA +RU	Aβ lap +QA -RU	Aβ lap +QA +RU	Aβ -QA -RU	Aβ -QA +RU	Aβ lap -QA -RU	Aβ lap -QA +RU
Aβ +QA -RU		n.s.	n.s.	< 0.01	< 0.0001	< 0.0001	< 0.0001	< 0.0001
Aβ +QA +RU			n.s.	n.s.	< 0.0001	< 0.0001	< 0.0001	< 0.0001
Aβ lap +QA -RU				< 0.05	< 0.0001	< 0.0001	< 0.0001	< 0.0001
Aβ lap +QA +RU					< 0.0001	< 0.01	< 0.0001	< 0.0001
Aβ -QA -RU						n.s.	n.s.	n.s.
Aβ -QA +RU							n.s.	n.s.
Aβ lap -QA -RU								n.s.
Aβ lap -QA +RU								
Day 36	Aβ +QA -RU	Aβ +QA +RU	Aβ lap +QA -RU	Aβ lap +QA +RU	Aβ -QA -RU	Aβ -QA +RU	Aβ lap -QA -RU	Aβ lap -QA +RU
Aβ +QA -RU		n.s.	n.s.	n.s.	< 0.0001	< 0.0001	< 0.001	< 0.0001
Aβ +QA +RU			n.s.	n.s.	< 0.0001	< 0.0001	n.s.	< 0.0001
Aβ lap +QA -RU				n.s.	< 0.0001	< 0.0001	< 0.01	< 0.0001
Aβ lap					< 0.0001	< 0.0001	< 0.01	< 0.0001

+QA +RU							
Aβ -QA -RU					n.s.	< 0.05	n.s.
Aβ -QA +RU						n.s.	n.s.
Aβ lap -QA -RU							< 0.001
Aβ lap -QA +RU							

3.3 Discussion

PICALM is linked to sporadic AD. A number of publications have described the role of PICALM in $A\beta_{42}$ production. However, the contribution of PICALM to modulating the downstream effect of $A\beta_{42}$ toxicity is unknown. My work provides a new link between the *Drosophila* homologue of PICALM, *lap* and glutamatergic transmission in Alzheimer's disease.

3.3.1 Autophagy and UPR in AD

Autophagy and UPR have been reported to be impaired in AD. My results have found that Atg8 expression was not altered upon Aβ expression. However, I cannot exclude the possibility that autophagy is changed in our model because autophagy is a multi-step process. In the future, it would be good to investigate the expression of more autophagy markers, such as p62.

My data have another limitation that it is still not understood whether UPR activity is activated or inhibited in AD. This limitation is caused by the fact that Grp78 is not a good marker of UPR induction. The future work needs to examine the expression of other UPR markers like Xbp1 mRNA and Grp78 mRNA levels.

3.3.2 Imbalance in glutamatergic transmission in AD

My work has shown that $A\beta_{42}$ expression leads to VGlut accumulation, which could increase

glutamate release. Elevated extracellular glutamate concentrations can give rise to glutamate excitotoxicity (Abramov et al., 2009; Ping et al., 2015). Alterations in expression of glutamate transporters have been observed in sporadic AD patients, mouse AD models and excess glutamate release is found in an *in vitro* model of AD (Cummings et al., 2015; Hefendehl et al., 2016; Li et al., 2009; Talantova et al., 2013). Presynaptic glutamate has been reported to negatively modulate the number of GluRII receptors (Featherstone et al., 2002). Therefore, $A\beta_{42}$ could possibly affect GluRII localization as well, again leading to an imbalance in glutamatergic transmission.

3.3.3 Contributions of glia in AD progression

Astrocyte and microglia are over-activated in AD. They take up $A\beta_{42}$ peptides and promote their clearance. Here, I show that *lap* over-expression in glial cells might protect neurons from $A\beta_{42}$ toxicity without affecting $A\beta_{42}$ levels. However, as QF2 and quinic acid are toxic (Riabinina et al., 2015), I cannot exclude the possibility that *lap* expression only reduces QF2 or quinic acid induced toxicity. Moreover, the feeding quinic acid and RU486 exacerbates toxicity compared to feeding quinic acid alone. Finally, the presence of the *lap* construct gives rise to lifespan extension. It is unknown whether the neuroprotection of glial *lap* is specific to $A\beta_{42}$ toxicity. Taken together, I do not think that the Q system is a good binary expression system to investigate gene function because it might confer exogenous toxicity.

3.3.4 Role of *lap* in longevity

A GWAS study has linked PICALM to longevity. However, the role of *lap* in the ageing process is still unclear. I show that inhibition of *lap* promotes longevity. Given that glutamatergic neurotransmission declines with age (Segovia et al., 2001), this lifespan extension could possibly result from an increase in VGlut localization and glutamatergic transmission by the downregulation of *lap*. My work has used a genetically encoded transmitter indicator (GETI) to visualize glutamate dynamics in larval VNC. It will be interesting to test whether this method allows for detecting extracellular glutamate in adults' brains and therefore revealing changes of glutamatergic transmission with age.

My work has showed that *lap* ameliorates Aβ toxicity. *Lap* reduces the accumulation of vesicular glutamate transporters (VGlut) near the pre-synaptic active zone and therefore reduces glutamatergic transmission.

4. Roles of BIN1 and RAB5 in Alzheimer's disease

4.1 Background

I showed in Chapter 3 that *lap* slightly diminishes Aβ toxicity, but its downstream effector is unknown. Although the expression of other clathrin-mediated endocytic proteins is altered in AD, the link between these proteins and disease progression is not firmly established.

Clathrin-dependent endocytosis starts with nucleation. This nucleation localizes at the sites where clathrin will be recruited. At the same time, receptors on the plasma membrane are recruited to the clathrin-coated pits by the adaptor protein AP2 (Blondeau et al., 2004; Honing et al., 2005; Ohno et al., 1995). AP2 interacts with different accessory adaptor proteins to select different cargos (Collins et al., 2002; Kelly et al., 2008). These accessory proteins are divided into two main groups: AP180 (also known as PICALM) and epsin (Chidambaram et al., 2008; Dittman and Kaplan, 2006; Ford et al., 2002; Ford et al., 2001; Reider et al., 2009; Stimpson et al., 2009). After the cargo selection, the clathrin cage is polymerized and assembled into vesicles (Boucrot et al., 2010; Motley et al., 2003; Saffarian et al., 2009; Tebar et al., 1996). Then vesicles are cliped by dynamin (Ferguson et al., 2009; Kosaka and Ikeda, 1983; Sundborger et al., 2011; Wigge et al., 1997), which curves the vesicle neck along with amphiphysin and endophilin, allowing the vesicle to detach from the plasma membrane (Bashkirov et al., 2008; Hinshaw and Schmid, 1995; Macia et al., 2006; Roux et al., 2006; Stowell et al., 1999; Sweitzer and Hinshaw, 1998; van der Bliek et al., 1993). The clathrin coat is then disassembled by HSC70 and auxilin (also known as GAK) (Fotin et al., 2004; Massol et al., 2006; Rapoport et al., 2008; Scheele et al., 2001; Schlossman et al., 1984; Taylor et al., 2011; Xing et al., 2010). Once the vesicle is eased, the subsequent cascade is vesicle trafficking, docking and fusion. Vesicle trafficking is mediated by two families of GTPases: Rab and Arf. They serve as a switch to regulate activities of their effectors (Pryor et al., 2008). Rab and Arf are activated by conversion from a GDP-bound to a GTP-bound form, catalyzed by guanidine exchange factors (GEFs) (Delprato et al., 2004). Then the GTP-bound form can be

switched back to the GDP-bound form by GTPase-activating proteins (GAPs) (Eathiraj et al., 2005). Inactive Rabs are further stabilized by GDP dissociation inhibitor (GDIs) while they are recycled back to the cytosol (Matsui et al., 1990). The Rab family is composed of at least 38 proteins (Haas et al., 2007) and the Arf family comprises of 6 proteins and several relatives (Kahn et al., 2006; Pasqualato et al., 2002). Different proteins are localized at distinct membrane microdomains, so they are specific to particular intracellular trafficking pathways. For example, Rab4 and Rab5 are mainly located at early endosome (Gorvel et al., 1991; Rubino et al., 2000). Rab4 is also found in recycling endosome as well as Rab11 (Sonnichsen et al., 2000). Rab7 and Rab9 are existed in late endosome (Barbero et al., 2002). RAB5 regulates the transport of cargos to early endosomes, whereas its effector, VPS39, activates Rab7 through RAB7 GEF activity (Rink et al., 2005). This allows for cargos to be transported to late endosomes. Rab proteins also contribute to vesicle tethering and fusion through the recruitment of membrane-tethering factors and t-SNARE respectively. Vesicle docking is required for the closing of the vesicle membrane and the target membrane. This process is mediated by membrane-tethering factors and Sec1-Munc18 protein (SM proteins). Membrane-tethering factors consist in two classes: the coiled-coil (e.g. golgins) and the multisubunit tethering complexes (e.g. Exocyst). Membrane-tethering factors work together with SM proteins (e.g. vps) to promote SNARE assembly (Archbold et al., 2014; Block et al., 1988; Clary et al., 1990; Ma et al., 2013a; McNew et al., 2000; Miller et al., 2011; Zick and Wickner, 2014). SNAREs are more crucial to membrane fusion, rather than vesicle tethering. They are categorized into v-SNAREs such as synaptobrevin and t-SNAREs like syntaxin and SNAP25. The association of synaptobrevin, syntaxin and SNAP25 between the two membranes forms a *trans*-SNARE complex that drives membrane fusion. During membrane fusion, this *trans*-SNARE complex converts to a *cis*-SNARE complex that is subsequently disassembled by NSF and SNAP. There are 20 or more SNAREs that also specify different intracellular trafficking pathways (Hanson et al., 1997). In the process of exocytosis, vesicle fusion is triggered by Ca^{2+} via its sensor synaptotagmin (Fernandez-Chacon et al., 2001; Geppert et al., 1994). When cargos enter early endosomes, they are delivered to lysosomes for degradation or to recycling endosomes for secretion. This event is regulated by the ESCRT (endosomal sorting complex required for transport). These pathways are a downstream

cascade of the clathrin-mediated endocytosis (Henne et al., 2011; Williams and Urbe, 2007). However, whether they are involved in AD pathogenesis is rarely studied.

BIN1 plays a crucial role in intracellular endosome trafficking through interaction with the GTPase dynamin (Takei et al., 1999). BIN1 mice knockouts present learning deficits (Di Paolo et al., 2002). It is not clear whether BIN1 is increased or decreased in AD (Chapuis et al., 2013; Glennon et al., 2013) and so BIN1's role in AD pathology is still unclear. BIN1 has mostly been implicated in tau pathology, however its role is unclear, with some studies suggesting that upregulation blocks the spread of tau (Calafate et al., 2016) while others suggesting that downregulation ameliorates tau toxicity (Chapuis et al., 2013). BIN1 also plays a role in Aβ production, with reduction of BIN1 linked to increased BACE1 and Aβ production (Miyagawa et al., 2016; Ubelmann et al., 2017), however, whether it plays a role in downstream Aβ toxicity remains unknown.

Glutamate release is abnormal with Aβ expression (Cummings et al., 2015; Hefendehl et al., 2016; Li et al., 2009; Talantova et al., 2013), while glutamate excitotoxicity is also attributed to the altered localization of glutamate receptors. Aβ affects the localization of glutamate receptors. For instance, Aβ expression leads to a reduction in AMPAR and NMDAR from the cell surface (Hsieh et al., 2006; Shankar et al., 2007; Snyder et al., 2005; Zhao et al., 2010). However, more recently, this idea has been challenged. Firstly, NR2B subunits of NMDARs are found to be activated by Aβ oligomers. NR2B antagonist ameliorates Aβ-mediated neurotoxicity (Hu et al., 2009a; Li et al., 2009; Li et al., 2011; Talantova et al., 2013). Therefore, NR2B activation could be responsible for Aβ-mediated excitotoxicity. Secondly, a large body of evidence shows that high doses of Aβ give rise to the internalization of GluA1 subunits of AMPAR from the cell surface, while low doses leads to the accumulate GluA1 subunits on the plasma membrane. Also this might explain why Aβ leads to glutamate excitotoxicity and synaptic loss (Liu et al., 2010; Whitcomb et al., 2015).

I performed a small-scale targeted genetic screen of endocytic-exocytic genes and identified *Rab5*, *EndoA*, *Bin1* and *Snap25* as suppressors of $A\beta_{42}$-induced degeneration. I showed that

Amph, the BIN1 orthologue, localization was disrupted upon Aβ expression and restored by *lap*. I also showed that *Amph* modulated the localization of glutamate receptors (GluRII) which was also altered by Aβ expression. Therefore, these results suggest that *Amph* might be downstream effectors of *lap*, and contribute to the amelioration in Aβ pathology.

4.2 Results

4.2.1 Endocytic and exocytic regulators modify $A\beta_{42}$ toxicity

I have shown that *lap* modestly attenuated Aβ toxicity. I next investigated whether other endocytic-exocytic proteins were involved with $A\beta_{42}$ toxicity. As PICALM physically interacted with endocytic genes like VAMP2 (*nSyb*), Rab5 and Rab11 (Zhao et al., 2015b), I performed a genetic screen of all accessible lines over-expressing genes regulating endocytosis or endocytic recycling. Among them, *Rab4*, *Rab8*, *Rab10* and *Rab11* mediate endocytic recycling, whereas *Rab5* and *Rab7* regulate endocytosis. In particular, *Rab5* contributes to trafficking from the plasma membrane to early endosomes and *Rab7* controls transporting from early endosomes to late endosomes. In addition to this, I screened genes engaged in vesicle formation. For example, clathrin helps to form coated vesicles. *Epsin* (*Lqf*) and *Eps15* (other types of adaptors) recruit cargos to the plasma membrane. *Bin1* (*Amph*), *Dynamin* (*Shi*) and *EndoA* are involved with vesicle scission and release. *Aux* is involved in the disassembly of coated vesicles. *Snap25* is widely located in the plasma membrane and in multi-vesicular bodies (MVBs) that drives vesicle fusion.

I crossed the lines over-expressing these genes to $A\beta_{42}$-expressing flies under the control of the neuronal elav promoter and induced gene expression in adult flies by feeding RU once the flies has eclosed. I then monitored their lifespan relative to flies over-expressing $A\beta_{42}$ alone. This screen showed that apart from the overexpression of wild type *Rab5*, overexpression of *Rab4*, *Rab7*, *Rab8*, *Rab10* and *Rab11* (Rab11-GFP) dramatically exacerbated $A\beta_{42}$ toxicity (Rab11-HA did not decrease lifespan of $A\beta_{42}$-expressing flies) (Figure 4.1, Figure 4.2 and Table 4.1, mean lifespan, Aβ RU200: 100 %; Aβ Snap25 RU200: 108 %; Aβ Syt RU200: 103 %; Aβ nSyb RU200: 100 %; Aβ Eps15 RU200: 100 %; Aβ Shi RU200: 100 %; Aβ Rab5[CA]

RU200: 100 %; Aβ Rab11-HA RU200: 100 %; Aβ Rab14 RU200: 97 %; Aβ Aux RU200: 92 %; Aβ Rab7 RU200: 92 %; Aβ Clc RU200: 89 %; Aβ Rab11-GFP RU200: 89 %; Aβ Rab30 RU200: 89 %; Aβ Rab4 RU200: 87 %; Aβ Rab8 RU200: 87 %; Aβ Lqf RU200: 84 %, n > 100 per condition. p was shown in Figure 4.1, log-rank test).

Consistent with a study on mammalian neurons, these results support the idea that active endocytosis, but not membrane recycling, can reverse $A\beta_{42}$–induced neurodegenerative defects (Treusch et al., 2011). However, my work further suggested that not all endocytic factors were beneficial in AD amelioration and some actually accelerated AD progression.

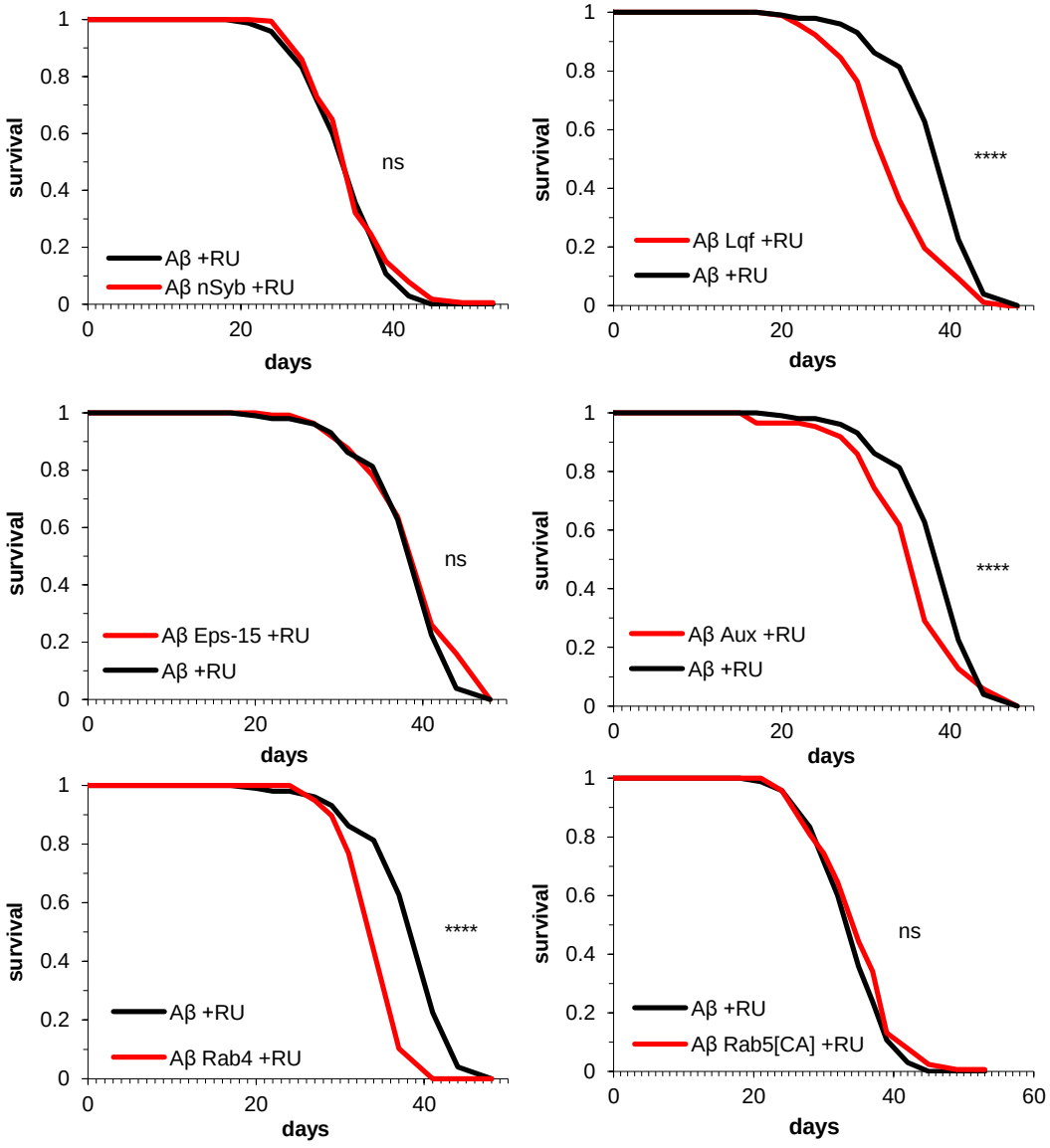

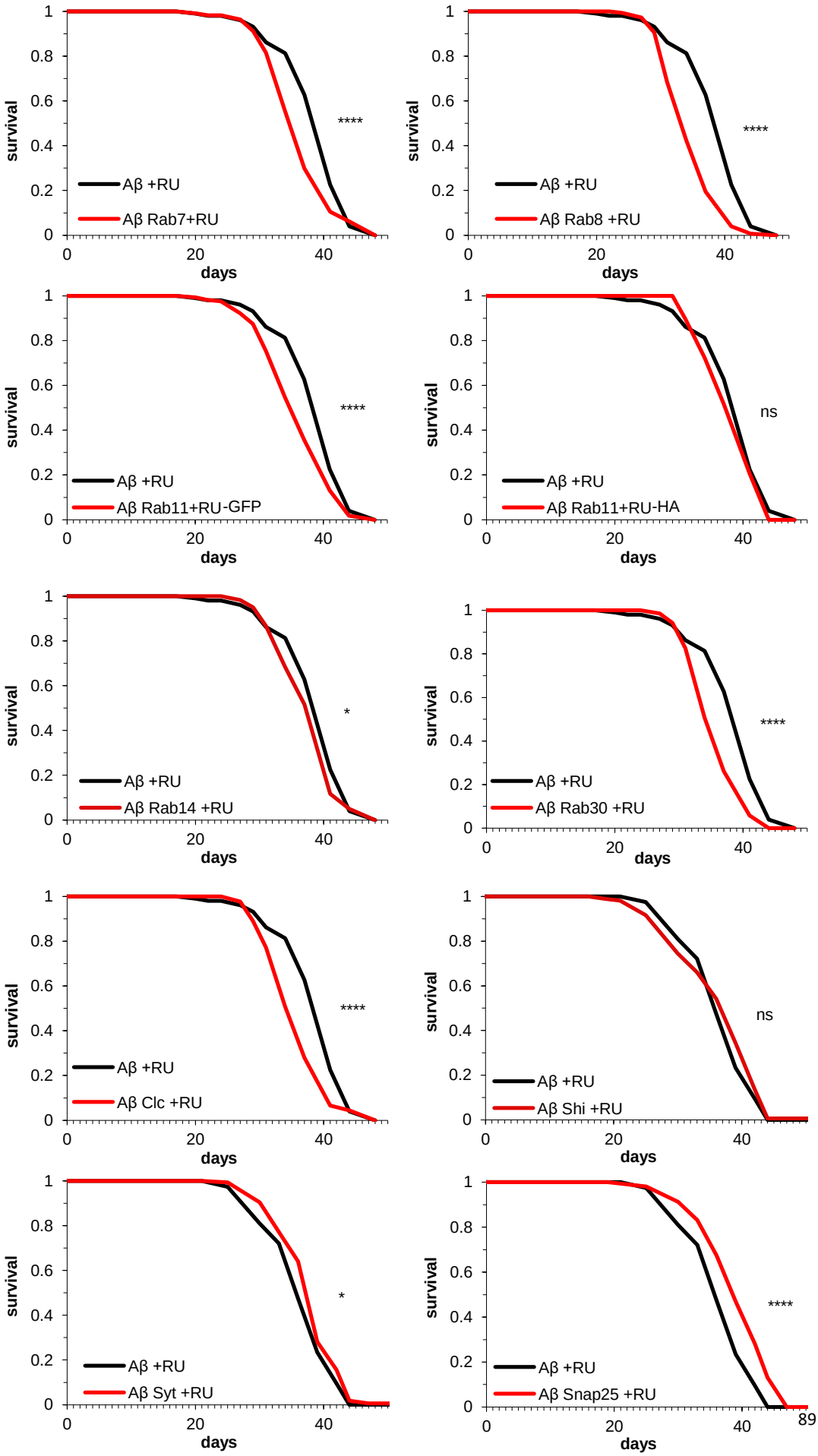
survival
days
Aβ +RU
Aβ Rab7+RU
****
Aβ Rab8 +RU
Aβ Rab11+RU-GFP
Aβ Rab11+RU-HA
ns
Aβ Rab14 +RU
*
Aβ Rab30 +RU
Aβ Clc +RU
Aβ Shi +RU
Aβ Syt +RU
Aβ Snap25 +RU

Figure 4.1 A genetic screen identifies regulators of $A\beta_{42}$ toxicity. Survival curves of flies expressing Aβ with endocytic-exocytic gene (red) or not (black) in adult neurons (+RU), n > 100. *p < 0.05, **p < 0.01, ***p < 0.001, ****p < 0.0001, n.s., not significant, comparison by log-rank test.

Table 4.1 Endocytic-exocytic genes in the *Drosophila* screen

Human gene	*Drosophila* homolog	Function	Effect on lifespan
BIN1	Amph	Vesicular scission	Increased
CD2AP	Cindr	Vesicular formation	Decreased
CLC	Clc	Vesicular formation	Decreased
DYNAMIN	Shi	Vesicular scission	NA
ENDOA	EndoA	Vesicular scission	Increased
EPS15	Eps15	Cargo selection	Decreased
EPSIN	Iqf	Cargo selection	Decreased
GAK	Aux	Vesicular disassembly	Decreased
RAB4	Rab4	Early endosome	Decreased
RAB5	Rab5	Early endosome	Increased
RAB7	Rab7	Late endosome	Decreased
RAB8	Rab8	Recycling endosome	Decreased
RAB10	Rab10	Recycling endosome	Decreased
RAB11	Rab11	Recycling endosome	Decreased
RAB14	Rab14	Recycling endosome	NA
SNAP25	Snap25	Exocytosis	Increased
SYT1	Syt	Exocytosis	Increased
VAMP2	nSyb	Endocytosis	NA

4.2.2 *Rab5*, *EndoA* and *Snap25* ameliorates $A\beta_{42}$ vulnerability

Although I found that a number of components did not improve $A\beta_{42}$ toxicity, I found that *Rab5*, *EndoA* and *Snap5* could alleviate $A\beta_{42}$ toxicity. In particular, I found that over-expression of wild type *Rab5* alleviated $A\beta_{42}$ toxicity, while active *Rab5* elevated $A\beta_{42}$ toxicity. Wild type *Rab5*

overexpression extended lifespan (Figure 4.2A, mean lifespan, Aβ RU0: 100 %; Aβ RU200: 49 %; Aβ Rab5 RU0: 106 %; Aβ Rab5 RU200: 58 %, n > 120 per condition. p was shown in Figure 4.2B, log-rank test) and also delayed the onset of climbing defects of $A\beta_{42}$-expressing flies (Figure 4.2B, PI, day 6, Aβ RU0: 89.67 ± 0.36 %; Aβ RU200: 91.36 ± 1.55 %; Aβ Rab5 RU0: 93.8 ± 0.56 %; Aβ Rab5 RU200: 93.84 ± 1.41 %; day 11, Aβ RU0: 90.42 ± 1.67 %; Aβ RU200: 94.96 ± 1.98 %; Aβ Rab5 RU0: 93.59 ± 0.74 %; Aβ Rab5 RU200: 89.49 ± 0.36 %; day 14, Aβ RU0: 90.77 ± 1.96 %; Aβ RU200: 79.74 ± 0.74 %; Aβ Rab5 RU0: 85.38 ± 3.26 %; Aβ Rab5 RU200: 91.67 ± 1.04 %; day 18, Aβ RU0: 88.16 ± 0.76 %; Aβ RU200: 71.16 ± 1.16 %; Aβ Rab5 RU0: 83.21 ± 1.51 %; Aβ Rab5 RU200: 77.48 ± 3.41 %; day 21, Aβ RU0: 84.8 ± 1.77 %; Aβ RU200: 50.67 ± 2.45 %; Aβ Rab5 RU0: 80.92 ± 1.76 %; Aβ Rab5 RU200: 58.7 ± 3.38 %; day 25, Aβ RU0: 82.2 ± 1.78 %; Aβ RU200: 36.34 ± 3.2 %; Aβ Rab5 RU0: 78.09 ± 4.58 %; Aβ Rab5 RU200: 44.84 ± 1.05 %, n = 3 per condition. Interaction of time and genotype, $p < 0.0001$; time, $p < 0.0001$, genotype, $p < 0.0001$, two-ways ANOVA). Although the Aβ Rab5 RU0 condition showed a lifespan increase when comparing to the Aβ RU0 condition, the Aβ Rab5 RU200 condition had relative longer lifespan compared to the Aβ RU200 condition (Mean lifespan of Aβ RU200 vs Aβ RU0 is 49%; mean lifespan of Aβ Rab5 RU200 vs Aβ Rab5 RU0 is 55%). Moreover, *EndoA* over-expression exclusively restored the lifespan of $A\beta_{42}$-expressing flies from 50% to 62% (Figure 4.2D, mean lifespan, Aβ RU0: 100 %; Aβ RU200: 50 %; Aβ EndoA RU0: 95 %; Aβ EndoA RU200: 59 %, n > 120 per condition. p was shown in Figure 4.2D, log-rank test) and *Snap25* over-expression attenuated their locomotor defects (Figure 4.2E, PI, day 7, Aβ RU0: 91.33 ± 1.45 %; Aβ RU200: 88.19 ± 1.84 %; Aβ Snap25 RU0: 69.33 ± 2.37 %; Aβ Snap25 RU200: 89.7 ± 3.07 %; day 14, Aβ RU0: 95.33 ± 1.33 %; Aβ RU200: 82.23 ± 1.05 %; Aβ Snap25 RU0: 66.77 ± 1.83 %; Aβ Snap25 RU200: 72.67 ± 1.27 %; day 24, Aβ RU0: 90.57 ± 2.5 %; Aβ RU200: 51.9 ± 1.66 %; Aβ Snap25 RU0: 64.93 ± 3.42 %; Aβ Snap25 RU200: 63.21 ± 2.09 %; day 28, Aβ RU0: 79.25 ± 2.78 %; Aβ RU200: 24.06 ± 1.2 %; Aβ Snap25 RU0: 46.12 ± 8.01 %; Aβ Snap25 RU200: 32.36 ± 3.68 %; day 31, Aβ RU0: 70.75 ± 2.78 %; Aβ RU200: 16.18 ± 1.47 %; Aβ Snap25 RU0: 41.32 ± 2.5 %; Aβ Snap25 RU200: 24.36 ± 0.03 %, n = 3 per condition. Interaction of time and genotype, $p < 0.0001$; time, $p < 0.0001$, genotype, $p < 0.0001$, two-ways ANOVA). As mean lifespan of the Aβ EndoA RU0 condition was shorter than that of the Aβ RU0 condition and locomotor

performance of the Aβ Snap25 RU0 condition was worse than that of the Aβ RU0 condition, if all uninduced conditions have the same lifespan and locomotor performance, co-expression of Aβ and *EndoA* might show a bigger lifespan increase and co-expression of Aβ and *Snap25* might have a better alleviation of locomotor defects. Similar to *lap*, neuroprotection of these genes was independent of $A\beta_{42}$ clearance (Figure 4.2C and F). Collectively, my work suggested a lap-EndoA-Rab5-Snap25 pathway that protected neurons from $A\beta_{42}$ toxicity.

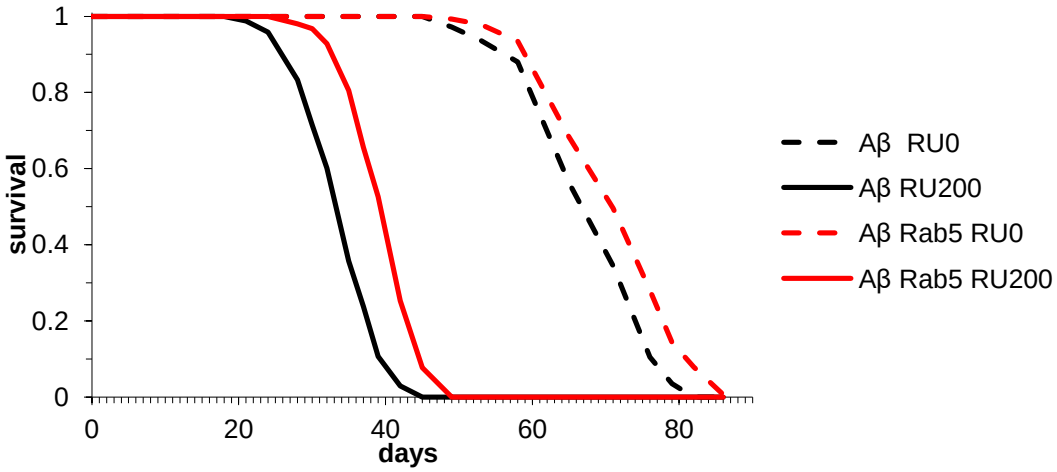

(A)

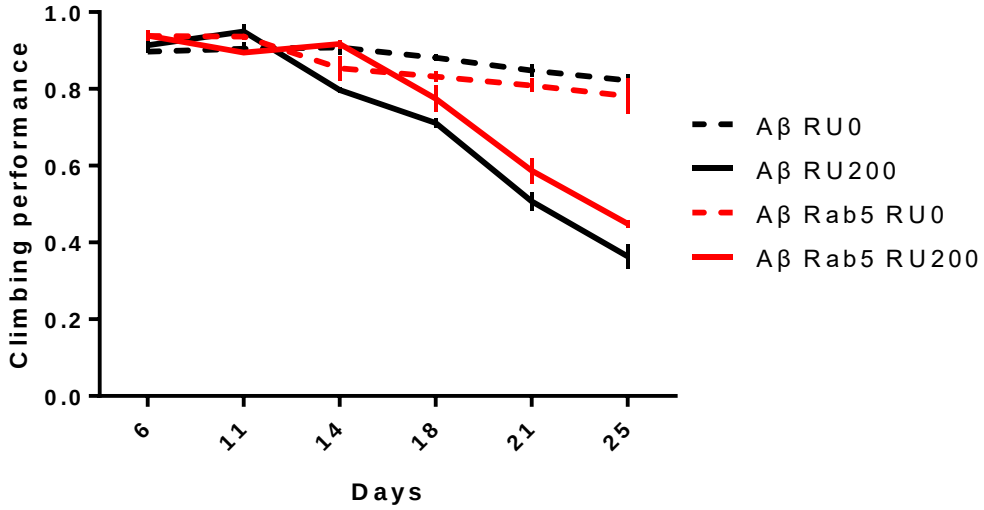

(B)

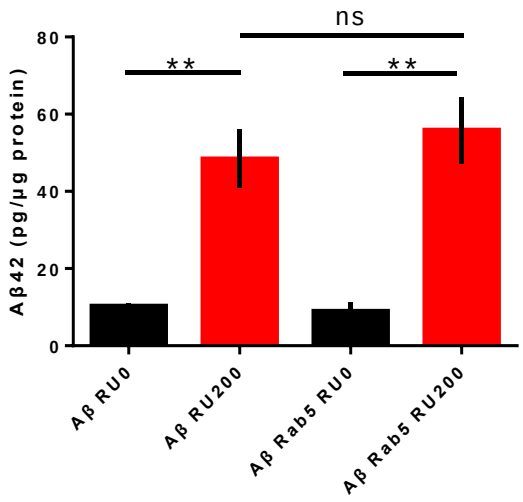
ns
**
**
Aβ42 (pg/µg protein)
80
60
40
20
0
Aβ RU0
Aβ RU200
Aβ Rab5 RU0
Aβ Rab5 RU200

(C)

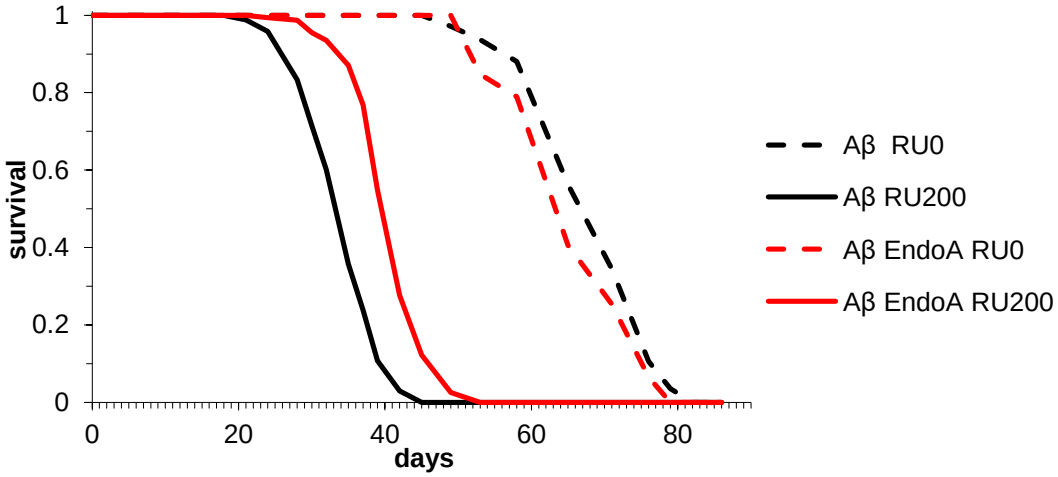
survival
1
0.8
0.6
0.4
0.2
0
0
20
40
60
80
days
Aβ RU0
Aβ RU200
Aβ EndoA RU0
Aβ EndoA RU200

(D)

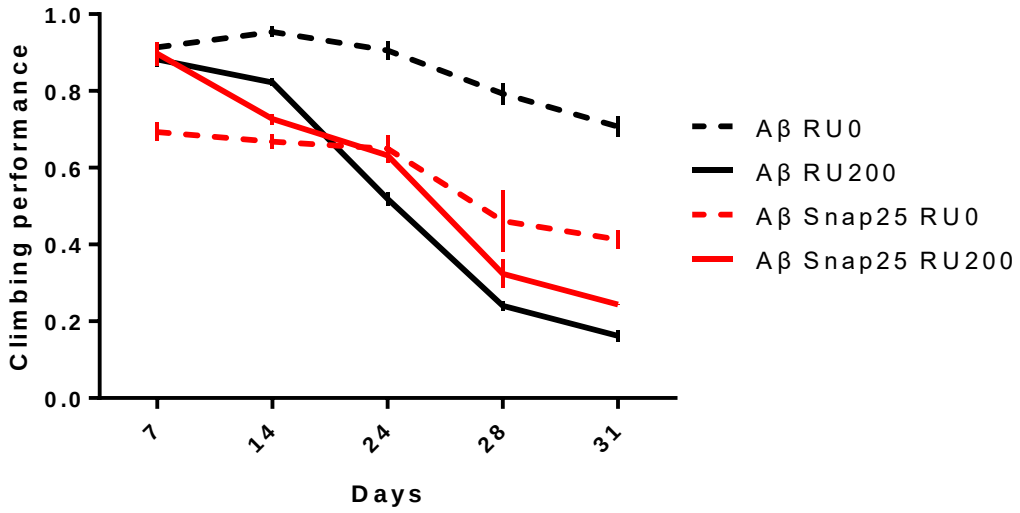

(E)

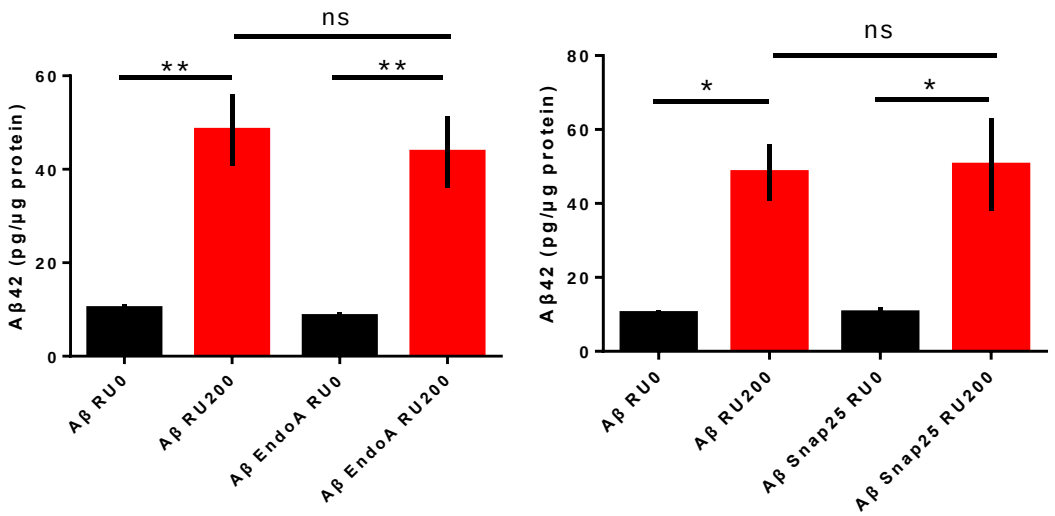

(F)

Figure 4.2 *Rab5* delays onset of Aβ-induced neurodegeneration.

(A) Lifespan curves of flies expressing Aβ with or without *Rab5* wild type version in neurons (+RU) and uninduced controls (-RU). Genotypes: UAS-Aβ; elavGS, UAS-Aβ/UAS-rab5; elavGS. n > 120. Aβ RU0 vs Aβ RU200, $p < 0.0001$; Aβ RU0 vs Aβ Rab5 RU0, $p < 0.0001$; Aβ Rab5 RU0 vs Aβ Rab5 RU200, $p < 0.0001$; Aβ RU200 vs Aβ Rab5 RU200, $p < 0.0001$, comparison by log-rank test.

(B) Locomotor performance index for the same flies plotted over time. n = 3. Genotypes are as above. Interaction of time and genotype, $p < 0.0001$; time, $p < 0.0001$, genotype, $p < 0.0001$, determined by two-ways ANOVA followed by Tukey's *post-hoc* test. Statistical analyses were shown in Table 4.2.

(C) $A\beta_{42}$ protein levels, measured by ELISA, in the heads of 24-day-old flies. Co-expression of Aβ and *Rab5* did not

change $A\beta_{42}$ levels when comparing Aβ-expressing flies. Means ± SEM, n = 3. ***p < 0.001, determined by one-way ANOVA; Aβ RU0 vs Aβ RU200, **p < 0.01; Aβ RU0 vs Aβ Rab5 RU0, n.s., not significant; Aβ Rab5 RU0 vs Aβ Rab5 RU200, **p < 0.01; Aβ RU200 vs Aβ Rab5 RU200, n.s., not significant, comparison by Tukey's *post-hoc* test.

(D) Adult survival of flies harboring Aβ with or without *EndoA* in adult neurons (+RU) and uninduced controls (-RU). Over-expression of *EndoA* modestly suppressed shortened lifespan induced by Aβ, n > 120. Aβ RU0 vs Aβ RU200, p < 0.0001; Aβ RU0 vs Aβ EndoA RU0, n.s., not significant; Aβ EndoA RU0 vs Aβ EndoA RU200, p < 0.0001; Aβ RU200 vs Aβ EndoA RU200, p < 0.0001, by log-rank test.

(E) Climbing index of flies expressing Aβ with or without *Snap25* in adult neurons (+RU) and uninduced controls (-RU). Overexpression of *Snap25* attenuated climbing defects induced by Aβ, n = 3. Interaction of time and genotype, p < 0.0001; time, p < 0.0001, genotype, p < 0.0001, determined by two-ways ANOVA followed by Tukey's *post-hoc* test. Statistical analyses were shown in Table 4.3.

(F) Flies expressing Aβ had similar levels of $A\beta_{42}$ when comparing flies expressing either Aβ EnodA or Aβ Snap25, indicating that *EnodA* and *Snap25* do not alter Aβ clearance. Means ± SEM, n = 3. **p < 0.01, determined by one-way ANOVA; *p < 0.05, **p < 0.01, ns, not significant, by Tukey's *post-hoc* test.

Table 4.2 Statistical summary of locomotor performance index of flies expressing Aβ with or without *Rab5*

Day 6	Aβ RU0	Aβ RU200	Aβ Rab5 RU0	Aβ Rab5 RU200
Aβ RU0		n.s.	n.s.	n.s.
Aβ RU200			n.s.	n.s.
Aβ Rab5 RU0				n.s.
Aβ Rab5 RU200				
Day 11	Aβ RU0	Aβ RU200	Aβ Rab5 RU0	Aβ Rab5 RU200
Aβ RU0		n.s.	n.s.	n.s.
Aβ RU200			n.s.	n.s.
Aβ Rab5 RU0				n.s.
Aβ Rab5 RU200				
Day 14	Aβ RU0	Aβ RU200	Aβ Rab5 RU0	Aβ Rab5 RU200
Aβ RU0		< 0.01	n.s.	n.s.
Aβ RU200			n.s.	< 0.001

Aβ Rab5 RU0				< 0.001
Aβ Rab5 RU200				
Day 18	Aβ RU0	Aβ RU200	Aβ Rab5 RU0	Aβ Rab5 RU200
Aβ RU0		< 0.0001	n.s.	< 0.01
Aβ RU200			< 0.001	n.s.
Aβ Rab5 RU0				n.s.
Aβ Rab5 RU200				
Day 21	Aβ RU0	Aβ RU200	Aβ Rab5 RU0	Aβ Rab5 RU200
Aβ RU0		< 0.0001	n.s.	< 0.0001
Aβ RU200			< 0.0001	< 0.05
Aβ Rab5 RU0				< 0.0001
Aβ Rab5 RU200				
Day 25	Aβ RU0	Aβ RU200	Aβ Rab5 RU0	Aβ Rab5 RU200
Aβ RU0		< 0.0001	n.s.	< 0.0001
Aβ RU200			< 0.0001	< 0.05
Aβ Rab5 RU0				< 0.0001
Aβ Rab5 RU200				

Table 4.3 Statistical summary of locomotor performance index of flies expressing Aβ with or without *Snap25*

Day 7	Aβ RU0	Aβ RU200	Aβ Snap25 RU0	Aβ Snap25 RU200
Aβ RU0		n.s.	< 0.0001	n.s.
Aβ RU200			< 0.001	n.s.
Aβ Snap25 RU0				< 0.0001
Aβ Snap25 RU200				
Day 14	Aβ RU0	Aβ RU200	Aβ Snap25 RU0	Aβ Snap25 RU200
Aβ RU0		< 0.05	< 0.0001	< 0.0001
Aβ RU200			< 0.01	n.s.
Aβ Snap25 RU200				n.s.
Aβ Snap25 RU200				

Day 24	Aβ RU0	Aβ RU200	Aβ Snap25 RU0	Aβ Snap25 RU200
Aβ RU0		< 0.0001	< 0.0001	< 0.0001
Aβ RU200			< 0.05	< 0.05
Aβ Snap25 RU0				n.s.
Aβ Snap25 RU200				
Day 28	Aβ RU0	Aβ RU200	Aβ Snap25 RU0	Aβ Snap25 RU200
Aβ RU0		< 0.0001	< 0.0001	< 0.0001
Aβ RU200			< 0.0001	< 0.05
Aβ Snap25 RU0				< 0.01
Aβ Snap25 RU200				
Day 31	Aβ RU0	Aβ RU200	Aβ Snap25 RU0	Aβ Snap25 RU200
Aβ RU0		< 0.0001	< 0.0001	< 0.0001
Aβ RU200			< 0.0001	< 0.05
Aβ Snap25 RU0				< 0.001
Aβ Snap25 RU200				

4.2.3 *Amph* alleviates $A\beta_{42}$ toxicity

Together with *Rab5*, *EndoA* and *Snap25*, *Amph* was another hit to ameliorate Aβ toxicity. *Amph* is the *Drosophila* homologue of BIN1 that is linked to AD. Like *EndoA*, *Amph* is involved in vesicle scission. *Amph* slightly prolonged the lifespan of $A\beta_{42}$-expressing flies (Fig 4.3A, Aβ RU0: 100 %; Aβ RU200: 47 %; Aβ Amph RU0: 100 %; Aβ Amph RU200: 51 %, n > 120 per condition. p was shown in Figure 4.3A, log-rank test; Figure 4.3B, day 5, Aβ RU0: 87.64 ± 9.4 %; Aβ RU200: 81.41 ± 4.6 %; Aβ Amph RU0: 91.48 ± 0.74 %; Aβ Amph RU200: 90.94 ± 2.02 %; day 8, Aβ RU0: 92.84 ± 2.64 %; Aβ RU200: 67.26 ± 1.49 %; Aβ Amph RU0: 83.22 ± 1 %; Aβ Amph RU200: 86.27 ± 0.42 %; day 11, Aβ RU0: 86.61 ± 1.72 %; Aβ RU200: 59.57 ± 2.46 %; Aβ Amph RU0: 79.37 ± 2.78 %; Aβ Amph RU200: 83.97 ± 1.4 %; day 14, Aβ RU0: 87 ± 2.65 %; Aβ RU200: 54.71 ± 3.22 %; Aβ Amph RU0: 74.52 ± 5.67 %; Aβ Amph RU200: 67.35 ± 0 %; day 18, Aβ RU0: 87.58 ± 1.63 %; Aβ RU200: 32.52 ± 2.93 %; Aβ Amph RU0: 72.36 ± 2.85 %; Aβ Amph RU200: 36.47 ± 2.98 %; day 23, Aβ RU0: 82.49 ± 2.39 %; Aβ RU200: 8.33 ±

2.79 %; Aβ Amph RU0: 62.77 ± 2.18 %; Aβ Amph RU200: 19.58 ± 1.82 %; day 26, Aβ RU0: 70.19 ± 1.11 %; Aβ RU200: 2.56 ± 1.28 %; Aβ Amph RU0: 57.08 ± 1.5 %; Aβ Amph RU200: 5.83 ± 0.42 %, n = 3 per condition. Interaction of time and genotype, $p < 0.0001$; time, $p < 0.0001$, genotype, $p < 0.0001$, two-ways ANOVA) without affecting Aβ levels (Fig 4.3D, Aβ RU0: 4.02 ± 0.01 pg/ug protein; Aβ RU200: 58.54 ± 8.14 pg/ug protein; Aβ Amph RU0: 3.50 ± 0.73 pg/ug protein; Aβ lap RU200: 73.28 ± 1.89 pg/ug protein, n = 3 per condition; $p < 0.0001$; one-way ANOVA). This suggested that *Amph* plays a role in downstream Aβ toxicity. RNAi of *Amph*, on the other hand, worsened the phenotype of Aβ expressing flies (Figure 4.3C, Aβ RU0: 100 %; Aβ RU200: 59 %; Aβ Amph RNAi RU0: 100 %; Aβ Amph RNAi RU200: 56 %, n > 120 per condition. p was shown in Figure 4.3C, log-rank test). These findings are in line with the fact that the *Amph* mutant was reported to display a flightless phenotype and climbing defects (Leventis et al., 2001; Razzaq et al., 2001). However, *Amph* is expressed post-synaptically (Razzaq et al., 2001; Zelhof et al., 2001) and participates in protein localization.

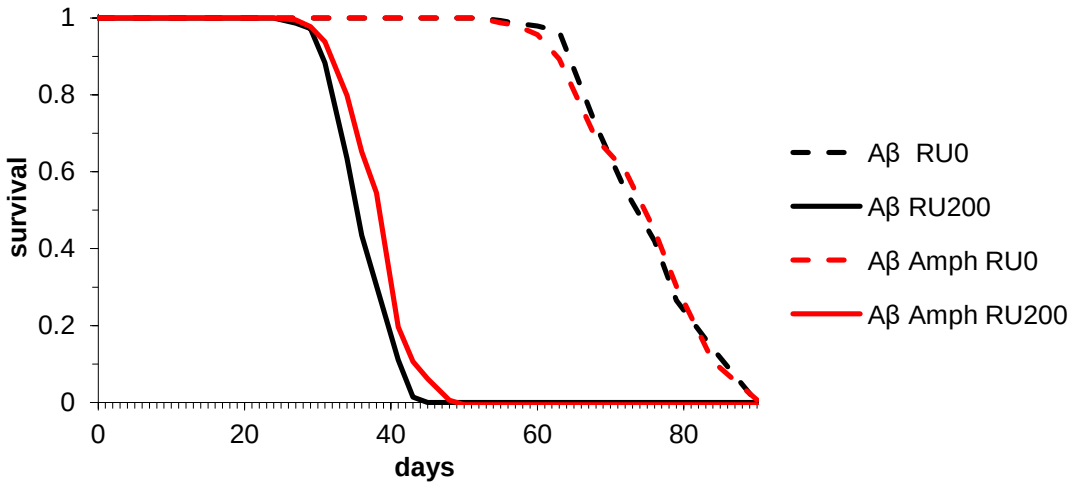

(A)

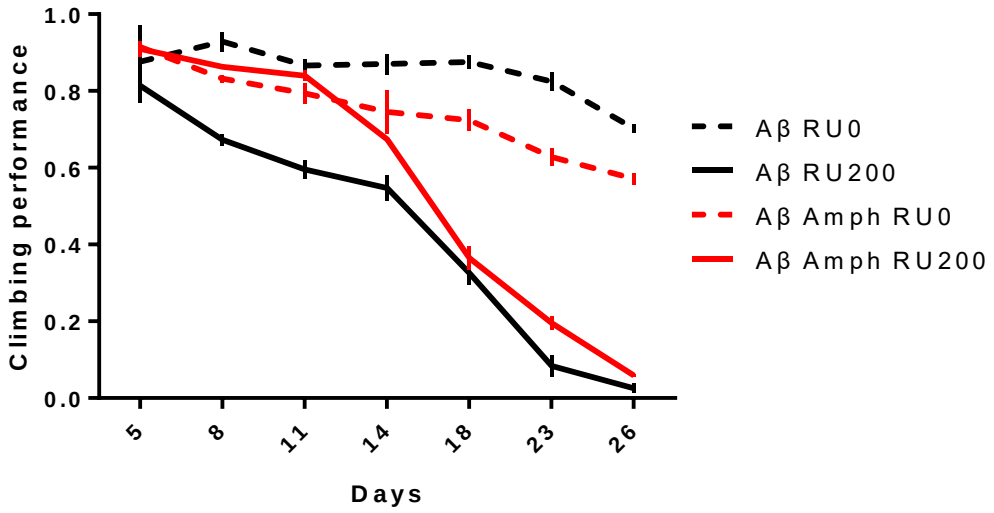
Climbing performance
1.0
0.8
0.6
0.4
0.2
0.0
5
8
11
14
18
23
26
Days
Aβ RU0
Aβ RU200
Aβ Amph RU0
Aβ Amph RU200

(B)

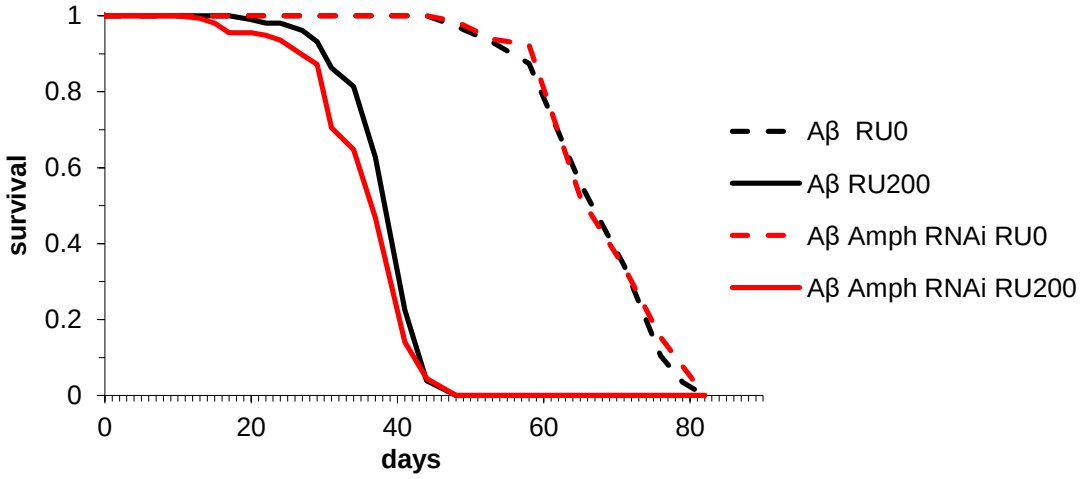
survival
1
0.8
0.6
0.4
0.2
0
0
20
40
60
80
days
Aβ RU0
Aβ RU200
Aβ Amph RNAi RU0
Aβ Amph RNAi RU200

(C)

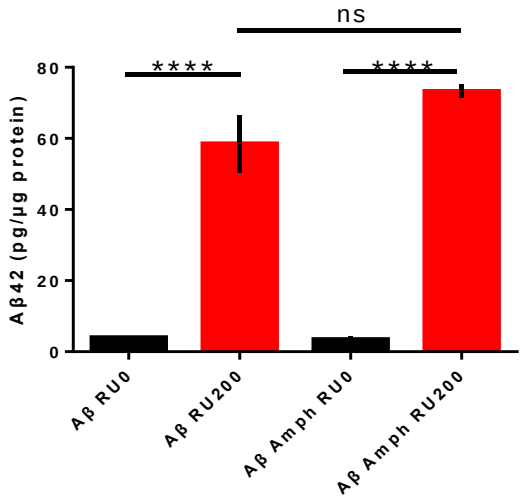
ns
****
****
Aβ42 (pg/µg protein)
80
60
40
20
0
Aβ RU0
Aβ RU200
Aβ Amph RU0
Aβ Amph RU200

(D)

Figure 4.3 *Amph* reduces $A\beta_{42}$ toxicity.

(A) Survival curves of flies expressing Aβ with *Amph* or not in adult neurons (+RU) and uninduced controls (-RU). Over-expression of *Amph* in neurons restored lifespan, n > 120. Aβ RU0 vs Aβ RU200, $p < 0.0001$; Aβ RU0 vs Aβ Amph RU0, n.s., not significant; Aβ Amph RU0 vs Aβ Amph RU200, $p < 0.0001$; Aβ RU200 vs Aβ Amph RU200, $p < 0.01$, by log-rank test.

(B) Locomotor performance index of flies of the same genotypes. Aβ caused climbing defects, which was diminished by expression of *Amph*, n = 3. Interaction of time and genotype, $p < 0.0001$; time, $p < 0.0001$, genotype, $p < 0.0001$, comparison by two-ways ANOVA followed by Tukey's *post-hoc* test. Statistical analyses were shown in Table 4.4.

(C) Survival curves of flies expressing Aβ with *Amph* RNAi or not in adult neurons (+RU) and uninduced controls (-RU). Downregulation of *Amph* suppressed lifespan, n > 120. Aβ RU0 vs Aβ RU200, $p < 0.0001$; Aβ RU0 vs Aβ Amph RNAi RU0, n.s., not significant; Aβ Amph RNAi RU0 vs Aβ Amph RNAi RU200, $p < 0.0001$; Aβ RU200 vs Aβ Amph RNAi RU200, $p < 0.01$, by log-rank test.

(D) $A\beta_{42}$ protein levels, measured by ELISA, in the heads of 21-day-old flies expressing Aβ with *Amph* or not in neurons (+RU) and uninduced controls (-RU). Means ± SEM, n = 3. ****$p < 0.0001$, by one-way ANOVA; Aβ RU0 vs Aβ RU200, ****$p < 0.0001$; Aβ RU0 vs Aβ Amph RU0, n.s., not significant; Aβ Amph RU0 vs Aβ Amph RU200, ****$p < 0.0001$; Aβ RU200 vs Aβ Amph RU200, n.s., not significant, by Tukey's *post-hoc* test.

Table 4.4 Statistical summary of locomotor performance index of flies expressing Aβ with or without *Amph*

Day 5	Aβ RU0	Aβ RU200	Aβ Amph RU0	Aβ Amph RU200
Aβ RU0		n.s.	n.s.	n.s.
Aβ RU200			n.s.	n.s.
Aβ Amph RU0				n.s.
Aβ lap RNAi RU200				
Day 8	Aβ RU0	Aβ RU200	Aβ Amph RU0	Aβ Amph RU200
Aβ RU0		< 0.0001	n.s.	n.s.
Aβ RU200			< 0.01	< 0.001
Aβ Amph RU0				n.s.
Aβ Amph RU200				
Day 11	Aβ RU0	Aβ RU200	Aβ Amph RU0	Aβ Amph RU200

Aβ RU0		< 0.0001	n.s.	n.s.
Aβ RU200			< 0.0001	< 0.0001
Aβ Amph RU0				n.s.
Aβ Amph RU200				
Day 14	Aβ RU0	Aβ RU200	Aβ Amph RU0	Aβ Amph RU200
Aβ RU0		< 0.0001	< 0.05	< 0.001
Aβ RU200			< 0.0001	< 0.05
Aβ Amph RU0				n.s.
Aβ Amph RU200				
Day 18	Aβ RU0	Aβ RU200	Aβ Amph RU0	Aβ Amph RU200
Aβ RU0		< 0.0001	< 0.01	< 0.0001
Aβ RU200			< 0.0001	n.s.
Aβ Amph RU0				< 0.0001
Aβ Amph RU200				
Day 23	Aβ RU0	Aβ RU200	Aβ Amph RU0	Aβ Amph RU200
Aβ RU0		< 0.0001	< 0.001	< 0.0001
Aβ RU200			< 0.0001	< 0.05
Aβ Amph RU0				< 0.0001
Aβ Amph RU200				
Day 26	Aβ RU0	Aβ RU200	Aβ Amph RU0	Aβ Amph RU200
Aβ RU0		< 0.0001	< 0.05	< 0.0001
Aβ RU200			< 0.0001	n.s.
Aβ Amph RU0				< 0.0001
Aβ Amph RU200				

4.2.4 *Amph* modulates GluRII accumulation

Amph has been shown to modulate the localization of Dlg. Dlg is the *Drosophila* homolog of the PSD-95 protein that stabilizes glutamate receptors (GluRII) (Razzaq et al., 2001; Zelhof et al., 2001). GluRII is composed of regulatory GluRIIA, GluRIIB and constitutive GluRIIC,

GluRIIA was found to increase postsynaptic sensitivity, while GluRIIB decreased it (Davis et al., 1998; DiAntonio et al., 1999; Petersen et al., 1997; Schuster et al., 1991). I checked whether *Amph* regulated GluRII localization. I used Mef2-Gal4 to express $A\beta_{42}$ post-synaptically and imaged GluRII localization in larval NMJ. I found that GluRIIA substantially accumulated on the plasma membrane (Figure 4.4A, Mef2: 100 $\pm$ 6.46 %, n = 7; Mef2 > Aβ: 164 $\pm$ 23.01 %, n = 8; Mef2 > Amph: 44.52 $\pm$ 4.16 %, n = 10; Mef2 > Aβ Amph: 47 $\pm$ 3.31, n = 10. $p < 0.0001$; one-way ANOVA), while GluRIIB decreased upon $A\beta_{42}$ exposure (Figure 4.4B, Mef2: 100 $\pm$ 19.62 %, n = 10; Mef2 > Aβ: 23.11 $\pm$ 7.64 %, n = 10; Mef2 > Amph: 14.77 $\pm$ 4.13 %, n = 8; Mef2 > Aβ Amph: 23.83 $\pm$ 9.39, n = 8. $p < 0.001$; one-way ANOVA). GluRIIC localization was not changed (Figure 4.4C, Mef2: 100 $\pm$ 19.07 %, n = 8; Mef2 > Aβ: 102.4 $\pm$ 15.21 %, n = 10; Mef2 > Amph: 41.46 $\pm$ 17.95 %, n = 7; Mef2 > Aβ Amph: 26.11 $\pm$ 9.72, n = 7. $p < 0.01$; one-way ANOVA), suggesting that Aβ expression can alter the composition of GluRII receptors post-synaptically. In fact, the elevated Aβ levels lead to hyperexcitability (Ping et al., 2015). Next we over-expressed *Amph* post-synaptically leading to a dramatic decrease in the localization of all the GluRII subunits at the NMJ (Fig 4.4A, B and C), indicating that *Amph* modulates glutamate receptor localization. Given that *Amph* also reduced the accumulation of GluRII without Aβ expression, this suggested that *Amph* modulates the localization of GluRII independent of Aβ induction, namely, *Amph* is a modulator of Aβ toxicity. In conclusion, Aβ expression leads to an increase in GluRIIA accumulation at the synapse with glutamate excitotoxicity, whereas *Amph* decreases GluRIIA levels back down and therefore reduces glutamate excitotoxicity.

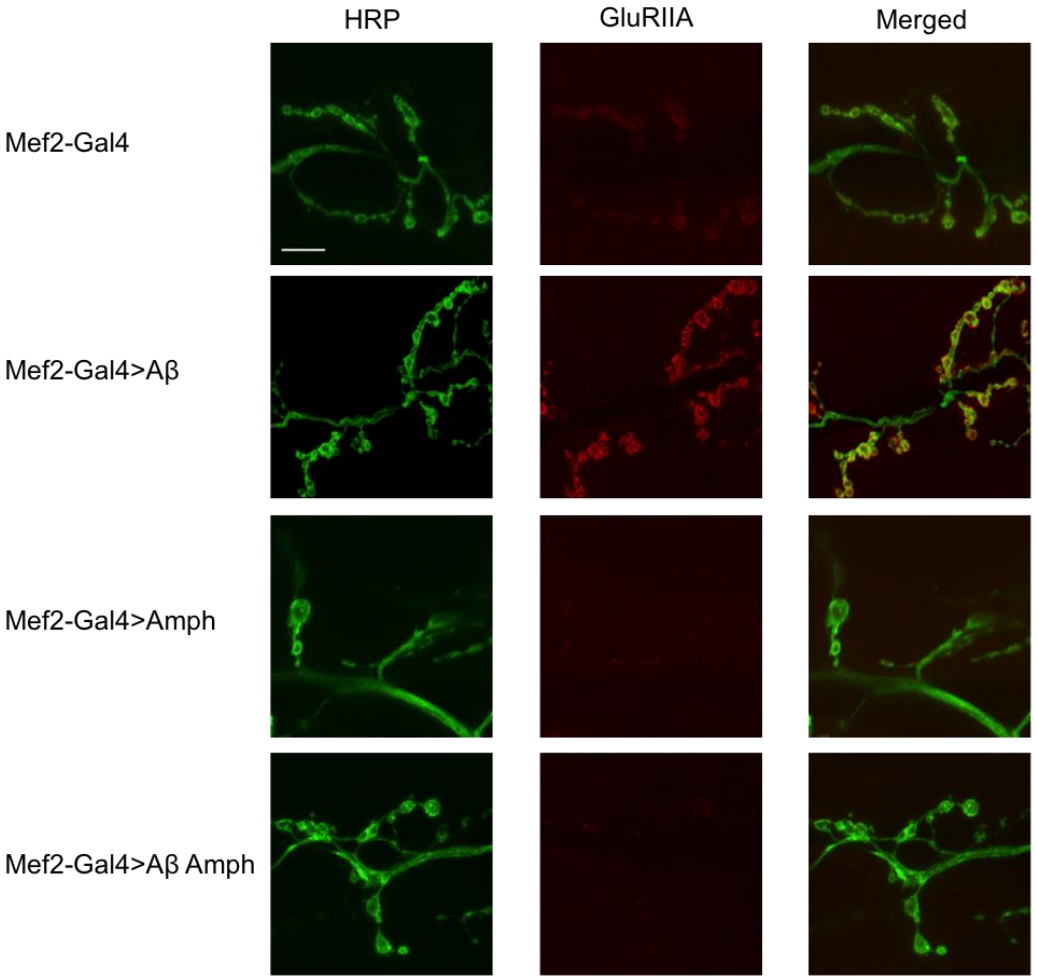
HRP
GluRIIA
Merged
Mef2-Gal4
Mef2-Gal4>Aβ
Mef2-Gal4>Amph
Mef2-Gal4>Aβ Amph

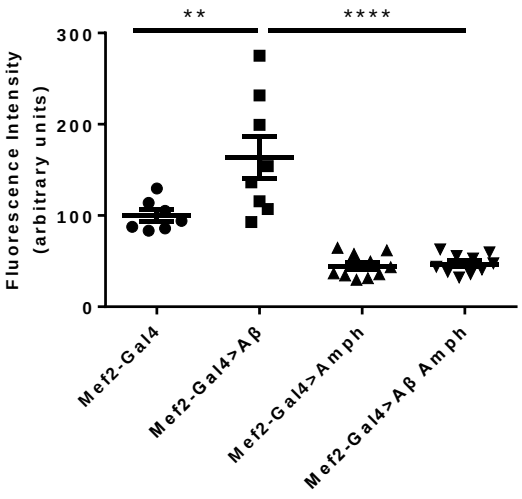
**
****
300
200
100
0
Fluorescence Intensity
(arbitrary units)
Mef2-Gal4
Mef2-Gal4>Aβ
Mef2-Gal4>Amph
Mef2-Gal4>Aβ Amph

(A)

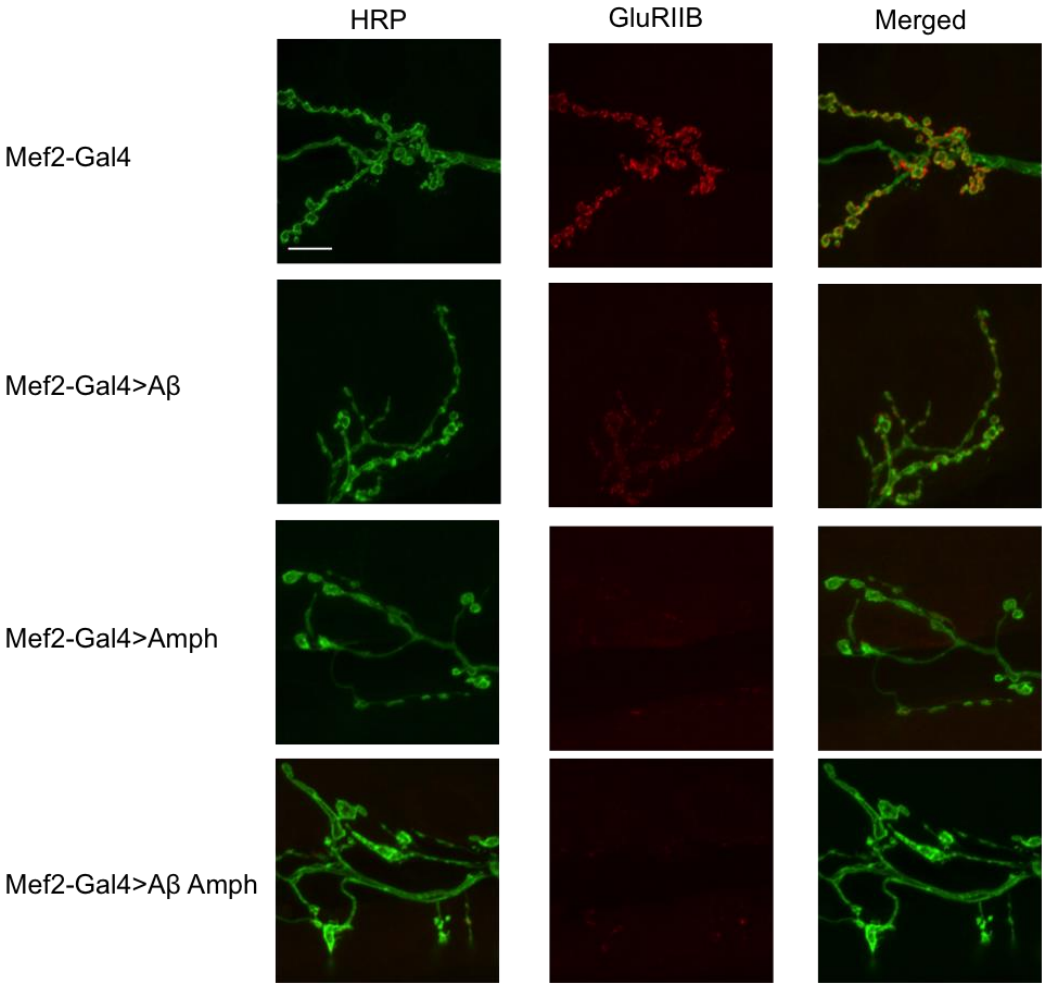
HRP
GluRIIB
Merged
Mef2-Gal4
Mef2-Gal4>Aβ
Mef2-Gal4>Amph
Mef2-Gal4>Aβ Amph

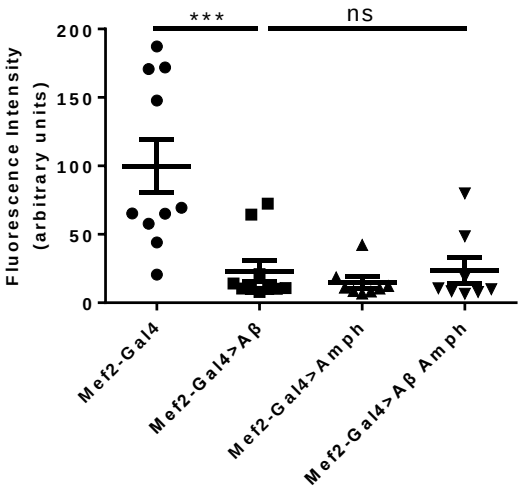
***
ns
Fluorescence Intensity (arbitrary units)
200
150
100
50
0
Mef2-Gal4
Mef2-Gal4>Aβ
Mef2-Gal4>Amph
Mef2-Gal4>Aβ Amph

(B)

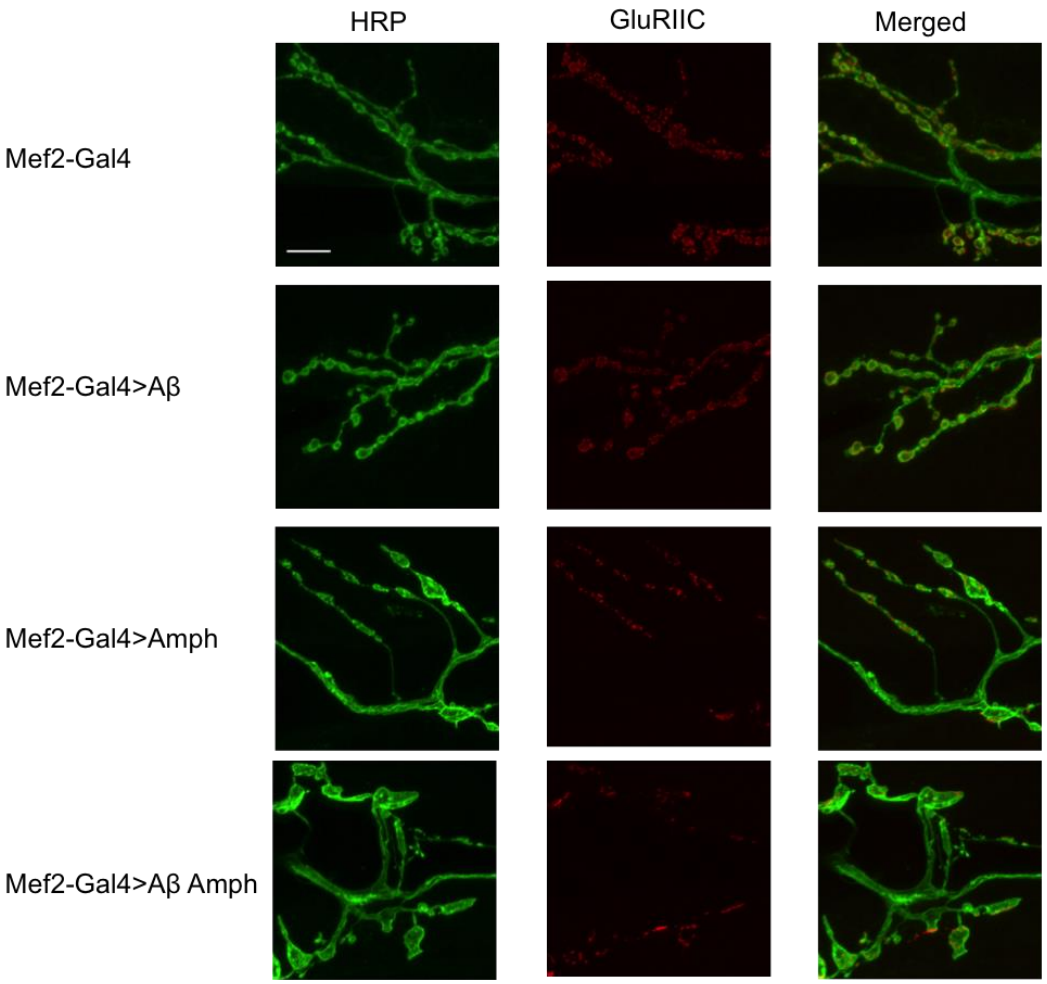

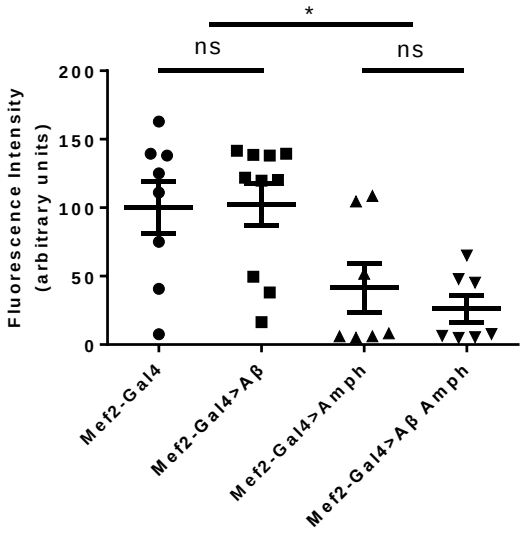

(C)

Figure 4.4 *Amph* modulates GluRIIA, GluRIIB and GluRIIC localization.

(A) Confocal images of the NMJ of wandering third-instar larvae expressing Aβ, *Amph* or both driven by Mef2-Gal4. Fluorescence intensity scores are plotted as means ± SEM, n ≥ 7. Genotypes: Mef2-Gal4, UAS-Aβ; Mef2-Gal4, UAS-amph; Mef2-Gal4, UAS-Aβ; UAS-amph/Mef2-Gal4. ****p < 0.0001, determined by one-way ANOVA; control

(Mef2-Gal4) vs Aβ, **p < 0.01; control vs Amph, **p < 0.01; Amph vs Aβ Amph, n.s., not significant; Aβ vs Aβ Amph, ****p < 0.0001, comparison by Tukey's *post-hoc* test. Scale bar, 10 μm.

(B) Quantification of GluRIIB fluorescence at the NMJ of wandering third-instar larvae expressing Aβ, *Amph* or both driven by Mef2-Gal4, plotted as means ± SEM, n ≥ 8. Genotypes: Mef2-Gal4, UAS-Aβ; Mef2-Gal4, UAS-amph; Mef2-Gal4, UAS-Aβ; UAS-amph/Mef2-Gal4. ***p < 0.001, by one-way ANOVA; control (Mef2-Gal4) vs Aβ, ***p < 0.001; control vs Amph, ***p < 0.001; Amph vs Aβ Amph, n.s., not significant; Aβ vs Aβ Amph, n.s., not significant, by Tukey's *post-hoc* test. Scale bar, 10 μm.

(C) Quantification of GluRIIC fluorescence at the NMJ of wandering third-instar larvae expressing Aβ, *Amph* or both driven by Mef2-Gal4, plotted as means ± SEM, n ≥ 7. Genotypes are as above. **p < 0.01, by one-way ANOVA; control (Mef2-Gal4) vs Aβ, n.s., not significant; control vs Amph, *p < 0.05; Amph vs Aβ Amph, n.s., not significant; Aβ vs Aβ Amph, *p < 0.05, by Tukey's *post-hoc* test. Scale bar, 10 μm.

4.2.5 Loss of Amph is rescued by *lap*

Next I further examined the effect of Aβ on *Amph* expression and localization. *Amph* is post-synaptic whereas our previous data suggest Aβ and *lap* act pre-synaptically. I therefore assessed Amph localization at the NMJ while expressed Aβ both pre-synaptically with D42-Gal4 or post-sypaptically with Mef2-Gal4. Interestingly I saw that, in both cases, Amph abundance was significantly decreased upon $A\beta_{42}$ expression (Figure 4.5A and B, Mef2: 100 ± 9.49 %, n = 5; Mef2 > Aβ: 30.76 ± 5.7 %, n = 7. p < 0.001; Student's t-test). Over-expression of *lap* pre-synaptically together with $A\beta_{42}$ rescued Amph localization at the NMJ (Fig 4.5A, D42: 100 ± 9.3 %, n = 7; D42 > Aβ: 37.38 ± 6.81 %, n = 7; D42 > lap: 116.6 ± 15.36 %, n = 9; D42 > Aβ lap: 108.6 ± 10.1, n = 10. p < 0.001; one-way ANOVA). Amph localization has been shown previously to be post-synaptic, so it is really intriguing that pre-synaptic proteins can effect localization of Amph post-synaptically.

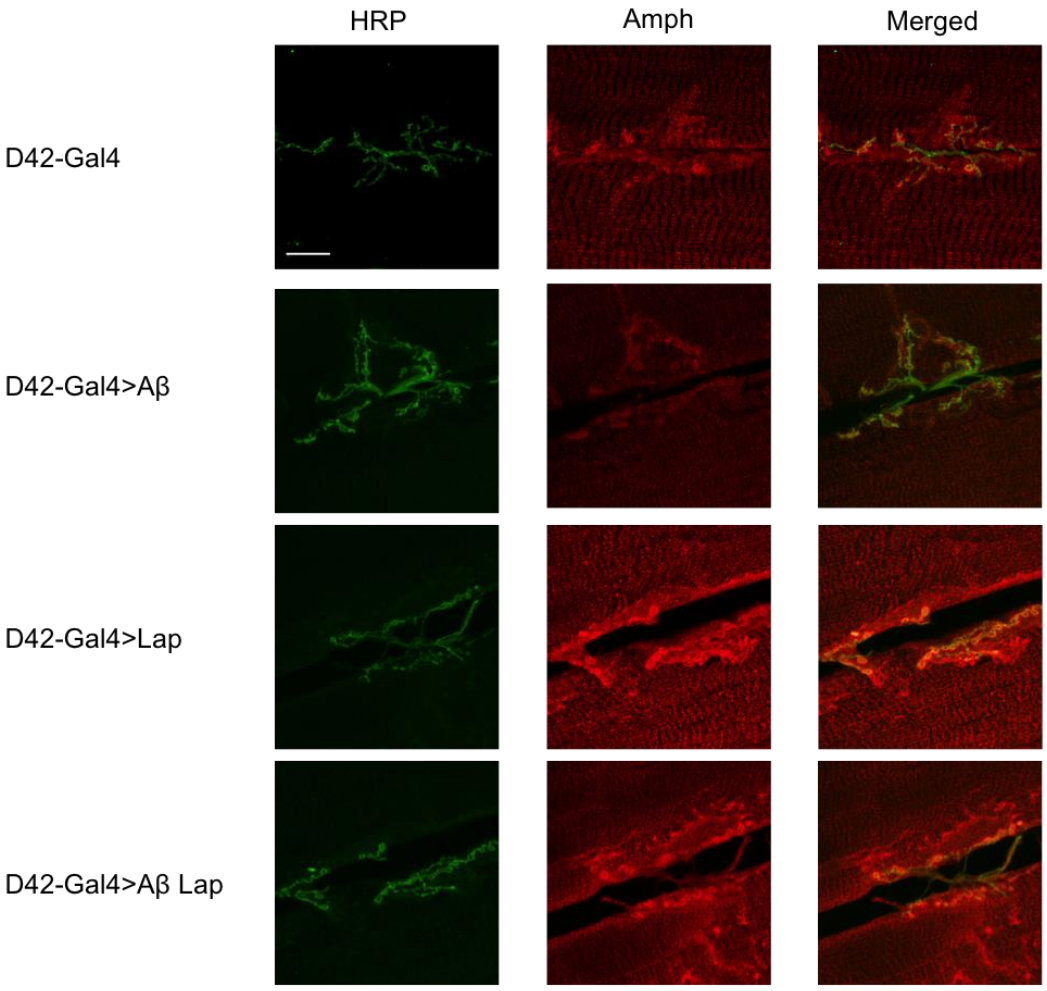
HRP
Amph
Merged
D42-Gal4
D42-Gal4>Aβ
D42-Gal4>Lap
D42-Gal4>Aβ Lap

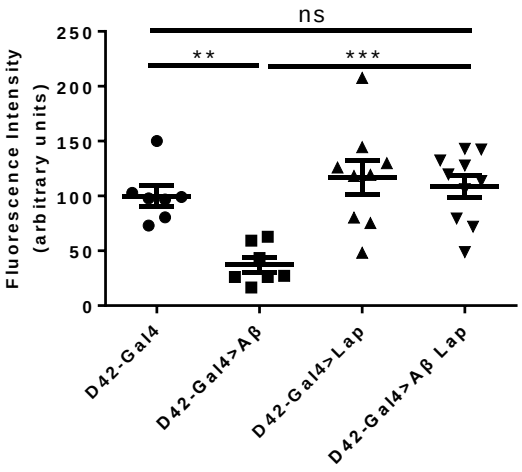
ns
**
***
Fluorescence Intensity (arbitrary units)
250
200
150
100
50
0
D42-Gal4
D42-Gal4>Aβ
D42-Gal4>Lap
D42-Gal4>Aβ Lap

(A)

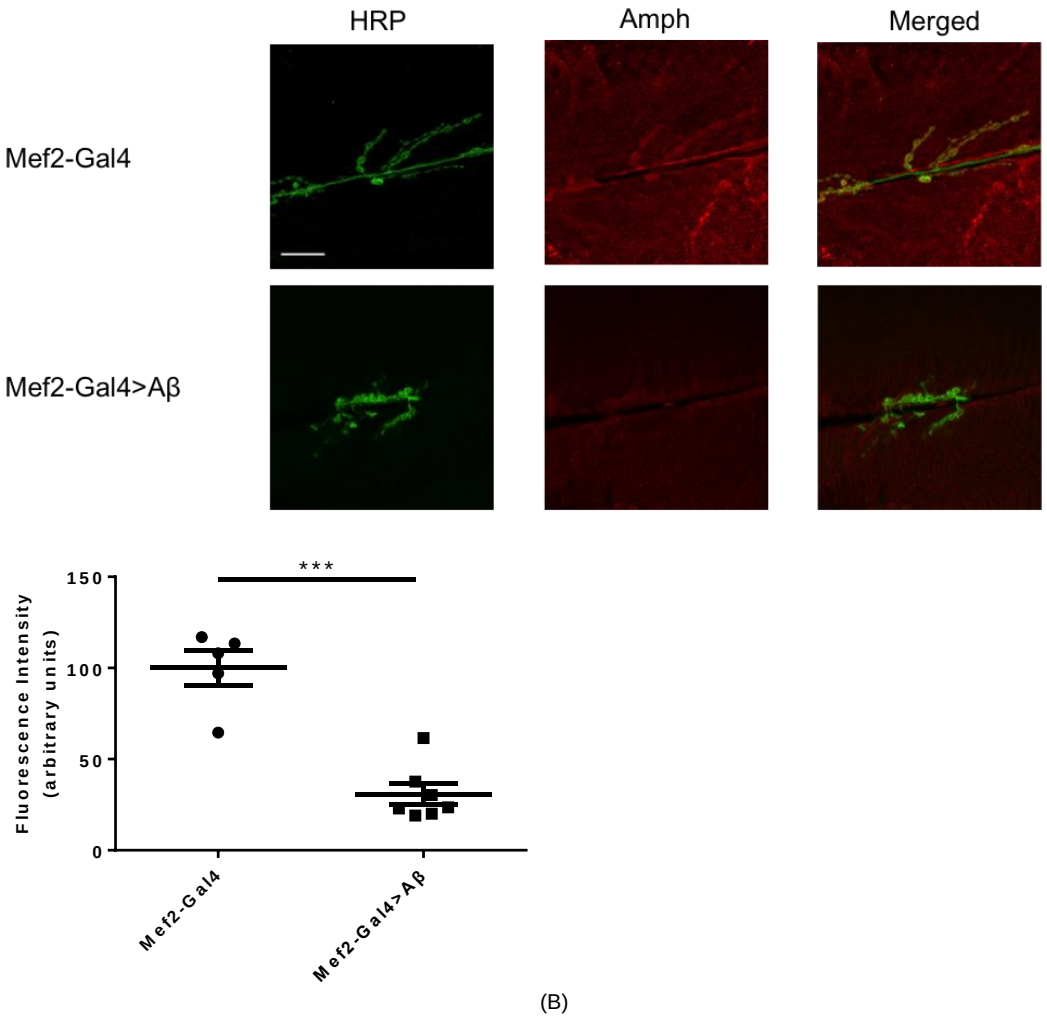

(B)

Figure 4.5 *Lap* restores Amph intensity in Aβ-expressing flies.

(A) Quantification of Amph fluorescence at the NMJ of wandering third-instar larvae expressing Aβ, *lap* or both driven by D42-Gal4, plotted as means ± SEM, n ≥ 7. Genotypes are as above. ***p < 0.001, determined by one-way ANOVA; control (D42-Gal4) vs Aβ, **p < 0.01; control vs Amph, n.s., not significant; Amph vs Aβ Amph, n.s., not significant; Aβ vs Aβ Amph, ***p < 0.001, comparison by Tukey's *post-hoc* test. Scale bar, 20 μm.

(B) Quantification of Amph fluorescence at the NMJ of wandering third-instar larvae expressing Aβ or not driven by Mef2-Gal4, plotted as means ± SEM, n ≥ 5. Genotypes: Mef2-Gal4, UAS-Aβ; Mef2-Gal4. ***p < 0.001, comparison by Student's t-test. Scale bar, 20 μm.

4.2.6 *Lap* and *Amph* modulate glutamatergic transmission

I proposed a model where *lap* and *Amph* collaborated to modulate glutamatergic transmission and so affected disease progression. First, *lap* participated in vesicle formation and cargo selection. The cargo included VGlut. Second, *lap* rescued Amph accumulation at the NMJ

which decreased upon Aβ expression. *Amph* modulated the localization of glutamate receptors (GluRII) and so affected disease development (Figure 4.6).

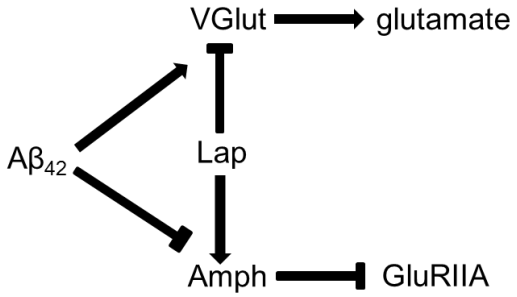

Figure 4.6 A model depicting the possible signalling pathways linking $A\beta_{42}$ to glutamatergic transmission seen in AD. Aβ causes the accumulation of VGlut and loss of Amph. *Lap* promotes the endocytosis of VGlut and therefore reduces glutamate release. *Lap* also rescues the loss of Amph, which leads to retrival of GluRIIA.

4.3 Discussion

4.3.1 Endocytosis is important for Aβ pathology

Endocytosis is severely impaired in AD, but secretion remains intact. An *in vitro* study has indicated that PICALM can ameliorate AD toxicity through eliminating endocytic defects (Treusch et al., 2011). My study has supported this *in vivo*. Furthermore, other endocytic genes also attenuate AD vulnerability including *Rab5*, *EndoA* and *Snap25*. *Rab5* is localized at the plasma membrane, clathrin-coated pits, and recycling endosomes, which plays a role in mediating the formation of clathrin coated pits at the plasma membrane (McLauchlan et al., 1998), as well as a primary role in the fusion of endocytic vesicles with early endosomes. In previous studies, *Rab5* was reported to be involved with $A\beta_{42}$ production (Grbovic et al., 2003; Kim et al., 2016). *EndoA* also plays an important role in clathrin-mediated endocytosis through controlling membrane tubulation and membrane association (Matta et al., 2012). A prior report has revealed that EndoA directly interacts with VGlut (Vinatier et al., 2006). It remains to be seen elusive whether *EndoA*'s neuroprotection is dependent on removing excess VGlut from the synaptic terminal. *Snap25* regulates both endocytosis and exocytosis via membrane fusion (Zhang et al., 2013). Gain of *Snap25* compromises the Ca^{2+} responsiveness in glutamatergic synapses, while its absence gives rise to the ADHD phenotype (Feng et al., 2005).

I also showed that not all endocytic genes were able to suppress Aβ toxicity. For example, *epsin* and *dynamin*-mediated endocytosis exacerbated Aβ toxicity. CD2AP is linked to AD by GWAS (Naj et al., 2011) and is involved in the regulation of receptor endocytosis (Cormont et al., 2003). The *Drosophila* homolog of CD2AP, *Cindr*, also increased Aβ toxicity. Moreover, almost all exocytic genes I screened accelerated AD progression, so it would be interesting to investigate whether the slowdown of membrane recycling can diminish Aβ toxicity.

4.3.2 Alterations in the ratio of GluRIIA/GluRIIB in AD

I showed that Aβ expression led to an increase in GluRIIA, concomitant with a decrease in GluRIIB. Aβ has been reported to up-regulate calcium permeable (CP) GluA1-containing AMPARs, while down-regulating calcium impermeable (CI) GluA2-containing AMPARs in mammalian neurons. This alteration is attributed to the fact that expression of GluRIIA reduces GluRIIB expression (Sigrist et al., 2002). The switch from CI-AMPARs to CP-AMPARs induces a Ca^{2+} influx and elevates intracellular Ca^{2+} loads that results in ER stress and neuronal toxicity (Liu et al., 2010; Whitcomb et al., 2015).

4.3.3 *Amph* is a modulator of GluRII localization

Amph also plays an important role in endocytosis, and again its role in Aβ toxicity remains unexplored. Amph localization is disrupted upon Aβ expression. Moreover, this defect is rescued by *lap* expression. This study highlights a role for *Amph* in regulating the localization of the glutamate receptor GluRII at the synapse since my data also show that *Amph* decreases GluRIIA levels postsynaptically. Taken together, since this counteracts Aβ's effect on GluRIIA localization, this could contribute to its suppression of Aβ toxicity.

4.3.4 Feedback control of glutamatergic transmission

As discussed in chapter 3, presynaptic glutamate has been reported to negatively modulate the number of GluRII receptors (Featherstone et al., 2002). In turn, GluRII also mediates presynaptic glutamate release via retrograde signals. An upregulation of GluRIIA and a downregulation of GluRIIB increase postsynaptic sensitivity and elicit a compensation to

decrease presynaptic glutamate release (DiAntonio et al., 1999). However, it will be interesting to know whether *lap*, via *Amph*, could possibly modulate GluRII localization and *Amph*, via retrograde signals, could modulate VGlut localization.

My work has demonstrated that *Rab5*, *EndoA*, *Snap25* and *Amph* suppress Aβ toxicity. Among them, Amph accumulation at the NMJ is rescued by *lap*. *Amph* reduces the accumulation of glutamate receptors (GluRIIA) at the NMJ and therefore could account for its suppression of Aβ toxicity.

5. Genome-wide screen for suppressors of $A\beta_{42}$ toxicity

5.1 Background

Most AD cases are sporadic AD (SAD), but 1% is familial AD (FAD). Both types of cases are thought to be caused by amyloid-β peptide (Aβ) accumulation and tau hyperphosphorylation, resulting in amyloid plaques and neurofibrillary tangles. A century of research on AD has revealed several molecular mechanisms underlying Aβ toxicity. For example, Aβ oligomers disrupt processes such as cell signaling, epigenetic, endocytosis and ER stress (Gjoneska et al., 2015; Minami et al., 2014; Seo et al., 2014; Suberbielle et al., 2015). However, there is still no effective treatment for AD. Therefore, novel therapies are desperately needed to delay the onset of symptoms, slow disease progression or reverse the course of this disease.

Drosophila has proven to be a powerful model system for rapidly screening therapeutic targets in neurodegenerative diseases such as Huntington's disease (HD), AD, Amyotrophic lateral sclerosis (ALS) and Spinocerebellar ataxia (SCA) disease models (Kim et al., 2014; Lasagna-Reeves et al., 2016; Lu et al., 2013; Park et al., 2013). An example of this is its rough eye phenotype (REP), which allows for high-throughput screening. Using a REP screen, my collaborators performed a genome-wide genetic screen to identify modifiers of Aβ toxicity. I took their primary hits, validated them and checked for rescue of adult phenotypes such as negative geotaxis and lifespan analysis.

This unbiased screen identified 4 of gene-knockdown suppressors of $A\beta_{42}$ toxicity. They were *CG15011*, *Larp*, *Pxn*, and *Sodh2*.

5.2 Materials and Methods

5.2.1 *Drosophila* screening in the eye

UAS-Aβ; GMR-GAL4 flies were crossed to RNAi flies at 29°C on SYA food. We stuck fly heads

on a 45°-angled piece of wood, such that the left eye pointed to the top. Eye phenotypes of anesthetized female flies were evaluated with a Leica MZ 75 stereomicroscope and photographed with a Leica M 165C. Scoring of the REP was performed. Comparison of scores was performed by a Student's t-test of the conditions of interest using the Prism software.

In detail, we first analyzed the effect of the construct independent of $A\beta_{42}$ toxicity in the progeny of crosses of GMR-Gal4 stock with each RNAi line. We assessed eye morphology while sorting the progeny of the crosses and excluded RNAi strains that modulated eye appearance. We further crossed the GMR-Gal4 > UAS-$A\beta_{42}$/Cyo stock with each RNAi/UAS line. We also crossed the GMR-Gal4 > UAS-$A\beta_{42}$ line with w^- w^{1118} lines as a control line. We assessed the effect of the construct on $A\beta_{42}$ toxicity in the non Cyo progeny. We chose the GMR-Gal4 > UAS-$A\beta_{42}$ line in the first generation as the control to cover the different numbers of UAS and different doses of the w^+ gene expressed in the screened lines as these may modulate $A\beta_{42}$ toxicity. The screened lines were crossed over several times and each time the two controls were crossed in parallel. We always compared the screened lines with controls of the same day. The progeny was anesthetized until the REP measurement. We photographed and quantified only female flies, which are bigger. We analyzed 10 flies per screened line and per control, with exceptions for lethality. We compared the changes of the REP between the screened line and the controls (10 values for the screened line versus 10 values for the control) by scoring. We calculated the scores of the REP and determined significant modifiers based on the scores (45 RNAi lines + 4 overexpression lines = 49 lines in total).

For significant modifiers, they were re-tested in an independent lab (by me). For the graphs and table, we calculated the mean of the median of each experiment. We also tested overexpression lines when available. To avoid any false positive results, we performed an independent screen using a different GMR-Gal4 > UAS-$A\beta_{42}$/Cyo stock. This way, several primary hits in the first screen went in the opposite direction in the second screen (Figure 5.1D). To be robust, RNAi lines were considered positive only if they suppressed the REP either in the screen done by my collaborators or my screen. For these reasons, the 30 primary hits were considered as positive hits as RNAi lines of these genes suppressed $A\beta_{42}$ toxicity.

5.3 Results

5.3.1 Genome-wide screen for modifiers of $A\beta_{42}$ toxicity

My collaborators used the well characterized *Drosophila* model expressing human $A\beta_{42}$ under the control of the GMR-Gal4 driver for the primary screen (Crowther et al., 2005). This model recapitulated key features of AD like rough eye phenotype (REP), shortened lifespan and locomotor deficits. REP has proven to be successful in screening modifiers in other neurodegenerative diseases. Using the REP (Figure 5.1B), my collaborators screened 7593 strains corresponded to 7025 genes and covered 88% of the *Drosophila* genome. Firstly, they excluded 866 RNAi strains that modulated eye appearance under the control of GMR-Gal4 alone. Secondly, they screened 6727 RNAi strains from Vienna *Drosophila* RNAi Center (VDRC). This primary screen identified 938 primary hits including 625 subtle enhancers and 313 subtle suppressors. Among these hits, 45 showed strong modification (24 suppressors, 15 enhancers and 6 lethality) (Figure 5.1A). To validate the roles of these preliminary hits in $A\beta_{42}$ toxicity, I conducted the subsequent screen with a different $A\beta_{42}$-expressing strain that expressed two copies of $A\beta_{42}$ and displayed more severe neuronal dysfunction (Casas-Tinto et al., 2011). I found that 27 hits exhibited reproducible and consistent results in two independent screens (16 suppressors and 11 enhancers) (Figure 5.1C and D). Gene ontology (GO) term analysis of the entire set of hits from the screen grouped them into five groups including endocytic trafficking, mitochondrial biogenesis, metabolic process, signaling transduction and transcription (Table 5.1). Notably, there was no overlap between the hits found in this genome-wide screen and those in a previous mini screen (Cao et al., 2008).

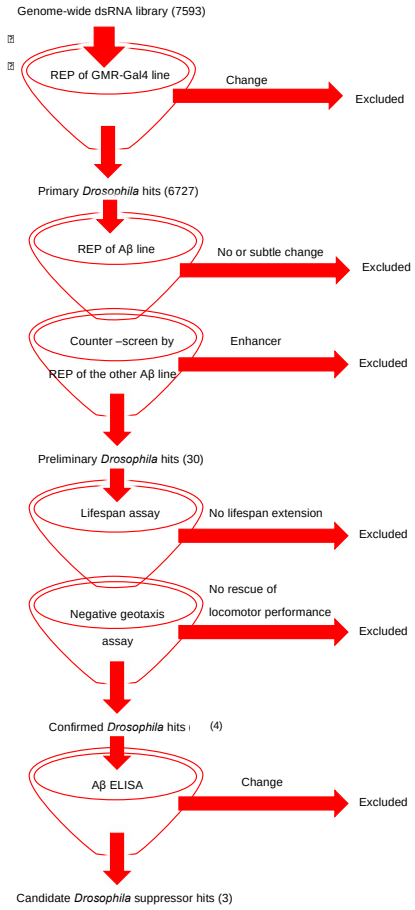
Genome-wide dsRNA library (7593)
REP of GMR-Gal4 line
Change
Excluded
Primary Drosophila hits (6727)
REP of Aβ line
No or subtle change
Excluded
Counter –screen by
REP of the other Aβ line
Enhancer
Excluded
Preliminary Drosophila hits (30)
Lifespan assay
No lifespan extension
Excluded
Negative geotaxis
assay
No rescue of
locomotor performance
Excluded
Confirmed Drosophila hits (4)
Aβ ELISA
Change
Excluded
Candidate Drosophila suppressor hits (3)

(A)

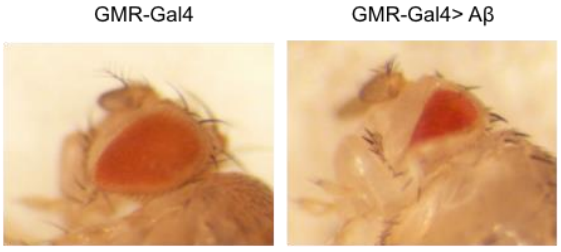
GMR-Gal4
GMR-Gal4> Aβ

(B)

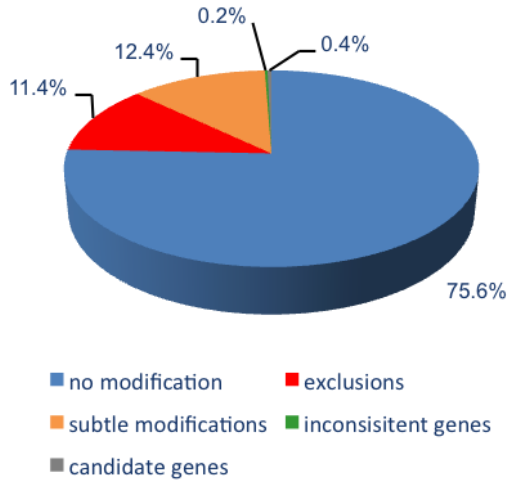

(C)

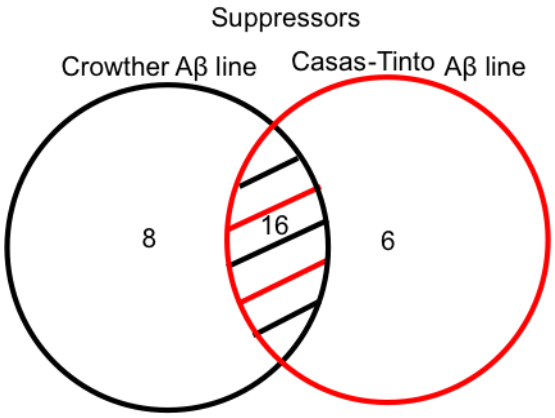

(D)

Figure 5.1 Primary genome-wide screens for the REP modifiers in *Drosophila*.

(A) Flow chart for the unbiased screen in *Drosophila*. REP is used to assess the $A\beta_{42}$ toxicity in the primary genetic screen that is followed by lifespan and locomotor assay to monitor the $A\beta_{42}$–induced defects. siRNA lines that reduce $A\beta_{42}$ toxicity in all assessments are regarded as potential suppressors.

(B) Schematic of the REP for modifiers of Aβ toxicity.

(C) Pie chart of RNAi strains scored in the screen.

(D) Venn diagram of the identified suppressor candidates.

Table 5.1 *Drosophila* RNAi genes that enhance or suppress Aβ toxicity using two independent $A\beta_{42}$-expressing lines.

Drosophila gene	Human homolog	Function	Type
CG1965	GCFC1	DNA binding protein	Increased

CG6972		Protein of unknown function	Increased
CG8086	ODF3	Protein required for sperm movement	Increased
CAH2	CA2	Carbonic anhydrase	Increased
DHC64C	DYNC1H1	Dynein heavy chain	Increased
ETS97D	GABPA	DNA-binding protein	Increased
NUB	POU2F1	Transcription factor of the POU family	Increased
R	RAP1A	Ras-related protein	Increased
RAB30	RAB30	Intra-Golgi traffic	Increased
SMOX	SMAD3	Transcription factor of the TGFβ family	Increased
SPX	SF3B4	Nuclear mRNA splicing protein	Increased
CG7757	PRPF3	Protein of the U4 and U6 snRNPs	Decreased
CG7849	TRUB2	Pseudouridine synthesis	Decreased
CG15011	NFXL1	Nuclear transcription factor	Decreased
CG16886		Protein of unknown function	Decreased
ARFGAP3	ARFGAP3	GTPase-activating proteins for ARF	Decreased
BAP60	SMARCD3	Part of the SWI/SNF complex	Decreased
MED15	MED15	Transcription factor of the Gal4 family	Decreased
MRPL15	MRPL15	Mitochondrial mRNA translation protein	Decreased
LILII	AFF4	Transcription factor of the AF4 family	Decreased
PXN	PXDN	Enzyme in extracellular matrix	Decreased
RNO	PHF16	Histone H4-specific acetyltransferase	Decreased
RTF1	RTF1	RNA polymerase-associated protein	Decreased
SF2	SRSF1	Nuclear mRNA splicing protein	Decreased
SODH2	SORD	Sorbitol pathway	Decreased
SU(TPL)	ELL2	RNA polymerase II elongation factor	Decreased

5.3.2 Secondary validation in *Drosophila* adulthood

To evaluate the contributions of preliminary hits on AD in adulthood, I used the $A\beta_{42}$-expressing fly described in chapter 3 and 4. Elav-GS is induced in the nervous system

upon eclosion. These $A\beta_{42}$-expressing flies displayed locomotor performance impairment and reduced lifespan. I crossed all the suppressor RNAi lines identified above and scored their lifespan. I also obtained all available *Drosophila* over-expression strains that corresponded to gene-knockdown enhancers in the first screen and crossed them to $A\beta_{42}$-expressing flies. The lifespan analysis yielded 17 of the 30 hits that increased the shortened lifespan of $A\beta_{42}$-expressing flies and no overexpression lines that extended the lifespan of $A\beta_{42}$-expressing flies (Figure 5.2, mean lifespan, Aβ RU200: 100 %; Aβ Btl RNAi RU200: 103 %; Aβ Cdk5α RNAi RU200: 103 %; Aβ Pxn RNAi RU200: 103 %; Aβ Rtf1 RNAi RU200: 103 %; Aβ Sodh2 RNAi RU200: 106 %; Aβ mRpL15 RNAi RU200: 106 %; Aβ Nat1 RNAi RU200: 106 %; Aβ Gβ13F RNAi RU200: 106 %; Aβ CG16886 RNAi RU200: 109 %; Aβ Med15 RNAi RU200: 112 %; Aβ Kermit RNAi RU200: 112 %; Aβ CG13889 RNAi RU200: 115 %; Aβ CG15011 RNAi RU200: 115 %; Aβ Lilli RNAi RU200: 115 %; Aβ CG7849 RNAi RU200: 118 %; Aβ Larp RNAi RU200: 118 %; Aβ CG7757 RNAi RU200: 129 %, n > 100 per condition. p was shown in Figure 5.2, log-rank test).

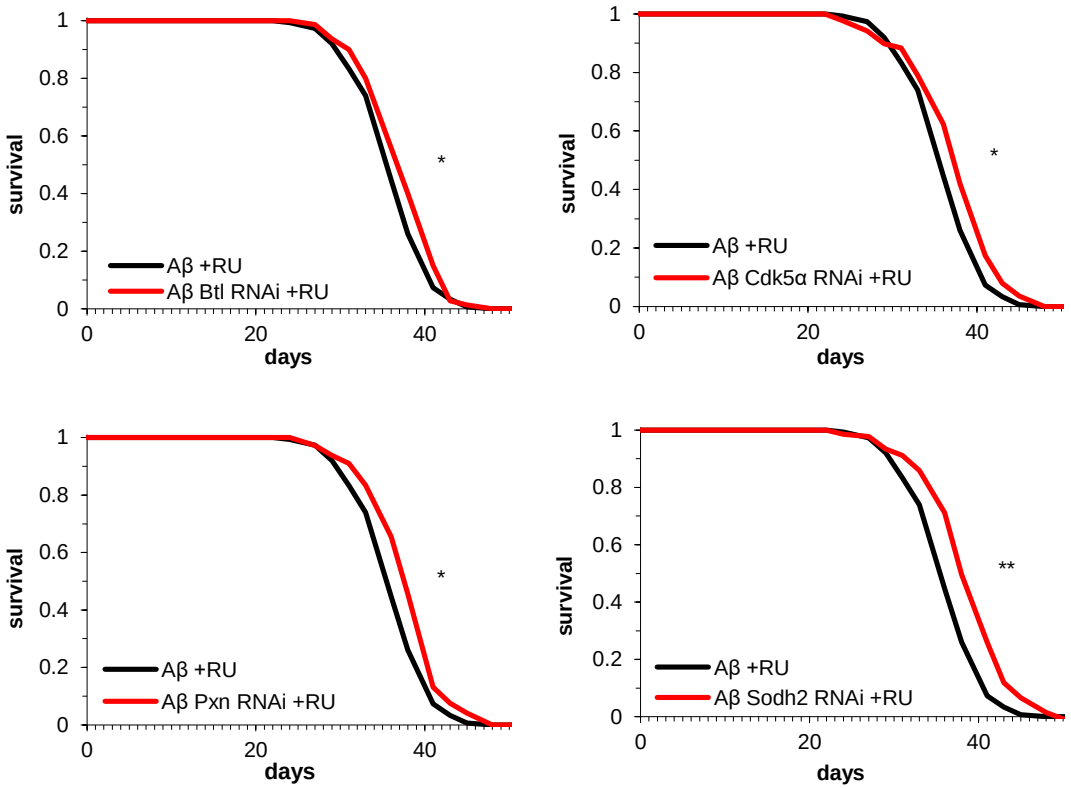

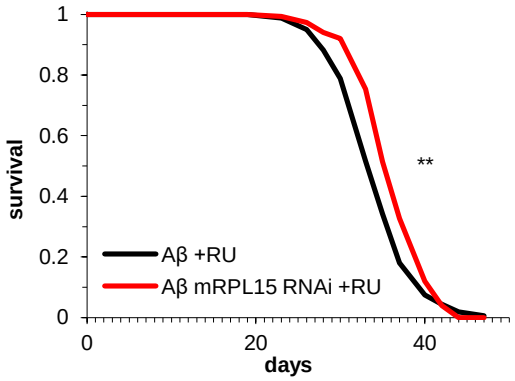
survival
days
Aβ +RU
Aβ mRPL15 RNAi +RU
**

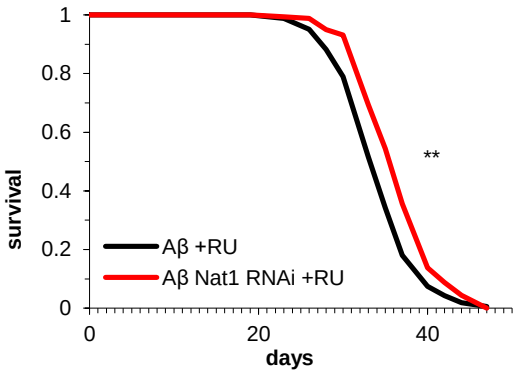
survival
days
Aβ +RU
Aβ Nat1 RNAi +RU
**

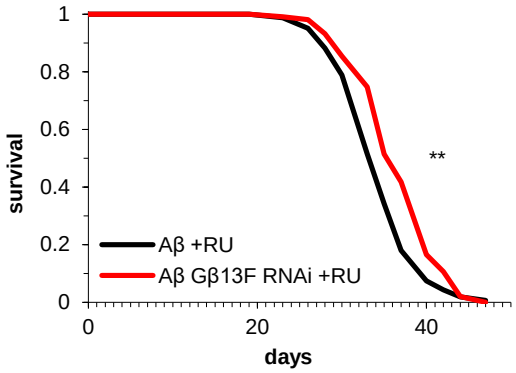
survival
days
Aβ +RU
Aβ Gβ13F RNAi +RU
**

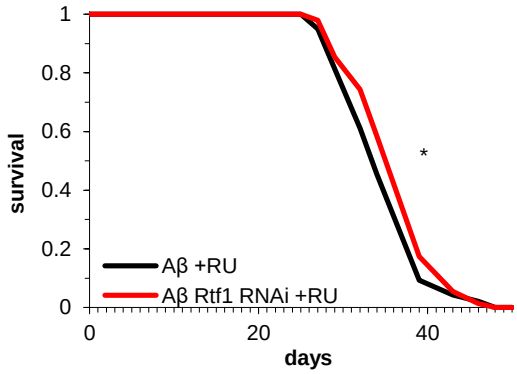
survival
days
Aβ +RU
Aβ Rtf1 RNAi +RU
*

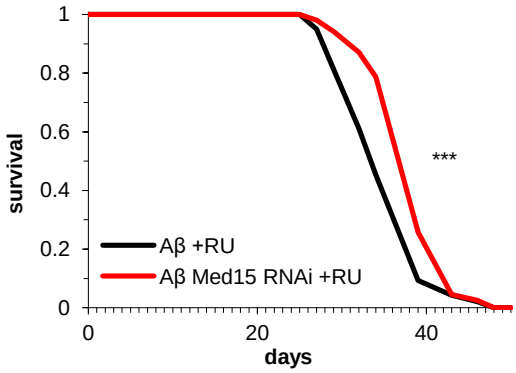
survival
days
Aβ +RU
Aβ Med15 RNAi +RU
***

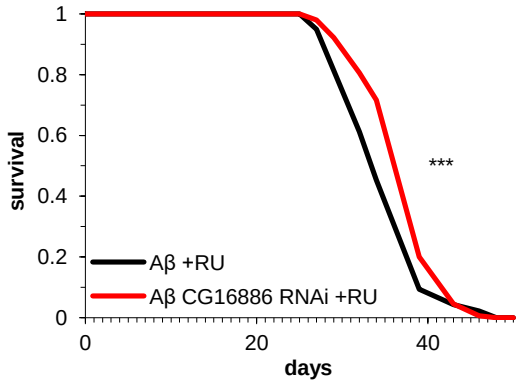
survival
days
Aβ +RU
Aβ CG16886 RNAi +RU
***

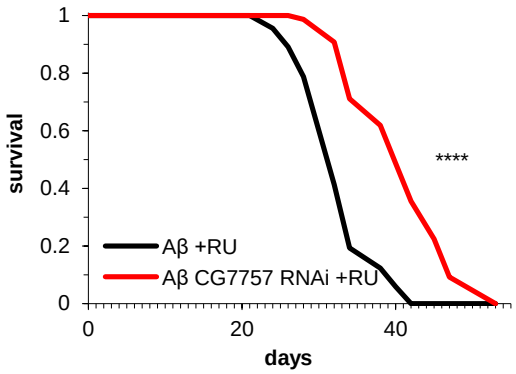
survival
days
Aβ +RU
Aβ CG7757 RNAi +RU
****

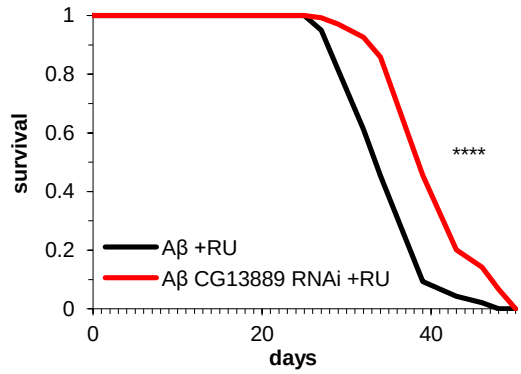
survival
days
Aβ +RU
Aβ CG13889 RNAi +RU
****

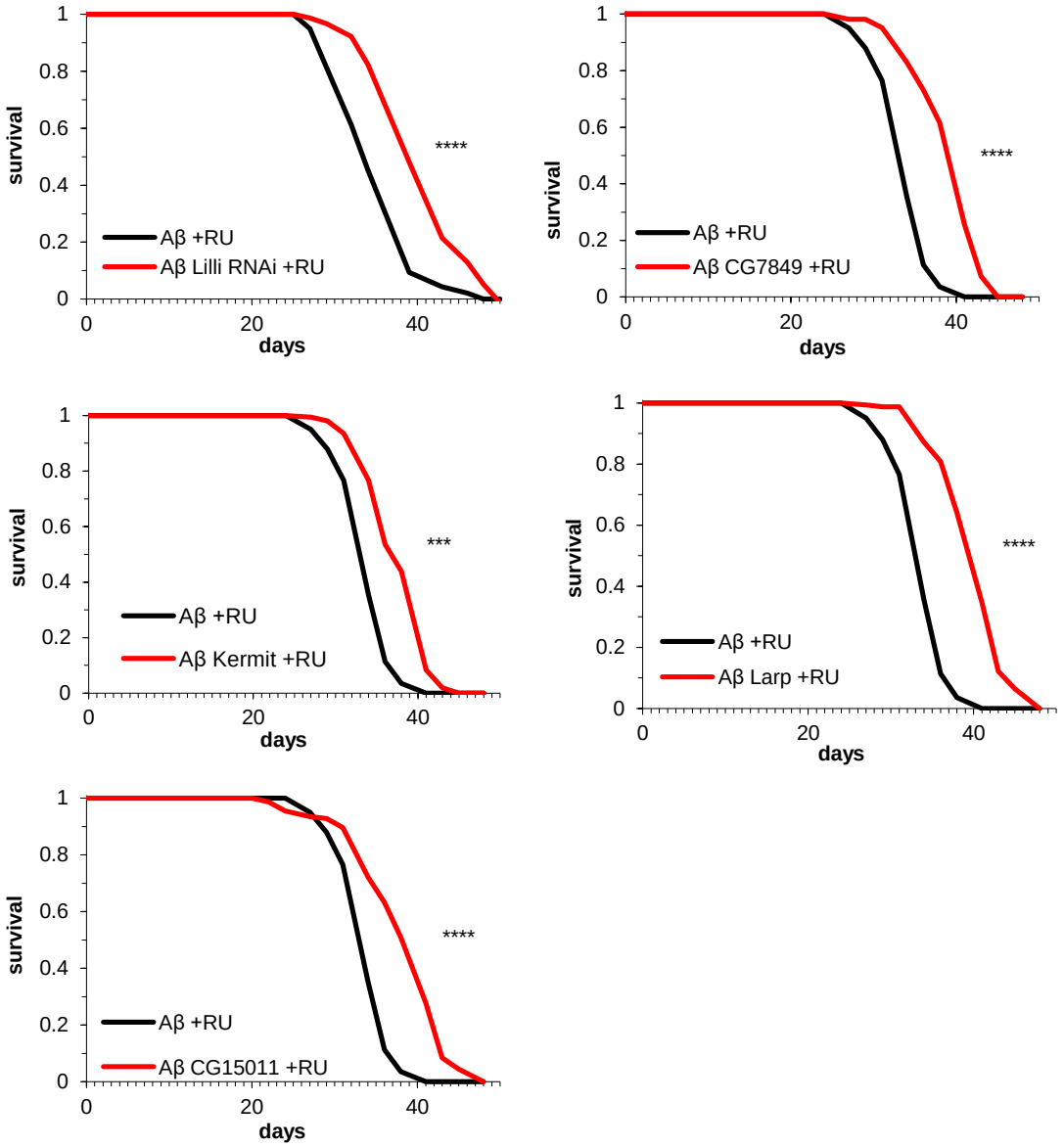

Figure 5.2 Secondary validation screens in *Drosophila* adults for genetic modifiers of $A\beta_{42}$ toxicity. Survival curves of flies expressing Aβ with shRNA hits (red) or not (black) in adult neurons (+RU), n > 100. *p < 0.05, **p < 0.01,***p < 0.001, ****p < 0.0001, comparison by log-rank test.

5.3.3 Counter validation in *Drosophila* adulthood

Based on 17 potential hits from lifespan analysis, I assessed effects of these hits on the locomotor performance of $A\beta_{42}$-expressing flies. The first behavioral analysis examined all RNAi lines without backcrossing and found that 3 candidate genes improved climbing performance of $A\beta_{42}$-expressing flies. They were *Pxn*, *Sodh2* and *Rtf1* (Figure 5.3A). As my previous data showed that the $A\beta_{42}$-expressing flies displayed locomotor deficits from day 14

onwards, I measured the climbing performance on day 7 and day 15 in the second behavioral analysis. The second behavioral analysis assessed all RNAi lines with backcrossing and revealed 4 hits were able to attenuate climbing deficits of $A\beta_{42}$-expressing flies. They were *CG15011*, *Larp*, *Pxn*, and *Sodh2* (Figure 5.3B, PI, day 7, Aβ RU200: 92.84 ± 2.64 %; Aβ CG15011 RNAi RU200: 90.94 ± 2.61 %; Aβ Larp RNAi RU200: 93 ± 2.65 %; Aβ Pxn RNAi RU200: 90.63 ± 1.04 %; Aβ Sodh2 RNAi RU200: 90.19 ± 0.64 %; day 15, Aβ RU200: 68.57 ± 1.64 %; Aβ CG15011 RNAi RU200: 81.11 ± 2.57 %; Aβ Larp RNAi RU200: 85.37 ± 2.38 %; Aβ Pxn RNAi RU200: 81.06 ± 2.85 %; Aβ Sodh2 RNAi RU200: 78.23 ± 1.23 %, n = 3 per condition. p was shown in Figure 5.3B, two-ways ANOVA). These 4 modifiers acted as significant knockdown suppressors to modify $A\beta_{42}$ toxicity, which were reproducible and consistent in all assessments. It was important to note that 4 genes showed potential improvements of climbing performance. They were *cep290* (*CG13889*), *Gβ13F*, *Lilli* and *Prp3* (*CG7757*) (Figure 5.3B, PI, day 7, Aβ RU200: 92.84 ± 2.64 %; Aβ cep290 RNAi RU200: 98.26 ± 0.92 %; Aβ Gβ13F RNAi RU200: 96.18 ± 0.92 %; Aβ Lilli RNAi RU200: 96.18 ± 0.69 %; Aβ Prp3 RNAi RU200: 92.6 ± 1.34 %; day 15, Aβ RU200: 68.57 ± 1.64 %; Aβ cep290 RNAi RU200: 80.65 ± 4.09 %; Aβ Gβ13F RNAi RU200: 76.84 ± 0.5 %; Aβ Lilli RNAi RU200: 76.69 ± 1.4 %; Aβ Prp3 RNAi RU200: 78.88 ± 1.68 %, n = 3 per condition. p was shown in Figure 5.3B, two-ways ANOVA). It remains to investigate whether these 4 candidates will show significant improvements of climbing performance after 15 days. Given that *Rtf1* was excluded in the second screen after backcrossing and *CG15011* and *Larp* did not appear in the first screen, my work also emphasized the importance of backcrossing.

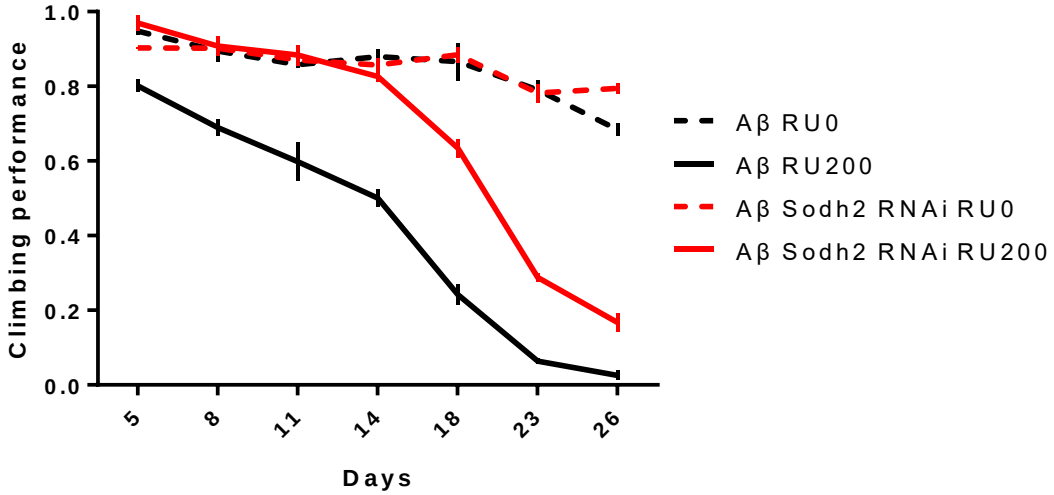
Climbing performance
1.0
0.8
0.6
0.4
0.2
0.0
5
8
11
14
18
23
26
Days
Aβ RU0
Aβ RU200
Aβ Sodh2 RNAi RU0
Aβ Sodh2 RNAi RU200

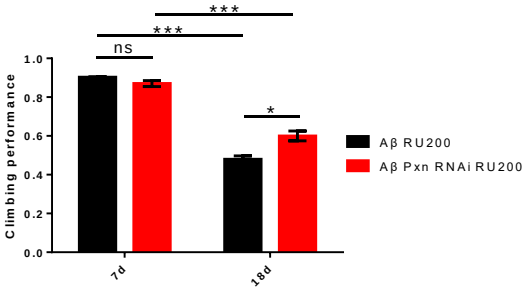
***
***
ns
*
Climbing performance
7d
18d
Aβ RU200
Aβ Pxn RNAi RU200

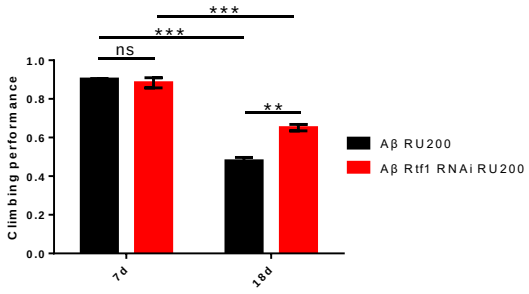
***
***
ns
**
Climbing performance
7d
18d
Aβ RU200
Aβ Rtf1 RNAi RU200

(A)

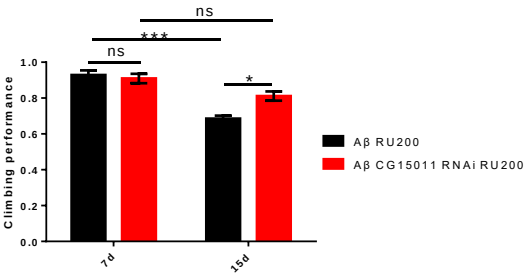
ns
***
ns
*
Climbing performance
7d
15d
Aβ RU200
Aβ CG15011 RNAi RU200

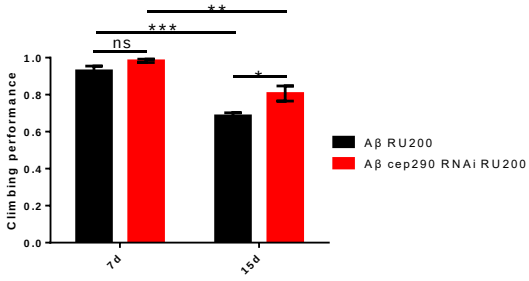
**
***
ns
*
Climbing performance
7d
15d
Aβ RU200
Aβ cep290 RNAi RU200

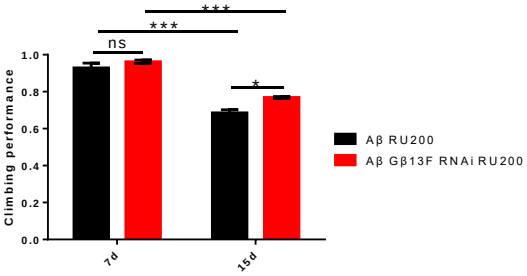
***
***
ns
*
Climbing performance
7d
15d
Aβ RU200
Aβ Gβ13F RNAi RU200

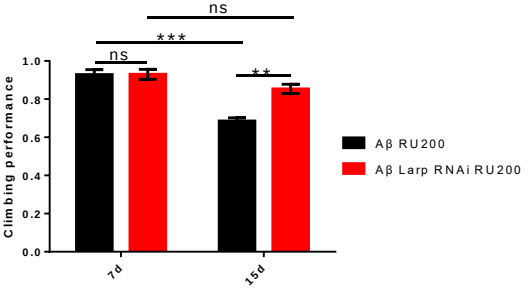
ns
***
ns
**
Climbing performance
7d
15d
Aβ RU200
Aβ Larp RNAi RU200

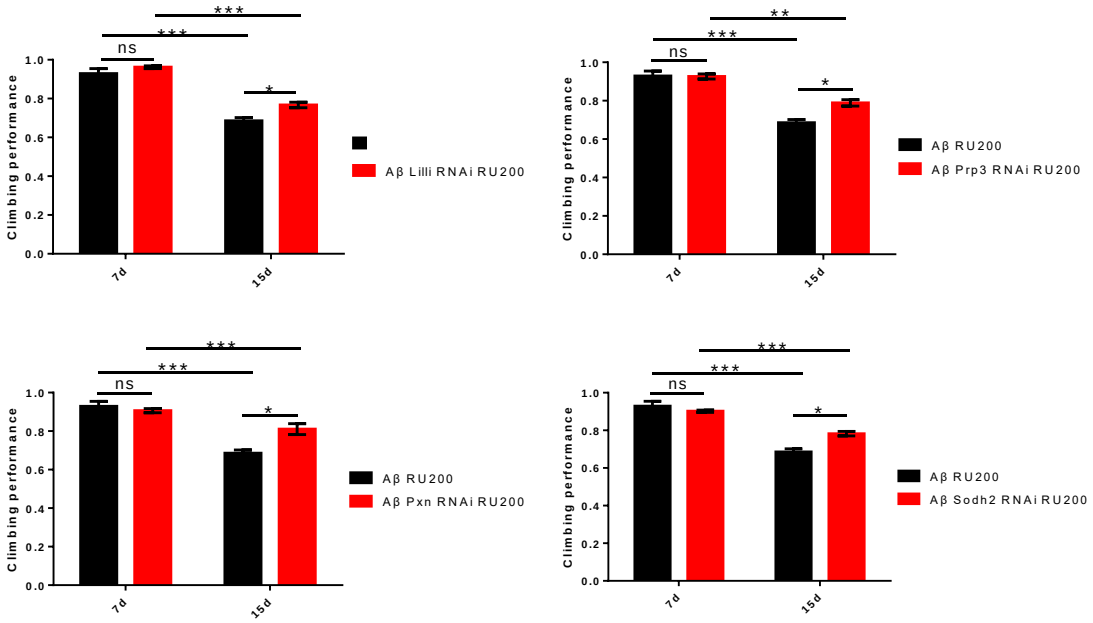

(B)

Figure 5.3 *In vivo* validation of the hits from the secondary screen. Climbing performance index of flies of the potential knockdown suppressors, n = 3 (50 animals per condition). *p < 0.05; **p < 0.01; ***p < 0.001; n.s., not significant, determined by two-ways ANOVA followed by Tukey's *post-hoc* test. Statistical analyses were shown in Table 5.2.

Table 5.2 Statistical summary of locomotor performance index of flies expressing Aβ with or without *Sodh2* RNAi

Day 5	Aβ RU0	Aβ RU200	Aβ Sodh2 RNAi RU0	Aβ Sodh2 RNAi RU200
Aβ RU0		< 0.001	n.s.	n.s.
Aβ RU200			< 0.05	< 0.0001
Aβ Sodh2 RNAi RU0				n.s.
Aβ Sodh2 RNAi RU200				
Day 8	Aβ RU0	Aβ RU200	Aβ Sodh2 RNAi RU0	Aβ Sodh2 RNAi RU200
Aβ RU0		< 0.0001	n.s.	n.s.
Aβ RU200			< 0.0001	< 0.0001
Aβ Sodh2 RNAi RU0				n.s.
Aβ Sodh2 RNAi RU200				
Day 11	Aβ RU0	Aβ RU200	Aβ Sodh2 RNAi RU0	Aβ Sodh2 RNAi RU200
Aβ RU0		< 0.0001	n.s.	n.s.
Aβ RU200			< 0.0001	< 0.0001

Aβ Sodh2 RNAi RU0				n.s.
Aβ Sodh2 RNAi RU200				
Day 14	Aβ RU0	Aβ RU200	Aβ Sodh2 RNAi RU0	Aβ Sodh2 RNAi RU200
Aβ RU0		< 0.0001	n.s.	n.s.
Aβ RU200			< 0.0001	< 0.0001
Aβ Sodh2 RNAi RU0				n.s.
Aβ Sodh2 RNAi RU200				
Day 18	Aβ RU0	Aβ RU200	Aβ Sodh2 RNAi RU0	Aβ Sodh2 RNAi RU200
Aβ RU0		< 0.0001	n.s.	< 0.0001
Aβ RU200			< 0.0001	< 0.0001
Aβ Sodh2 RNAi RU0				< 0.0001
Aβ Sodh2 RNAi RU200				
Day 23	Aβ RU0	Aβ RU200	Aβ Sodh2 RNAi RU0	Aβ Sodh2 RNAi RU200
Aβ RU0		< 0.0001	n.s.	< 0.0001
Aβ RU200			< 0.0001	< 0.0001
Aβ Sodh2 RNAi RU0				< 0.0001
Aβ Sodh2 RNAi RU200				
Day 26	Aβ RU0	Aβ RU200	Aβ Sodh2 RNAi RU0	Aβ Sodh2 RNAi RU200
Aβ RU0		< 0.0001	< 0.01	< 0.0001
Aβ RU200			< 0.0001	< 0.001
Aβ Sodh2 RNAi RU0				< 0.0001
Aβ Sodh2 RNAi RU200				

Statistical summary of locomotor performance index of flies expressing Aβ with or without shRNA

First locomotor assay	Interaction of time and genotype	time	genotype
Sodh2	p < 0.0001	p < 0.0001	p < 0.0001
Pxn	p < 0.01	p < 0.0001	p < 0.05
Rtf1	p < 0.001	p < 0.0001	p < 0.01
Second locomotor assay	Interaction of time and genotype	time	genotype

CG15011	p < 0.05	p < 0.0001	p < 0.05
cep290	ns	p < 0.0001	p < 0.05
Gβ13F	ns	p < 0.0001	p < 0.01
Larp	p < 0.01	p < 0.001	p < 0.01
Lilli	ns	p < 0.001	p < 0.05
Prp3	ns	p < 0.001	p < 0.05
Pxn	p < 0.01	p < 0.0001	p < 0.05
Sodh2	p < 0.01	p < 0.0001	p < 0.05

5.3.4 $A\beta_{42}$ measurement

I next measured total $A\beta_{42}$ levels in flies described above using Aβ ELISA. I found that downregulation of *Prp3* (*CG7757*) and *CG15011* reduced $A\beta_{42}$ levels, while other genes did not change (Figure 5.4, Aβ RU0: 4.02 ± 0.01 pg/ug protein; Aβ RU200: 48.63 ± 4.71 pg/ug protein; Aβ CG15011 RNAi RU200: 24.8 ± 4.87 pg/ug protein; Aβ Prp3 RNAi RU200: 34.97 ± 10.74 pg/ug protein, Aβ Btl RNAi RU200: 59.84 ± 14.31 pg/ug protein; Aβ Cdk5α RNAi RU200: 69.83 ± 12.76 pg/ug protein; Aβ Gβ13F RNAi RU200: 45.13 ± 8.41 pg/ug protein; Aβ Larp RNAi RU200: 39.1 ± 17.21 pg/ug protein; Aβ mRpL15 RNAi RU200: 44.92 ± 2.5 pg/ug protein; Aβ Nat1 RNAi RU200: 45.54 ± 11.08 pg/ug protein; Aβ Pxn RNAi RU200: 65.26 ± 23.41 pg/ug protein; Aβ Sodh2 RNAi RU200: 64.82 ± 10.21 pg/ug protein, n = 3 per condition. p < 0.05, one-way ANOVA). To eliminate the possibility that these genes alter $A\beta_{42}$ transcription, in the future I intend to monitor $A\beta_{42}$ transcription by RT-qPCR.

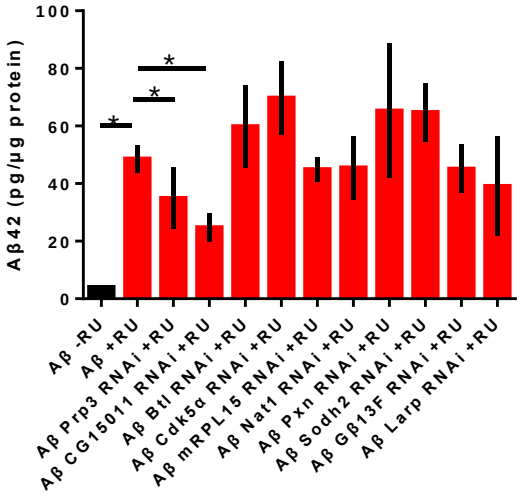

Figure 5.4 $A\beta_{42}$ protein levels, measured by ELISA, in the heads of 21-day-old flies expressing Aβ or Aβ shRNA hits in neurons (+RU) and uninduced controls (-RU). Means ± SEM, n = 3. *p < 0.05, determined by one-way ANOVA, *p < 0.05, comparison by Tukey's *post-hoc* test.

5.4 Discussion

5.4.1 Potential pathways underpinning novel modifiers of $A\beta_{42}$ toxicity

Reducing $A\beta_{42}$ levels was believed to be an effective strategy in AD treatment. However, drugs that promoted $A\beta_{42}$ clearance failed to ameliorate symptoms in patients with mild dementia (Abbott and Dolgin, 2016), indicating that decreasing $A\beta_{42}$ levels may not be sufficient to attenuated AD symptoms once the disease is established. Here I present a genome-wide screen to identify modifiers of Aβ toxicity and Aβ levels. Together with my collaborators, we identified 3 suppressors of Aβ toxicity and 1 suppressors of Aβ abundance in *Drosophila*. Inhibition of *Prp3* and *CG15011* reduced Aβ levels. However, only knockdown of *CG15011* attenuated all Aβ-induced phenotype. Reduction in *Larp*, *Pxn* and *Sodh2* suppressed the toxic effects of Aβ and ameliorated Aβ-induced neurodegeneration without influencing Aβ levels. However, *Larp* RNAi showed a decreasing tendency in Aβ levels, though not at a statistically significant level. I have not measured the impact of *Lilli* and *cep290* on Aβ levels.

Sodh-2 is a *Drosophila* orthologue of sorbitol dehydrogenase (SDH) and appears as an enzyme that converts sorbitol into fructose. Inhibition of SDH was reported to suppress neurodysfunction in diabetes (Cameron et al., 1997; Ng et al., 1998; Obrosova et al., 1999; Tilton et al., 1995). As previously shown, AD gave rise to progressive impairment of metabolic processes, indicating that metabolic interventions might ameliorate the AD phenotype (Niccoli et al., 2016; Tien et al., 2016; Winkler et al., 2015; Yoon et al., 2012). Peroxiredoxin (*Pxn*) is a secreted peroxidase and has never linked to AD (Colon and Bhave, 2016; Nelson et al., 1994). Peroxiredoxin, a related peroxidase, has been shown to be upregulated in APP mice and AD patient brains (Schonberger et al., 2001; Sizova et al., 2007). Peroxidasin (*Pxn*) is the other peroxidase that secrets into the ECM. It remains unclear why a reduction in an antioxidant protein is neuroprotective. *Gβ13F* is a subunit of G protein. Its mutation is linked to

neurodevelopmental disorder (Petrovski et al., 2016; Ramaker et al., 2013). *Larp* regulates translation of specific classes of mRNAs, which is downstream of the mTORC (Fonseca et al., 2015; Hong et al., 2017; Lahr et al., 2017; Tcherkezian et al., 2014). *Lilli* is required for mRNA transcription (Lin et al., 2010). However, gain of function mutations in its homologue AFF4 causes a developmental syndrome (Izumi et al., 2015). *Cep290* encodes a centrosomal protein (Sayer et al., 2006; Valente et al., 2006). The link between these hits and AD progression has not been firmly established.

5.4.2 Inhibition of exocytic genes does not attenuate $A\beta_{42}$ toxicity

As discussed in chapter 4, it is unclear whether the block of endocytic recycling can suppress Aβ toxicity. Here a genome-wide screen included genes that are involved in endocytic recycling. However, RNAi of these genes did not show a reduction in Aβ toxicity. The function of endocytic recycling in AD is under debate. On one hand, limitation of endocytic recycling could enhance Aβ elimination through lysosomal degradation (Li et al., 2012); on the other hand, abundant Aβ accumulation gives rise to enlarged endosomes, abnormal multivesicular bodies (MVBs) and lysosomal accumulation (Edgar et al., 2015; Gowrishankar et al., 2015; Sollvander et al., 2016). Therefore, this controversy might explain why any manipulation of endocytic recycling is detrimental to AD progression.

In summary, my study combined different screening strategies to identify at least 4 modifiers of Aβ toxicity. The identified hits are novel modulators, and so could provide novel avenues for modulation of downstream Aβ toxicity.

6. Perspectives

6.1 *Lap* and *Amph* suppress $A\beta_{42}$ toxicity

My work demonstrated that *lap* is an interacting partner of glutamate transporters and *Amph* is a novel modulator of glutamate receptors. Based on the work in chapters 3 and 4, I proposed a model where *lap* and *Amph* collaborated to modulate glutamatergic transmission and so affected disease progression (Figure 6.1). Firstly, *lap* participated in vesicle formation and cargo selection. The cargo included VGlut. Secondly, *EndoA* engaged in membrane tubulation and membrane association. Thirdly, *Rab5* was involved in translocation from the plasma membrane to early endosomes. Finally, *Snap25* played an important role in membrane fusion. Their over-expressions all slightly reduced $A\beta_{42}$ toxicity. In addition to this, *lap* also rescued Amph accumulation at the NMJ which decreased upon Aβ expression. *Amph* modulated the localization of glutamate receptors (GluRII) and so affected disease development.

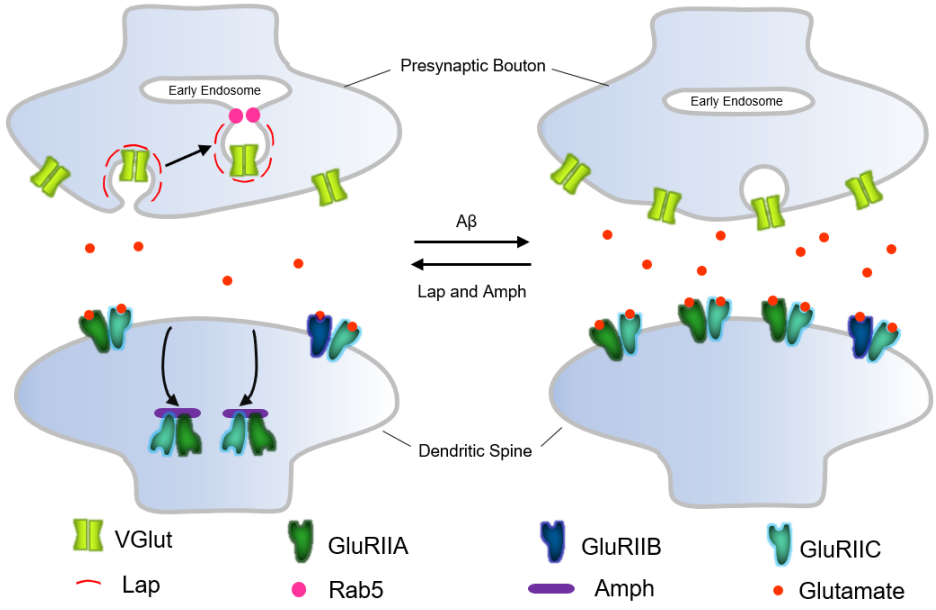

Figure 6.1 Schematic of *lap* and *Amph* in glutamatergic transmission. *Lap* promotes endocytosis of VGlut and this process might be mediated by *Rab5*. *Amph* leads to retrival of GluRIIA and GluRIIC in a manner dependent on *Dlg*.

This work indicated that the neuroprotection of *lap* could possibly be dependent on its role in endocytic recycling. However, my work lacks direct evidence to demonstrate that *lap* regulated

VGlut traffick. Recently Ventimiglia and Bargmann used VGLUT-pHluorin to monitor VGlut exocytosis and retrieval in *C. elegans*. pHluorin is a highly pH-sensitive variant of the green fluorescent protein that is minimally fluorescent at the acidic pH conditions, but highly fluorescence at neutral pH conditions (Miesenbock et al., 1998). Given that early endosomes provide acidic pH conditions, while the plasma membrane creates neutral pH conditions, synaptic vesicle exocytosis markedly increases the fluorescence when pHluorin fusion proteins target to the plasma membrane, while the subsequent endocytosis and reacidification in early endosomes quenches fluorescence, providing distinction at multiple stages of the synaptic vesicle cycle ((Di Giovanni and Sheng, 2015; Fernandez-Alfonso and Ryan, 2008; Li et al., 2005; Sankaranarayanan and Ryan, 2000). Linking pHluorin to VGLUT, Ventimiglia and Bargmann demonstrated that *unc-11*, a *C. elegans* homologue of PICALM, accelerated the endocytosis-reacidification process (Ventimiglia and Bargmann, 2017). It will be interesting for subsequent research to investigate whether the endocytosis process of VGlut is slowed down in our AD models using the VGLUT-pHluorin reportor and whether *lap* overexpression rescues this deficit.

In addition to this, although I have identified *Rab5* as a suppressor of $A\beta_{42}$ toxicity, its relationship with *lap* is unclear. In the mammalian model of AD, RAB5 was found to interact with PICALM (Zhao et al., 2015b), suggesting that it was a downstream effector of PICALM. However, in our *Drosophila* model, the relationship between *Rab5* and *lap* remained elusive. If *Rab5* is a downstream effector of *lap*, it might also regulate VGlut localization. Therefore, a quick way to elucidate the relationship between *Rab5* and *lap* is to look at whether the blockade of *Rab5* expression prevented *lap*-mediated VGlut recycling at the larval NMJ.

Moreover, this work clearly elucidated the relationship between *lap* and *Amph*, namely, *lap* increased Amph intensity at the NMJ upon Aβ expression. Given that this work also showed that *Amph* modulated the localization of GluRII receptors, it will be interesting to understand whether *lap*, via *Amph*, could possibly modulate the localization of GluRII receptors. In turn, GluRII receptors were found to mediate presynaptic glutamate release via retrograde signals. (DiAntonio et al., 1999). Based on this observation, it will be not surprising that *Amph* affects

glutamate release.

Finally, it is essential to validate the conserved function of PICALM and BIN1 in mammalian models of AD. Given that impacts of PICALM and BIN1 on APP processing are well studied, the future work should pay more attention to their contributions to Aβ toxicity. However, Aβ expressing mice lack AD phenotypes (Hsiao et al., 1996; Mucke et al., 2000). Therefore, the following studies will be dependent on a cell model of AD.

6.2 $A\beta_{42}$ expression leads to glutamate excitotoxicity in the short term

Here I used a genetically encoded glutamate indicator, iGluSnFR, to visualize glutamate dynamic and showed that extracellular glutamate is elevated upon $A\beta_{42}$ expression. My work also suggests that an increase in extracellular glutamate might be due to the presynaptic accumulation of VGlut. This glutamate excitotoxicity was also observed in mammalian models of AD (Abramov et al., 2009; Hynd et al., 2004). It was speculated to be caused by either enhancement in glutamate release (Cummings et al., 2015) or impairment in glutamate uptake, giving rise to excess extracellular glutamate (Hefendehl et al., 2016; Li et al., 2009; Talantova et al., 2013). My work provids further evidence to demonstrate that $A\beta_{42}$-induced glutamate toxicity in *vivo*.

My work also found that GluRIIA accumulated more on the plasma membrane, while GluRIIB accumulated less upon the short-time exposure of $A\beta_{42}$ (the L3 larvae). This observation supported previous *in vitro* studies. In the past, the long-term $A\beta_{42}$ exposure was found to lead to endocytosis of AMPARs and NMDARs, suggesting that $A\beta_{42}$ expression gave rise to a decrease in glutamate receptors (Hsieh et al., 2006; Shankar et al., 2007; Snyder et al., 2005; Zhao et al., 2010). More recent work revealed that although GluN2A was down-regulated upon $A\beta_{42}$ expression, GluN2B was transiently up-regulated (Hu et al., 2009a; Li et al., 2009; Li et al., 2011; Talantova et al., 2013). This observation correlated with the fact that GluN2A induced memory formation, while GluN2B induced memory decay. This different observation might be attributed to the time of $A\beta_{42}$ exposure. Acute exposure of $A\beta_{42}$ oligomers also conferred an

increase in GluA1 on the plasma membrane (Liu et al., 2010; Whitcomb et al., 2015). This finding was consistent with the fact that Ca^{2+} influx shortly increased as the primary response to $A\beta_{42}$ exposure (Lauren et al., 2009; Um et al., 2013; Um et al., 2012). Furthermore, knockout of a specific AMPAR subunit protected against $A\beta_{42}$–induced synaptic toxicity (Reinders et al., 2016). My finding raised the question as to whether $A\beta_{42}$ expression changed the GluRIIA/GluIIB ratio. Also, it remains elusive whether an increase in GluRIIA and a decrease in GluRIIB changed synaptic strength.

Apart from this, glutamate excitotoxicity in the short term might finally attenuate glutamatergic neurotransmission in the long term through hemostatic scaling. Firstly, Presynaptic glutamate negatively modulates the number of GluRII receptors (Featherstone et al., 2002). Secondly, GluRII reduces presynaptic glutamate release via retrograde signals (DiAntonio et al., 1999). In fact, long-time expression of $A\beta_{42}$ caused glutamatergic defects in adult flies at 28 days (Sofola et al., 2010). This time-dependent toxicity was also observed in the murine model, finding that the surface expression of GluN2B elevated at 15 minutes and then returned to baseline by 60 minutes after incubation with $A\beta_{42}$ (Lauren et al., 2009; Um et al., 2013; Um et al., 2012).

Given that I have provided an example of using iGluSnFR to visualize glutamate dynamics in the larval VNC, it will be interesting to test whether this method allows for detecting extracellular glutamate in adults' brains and therefore detecting the effect of the long-term expression of $A\beta_{42}$ on glutamatergic transmission.

Collectively, my work provided a new insight into the mechanism underlying AD progression, namely, $A\beta_{42}$ resulted in not only excitotoxicity of glutamate receptors but also excess glutamate release. As far as I know, one NMDAR antagonist memantine has been used in AD treatment (Bormann, 1989; Lipton, 2006; Milnerwood et al., 2010; Okamoto et al., 2009; Parsons et al., 1999; Suhs et al., 2014; Talantova et al., 2013; Wang and Zhang, 2005). However, it remains elusive whether VGLUT antagonists also attenuate AD phenotypes. Riluzole is a glutamate modulator that reduces glutamate release (Martin et al., 1993) and

facilitates astrocytic glutamate uptake (Banasr et al., 2010; Frizzo et al., 2004; Fumagalli et al., 2008). These findings suggest that riluzole will be a potential drug for AD treatment through preventing excessive glutamate overflow to the extrasynaptic space (Banasr et al., 2010; Brennan et al., 2010; Chowdhury et al., 2008). In fact, riluzole is a FDA (the US food and drug administration) approved drug in clinical trials for the treatment of MND (motor neuron disease) patients (Bensimon et al., 1994; Gurney, 1997). Therefore, it will be interesting to explore whether riluzole will have any therapeutic intervention of AD pathology.

6.3 Roles of glia in AD pathology

PICALM is enriched in endothelial cells and microglia. This indicates that PICALM in glial cells might contribute to AD progression. In this study, I used a new *Drosophila* model of AD and aimed to understand the role of glial *lap* in $A\beta_{42}$ toxicity.

Drosophila glial cells show great similarities with mammalian glial cells and represent a good example of the conservation between *Drosophila* and mammalian nervous systems. This highlights that *Drosophila* glial cells are a good model to elucidate the role of glial cells in AD progression. *Drosophila* nervous system also bears a wide variety of glial subtypes, although glial cells only represent 5–10% of the total cells in the *Drosophila* CNS. *Drosophila* glial cells are mainly constituted in cortex glia, ensheathing glia and astrocytes (Crews, 2010; Jacobs, 2000). Astrocytes affect neuronal development through FGF and TGF-β (Awasaki et al., 2008; Awasaki and Lee, 2011; Bialas and Stevens, 2013; Doherty et al., 2009; Muthukumar et al., 2014; Stork et al., 2014; Tasdemir-Yilmaz and Freeman, 2014). Moreover, astrocytes communicate with the mature neurons through glutamatergic transmission. Similar to mammalian astrocytes, *Drosophila* astrocytes express EAAT1 to promote glutamate clearance. In turn, the expression of EAAT1 is modulated by glutamate secreted from neurons (Benediktsson et al., 2012; Devaraju et al., 2013; Freeman et al., 2003; Yang et al., 2009). Both astrocytes and ensheathing glia are involved in debris clearance. For instance, ensheathing glia engulf axonal debris through activating the Draper receptor (Awasaki et al., 2006; Doherty et al., 2009; Doherty et al., 2014; Lu et al., 2014; MacDonald et al., 2006;

Macdonald et al., 2013; Ziegenfuss et al., 2008; Ziegenfuss et al., 2012). *Drosophila* glial cells are also found to facilitate the clearance of toxin proteins (Pearce et al., 2015). Besides that, *Drosophila* glial cells include perineural glia (PG) and subperineural glial cells (SPGs) that establish the BBB of flies (Auld et al., 1995; Baumgartner et al., 1996; Carlson et al., 2000; Leiserson et al., 2000; Schwabe et al., 2005). In particular, *Drosophila* PNS has the wrapping glia to wrap, support, and modulate the development and function of sensory and motor neurons (Beckervordersandforth et al., 2008; Leiserson et al., 2000; Stork et al., 2008). Collectively, the contributions of *Drosophila* glial cells to neurodegenerative diseases are the most understudied. Therefore, we should pay more attention to the role of *Drosophila* glial cells in AD progression.

My study has found that overexpression of *lap* in glial cells showed suppression of $A\beta_{42}$ toxicity. However, as this model confers exogenous toxicity of quinic acid (Riabinina et al., 2015), I cannot exclude the possibility that *lap* specifically reduced toxicity caused by quinic acid. Although this model takes this disadvantage, it might be still useful to investigate the glia-neuron communications in AD pathology (Pearce et al., 2015) because constitutive expression of QF2 is independent of feeding quinic acid. In addition to this, the other possible approach to drive gene expression is using the LexA-lexAop system, but this binary expression system is not inducible (Aso et al., 2014; Lai and Lee, 2006).

In the mammalian nervous system, approximately 90% of the cells in the brain are glial cells that surround neurons. Therefore, mammalian gilal cells are more complicated than *Drosophila* glial cells. Mammalian glial cells are categorized in oligodendrocytes, astrocytes and microglia. They are distinguished in morphology, origins, markers and function. Oligodendrocytes form the myelin sheath and wrap axons. They ensheath axons to enable fast transduction of electrical signals. Oligodendrocytes communicate with neurons through glutamatergic transmission, suggesting that oligodendrocytes are crucial to learning and memory (Fruhbeis et al., 2013; McKenzie et al., 2014). Oligodendrocytes support energy metabolism in the adjacent axons as well. Oligodendrocytes take up glucose from the blood and synthesize lactate (Funfschilling et al., 2012; Rinholm et al., 2011). Lactate is then

released by the monocarboxylate transporter MCT1 and imported into neurons (Lee et al., 2012). Furthermore, oligodendroglial glutamate receptors regulate glucose import of oligodendrocytes, indicating that glutamatergic transmission is coupled with glial metabolism (Saab et al., 2016). Given that PICALM is involved in glutamatergic transmission in my study, it is worthy of exploring whether PICALM affects oligodendrocyte-neuron communications and therefore AD pathology. As oligodendroglial glutamate receptor regulates glucose metabolism, it will be interesting to investigate the link between glutamatergic transmission and glucose metabolism in the AD case because glucose metabolism is impaired in the AD case (Carro et al., 2006; Carro et al., 2002; Craft et al., 2012; Dudek et al., 1997) Winkler et al., 2015; Niccoli et al., 2016).

The function of astrocytes is dependent on their secreted proteins. For example, astrocytes-secreted APOE enhances presynaptic function of glutamatergic synapses (Goritz et al., 2005; Mauch et al., 2001). As well as the control of synapse formation, astrocytes can communicate with neurons in a rapid way. Astrocytes release and take up diverse neurotransmitters such as calcium, glutamate and D-serine (Nett et al., 2002; Panatier et al., 2011; Perea and Araque, 2005; Verbich et al., 2012; Wang et al., 2006). These molecules modulate synaptic transmission and affect memory acquisition (Kronschlager et al., 2016). In turn, astrocytic activity is regulated by neuron-secreted glutamate (Yang et al., 2009).

In AD frequent dysregulation of glia is observed, for example, reactive astrogliosis is a common feature of AD. One prevailing view insists that reactive astrocytes lead to detrimental effects because of neurotoxic inflammation. These inflammatory molecules include a number of cytokines, chemokines and growth factors (Sofroniew, 2015; Sofroniew and Vinters, 2010). However, inhibition of reactive astrogliosis exacerbates disease progression in a mouse model of AD, indicating that reactive astrocytes may exert a beneficial function and increase neuronal survival (Nagele et al., 2004; Thal et al., 2000). Astrocytes confer benefits via diverse ways. Firstly, astrocytes internalize $A\beta_{42}$ and clear $A\beta_{42}$ peptides (Wyss-Coray et al., 2003). Secondly, astrocytes uptake excess extracellular glutamate and interfere with $A\beta_{42}$ toxicity without affecting $A\beta_{42}$ levels (Simpson et al., 2010). Although my work cannot conclude that *lap* in glial

cells reduced $A\beta_{42}$ toxicity, this work showed that *lap* in glial cells did not change $A\beta_{42}$ levels. As *Drosophila* glial cells are a counterpart to mammalian astrocytes, mammalian astrocytes might be not involved in $A\beta_{42}$ clearance but glutamate release. In fact, astrocytes are reported to release excess glutamate upon $A\beta_{42}$ exposure (Hu et al., 2009a; Li et al., 2009; Li et al., 2011; Talantova et al., 2013). An interesting possible future work would be to investigate whether PICALM in astrocytes modulates glutamatergic neurotransmission and therefore affects disease progression.

Microglial activation is also observed in AD. Microglia are either positive or negative modulators of AD. On one hand, microglial activation gives rise to inflammation and ROS production to exacerbate neurodegeneration (Block et al., 2007); on the other hand, activated microglia phagocytoses $A\beta_{42}$ peptides via the CCR2 receptor (Kobayashi et al., 1993), beclin (Lucin et al., 2013) or AD risk genes, TREM2 (Kleinberger et al., 2014; Ulland et al., 2017; Wang et al., 2015; Yeh et al., 2016) and CR1 (Fuhrmann et al., 2010), whereas the other AD risk gene, CD33, perturbs this $A\beta_{42}$ clearance (Griciuc et al., 2013).

Both astrocyte and microglia communicate with the brain endothelial cells and pericytes that form the blood-brain barrier (BBB). The BBB transcytoses proteins from the blood and brain. For example, a BBB breakdown is found in AD that increases BBB permeability (Zhao et al., 2015a; Zlokovic, 2008). The BBB breakdown incurs the decreased $A\beta_{42}$ transport across the BBB (loss of toxicity) and the increased entry of neurotoxic products into the brain. (gain of toxicity). $A\beta_{42}$ is effluxed into the BBB and degraded by neprilysin via binding to LRP1 (Deane et al., 2004; Winkler et al., 2015). This process is facilitated by PICALM (Zhao et al., 2015b). The BBB efflux of $A\beta_{42}$ is also mediated by an AD risk gene, CLU (Bell et al., 2007). Conversely, the other AD risk gene, APOE4, slows the internalized $A\beta_{42}$ (Bell et al., 2012; Deane et al., 2008). Efflux of $A\beta_{42}$ across the BBB is also interfered by RAGE (Deane et al., 2003; Deane et al., 2012). RAGE is a transporter on the cell surface of endothelial cells and physically interacts with $A\beta_{42}$. RAGE/ $A\beta_{42}$ interaction results in the accumulation of $A\beta_{42}$ in neurons, and so as expected intervention of the RAGE/ $A\beta_{42}$ interaction has been shown to reduce ROS and attenuate $A\beta_{42}$ damage (Yan et al., 1996). Overall, compared to studies on the function of

PICALM in the blood-brain barrier, studies on the function of PICALM in microglia are sparse. Given that *Drosophila* does not have a counterpart to mammalian microglia, a following possible study could investigate whether PICALM facilitate $A\beta_{42}$ clearance in microglia in a mammalian model of AD.

6.4 Potential mechanisms underlying identified modifiers of $A\beta_{42}$ toxicity

My work in chapter 5 has identified 4 potential gene-knockdown suppressors of $A\beta_{42}$ toxicity. As stated earlier, none of them were linked to AD risk. Given that *CG15011* regulated gene transcription and reduced Aβ levels, future works should identify whether its downregulation reduces Aβ transcription. As *Larp* mediated mRNA translation and showed a trend to decrease Aβ levels, the following work is evitable to investigate whether its downregulation reduces Aβ translation. Because Aβ species are produced from APP protein, its expression is independent of transcriptional and translational regulation in human brains. If these two genes change Aβ transcription or translation, they might not be the actual modifiers.

One potential gene knockdown suppressor is *Sodh-2*, a *Drosophila* orthologue of sorbitol dehydrogenase (SDH). Inhibition of SDH was reported to suppress neurodysfunction in diabetes (Cameron et al., 1997; Ng et al., 1998; Obrosova et al., 1999; Tilton et al., 1995), suggesting its downregulation might provide global neuroprotection. Most importantly, AD was shown to give rise to progressive impairment of metabolic processes, indicating that metabolic interventions might ameliorate the AD phenotype (Niccoli et al., 2016; Tien et al., 2016; Winkler et al., 2015; Yoon et al., 2012)

Another promising candidate is *Pxn*. Although the function of the PXN protein is unclear, it is well known that PXN is secreted into the ECM. Given that many secreted proteins such as APOE affect clearance of Aβ and formation of amyloid plaques (Bales et al., 2009; Fryer et al., 2005; Oakley et al., 2006; Youmans et al., 2012), this protein might be involved in formation of amyloid plaques.

It is important to note that 25% of *Drosophila* genes are not conserved in humans. Therefore, it will be necessary to confirm whether the contributions of these candidate suppressors of Aβ toxicity are conserved in mammalian models of AD. Given that these hits are supposed to modulate the downstream of Aβ toxicity, they may not affect APP processing. Therefore, future works could use APP KI mice or APP iPSCs-derived neurons.

In summary, this work aimed to investigate candidate modifiers of Aβ toxicity from GWAS and from a *Drosophila* screen. This work achieved this purpose by identifying *lap*, *Amph*, *Rab5, EndoA* and *Snap25* as potential gene-overexpression suppressors of $A\beta_{42}$ toxicity, and *CG15011*, *Larp*, *Pxn*, and *Sodh2* as gene-knockdown suppressors of $A\beta_{42}$ toxicity. This work also elucidated the molecular mechanisms underlying the protection of *lap* and *Amph* in Aβ pathogenesis which modulates glutamate transmission. Subsequent studies should mainly focus on validating the functional conservation of these candidate modifiers in a mammalian model of AD. Future works should also pay attention to elucidating the molecular mechanisms by which down-regulation of *CG15011*, *Larp*, *Pxn*, and *Sodh2* attenuates Aβ pathology.

7. References

Abbott, A., and Dolgin, E. (2016). Failed Alzheimer's trial does not kill leading theory of disease. Nature *540*, 15-16.

Abramov, E., Dolev, I., Fogel, H., Ciccotosto, G.D., Ruff, E., and Slutsky, I. (2009). Amyloid-beta as a positive endogenous regulator of release probability at hippocampal synapses. Nature neuroscience *12*, 1567-1576.

Akalal, D.B., Wilson, C.F., Zong, L., Tanaka, N.K., Ito, K., and Davis, R.L. (2006). Roles for Drosophila mushroom body neurons in olfactory learning and memory. Learning & memory *13*, 659-668.

Akalal, D.B., Yu, D., and Davis, R.L. (2010). A late-phase, long-term memory trace forms in the gamma neurons of Drosophila mushroom bodies after olfactory classical conditioning. The Journal of neuroscience : the official journal of the Society for Neuroscience *30*, 16699-16708.

Allen, M.J., and Godenschwege, T.A. (2010). Electrophysiological recordings from the Drosophila giant fiber system (GFS). Cold Spring Harbor protocols *2010*, pdb prot5453.

Alonso, A., Zaidi, T., Novak, M., Grundke-Iqbal, I., and Iqbal, K. (2001). Hyperphosphorylation induces self-assembly of tau into tangles of paired helical filaments/straight filaments. Proceedings of the National Academy of Sciences of the United States of America *98*, 6923-6928.

Alonso Adel, C., Li, B., Grundke-Iqbal, I., and Iqbal, K. (2006). Polymerization of hyperphosphorylated tau into filaments eliminates its inhibitory activity. Proceedings of the National Academy of Sciences of the United States of America *103*, 8864-8869.

Anandatheerthavarada, H.K., Biswas, G., Robin, M.A., and Avadhani, N.G. (2003). Mitochondrial targeting and a novel transmembrane arrest of Alzheimer's amyloid precursor protein impairs mitochondrial function in neuronal cells. The Journal of cell biology *161*, 41-54.

Andlauer, T.F., Scholz-Kornehl, S., Tian, R., Kirchner, M., Babikir, H.A., Depner, H., Loll, B., Quentin, C., Gupta, V.K., Holt, M.G.*, et al.* (2014). Drep-2 is a novel synaptic protein important for learning and memory. eLife *3*.

Ando, K., Brion, J.P., Stygelbout, V., Suain, V., Authelet, M., Dedecker, R., Chanut, A., Lacor, P., Lavaur, J., Sazdovitch, V.*, et al.* (2013). Clathrin adaptor CALM/PICALM is associated with neurofibrillary tangles and is cleaved in Alzheimer's brains. Acta neuropathologica *125*, 861-878.

Andreadis, A., Brown, W.M., and Kosik, K.S. (1992). Structure and novel exons of the human tau gene. Biochemistry *31*, 10626-10633.

Annaert, W.G., Levesque, L., Craessaerts, K., Dierinck, I., Snellings, G., Westaway, D., George-Hyslop, P.S., Cordell, B., Fraser, P., and De Strooper, B. (1999). Presenilin 1 controls gamma-secretase processing of amyloid precursor protein in pre-golgi compartments of hippocampal neurons. The Journal of cell biology *147*, 277-294.

Archbold, J.K., Whitten, A.E., Hu, S.H., Collins, B.M., and Martin, J.L. (2014). SNARE-ing the structures of Sec1/Munc18 proteins. Current opinion in structural biology *29*, 44-51.

Armakola, M., Higgins, M.J., Figley, M.D., Barmada, S.J., Scarborough, E.A., Diaz, Z., Fang, X., Shorter, J., Krogan, N.J., Finkbeiner, S.*, et al.* (2012). Inhibition of RNA lariat debranching enzyme suppresses TDP-43 toxicity in ALS disease models. Nature genetics *44*, 1302-1309.

Aso, Y., Sitaraman, D., Ichinose, T., Kaun, K.R., Vogt, K., Belliart-Guerin, G., Placais, P.Y., Robie, A.A., Yamagata, N., Schnaitmann, C.*, et al.* (2014). Mushroom body output neurons encode valence and guide memory-based action selection in Drosophila. eLife *3*, e04580.

Augustin, H., Allen, M.J., and Partridge, L. (2011). Electrophysiological recordings from the giant fiber pathway of D. melanogaster. Journal of visualized experiments : JoVE.

Augustin, H., Grosjean, Y., Chen, K., Sheng, Q., and Featherstone, D.E. (2007). Nonvesicular release of glutamate by glial xCT transporters suppresses glutamate receptor clustering in vivo.

The Journal of neuroscience : the official journal of the Society for Neuroscience *27*, 111-123.

Auld, V.J., Fetter, R.D., Broadie, K., and Goodman, C.S. (1995). Gliotactin, a novel transmembrane protein on peripheral glia, is required to form the blood-nerve barrier in Drosophila. Cell *81*, 757-767.

Awasaki, T., Lai, S.L., Ito, K., and Lee, T. (2008). Organization and postembryonic development of glial cells in the adult central brain of Drosophila. The Journal of neuroscience : the official journal of the Society for Neuroscience *28*, 13742-13753.

Awasaki, T., and Lee, T. (2011). New tools for the analysis of glial cell biology in Drosophila. Glia *59*, 1377-1386.

Awasaki, T., Tatsumi, R., Takahashi, K., Arai, K., Nakanishi, Y., Ueda, R., and Ito, K. (2006). Essential role of the apoptotic cell engulfment genes draper and ced-6 in programmed axon pruning during Drosophila metamorphosis. Neuron *50*, 855-867.

Baig, S., Joseph, S.A., Tayler, H., Abraham, R., Owen, M.J., Williams, J., Kehoe, P.G., and Love, S. (2010). Distribution and expression of picalm in Alzheimer disease. Journal of neuropathology and experimental neurology *69*, 1071-1077.

Baldassarro, V.A., Marchesini, A., Giardino, L., and Calza, L. (2017). Vulnerability of primary neurons derived from Tg2576 Alzheimer mice to oxygen and glucose deprivation: role of intraneuronal amyloid-beta accumulation and astrocytes. Disease models & mechanisms *10*, 671-678.

Bales, K.R., Liu, F., Wu, S., Lin, S., Koger, D., DeLong, C., Hansen, J.C., Sullivan, P.M., and Paul, S.M. (2009). Human APOE isoform-dependent effects on brain beta-amyloid levels in PDAPP transgenic mice. The Journal of neuroscience : the official journal of the Society for Neuroscience *29*, 6771-6779.

Ballatore, C., Lee, V.M., and Trojanowski, J.Q. (2007). Tau-mediated neurodegeneration in Alzheimer's disease and related disorders. Nature reviews Neuroscience *8*, 663-672.

Banasr, M., Chowdhury, G.M., Terwilliger, R., Newton, S.S., Duman, R.S., Behar, K.L., and Sanacora, G. (2010). Glial pathology in an animal model of depression: reversal of stress-induced cellular, metabolic and behavioral deficits by the glutamate-modulating drug riluzole. Molecular psychiatry *15*, 501-511.

Bao, H., Daniels, R.W., MacLeod, G.T., Charlton, M.P., Atwood, H.L., and Zhang, B. (2005). AP180 maintains the distribution of synaptic and vesicle proteins in the nerve terminal and indirectly regulates the efficacy of Ca2+-triggered exocytosis. Journal of neurophysiology *94*, 1888-1903.

Barbero, P., Bittova, L., and Pfeffer, S.R. (2002). Visualization of Rab9-mediated vesicle transport from endosomes to the trans-Golgi in living cells. The Journal of cell biology *156*, 511-518.

Barbour, B., Brew, H., and Attwell, D. (1988). Electrogenic glutamate uptake in glial cells is activated by intracellular potassium. Nature *335*, 433-435.

Bartus, R.T. (1979). Physostigmine and recent memory: effects in young and aged nonhuman primates. Science *206*, 1087-1089.

Bashkirov, P.V., Akimov, S.A., Evseev, A.I., Schmid, S.L., Zimmerberg, J., and Frolov, V.A. (2008). GTPase cycle of dynamin is coupled to membrane squeeze and release, leading to spontaneous fission. Cell *135*, 1276-1286.

Bass, T.M., Grandison, R.C., Wong, R., Martinez, P., Partridge, L., and Piper, M.D. (2007). Optimization of dietary restriction protocols in Drosophila. The journals of gerontology Series A, Biological sciences and medical sciences *62*, 1071-1081.

Baumann, K., Mandelkow, E.M., Biernat, J., Piwnica-Worms, H., and Mandelkow, E. (1993). Abnormal Alzheimer-like phosphorylation of tau-protein by cyclin-dependent kinases cdk2 and cdk5. FEBS letters *336*, 417-424.

Baumgartner, S., Littleton, J.T., Broadie, K., Bhat, M.A., Harbecke, R., Lengyel, J.A.,

Chiquet-Ehrismann, R., Prokop, A., and Bellen, H.J. (1996). A Drosophila neurexin is required for septate junction and blood-nerve barrier formation and function. Cell *87*, 1059-1068.

Baumkotter, F., Schmidt, N., Vargas, C., Schilling, S., Weber, R., Wagner, K., Fiedler, S., Klug, W., Radzimanowski, J., Nickolaus, S.*, et al.* (2014). Amyloid precursor protein dimerization and synaptogenic function depend on copper binding to the growth factor-like domain. The Journal of neuroscience : the official journal of the Society for Neuroscience *34*, 11159-11172.

Beckervordersandforth, R.M., Rickert, C., Altenhein, B., and Technau, G.M. (2008). Subtypes of glial cells in the Drosophila embryonic ventral nerve cord as related to lineage and gene expression. Mechanisms of development *125*, 542-557.

Behm-Ansmant, I., Rehwinkel, J., Doerks, T., Stark, A., Bork, P., and Izaurralde, E. (2006). mRNA degradation by miRNAs and GW182 requires both CCR4:NOT deadenylase and DCP1:DCP2 decapping complexes. Genes & development *20*, 1885-1898.

Beisiegel, U., Weber, W., Ihrke, G., Herz, J., and Stanley, K.K. (1989). The LDL-receptor-related protein, LRP, is an apolipoprotein E-binding protein. Nature *341*, 162-164.

Bell, R.D., Sagare, A.P., Friedman, A.E., Bedi, G.S., Holtzman, D.M., Deane, R., and Zlokovic, B.V. (2007). Transport pathways for clearance of human Alzheimer's amyloid beta-peptide and apolipoproteins E and J in the mouse central nervous system. Journal of cerebral blood flow and metabolism : official journal of the International Society of Cerebral Blood Flow and Metabolism *27*, 909-918.

Bell, R.D., Winkler, E.A., Singh, I., Sagare, A.P., Deane, R., Wu, Z., Holtzman, D.M., Betsholtz, C., Armulik, A., Sallstrom, J.*, et al.* (2012). Apolipoprotein E controls cerebrovascular integrity via cyclophilin A. Nature *485*, 512-516.

Benediktsson, A.M., Marrs, G.S., Tu, J.C., Worley, P.F., Rothstein, J.D., Bergles, D.E., and Dailey, M.E. (2012). Neuronal activity regulates glutamate transporter dynamics in developing astrocytes. Glia *60*, 175-188.

Benke, T.A., Luthi, A., Isaac, J.T., and Collingridge, G.L. (1998). Modulation of AMPA receptor unitary conductance by synaptic activity. Nature *393*, 793-797.

Bensimon, G., Lacomblez, L., and Meininger, V. (1994). A controlled trial of riluzole in amyotrophic lateral sclerosis. ALS/Riluzole Study Group. The New England journal of medicine *330*, 585-591.

Bentahir, M., Nyabi, O., Verhamme, J., Tolia, A., Horre, K., Wiltfang, J., Esselmann, H., and De Strooper, B. (2006). Presenilin clinical mutations can affect gamma-secretase activity by different mechanisms. Journal of neurochemistry *96*, 732-742.

Berger, J., Suzuki, T., Senti, K.A., Stubbs, J., Schaffner, G., and Dickson, B.J. (2001). Genetic mapping with SNP markers in Drosophila. Nature genetics *29*, 475-481.

Bialas, A.R., and Stevens, B. (2013). TGF-beta signaling regulates neuronal C1q expression and developmental synaptic refinement. Nature neuroscience *16*, 1773-1782.

Biere, A.L., Ostaszewski, B., Zhao, H., Gillespie, S., Younkin, S.G., and Selkoe, D.J. (1995). Co-expression of beta-amyloid precursor protein (betaAPP) and apolipoprotein E in cell culture: analysis of betaAPP processing. Neurobiol Dis *2*, 177-187.

Billingsley, M.L., and Kincaid, R.L. (1997). Regulated phosphorylation and dephosphorylation of tau protein: effects on microtubule interaction, intracellular trafficking and neurodegeneration. Biochem J *323 (Pt 3)*, 577-591.

Binder, L.I., Frankfurter, A., and Rebhun, L.I. (1985). The distribution of tau in the mammalian central nervous system. The Journal of cell biology *101*, 1371-1378.

Block, M.L., Zecca, L., and Hong, J.S. (2007). Microglia-mediated neurotoxicity: uncovering the molecular mechanisms. Nature reviews Neuroscience *8*, 57-69.

Block, M.R., Glick, B.S., Wilcox, C.A., Wieland, F.T., and Rothman, J.E. (1988). Purification of an N-ethylmaleimide-sensitive protein catalyzing vesicular transport. Proceedings of the National Academy of Sciences of the United States of America *85*, 7852-7856.

Blondeau, F., Ritter, B., Allaire, P.D., Wasiak, S., Girard, M., Hussain, N.K., Angers, A., Legendre-Guillemin, V., Roy, L., Boismenu, D.*, et al.* (2004). Tandem MS analysis of brain clathrin-coated vesicles reveals their critical involvement in synaptic vesicle recycling. Proceedings of the National Academy of Sciences of the United States of America *101*, 3833-3838.

Bloom, R.D., Bolin, P., Gandra, S.R., Scarlata, D., and Petersen, J. (2011). Impact on health-related quality of life in kidney transplant recipients with late posttransplant anemia administered darbepoetin alfa: results from the STRATA study. Transplantation proceedings *43*, 1593-1600.

Blum, A.L., Li, W., Cressy, M., and Dubnau, J. (2009). Short- and long-term memory in Drosophila require cAMP signaling in distinct neuron types. Current biology : CB *19*, 1341-1350.

Bogdanik, L., Mohrmann, R., Ramaekers, A., Bockaert, J., Grau, Y., Broadie, K., and Parmentier, M.L. (2004). The Drosophila metabotropic glutamate receptor DmGluRA regulates activity-dependent synaptic facilitation and fine synaptic morphology. The Journal of neuroscience : the official journal of the Society for Neuroscience *24*, 9105-9116.

Bormann, J. (1989). Memantine is a potent blocker of N-methyl-D-aspartate (NMDA) receptor channels. European journal of pharmacology *166*, 591-592.

Boto, T., Louis, T., Jindachomthong, K., Jalink, K., and Tomchik, S.M. (2014). Dopaminergic modulation of cAMP drives nonlinear plasticity across the Drosophila mushroom body lobes. Current biology : CB *24*, 822-831.

Boucrot, E., Saffarian, S., Zhang, R., and Kirchhausen, T. (2010). Roles of AP-2 in clathrin-mediated endocytosis. PloS one *5*, e10597.

Bouvier, M., Szatkowski, M., Amato, A., and Attwell, D. (1992). The glial cell glutamate uptake carrier countertransports pH-changing anions. Nature *360*, 471-474.

Bowen, D.M., Smith, C.B., White, P., and Davison, A.N. (1976). Neurotransmitter-related enzymes and indices of hypoxia in senile dementia and other abiotrophies. Brain *99*, 459-496.

Boyd-Kimball, D., Poon, H.F., Lynn, B.C., Cai, J., Pierce, W.M., Jr., Klein, J.B., Ferguson, J., Link, C.D., and Butterfield, D.A. (2006). Proteomic identification of proteins specifically oxidized in Caenorhabditis elegans expressing human Abeta(1-42): implications for Alzheimer's disease. Neurobiology of aging *27*, 1239-1249.

Braak, E., Braak, H., and Mandelkow, E.M. (1994). A sequence of cytoskeleton changes related to the formation of neurofibrillary tangles and neuropil threads. Acta Neuropathol *87*, 554-567.

Bramblett, G.T., Goedert, M., Jakes, R., Merrick, S.E., Trojanowski, J.Q., and Lee, V.M. (1993). Abnormal tau phosphorylation at Ser396 in Alzheimer's disease recapitulates development and contributes to reduced microtubule binding. Neuron *10*, 1089-1099.

Brand, A.H., and Perrimon, N. (1993). Targeted gene expression as a means of altering cell fates and generating dominant phenotypes. Development *118*, 401-415.

Brenman, J.E., Gao, F.B., Jan, L.Y., and Jan, Y.N. (2001). Sequoia, a tramtrack-related zinc finger protein, functions as a pan-neural regulator for dendrite and axon morphogenesis in Drosophila. Developmental cell *1*, 667-677.

Brennan, B.P., Hudson, J.I., Jensen, J.E., McCarthy, J., Roberts, J.L., Prescot, A.P., Cohen, B.M., Pope, H.G., Jr., Renshaw, P.F., and Ongur, D. (2010). Rapid enhancement of glutamatergic neurotransmission in bipolar depression following treatment with riluzole. Neuropsychopharmacology : official publication of the American College of Neuropsychopharmacology *35*, 834-846.

Brion, J.P., Couck, A.M., Robertson, J., Loviny, T.L., and Anderton, B.H. (1993). Neurofilament monoclonal antibodies RT97 and 8D8 recognize different modified epitopes in paired helical filament-tau in Alzheimer's disease. Journal of neurochemistry *60*, 1372-1382.

Buee, L., Bussiere, T., Buee-Scherrer, V., Delacourte, A., and Hof, P.R. (2000). Tau protein isoforms, phosphorylation and role in neurodegenerative disorders. Brain Res Brain Res Rev *33*, 95-130.

Burchell, V.S., Nelson, D.E., Sanchez-Martinez, A., Delgado-Camprubi, M., Ivatt, R.M., Pogson, J.H., Randle, S.J., Wray, S., Lewis, P.A., Houlden, H.*, et al.* (2013). The Parkinson's disease-linked proteins Fbxo7 and Parkin interact to mediate mitophagy. Nature neuroscience *16*, 1257-1265.

Burnett, C., Valentini, S., Cabreiro, F., Goss, M., Somogyvari, M., Piper, M.D., Hoddinott, M., Sutphin, G.L., Leko, V., McElwee, J.J.*, et al.* (2011). Absence of effects of Sir2 overexpression on lifespan in C. elegans and Drosophila. Nature *477*, 482-485.

Busciglio, J., Gabuzda, D.H., Matsudaira, P., and Yankner, B.A. (1993). Generation of beta-amyloid in the secretory pathway in neuronal and nonneuronal cells. Proceedings of the National Academy of Sciences of the United States of America *90*, 2092-2096.

Butner, K.A., and Kirschner, M.W. (1991). Tau protein binds to microtubules through a flexible array of distributed weak sites. The Journal of cell biology *115*, 717-730.

Buttini, M., Orth, M., Bellosta, S., Akeefe, H., Pitas, R.E., Wyss-Coray, T., Mucke, L., and Mahley, R.W. (1999). Expression of human apolipoprotein E3 or E4 in the brains of Apoe-/- mice: isoform-specific effects on neurodegeneration. The Journal of neuroscience : the official journal of the Society for Neuroscience *19*, 4867-4880.

Calafate, S., Flavin, W., Verstreken, P., and Moechars, D. (2016). Loss of Bin1 Promotes the Propagation of Tau Pathology. Cell reports *17*, 931-940.

Cameron, N.E., Cotter, M.A., Basso, M., and Hohman, T.C. (1997). Comparison of the effects of inhibitors of aldose reductase and sorbitol dehydrogenase on neurovascular function, nerve conduction and tissue polyol pathway metabolites in streptozotocin-diabetic rats. Diabetologia *40*, 271-281.

Campbell, R.A., Honegger, K.S., Qin, H., Li, W., Demir, E., and Turner, G.C. (2013). Imaging a population code for odor identity in the Drosophila mushroom body. The Journal of neuroscience : the official journal of the Society for Neuroscience *33*, 10568-10581.

Cao, W., Song, H.J., Gangi, T., Kelkar, A., Antani, I., Garza, D., and Konsolaki, M. (2008). Identification of novel genes that modify phenotypes induced by Alzheimer's beta-amyloid overexpression in Drosophila. Genetics *178*, 1457-1471.

Cao, X., and Sudhof, T.C. (2001). A transcriptionally [correction of transcriptively] active complex of APP with Fe65 and histone acetyltransferase Tip60. Science *293*, 115-120.

Capell, A., Grunberg, J., Pesold, B., Diehlmann, A., Citron, M., Nixon, R., Beyreuther, K., Selkoe, D.J., and Haass, C. (1998). The proteolytic fragments of the Alzheimer's disease-associated presenilin-1 form heterodimers and occur as a 100-150-kDa molecular mass complex. The Journal of biological chemistry *273*, 3205-3211.

Carlson, S.D., Juang, J.L., Hilgers, S.L., and Garment, M.B. (2000). Blood barriers of the insect. Annual review of entomology *45*, 151-174.

Carrano, A.C., Dillin, A., and Hunter, T. (2014). A Kruppel-like factor downstream of the E3 ligase WWP-1 mediates dietary-restriction-induced longevity in Caenorhabditis elegans. Nature communications *5*, 3772.

Carrano, A.C., Liu, Z., Dillin, A., and Hunter, T. (2009). A conserved ubiquitination pathway determines longevity in response to diet restriction. Nature *460*, 396-399.

Carrasquillo, M.M., Belbin, O., Hunter, T.A., Ma, L., Bisceglio, G.D., Zou, F., Crook, J.E., Pankratz, V.S., Sando, S.B., Aasly, J.O.*, et al.* (2011). Replication of BIN1 association with Alzheimer's disease and evaluation of genetic interactions. Journal of Alzheimer's disease : JAD *24*, 751-758.

Carrasquillo, M.M., Crook, J.E., Pedraza, O., Thomas, C.S., Pankratz, V.S., Allen, M., Nguyen, T., Malphrus, K.G., Ma, L., Bisceglio, G.D.*, et al.* (2015). Late-onset Alzheimer's risk variants in

memory decline, incident mild cognitive impairment, and Alzheimer's disease. Neurobiology of aging *36*, 60-67.

Carro, E., Trejo, J.L., Gerber, A., Loetscher, H., Torrado, J., Metzger, F., and Torres-Aleman, I. (2006). Therapeutic actions of insulin-like growth factor I on APP/PS2 mice with severe brain amyloidosis. Neurobiology of aging *27*, 1250-1257.

Carro, E., Trejo, J.L., Gomez-Isla, T., LeRoith, D., and Torres-Aleman, I. (2002). Serum insulin-like growth factor I regulates brain amyloid-beta levels. Nature medicine *8*, 1390-1397.

Casas-Tinto, S., Zhang, Y., Sanchez-Garcia, J., Gomez-Velazquez, M., Rincon-Limas, D.E., and Fernandez-Funez, P. (2011). The ER stress factor XBP1s prevents amyloid-beta neurotoxicity. Human molecular genetics *20*, 2144-2160.

Caspersen, C., Wang, N., Yao, J., Sosunov, A., Chen, X., Lustbader, J.W., Xu, H.W., Stern, D., McKhann, G., and Yan, S.D. (2005). Mitochondrial Abeta: a potential focal point for neuronal metabolic dysfunction in Alzheimer's disease. FASEB journal : official publication of the Federation of American Societies for Experimental Biology *19*, 2040-2041.

Ceglia, I., Reitz, C., Gresack, J., Ahn, J.H., Bustos, V., Bleck, M., Zhang, X., Martin, G., Simon, S.M., Nairn, A.C.*, et al.* (2015). APP intracellular domain-WAVE1 pathway reduces amyloid-beta production. Nature medicine *21*, 1054-1059.

Cerf, E., Gustot, A., Goormaghtigh, E., Ruysschaert, J.M., and Raussens, V. (2011). High ability of apolipoprotein E4 to stabilize amyloid-beta peptide oligomers, the pathological entities responsible for Alzheimer's disease. FASEB journal : official publication of the Federation of American Societies for Experimental Biology *25*, 1585-1595.

Cervantes-Sandoval, I., Martin-Pena, A., Berry, J.A., and Davis, R.L. (2013). System-like consolidation of olfactory memories in Drosophila. The Journal of neuroscience : the official journal of the Society for Neuroscience *33*, 9846-9854.

Chakraborty, R., Vepuri, V., Mhatre, S.D., Paddock, B.E., Miller, S., Michelson, S.J., Delvadia,

R., Desai, A., Vinokur, M., Melicharek, D.J., *et al.* (2011). Characterization of a Drosophila Alzheimer's disease model: pharmacological rescue of cognitive defects. PloS one *6*, e20799.

Chang, H., Ciani, S., and Kidokoro, Y. (1994). Ion permeation properties of the glutamate receptor channel in cultured embryonic Drosophila myotubes. The Journal of physiology *476*, 1-16.

Chang, M.Y., Boulden, J., Katz, J.B., Wang, L., Meyer, T.J., Soler, A.P., Muller, A.J., and Prendergast, G.C. (2007). Bin1 ablation increases susceptibility to cancer during aging, particularly lung cancer. Cancer Res *67*, 7605-7612.

Chapuis, J., Hansmannel, F., Gistelinck, M., Mounier, A., Van Cauwenberghe, C., Kolen, K.V., Geller, F., Sottejeau, Y., Harold, D., Dourlen, P., *et al.* (2013). Increased expression of BIN1 mediates Alzheimer genetic risk by modulating tau pathology. Molecular psychiatry *18*, 1225-1234.

Chen, C.C., Wu, J.K., Lin, H.W., Pai, T.P., Fu, T.F., Wu, C.L., Tully, T., and Chiang, A.S. (2012). Visualizing long-term memory formation in two neurons of the Drosophila brain. Science *335*, 678-685.

Chiang, H.C., Wang, L., Xie, Z., Yau, A., and Zhong, Y. (2010). PI3 kinase signaling is involved in Abeta-induced memory loss in Drosophila. Proceedings of the National Academy of Sciences of the United States of America *107*, 7060-7065.

Chidambaram, S., Zimmermann, J., and von Mollard, G.F. (2008). ENTH domain proteins are cargo adaptors for multiple SNARE proteins at the TGN endosome. Journal of cell science *121*, 329-338.

Choi, H.Y., Liu, Y., Tennert, C., Sugiura, Y., Karakatsani, A., Kroger, S., Johnson, E.B., Hammer, R.E., Lin, W., and Herz, J. (2013). APP interacts with LRP4 and agrin to coordinate the development of the neuromuscular junction in mice. eLife *2*, e00220.

Choi, S.H., Kim, Y.H., Hebisch, M., Sliwinski, C., Lee, S., D'Avanzo, C., Chen, H., Hooli, B.,

Asselin, C., Muffat, J.*, et al.* (2014). A three-dimensional human neural cell culture model of Alzheimer's disease. Nature *515*, 274-278.

Chowdhury, G.M., Banasr, M., de Graaf, R.A., Rothman, D.L., Behar, K.L., and Sanacora, G. (2008). Chronic riluzole treatment increases glucose metabolism in rat prefrontal cortex and hippocampus. Journal of cerebral blood flow and metabolism : official journal of the International Society of Cerebral Blood Flow and Metabolism *28*, 1892-1897.

Chung, C.Y., Khurana, V., Auluck, P.K., Tardiff, D.F., Mazzulli, J.R., Soldner, F., Baru, V., Lou, Y., Freyzon, Y., Cho, S.*, et al.* (2013). Identification and rescue of alpha-synuclein toxicity in Parkinson patient-derived neurons. Science *342*, 983-987.

Cisse, M., Halabisky, B., Harris, J., Devidze, N., Dubal, D.B., Sun, B., Orr, A., Lotz, G., Kim, D.H., Hamto, P.*, et al.* (2011). Reversing EphB2 depletion rescues cognitive functions in Alzheimer model. Nature *469*, 47-52.

Citron, M., Oltersdorf, T., Haass, C., McConlogue, L., Hung, A.Y., Seubert, P., Vigo-Pelfrey, C., Lieberburg, I., and Selkoe, D.J. (1992). Mutation of the beta-amyloid precursor protein in familial Alzheimer's disease increases beta-protein production. Nature *360*, 672-674.

Claridge-Chang, A., Roorda, R.D., Vrontou, E., Sjulson, L., Li, H., Hirsh, J., and Miesenbock, G. (2009). Writing memories with light-addressable reinforcement circuitry. Cell *139*, 405-415.

Clary, D.O., Griff, I.C., and Rothman, J.E. (1990). SNAPs, a family of NSF attachment proteins involved in intracellular membrane fusion in animals and yeast. Cell *61*, 709-721.

Cleveland, D.W., Hwo, S.Y., and Kirschner, M.W. (1977a). Physical and chemical properties of purified tau factor and the role of tau in microtubule assembly. J Mol Biol *116*, 227-247.

Cleveland, D.W., Hwo, S.Y., and Kirschner, M.W. (1977b). Purification of tau, a microtubule-associated protein that induces assembly of microtubules from purified tubulin. J Mol Biol *116*, 207-225.

Cohen, E., Bieschke, J., Perciavalle, R.M., Kelly, J.W., and Dillin, A. (2006). Opposing

activities protect against age-onset proteotoxicity. Science *313*, 1604-1610.

Cohen, E., Paulsson, J.F., Blinder, P., Burstyn-Cohen, T., Du, D., Estepa, G., Adame, A., Pham, H.M., Holzenberger, M., Kelly, J.W.*, et al.* (2009). Reduced IGF-1 signaling delays age-associated proteotoxicity in mice. Cell *139*, 1157-1169.

Collins, B.M., McCoy, A.J., Kent, H.M., Evans, P.R., and Owen, D.J. (2002). Molecular architecture and functional model of the endocytic AP2 complex. Cell *109*, 523-535.

Colon, S., and Bhave, G. (2016). Proprotein Convertase Processing Enhances Peroxidasin Activity to Reinforce Collagen IV. The Journal of biological chemistry *291*, 24009-24016.

Cook, D.G., Forman, M.S., Sung, J.C., Leight, S., Kolson, D.L., Iwatsubo, T., Lee, V.M., and Doms, R.W. (1997). Alzheimer's A beta(1-42) is generated in the endoplasmic reticulum/intermediate compartment of NT2N cells. Nature medicine *3*, 1021-1023.

Coomaraswamy, J., Kilger, E., Wolfing, H., Schafer, C., Kaeser, S.A., Wegenast-Braun, B.M., Hefendehl, J.K., Wolburg, H., Mazzella, M., Ghiso, J.*, et al.* (2010). Modeling familial Danish dementia in mice supports the concept of the amyloid hypothesis of Alzheimer's disease. Proceedings of the National Academy of Sciences of the United States of America *107*, 7969-7974.

Copeland, J.M., Cho, J., Lo, T., Jr., Hur, J.H., Bahadorani, S., Arabyan, T., Rabie, J., Soh, J., and Walker, D.W. (2009). Extension of Drosophila life span by RNAi of the mitochondrial respiratory chain. Current biology : CB *19*, 1591-1598.

Corder, E.H., Saunders, A.M., Strittmatter, W.J., Schmechel, D.E., Gaskell, P.C., Small, G.W., Roses, A.D., Haines, J.L., and Pericak-Vance, M.A. (1993). Gene dose of apolipoprotein E type 4 allele and the risk of Alzheimer's disease in late onset families. Science *261*, 921-923.

Cormont, M., Meton, I., Mari, M., Monzo, P., Keslair, F., Gaskin, C., McGraw, T.E., and Le Marchand-Brustel, Y. (2003). CD2AP/CMS regulates endosome morphology and traffic to the degradative pathway through its interaction with Rab4 and c-Cbl. Traffic *4*, 97-112.

Corrigan, F., Vink, R., Blumbergs, P.C., Masters, C.L., Cappai, R., and van den Heuvel, C. (2012). sAPPalpha rescues deficits in amyloid precursor protein knockout mice following focal traumatic brain injury. Journal of neurochemistry *122*, 208-220.

Cosentino, S., Scarmeas, N., Helzner, E., Glymour, M.M., Brandt, J., Albert, M., Blacker, D., and Stern, Y. (2008). APOE epsilon 4 allele predicts faster cognitive decline in mild Alzheimer disease. Neurology *70*, 1842-1849.

Couchie, D., Mavilia, C., Georgieff, I.S., Liem, R.K., Shelanski, M.L., and Nunez, J. (1992). Primary structure of high molecular weight tau present in the peripheral nervous system. Proceedings of the National Academy of Sciences of the United States of America *89*, 4378-4381.

Cousins, S.L., Hoey, S.E., Anne Stephenson, F., and Perkinton, M.S. (2009). Amyloid precursor protein 695 associates with assembled NR2A- and NR2B-containing NMDA receptors to result in the enhancement of their cell surface delivery. Journal of neurochemistry *111*, 1501-1513.

Cousins, S.L., Innocent, N., and Stephenson, F.A. (2013). Neto1 associates with the NMDA receptor/amyloid precursor protein complex. Journal of neurochemistry *126*, 554-564.

Craft, S., Baker, L.D., Montine, T.J., Minoshima, S., Watson, G.S., Claxton, A., Arbuckle, M., Callaghan, M., Tsai, E., Plymate, S.R.*, et al.* (2012). Intranasal insulin therapy for Alzheimer disease and amnestic mild cognitive impairment: a pilot clinical trial. Archives of neurology *69*, 29-38.

Crews, S.T. (2010). Axon-glial interactions at the Drosophila CNS midline. Cell adhesion & migration *4*, 67-71.

Crook, R., Verkkoniemi, A., Perez-Tur, J., Mehta, N., Baker, M., Houlden, H., Farrer, M., Hutton, M., Lincoln, S., Hardy, J.*, et al.* (1998). A variant of Alzheimer's disease with spastic paraparesis and unusual plaques due to deletion of exon 9 of presenilin 1. Nature medicine *4*, 452-455.

Crowther, D.C., Kinghorn, K.J., Miranda, E., Page, R., Curry, J.A., Duthie, F.A., Gubb, D.C., and Lomas, D.A. (2005). Intraneuronal Abeta, non-amyloid aggregates and neurodegeneration in a Drosophila model of Alzheimer's disease. Neuroscience *132*, 123-135.

Cummings, D.M., Liu, W., Portelius, E., Bayram, S., Yasvoina, M., Ho, S.H., Smits, H., Ali, S.S., Steinberg, R., Pegasiou, C.M.*, et al.* (2015). First effects of rising amyloid-beta in transgenic mouse brain: synaptic transmission and gene expression. Brain *138*, 1992-2004.

Daniels, R.W., Collins, C.A., Gelfand, M.V., Dant, J., Brooks, E.S., Krantz, D.E., and DiAntonio, A. (2004). Increased expression of the Drosophila vesicular glutamate transporter leads to excess glutamate release and a compensatory decrease in quantal content. The Journal of neuroscience : the official journal of the Society for Neuroscience *24*, 10466-10474.

Davies, P., and Maloney, A.J. (1976). Selective loss of central cholinergic neurons in Alzheimer's disease. Lancet *2*, 1403.

Davis, G.W., DiAntonio, A., Petersen, S.A., and Goodman, C.S. (1998). Postsynaptic PKA controls quantal size and reveals a retrograde signal that regulates presynaptic transmitter release in Drosophila. Neuron *20*, 305-315.

Davis, K.L., Mohs, R.C., Tinklenberg, J.R., Pfefferbaum, A., Hollister, L.E., and Kopell, B.S. (1978). Physostigmine: improvement of long-term memory processes in normal humans. Science *201*, 272-274.

Davis, R.L. (2011). Traces of Drosophila memory. Neuron *70*, 8-19.

Dawson, G.R., Seabrook, G.R., Zheng, H., Smith, D.W., Graham, S., O'Dowd, G., Bowery, B.J., Boyce, S., Trumbauer, M.E., Chen, H.Y.*, et al.* (1999). Age-related cognitive deficits, impaired long-term potentiation and reduction in synaptic marker density in mice lacking the beta-amyloid precursor protein. Neuroscience *90*, 1-13.

De Strooper, B., Beullens, M., Contreras, B., Levesque, L., Craessaerts, K., Cordell, B., Moechars, D., Bollen, M., Fraser, P., George-Hyslop, P.S.*, et al.* (1997). Phosphorylation,

subcellular localization, and membrane orientation of the Alzheimer's disease-associated presenilins. The Journal of biological chemistry *272*, 3590-3598.

De Strooper, B., Saftig, P., Craessaerts, K., Vanderstichele, H., Guhde, G., Annaert, W., Von Figura, K., and Van Leuven, F. (1998). Deficiency of presenilin-1 inhibits the normal cleavage of amyloid precursor protein. Nature *391*, 387-390.

Deane, R., Du Yan, S., Submamaryan, R.K., LaRue, B., Jovanovic, S., Hogg, E., Welch, D., Manness, L., Lin, C., Yu, J.*, et al.* (2003). RAGE mediates amyloid-beta peptide transport across the blood-brain barrier and accumulation in brain. Nature medicine *9*, 907-913.

Deane, R., Sagare, A., Hamm, K., Parisi, M., Lane, S., Finn, M.B., Holtzman, D.M., and Zlokovic, B.V. (2008). apoE isoform-specific disruption of amyloid beta peptide clearance from mouse brain. The Journal of clinical investigation *118*, 4002-4013.

Deane, R., Singh, I., Sagare, A.P., Bell, R.D., Ross, N.T., LaRue, B., Love, R., Perry, S., Paquette, N., Deane, R.J.*, et al.* (2012). A multimodal RAGE-specific inhibitor reduces amyloid beta-mediated brain disorder in a mouse model of Alzheimer disease. The Journal of clinical investigation *122*, 1377-1392.

Deane, R., Wu, Z., and Zlokovic, B.V. (2004). RAGE (yin) versus LRP (yang) balance regulates alzheimer amyloid beta-peptide clearance through transport across the blood-brain barrier. Stroke *35*, 2628-2631.

Delgado, R., Barla, R., Latorre, R., and Labarca, P. (1989). L-glutamate activates excitatory and inhibitory channels in Drosophila larval muscle. FEBS letters *243*, 337-342.

Delprato, A., Merithew, E., and Lambright, D.G. (2004). Structure, exchange determinants, and family-wide rab specificity of the tandem helical bundle and Vps9 domains of Rabex-5. Cell *118*, 607-617.

Denzel, M.S., Storm, N.J., Gutschmidt, A., Baddi, R., Hinze, Y., Jarosch, E., Sommer, T., Hoppe, T., and Antebi, A. (2014). Hexosamine pathway metabolites enhance protein quality

control and prolong life. Cell *156*, 1167-1178.

Derkach, V., Barria, A., and Soderling, T.R. (1999). Ca2+/calmodulin-kinase II enhances channel conductance of alpha-amino-3-hydroxy-5-methyl-4-isoxazolepropionate type glutamate receptors. Proceedings of the National Academy of Sciences of the United States of America *96*, 3269-3274.

Devaraju, P., Sun, M.Y., Myers, T.L., Lauderdale, K., and Fiacco, T.A. (2013). Astrocytic group I mGluR-dependent potentiation of astrocytic glutamate and potassium uptake. Journal of neurophysiology *109*, 2404-2414.

Devi, L., Prabhu, B.M., Galati, D.F., Avadhani, N.G., and Anandatheerthavarada, H.K. (2006). Accumulation of amyloid precursor protein in the mitochondrial import channels of human Alzheimer's disease brain is associated with mitochondrial dysfunction. The Journal of neuroscience : the official journal of the Society for Neuroscience *26*, 9057-9068.

Deyts, C., Clutter, M., Herrera, S., Jovanovic, N., Goddi, A., and Parent, A.T. (2016). Loss of presenilin function is associated with a selective gain of APP function. eLife *5*.

Deyts, C., Vetrivel, K.S., Das, S., Shepherd, Y.M., Dupre, D.J., Thinakaran, G., and Parent, A.T. (2012). Novel GalphaS-protein signaling associated with membrane-tethered amyloid precursor protein intracellular domain. The Journal of neuroscience : the official journal of the Society for Neuroscience *32*, 1714-1729.

Di Giovanni, J., and Sheng, Z.H. (2015). Regulation of synaptic activity by snapin-mediated endolysosomal transport and sorting. The EMBO journal *34*, 2059-2077.

Di Paolo, G., Sankaranarayanan, S., Wenk, M.R., Daniell, L., Perucco, E., Caldarone, B.J., Flavell, R., Picciotto, M.R., Ryan, T.A., Cremona, O.*, et al.* (2002). Decreased synaptic vesicle recycling efficiency and cognitive deficits in amphiphysin 1 knockout mice. Neuron *33*, 789-804.

DiAntonio, A., Petersen, S.A., Heckmann, M., and Goodman, C.S. (1999). Glutamate receptor

expression regulates quantal size and quantal content at the Drosophila neuromuscular junction. The Journal of neuroscience : the official journal of the Society for Neuroscience *19*, 3023-3032.

Dik, M.G., Jonker, C., Bouter, L.M., Geerlings, M.I., van Kamp, G.J., and Deeg, D.J. (2000). APOE-epsilon4 is associated with memory decline in cognitively impaired elderly. Neurology *54*, 1492-1497.

Dineley, K.T., Bell, K.A., Bui, D., and Sweatt, J.D. (2002a). beta -Amyloid peptide activates alpha 7 nicotinic acetylcholine receptors expressed in Xenopus oocytes. The Journal of biological chemistry *277*, 25056-25061.

Dineley, K.T., Xia, X., Bui, D., Sweatt, J.D., and Zheng, H. (2002b). Accelerated plaque accumulation, associative learning deficits, and up-regulation of alpha 7 nicotinic receptor protein in transgenic mice co-expressing mutant human presenilin 1 and amyloid precursor proteins. The Journal of biological chemistry *277*, 22768-22780.

Dittman, J.S., and Kaplan, J.M. (2006). Factors regulating the abundance and localization of synaptobrevin in the plasma membrane. Proceedings of the National Academy of Sciences of the United States of America *103*, 11399-11404.

Doherty, J., Logan, M.A., Tasdemir, O.E., and Freeman, M.R. (2009). Ensheathing glia function as phagocytes in the adult Drosophila brain. The Journal of neuroscience : the official journal of the Society for Neuroscience *29*, 4768-4781.

Doherty, J., Sheehan, A.E., Bradshaw, R., Fox, A.N., Lu, T.Y., and Freeman, M.R. (2014). PI3K signaling and Stat92E converge to modulate glial responsiveness to axonal injury. PLoS biology *12*, e1001985.

Dong, L.M., Wilson, C., Wardell, M.R., Simmons, T., Mahley, R.W., Weisgraber, K.H., and Agard, D.A. (1994). Human apolipoprotein E. Role of arginine 61 in mediating the lipoprotein preferences of the E3 and E4 isoforms. The Journal of biological chemistry *269*, 22358-22365.

Drechsel, D.N., Hyman, A.A., Cobb, M.H., and Kirschner, M.W. (1992). Modulation of the dynamic instability of tubulin assembly by the microtubule-associated protein tau. Molecular biology of the cell *3*, 1141-1154.

Drewes, G., Ebneth, A., Preuss, U., Mandelkow, E.M., and Mandelkow, E. (1997). MARK, a novel family of protein kinases that phosphorylate microtubule-associated proteins and trigger microtubule disruption. Cell *89*, 297-308.

Dubnau, J., Grady, L., Kitamoto, T., and Tully, T. (2001). Disruption of neurotransmission in Drosophila mushroom body blocks retrieval but not acquisition of memory. Nature *411*, 476-480.

DuBoff, B., Gotz, J., and Feany, M.B. (2012). Tau promotes neurodegeneration via DRP1 mislocalization in vivo. Neuron *75*, 618-632.

Duchek, P., and Rorth, P. (2001). Guidance of cell migration by EGF receptor signaling during Drosophila oogenesis. Science *291*, 131-133.

Duchek, P., Somogyi, K., Jekely, G., Beccari, S., and Rorth, P. (2001). Guidance of cell migration by the Drosophila PDGF/VEGF receptor. Cell *107*, 17-26.

Dudek, H., Datta, S.R., Franke, T.F., Birnbaum, M.J., Yao, R., Cooper, G.M., Segal, R.A., Kaplan, D.R., and Greenberg, M.E. (1997). Regulation of neuronal survival by the serine-threonine protein kinase Akt. Science *275*, 661-665.

Eathiraj, S., Pan, X., Ritacco, C., and Lambright, D.G. (2005). Structural basis of family-wide Rab GTPase recognition by rabenosyn-5. Nature *436*, 415-419.

Edgar, J.R., Willen, K., Gouras, G.K., and Futter, C.E. (2015). ESCRTs regulate amyloid precursor protein sorting in multivesicular bodies and intracellular amyloid-beta accumulation. Journal of cell science *128*, 2520-2528.

Ehlers, M.D. (2000). Reinsertion or degradation of AMPA receptors determined by activity-dependent endocytic sorting. Neuron *28*, 511-525.

Eisenberg, D., and Jucker, M. (2012). The amyloid state of proteins in human diseases. Cell *148*, 1188-1203.

El Mestikawy, S., Wallen-Mackenzie, A., Fortin, G.M., Descarries, L., and Trudeau, L.E. (2011). From glutamate co-release to vesicular synergy: vesicular glutamate transporters. Nature reviews Neuroscience *12*, 204-216.

Elias-Sonnenschein, L.S., Viechtbauer, W., Ramakers, I.H., Verhey, F.R., and Visser, P.J. (2011). Predictive value of APOE-epsilon4 allele for progression from MCI to AD-type dementia: a meta-analysis. Journal of neurology, neurosurgery, and psychiatry *82*, 1149-1156.

Elliott, K., Ge, K., Du, W., and Prendergast, G.C. (2000). The c-Myc-interacting adaptor protein Bin1 activates a caspase-independent cell death program. Oncogene *19*, 4669-4684.

Emond, M.R., Montgomery, J.M., Huggins, M.L., Hanson, J.E., Mao, L., Huganir, R.L., and Madison, D.V. (2010). AMPA receptor subunits define properties of state-dependent synaptic plasticity. The Journal of physiology *588*, 1929-1946.

Erecinska, M., Wantorsky, D., and Wilson, D.F. (1983). Aspartate transport in synaptosomes from rat brain. The Journal of biological chemistry *258*, 9069-9077.

Esselens, C., Oorschot, V., Baert, V., Raemaekers, T., Spittaels, K., Serneels, L., Zheng, H., Saftig, P., De Strooper, B., Klumperman, J.*, et al.* (2004). Presenilin 1 mediates the turnover of telencephalin in hippocampal neurons via an autophagic degradative pathway. J Cell Biol *166*, 1041-1054.

Eulalio, A., Huntzinger, E., Nishihara, T., Rehwinkel, J., Fauser, M., and Izaurralde, E. (2009). Deadenylation is a widespread effect of miRNA regulation. RNA *15*, 21-32.

Eulalio, A., Rehwinkel, J., Stricker, M., Huntzinger, E., Yang, S.F., Doerks, T., Dorner, S., Bork, P., Boutros, M., and Izaurralde, E. (2007). Target-specific requirements for enhancers of decapping in miRNA-mediated gene silencing. Genes & development *21*, 2558-2570.

Evans, K.C., Berger, E.P., Cho, C.G., Weisgraber, K.H., and Lansbury, P.T., Jr. (1995).

Apolipoprotein E is a kinetic but not a thermodynamic inhibitor of amyloid formation: implications for the pathogenesis and treatment of Alzheimer disease. Proceedings of the National Academy of Sciences of the United States of America *92*, 763-767.

Ewbank, J.J., Barnes, T.M., Lakowski, B., Lussier, M., Bussey, H., and Hekimi, S. (1997). Structural and functional conservation of the Caenorhabditis elegans timing gene clk-1. Science *275*, 980-983.

Fang, E.F., Kassahun, H., Croteau, D.L., Scheibye-Knudsen, M., Marosi, K., Lu, H., Shamanna, R.A., Kalyanasundaram, S., Bollineni, R.C., Wilson, M.A.*, et al.* (2016). NAD+ Replenishment Improves Lifespan and Healthspan in Ataxia Telangiectasia Models via Mitophagy and DNA Repair. Cell metabolism *24*, 566-581.

Farlow, M.R., He, Y., Tekin, S., Xu, J., Lane, R., and Charles, H.C. (2004). Impact of APOE in mild cognitive impairment. Neurology *63*, 1898-1901.

Farrer, L.A., Cupples, L.A., Haines, J.L., Hyman, B., Kukull, W.A., Mayeux, R., Myers, R.H., Pericak-Vance, M.A., Risch, N., and van Duijn, C.M. (1997). Effects of age, sex, and ethnicity on the association between apolipoprotein E genotype and Alzheimer disease. A meta-analysis. APOE and Alzheimer Disease Meta Analysis Consortium. Jama *278*, 1349-1356.

Featherstone, D.E., Rushton, E., and Broadie, K. (2002). Developmental regulation of glutamate receptor field size by nonvesicular glutamate release. Nature neuroscience *5*, 141-146.

Felkai, S., Ewbank, J.J., Lemieux, J., Labbe, J.C., Brown, G.G., and Hekimi, S. (1999). CLK-1 controls respiration, behavior and aging in the nematode Caenorhabditis elegans. The EMBO journal *18*, 1783-1792.

Feng, J., Bussiere, F., and Hekimi, S. (2001). Mitochondrial electron transport is a key determinant of life span in Caenorhabditis elegans. Developmental cell *1*, 633-644.

Feng, Y., Wigg, K.G., Makkar, R., Ickowicz, A., Pathare, T., Tannock, R., Roberts, W., Malone, M., Kennedy, J.L., Schachar, R.*, et al.* (2005). Sequence variation in the 3'-untranslated region of the dopamine transporter gene and attention-deficit hyperactivity disorder (ADHD). American journal of medical genetics Part B, Neuropsychiatric genetics : the official publication of the International Society of Psychiatric Genetics *139B*, 1-6.

Ferguson, S.M., Raimondi, A., Paradise, S., Shen, H., Mesaki, K., Ferguson, A., Destaing, O., Ko, G., Takasaki, J., Cremona, O.*, et al.* (2009). Coordinated actions of actin and BAR proteins upstream of dynamin at endocytic clathrin-coated pits. Developmental cell *17*, 811-822.

Fernandez-Alfonso, T., and Ryan, T.A. (2008). A heterogeneous "resting" pool of synaptic vesicles that is dynamically interchanged across boutons in mammalian CNS synapses. Brain cell biology *36*, 87-100.

Fernandez-Chacon, R., Konigstorfer, A., Gerber, S.H., Garcia, J., Matos, M.F., Stevens, C.F., Brose, N., Rizo, J., Rosenmund, C., and Sudhof, T.C. (2001). Synaptotagmin I functions as a calcium regulator of release probability. Nature *410*, 41-49.

Fernandez, M.A., Klutkowski, J.A., Freret, T., and Wolfe, M.S. (2014). Alzheimer presenilin-1 mutations dramatically reduce trimming of long amyloid beta-peptides (Abeta) by gamma-secretase to increase 42-to-40-residue Abeta. The Journal of biological chemistry *289*, 31043-31052.

Finelli, A., Kelkar, A., Song, H.J., Yang, H., and Konsolaki, M. (2004). A model for studying Alzheimer's Abeta42-induced toxicity in Drosophila melanogaster. Molecular and cellular neurosciences *26*, 365-375.

Fire, A., Xu, S., Montgomery, M.K., Kostas, S.A., Driver, S.E., and Mello, C.C. (1998). Potent and specific genetic interference by double-stranded RNA in Caenorhabditis elegans. Nature *391*, 806-811.

Flach, K., Hilbrich, I., Schiffmann, A., Gartner, U., Kruger, M., Leonhardt, M., Waschipky, H., Wick, L., Arendt, T., and Holzer, M. (2012). Tau oligomers impair artificial membrane integrity

and cellular viability. The Journal of biological chemistry *287*, 43223-43233.

Fleisher, A.S., Sowell, B.B., Taylor, C., Gamst, A.C., Petersen, R.C., Thal, L.J., and Alzheimer's Disease Cooperative, S. (2007). Clinical predictors of progression to Alzheimer disease in amnestic mild cognitive impairment. Neurology *68*, 1588-1595.

Fonseca, B.D., Zakaria, C., Jia, J.J., Graber, T.E., Svitkin, Y., Tahmasebi, S., Healy, D., Hoang, H.D., Jensen, J.M., Diao, I.T.*, et al.* (2015). La-related Protein 1 (LARP1) Represses Terminal Oligopyrimidine (TOP) mRNA Translation Downstream of mTOR Complex 1 (mTORC1). The Journal of biological chemistry *290*, 15996-16020.

Ford, D., Hoe, N., Landis, G.N., Tozer, K., Luu, A., Bhole, D., Badrinath, A., and Tower, J. (2007). Alteration of Drosophila life span using conditional, tissue-specific expression of transgenes triggered by doxycyline or RU486/Mifepristone. Experimental gerontology *42*, 483-497.

Ford, M.G., Mills, I.G., Peter, B.J., Vallis, Y., Praefcke, G.J., Evans, P.R., and McMahon, H.T. (2002). Curvature of clathrin-coated pits driven by epsin. Nature *419*, 361-366.

Ford, M.G., Pearse, B.M., Higgins, M.K., Vallis, Y., Owen, D.J., Gibson, A., Hopkins, C.R., Evans, P.R., and McMahon, H.T. (2001). Simultaneous binding of PtdIns(4,5)P2 and clathrin by AP180 in the nucleation of clathrin lattices on membranes. Science *291*, 1051-1055.

Fortress, A.M., Fan, L., Orr, P.T., Zhao, Z., and Frick, K.M. (2013). Estradiol-induced object recognition memory consolidation is dependent on activation of mTOR signaling in the dorsal hippocampus. Learning & memory *20*, 147-155.

Fotin, A., Cheng, Y., Grigorieff, N., Walz, T., Harrison, S.C., and Kirchhausen, T. (2004). Structure of an auxilin-bound clathrin coat and its implications for the mechanism of uncoating. Nature *432*, 649-653.

Fraser, A.G., Kamath, R.S., Zipperlen, P., Martinez-Campos, M., Sohrmann, M., and Ahringer, J. (2000). Functional genomic analysis of C. elegans chromosome I by systematic RNA

interference. Nature *408*, 325-330.

Freeman, M.R., Delrow, J., Kim, J., Johnson, E., and Doe, C.Q. (2003). Unwrapping glial biology: Gcm target genes regulating glial development, diversification, and function. Neuron *38*, 567-580.

Fremeau, R.T., Jr., Troyer, M.D., Pahner, I., Nygaard, G.O., Tran, C.H., Reimer, R.J., Bellocchio, E.E., Fortin, D., Storm-Mathisen, J., and Edwards, R.H. (2001). The expression of vesicular glutamate transporters defines two classes of excitatory synapse. Neuron *31*, 247-260.

Frizzo, M.E., Dall'Onder, L.P., Dalcin, K.B., and Souza, D.O. (2004). Riluzole enhances glutamate uptake in rat astrocyte cultures. Cellular and molecular neurobiology *24*, 123-128.

Frost, B., Jacks, R.L., and Diamond, M.I. (2009). Propagation of tau misfolding from the outside to the inside of a cell. The Journal of biological chemistry *284*, 12845-12852.

Fruhbeis, C., Frohlich, D., Kuo, W.P., Amphornrat, J., Thilemann, S., Saab, A.S., Kirchhoff, F., Mobius, W., Goebbels, S., Nave, K.A*., et al.* (2013). Neurotransmitter-triggered transfer of exosomes mediates oligodendrocyte-neuron communication. PLoS biology *11*, e1001604.

Fryer, J.D., Simmons, K., Parsadanian, M., Bales, K.R., Paul, S.M., Sullivan, P.M., and Holtzman, D.M. (2005). Human apolipoprotein E4 alters the amyloid-beta 40:42 ratio and promotes the formation of cerebral amyloid angiopathy in an amyloid precursor protein transgenic model. The Journal of neuroscience : the official journal of the Society for Neuroscience *25*, 2803-2810.

Fu, Y., Hsiao, J.H., Paxinos, G., Halliday, G.M., and Kim, W.S. (2016). ABCA7 Mediates Phagocytic Clearance of Amyloid-beta in the Brain. Journal of Alzheimer's disease : JAD *54*, 569-584.

Fuhrmann, M., Bittner, T., Jung, C.K., Burgold, S., Page, R.M., Mitteregger, G., Haass, C., LaFerla, F.M., Kretzschmar, H., and Herms, J. (2010). Microglial Cx3cr1 knockout prevents

neuron loss in a mouse model of Alzheimer's disease. Nature neuroscience *13*, 411-413.

Fumagalli, E., Funicello, M., Rauen, T., Gobbi, M., and Mennini, T. (2008). Riluzole enhances the activity of glutamate transporters GLAST, GLT1 and EAAC1. European journal of pharmacology *578*, 171-176.

Funfschilling, U., Supplie, L.M., Mahad, D., Boretius, S., Saab, A.S., Edgar, J., Brinkmann, B.G., Kassmann, C.M., Tzvetanova, I.D., Mobius, W.*, et al.* (2012). Glycolytic oligodendrocytes maintain myelin and long-term axonal integrity. Nature *485*, 517-521.

Galderisi, U., Di Bernardo, G., Cipollaro, M., Jori, F.P., Piegari, E., Cascino, A., Peluso, G., and Melone, M.A. (1999). Induction of apoptosis and differentiation in neuroblastoma and astrocytoma cells by the overexpression of Bin1, a novel Myc interacting protein. Journal of cellular biochemistry *74*, 313-322.

Games, D., Adams, D., Alessandrini, R., Barbour, R., Berthelette, P., Blackwell, C., Carr, T., Clemens, J., Donaldson, T., Gillespie, F.*, et al.* (1995). Alzheimer-type neuropathology in transgenic mice overexpressing V717F beta-amyloid precursor protein. Nature *373*, 523-527.

Gao, F.B., Brenman, J.E., Jan, L.Y., and Jan, Y.N. (1999). Genes regulating dendritic outgrowth, branching, and routing in Drosophila. Genes & development *13*, 2549-2561.

Gao, F.B., Kohwi, M., Brenman, J.E., Jan, L.Y., and Jan, Y.N. (2000). Control of dendritic field formation in Drosophila: the roles of flamingo and competition between homologous neurons. Neuron *28*, 91-101.

Gargano, J.W., Martin, I., Bhandari, P., and Grotewiel, M.S. (2005). Rapid iterative negative geotaxis (RING): a new method for assessing age-related locomotor decline in Drosophila. Experimental gerontology *40*, 386-395.

Geppert, M., Goda, Y., Hammer, R.E., Li, C., Rosahl, T.W., Stevens, C.F., and Sudhof, T.C. (1994). Synaptotagmin I: a major Ca2+ sensor for transmitter release at a central synapse. Cell *79*, 717-727.

Giraldez, A.J., Mishima, Y., Rihel, J., Grocock, R.J., Van Dongen, S., Inoue, K., Enright, A.J., and Schier, A.F. (2006). Zebrafish MiR-430 promotes deadenylation and clearance of maternal mRNAs. Science *312*, 75-79.

Girard, S.D., Jacquet, M., Baranger, K., Migliorati, M., Escoffier, G., Bernard, A., Khrestchatisky, M., Feron, F., Rivera, S., Roman, F.S.*, et al.* (2014). Onset of hippocampus-dependent memory impairments in 5XFAD transgenic mouse model of Alzheimer's disease. Hippocampus *24*, 762-772.

Gitler, A.D., Chesi, A., Geddie, M.L., Strathearn, K.E., Hamamichi, S., Hill, K.J., Caldwell, K.A., Caldwell, G.A., Cooper, A.A., Rochet, J.C.*, et al.* (2009). Alpha-synuclein is part of a diverse and highly conserved interaction network that includes PARK9 and manganese toxicity. Nature genetics *41*, 308-315.

Gjoneska, E., Pfenning, A.R., Mathys, H., Quon, G., Kundaje, A., Tsai, L.H., and Kellis, M. (2015). Conserved epigenomic signals in mice and humans reveal immune basis of Alzheimer's disease. Nature *518*, 365-369.

Glenner, G.G., and Wong, C.W. (1984a). Alzheimer's disease and Down's syndrome: sharing of a unique cerebrovascular amyloid fibril protein. Biochem Biophys Res Commun *122*, 1131-1135.

Glenner, G.G., and Wong, C.W. (1984b). Alzheimer's disease: initial report of the purification and characterization of a novel cerebrovascular amyloid protein. Biochem Biophys Res Commun *120*, 885-890.

Glennon, E.B., Whitehouse, I.J., Miners, J.S., Kehoe, P.G., Love, S., Kellett, K.A., and Hooper, N.M. (2013). BIN1 is decreased in sporadic but not familial Alzheimer's disease or in aging. PloS one *8*, e78806.

Goate, A., Chartier-Harlin, M.C., Mullan, M., Brown, J., Crawford, F., Fidani, L., Giuffra, L., Haynes, A., Irving, N., James, L.*, et al.* (1991). Segregation of a missense mutation in the amyloid precursor protein gene with familial Alzheimer's disease. Nature *349*, 704-706.

Goedert, M., and Jakes, R. (1990). Expression of separate isoforms of human tau protein: correlation with the tau pattern in brain and effects on tubulin polymerization. The EMBO journal *9*, 4225-4230.

Goedert, M., Jakes, R., Crowther, R.A., Six, J., Lubke, U., Vandermeeren, M., Cras, P., Trojanowski, J.Q., and Lee, V.M. (1993). The abnormal phosphorylation of tau protein at Ser-202 in Alzheimer disease recapitulates phosphorylation during development. Proceedings of the National Academy of Sciences of the United States of America *90*, 5066-5070.

Goedert, M., and Spillantini, M.G. (2006). A century of Alzheimer's disease. Science *314*, 777-781.

Goedert, M., Spillantini, M.G., Jakes, R., Rutherford, D., and Crowther, R.A. (1989a). Multiple isoforms of human microtubule-associated protein tau: sequences and localization in neurofibrillary tangles of Alzheimer's disease. Neuron *3*, 519-526.

Goedert, M., Spillantini, M.G., Potier, M.C., Ulrich, J., and Crowther, R.A. (1989b). Cloning and sequencing of the cDNA encoding an isoform of microtubule-associated protein tau containing four tandem repeats: differential expression of tau protein mRNAs in human brain. The EMBO journal *8*, 393-399.

Goedert, M., Wischik, C.M., Crowther, R.A., Walker, J.E., and Klug, A. (1988). Cloning and sequencing of the cDNA encoding a core protein of the paired helical filament of Alzheimer disease: identification as the microtubule-associated protein tau. Proceedings of the National Academy of Sciences of the United States of America *85*, 4051-4055.

Golic, K.G., and Lindquist, S. (1989). The FLP recombinase of yeast catalyzes site-specific recombination in the Drosophila genome. Cell *59*, 499-509.

Gonczy, P., Echeverri, C., Oegema, K., Coulson, A., Jones, S.J., Copley, R.R., Duperon, J., Oegema, J., Brehm, M., Cassin, E.*, et al.* (2000). Functional genomic analysis of cell division in C. elegans using RNAi of genes on chromosome III. Nature *408*, 331-336.

Gong, B., Cao, Z., Zheng, P., Vitolo, O.V., Liu, S., Staniszewski, A., Moolman, D., Zhang, H., Shelanski, M., and Arancio, O. (2006). Ubiquitin hydrolase Uch-L1 rescues beta-amyloid-induced decreases in synaptic function and contextual memory. Cell *126*, 775-788.

Goritz, C., Mauch, D.H., and Pfrieger, F.W. (2005). Multiple mechanisms mediate cholesterol-induced synaptogenesis in a CNS neuron. Molecular and cellular neurosciences *29*, 190-201.

Gorvel, J.P., Chavrier, P., Zerial, M., and Gruenberg, J. (1991). rab5 controls early endosome fusion in vitro. Cell *64*, 915-925.

Gotz, J., Chen, F., van Dorpe, J., and Nitsch, R.M. (2001). Formation of neurofibrillary tangles in P301l tau transgenic mice induced by Abeta 42 fibrils. Science *293*, 1491-1495.

Gotz, J., Probst, A., Spillantini, M.G., Schafer, T., Jakes, R., Burki, K., and Goedert, M. (1995). Somatodendritic localization and hyperphosphorylation of tau protein in transgenic mice expressing the longest human brain tau isoform. The EMBO journal *14*, 1304-1313.

Gotz, J., Streffer, J.R., David, D., Schild, A., Hoerndli, F., Pennanen, L., Kurosinski, P., and Chen, F. (2004). Transgenic animal models of Alzheimer's disease and related disorders: histopathology, behavior and therapy. Molecular psychiatry *9*, 664-683.

Gowrishankar, S., Yuan, P., Wu, Y., Schrag, M., Paradise, S., Grutzendler, J., De Camilli, P., and Ferguson, S.M. (2015). Massive accumulation of luminal protease-deficient axonal lysosomes at Alzheimer's disease amyloid plaques. Proceedings of the National Academy of Sciences of the United States of America *112*, E3699-3708.

Graeber, M.B., Kosel, S., Egensperger, R., Banati, R.B., Muller, U., Bise, K., Hoff, P., Moller, H.J., Fujisawa, K., and Mehraein, P. (1997). Rediscovery of the case described by Alois Alzheimer in 1911: historical, histological and molecular genetic analysis. Neurogenetics *1*, 73-80.

Grbovic, O.M., Mathews, P.M., Jiang, Y., Schmidt, S.D., Dinakar, R., Summers-Terio, N.B., Ceresa, B.P., Nixon, R.A., and Cataldo, A.M. (2003). Rab5-stimulated up-regulation of the endocytic pathway increases intracellular beta-cleaved amyloid precursor protein carboxyl-terminal fragment levels and Abeta production. The Journal of biological chemistry *278*, 31261-31268.

Greer, E.L., Maures, T.J., Hauswirth, A.G., Green, E.M., Leeman, D.S., Maro, G.S., Han, S., Banko, M.R., Gozani, O., and Brunet, A. (2010). Members of the H3K4 trimethylation complex regulate lifespan in a germline-dependent manner in C. elegans. Nature *466*, 383-387.

Greer, E.L., Maures, T.J., Ucar, D., Hauswirth, A.G., Mancini, E., Lim, J.P., Benayoun, B.A., Shi, Y., and Brunet, A. (2011). Transgenerational epigenetic inheritance of longevity in Caenorhabditis elegans. Nature *479*, 365-371.

Griciuc, A., Serrano-Pozo, A., Parrado, A.R., Lesinski, A.N., Asselin, C.N., Mullin, K., Hooli, B., Choi, S.H., Hyman, B.T., and Tanzi, R.E. (2013). Alzheimer's disease risk gene CD33 inhibits microglial uptake of amyloid beta. Neuron *78*, 631-643.

Guardia-Laguarta, C., Pera, M., Clarimon, J., Molinuevo, J.L., Sanchez-Valle, R., Llado, A., Coma, M., Gomez-Isla, T., Blesa, R., Ferrer, I.*, et al.* (2010). Clinical, neuropathologic, and biochemical profile of the amyloid precursor protein I716F mutation. Journal of neuropathology and experimental neurology *69*, 53-59.

Guerreiro, R., Wojtas, A., Bras, J., Carrasquillo, M., Rogaeva, E., Majounie, E., Cruchaga, C., Sassi, C., Kauwe, J.S., Younkin, S.*, et al.* (2013). TREM2 variants in Alzheimer's disease. The New England journal of medicine *368*, 117-127.

Guo, H.F., Tong, J., Hannan, F., Luo, L., and Zhong, Y. (2000). A neurofibromatosis-1-regulated pathway is required for learning in Drosophila. Nature *403*, 895-898.

Guo, H.F., and Zhong, Y. (2006). Requirement of Akt to mediate long-term synaptic depression in Drosophila. The Journal of neuroscience : the official journal of the Society for Neuroscience

26, 4004-4014.

Gurney, M.E. (1997). Transgenic animal models of familial amyotrophic lateral sclerosis. Journal of neurology *244 Suppl 2*, S15-20.

Gustke, N., Trinczek, B., Biernat, J., Mandelkow, E.M., and Mandelkow, E. (1994). Domains of tau protein and interactions with microtubules. Biochemistry *33*, 9511-9522.

Haas, A.K., Yoshimura, S., Stephens, D.J., Preisinger, C., Fuchs, E., and Barr, F.A. (2007). Analysis of GTPase-activating proteins: Rab1 and Rab43 are key Rabs required to maintain a functional Golgi complex in human cells. Journal of cell science *120*, 2997-3010.

Haass, C., Koo, E.H., Mellon, A., Hung, A.Y., and Selkoe, D.J. (1992). Targeting of cell-surface beta-amyloid precursor protein to lysosomes: alternative processing into amyloid-bearing fragments. Nature *357*, 500-503.

Hamanaka, H., Katoh-Fukui, Y., Suzuki, K., Kobayashi, M., Suzuki, R., Motegi, Y., Nakahara, Y., Takeshita, A., Kawai, M., Ishiguro, K.*, et al.* (2000). Altered cholesterol metabolism in human apolipoprotein E4 knock-in mice. Human molecular genetics *9*, 353-361.

Han, S., Schroeder, E.A., Silva-Garcia, C.G., Hebestreit, K., Mair, W.B., and Brunet, A. (2017). Mono-unsaturated fatty acids link H3K4me3 modifiers to C. elegans lifespan. Nature *544*, 185-190.

Han, T.H., Dharkar, P., Mayer, M.L., and Serpe, M. (2015). Functional reconstitution of Drosophila melanogaster NMJ glutamate receptors. Proceedings of the National Academy of Sciences of the United States of America *112*, 6182-6187.

Hanger, D.P., Hughes, K., Woodgett, J.R., Brion, J.P., and Anderton, B.H. (1992). Glycogen synthase kinase-3 induces Alzheimer's disease-like phosphorylation of tau: generation of paired helical filament epitopes and neuronal localisation of the kinase. Neuroscience letters *147*, 58-62.

Hanley, J.G., and Henley, J.M. (2005). PICK1 is a calcium-sensor for NMDA-induced AMPA

receptor trafficking. The EMBO journal *24*, 3266-3278.

Hanson, P.I., Roth, R., Morisaki, H., Jahn, R., and Heuser, J.E. (1997). Structure and conformational changes in NSF and its membrane receptor complexes visualized by quick-freeze/deep-etch electron microscopy. Cell *90*, 523-535.

Hardy, J. (2006). A hundred years of Alzheimer's disease research. Neuron *52*, 3-13.

Hardy, J., and Selkoe, D.J. (2002). The amyloid hypothesis of Alzheimer's disease: progress and problems on the road to therapeutics. Science *297*, 353-356.

Harel, A., Wu, F., Mattson, M.P., Morris, C.M., and Yao, P.J. (2008). Evidence for CALM in directing VAMP2 trafficking. Traffic *9*, 417-429.

Harold, D., Abraham, R., Hollingworth, P., Sims, R., Gerrish, A., Hamshere, M.L., Pahwa, J.S., Moskvina, V., Dowzell, K., Williams, A.*, et al.* (2009). Genome-wide association study identifies variants at CLU and PICALM associated with Alzheimer's disease. Nature genetics *41*, 1088-1093.

Harrison, D.E., Strong, R., Sharp, Z.D., Nelson, J.F., Astle, C.M., Flurkey, K., Nadon, N.L., Wilkinson, J.E., Frenkel, K., Carter, C.S.*, et al.* (2009). Rapamycin fed late in life extends lifespan in genetically heterogeneous mice. Nature *460*, 392-395.

Hartmann, T., Bieger, S.C., Bruhl, B., Tienari, P.J., Ida, N., Allsop, D., Roberts, G.W., Masters, C.L., Dotti, C.G., Unsicker, K.*, et al.* (1997). Distinct sites of intracellular production for Alzheimer's disease A beta40/42 amyloid peptides. Nature medicine *3*, 1016-1020.

Hatters, D.M., Zhong, N., Rutenber, E., and Weisgraber, K.H. (2006). Amino-terminal domain stability mediates apolipoprotein E aggregation into neurotoxic fibrils. Journal of molecular biology *361*, 932-944.

Heckmann, M., Bufler, J., Franke, C., and Dudel, J. (1996). Kinetics of homomeric GluR6 glutamate receptor channels. Biophysical journal *71*, 1743-1750.

Hefendehl, J.K., LeDue, J., Ko, R.W., Mahler, J., Murphy, T.H., and MacVicar, B.A. (2016). Mapping synaptic glutamate transporter dysfunction in vivo to regions surrounding Abeta plaques by iGluSnFR two-photon imaging. Nature communications *7*, 13441.

Hefter, D., Kaiser, M., Weyer, S.W., Papageorgiou, I.E., Both, M., Kann, O., Muller, U.C., and Draguhn, A. (2016). Amyloid Precursor Protein Protects Neuronal Network Function after Hypoxia via Control of Voltage-Gated Calcium Channels. The Journal of neuroscience : the official journal of the Society for Neuroscience *36*, 8356-8371.

Heimbucher, T., Liu, Z., Bossard, C., McCloskey, R., Carrano, A.C., Riedel, C.G., Tanasa, B., Klammt, C., Fonslow, B.R., Riera, C.E.*, et al.* (2015). The Deubiquitylase MATH-33 Controls DAF-16 Stability and Function in Metabolism and Longevity. Cell metabolism *22*, 151-163.

Henne, W.M., Buchkovich, N.J., and Emr, S.D. (2011). The ESCRT pathway. Dev Cell *21*, 77-91.

Hick, M., Herrmann, U., Weyer, S.W., Mallm, J.P., Tschape, J.A., Borgers, M., Mercken, M., Roth, F.C., Draguhn, A., Slomianka, L.*, et al.* (2015). Acute function of secreted amyloid precursor protein fragment APPsalpha in synaptic plasticity. Acta Neuropathol *129*, 21-37.

Hinshaw, J.E., and Schmid, S.L. (1995). Dynamin self-assembles into rings suggesting a mechanism for coated vesicle budding. Nature *374*, 190-192.

Hirai, K., Aliev, G., Nunomura, A., Fujioka, H., Russell, R.L., Atwood, C.S., Johnson, A.B., Kress, Y., Vinters, H.V., Tabaton, M.*, et al.* (2001). Mitochondrial abnormalities in Alzheimer's disease. The Journal of neuroscience : the official journal of the Society for Neuroscience *21*, 3017-3023.

Hoe, H.S., Fu, Z., Makarova, A., Lee, J.Y., Lu, C., Feng, L., Pajoohesh-Ganji, A., Matsuoka, Y., Hyman, B.T., Ehlers, M.D.*, et al.* (2009). The effects of amyloid precursor protein on postsynaptic composition and activity. The Journal of biological chemistry *284*, 8495-8506.

Holcomb, L., Gordon, M.N., McGowan, E., Yu, X., Benkovic, S., Jantzen, P., Wright, K., Saad,

I., Mueller, R., Morgan, D.*, et al.* (1998). Accelerated Alzheimer-type phenotype in transgenic mice carrying both mutant amyloid precursor protein and presenilin 1 transgenes. Nature medicine *4*, 97-100.

Hollingworth, P., Harold, D., Sims, R., Gerrish, A., Lambert, J.C., Carrasquillo, M.M., Abraham, R., Hamshere, M.L., Pahwa, J.S., Moskvina, V.*, et al.* (2011). Common variants at ABCA7, MS4A6A/MS4A4E, EPHA1, CD33 and CD2AP are associated with Alzheimer's disease. Nature genetics *43*, 429-435.

Holtzman, D.M., Bales, K.R., Tenkova, T., Fagan, A.M., Parsadanian, M., Sartorius, L.J., Mackey, B., Olney, J., McKeel, D., Wozniak, D.*, et al.* (2000). Apolipoprotein E isoform-dependent amyloid deposition and neuritic degeneration in a mouse model of Alzheimer's disease. Proceedings of the National Academy of Sciences of the United States of America *97*, 2892-2897.

Holtzman, D.M., Bales, K.R., Wu, S., Bhat, P., Parsadanian, M., Fagan, A.M., Chang, L.K., Sun, Y., and Paul, S.M. (1999). Expression of human apolipoprotein E reduces amyloid-beta deposition in a mouse model of Alzheimer's disease. The Journal of clinical investigation *103*, R15-R21.

Hong, M., Zhukareva, V., Vogelsberg-Ragaglia, V., Wszolek, Z., Reed, L., Miller, B.I., Geschwind, D.H., Bird, T.D., McKeel, D., Goate, A.*, et al.* (1998). Mutation-specific functional impairments in distinct tau isoforms of hereditary FTDP-17. Science *282*, 1914-1917.

Hong, S., Freeberg, M.A., Han, T., Kamath, A., Yao, Y., Fukuda, T., Suzuki, T., Kim, J.K., and Inoki, K. (2017). LARP1 functions as a molecular switch for mTORC1-mediated translation of an essential class of mRNAs. eLife *6*.

Honing, S., Ricotta, D., Krauss, M., Spate, K., Spolaore, B., Motley, A., Robinson, M., Robinson, C., Haucke, V., and Owen, D.J. (2005). Phosphatidylinositol-(4,5)-bisphosphate regulates sorting signal recognition by the clathrin-associated adaptor complex AP2. Molecular cell *18*, 519-531.

Houlden, H., Crook, R., Dolan, R.J., McLaughlin, J., Revesz, T., and Hardy, J. (2001). A novel presenilin mutation (M233V) causing very early onset Alzheimer's disease with Lewy bodies. Neurosci Lett *313*, 93-95.

Hsiao, K., Chapman, P., Nilsen, S., Eckman, C., Harigaya, Y., Younkin, S., Yang, F., and Cole, G. (1996). Correlative memory deficits, Abeta elevation, and amyloid plaques in transgenic mice. Science *274*, 99-102.

Hsieh, H., Boehm, J., Sato, C., Iwatsubo, T., Tomita, T., Sisodia, S., and Malinow, R. (2006). AMPAR removal underlies Abeta-induced synaptic depression and dendritic spine loss. Neuron *52*, 831-843.

Hu, N.W., Klyubin, I., Anwyl, R., and Rowan, M.J. (2009a). GluN2B subunit-containing NMDA receptor antagonists prevent Abeta-mediated synaptic plasticity disruption in vivo. Proceedings of the National Academy of Sciences of the United States of America *106*, 20504-20509.

Hu, W., Qiu, B., Guan, W., Wang, Q., Wang, M., Li, W., Gao, L., Shen, L., Huang, Y., Xie, G.*, et al.* (2015). Direct Conversion of Normal and Alzheimer's Disease Human Fibroblasts into Neuronal Cells by Small Molecules. Cell stem cell *17*, 204-212.

Hu, X., Crick, S.L., Bu, G., Frieden, C., Pappu, R.V., and Lee, J.M. (2009b). Amyloid seeds formed by cellular uptake, concentration, and aggregation of the amyloid-beta peptide. Proceedings of the National Academy of Sciences of the United States of America *106*, 20324-20329.

Huang, C., Wang, P., Xie, Z., Wang, L., and Zhong, Y. (2013). The differential requirement of mushroom body alpha/beta subdivisions in long-term memory retrieval in Drosophila. Protein & cell *4*, 512-519.

Huang, C., Zheng, X., Zhao, H., Li, M., Wang, P., Xie, Z., Wang, L., and Zhong, Y. (2012). A permissive role of mushroom body alpha/beta core neurons in long-term memory consolidation in Drosophila. Current biology : CB *22*, 1981-1989.

Huang, Y.A., Zhou, B., Wernig, M., and Sudhof, T.C. (2017). ApoE2, ApoE3, and ApoE4 Differentially Stimulate APP Transcription and Abeta Secretion. Cell *168*, 427-441 e421.

Hynd, M.R., Scott, H.L., and Dodd, P.R. (2004). Glutamate-mediated excitotoxicity and neurodegeneration in Alzheimer's disease. Neurochemistry international *45*, 583-595.

Iijima, K., Liu, H.P., Chiang, A.S., Hearn, S.A., Konsolaki, M., and Zhong, Y. (2004). Dissecting the pathological effects of human Abeta40 and Abeta42 in Drosophila: a potential model for Alzheimer's disease. Proceedings of the National Academy of Sciences of the United States of America *101*, 6623-6628.

Innerarity, T.L., and Mahley, R.W. (1978). Enhanced binding by cultured human fibroblasts of apo-E-containing lipoproteins as compared with low density lipoproteins. Biochemistry *17*, 1440-1447.

Ishii, K., Tamaoka, A., Mizusawa, H., Shoji, S., Ohtake, T., Fraser, P.E., Takahashi, H., Tsuji, S., Gearing, M., Mizutani, T.*, et al.* (1997). Abeta1-40 but not Abeta1-42 levels in cortex correlate with apolipoprotein E epsilon4 allele dosage in sporadic Alzheimer's disease. Brain research *748*, 250-252.

Israel, M.A., Yuan, S.H., Bardy, C., Reyna, S.M., Mu, Y., Herrera, C., Hefferan, M.P., Van Gorp, S., Nazor, K.L., Boscolo, F.S.*, et al.* (2012). Probing sporadic and familial Alzheimer's disease using induced pluripotent stem cells. Nature *482*, 216-220.

Izumi, K., Nakato, R., Zhang, Z., Edmondson, A.C., Noon, S., Dulik, M.C., Rajagopalan, R., Venditti, C.P., Gripp, K., Samanich, J.*, et al.* (2015). Germline gain-of-function mutations in AFF4 cause a developmental syndrome functionally linking the super elongation complex and cohesin. Nature genetics *47*, 338-344.

Jacobs, J.R. (2000). The midline glia of Drosophila: a molecular genetic model for the developmental functions of glia. Progress in neurobiology *62*, 475-508.

Jacobsen, H., Reinhardt, D., Brockhaus, M., Bur, D., Kocyba, C., Kurt, H., Grim, M.G.,

Baumeister, R., and Loetscher, H. (1999). The influence of endoproteolytic processing of familial Alzheimer's disease presenilin 2 on abeta42 amyloid peptide formation. The Journal of biological chemistry *274*, 35233-35239.

Jamsa, A., Belda, O., Edlund, M., and Lindstrom, E. (2011). BACE-1 inhibition prevents the gamma-secretase inhibitor evoked Abeta rise in human neuroblastoma SH-SY5Y cells. J Biomed Sci *18*, 76.

Jobim, P.F., Pedroso, T.R., Christoff, R.R., Werenicz, A., Maurmann, N., Reolon, G.K., and Roesler, R. (2012a). Inhibition of mTOR by rapamycin in the amygdala or hippocampus impairs formation and reconsolidation of inhibitory avoidance memory. Neurobiology of learning and memory *97*, 105-112.

Jobim, P.F., Pedroso, T.R., Werenicz, A., Christoff, R.R., Maurmann, N., Reolon, G.K., Schroder, N., and Roesler, R. (2012b). Impairment of object recognition memory by rapamycin inhibition of mTOR in the amygdala or hippocampus around the time of learning or reactivation. Behavioural brain research *228*, 151-158.

Jonassen, T., Larsen, P.L., and Clarke, C.F. (2001). A dietary source of coenzyme Q is essential for growth of long-lived Caenorhabditis elegans clk-1 mutants. Proceedings of the National Academy of Sciences of the United States of America *98*, 421-426.

Jonassen, T., Proft, M., Randez-Gil, F., Schultz, J.R., Marbois, B.N., Entian, K.D., and Clarke, C.F. (1998). Yeast Clk-1 homologue (Coq7/Cat5) is a mitochondrial protein in coenzyme Q synthesis. The Journal of biological chemistry *273*, 3351-3357.

Jones, M.A., Gargano, J.W., Rhodenizer, D., Martin, I., Bhandari, P., and Grotewiel, M. (2009). A forward genetic screen in Drosophila implicates insulin signaling in age-related locomotor impairment. Experimental gerontology *44*, 532-540.

Jonsson, T., Stefansson, H., Steinberg, S., Jonsdottir, I., Jonsson, P.V., Snaedal, J., Bjornsson, S., Huttenlocher, J., Levey, A.I., Lah, J.J.*, et al.* (2013). Variant of TREM2 associated with the risk of Alzheimer's disease. The New England journal of medicine *368*, 107-116.

Juhasz, G., Erdi, B., Sass, M., and Neufeld, T.P. (2007). Atg7-dependent autophagy promotes neuronal health, stress tolerance, and longevity but is dispensable for metamorphosis in Drosophila. Genes & development *21*, 3061-3066.

Kabeya, Y., Mizushima, N., Ueno, T., Yamamoto, A., Kirisako, T., Noda, T., Kominami, E., Ohsumi, Y., and Yoshimori, T. (2000). LC3, a mammalian homologue of yeast Apg8p, is localized in autophagosome membranes after processing. The EMBO journal *19*, 5720-5728.

Kahn, R.A., Cherfils, J., Elias, M., Lovering, R.C., Munro, S., and Schurmann, A. (2006). Nomenclature for the human Arf family of GTP-binding proteins: ARF, ARL, and SAR proteins. The Journal of cell biology *172*, 645-650.

Kajava, A.V., Baxa, U., and Steven, A.C. (2010). Beta arcades: recurring motifs in naturally occurring and disease-related amyloid fibrils. FASEB journal : official publication of the Federation of American Societies for Experimental Biology *24*, 1311-1319.

Kamboh, M.I., Demirci, F.Y., Wang, X., Minster, R.L., Carrasquillo, M.M., Pankratz, V.S., Younkin, S.G., Saykin, A.J., Alzheimer's Disease Neuroimaging, I., Jun, G.*, et al.* (2012). Genome-wide association study of Alzheimer's disease. Translational psychiatry *2*, e117.

Kanai, Y., Nussberger, S., Romero, M.F., Boron, W.F., Hebert, S.C., and Hediger, M.A. (1995). Electrogenic properties of the epithelial and neuronal high affinity glutamate transporter. The Journal of biological chemistry *270*, 16561-16568.

Kanatsu, K., Morohashi, Y., Suzuki, M., Kuroda, H., Watanabe, T., Tomita, T., and Iwatsubo, T. (2014). Decreased CALM expression reduces Abeta42 to total Abeta ratio through clathrin-mediated endocytosis of gamma-secretase. Nature communications *5*, 3386.

Kanekiyo, T., Cirrito, J.R., Liu, C.C., Shinohara, M., Li, J., Schuler, D.R., Shinohara, M., Holtzman, D.M., and Bu, G. (2013). Neuronal clearance of amyloid-beta by endocytic receptor LRP1. The Journal of neuroscience : the official journal of the Society for Neuroscience *33*, 19276-19283.

Kaneko, T., Fujiyama, F., and Hioki, H. (2002). Immunohistochemical localization of candidates for vesicular glutamate transporters in the rat brain. The Journal of comparative neurology *444*, 39-62.

Kanemaru, K., Takio, K., Miura, R., Titani, K., and Ihara, Y. (1992). Fetal-type phosphorylation of the tau in paired helical filaments. Journal of neurochemistry *58*, 1667-1675.

Kang, J., Lemaire, H.G., Unterbeck, A., Salbaum, J.M., Masters, C.L., Grzeschik, K.H., Multhaup, G., Beyreuther, K., and Muller-Hill, B. (1987). The precursor of Alzheimer's disease amyloid A4 protein resembles a cell-surface receptor. Nature *325*, 733-736.

Kanner, B.I., and Bendahan, A. (1982). Binding order of substrates to the sodium and potassium ion coupled L-glutamic acid transporter from rat brain. Biochemistry *21*, 6327-6330.

Kanner, B.I., and Sharon, I. (1978). Active transport of L-glutamate by membrane vesicles isolated from rat brain. Biochemistry *17*, 3949-3953.

Katsurabayashi, S., Kawano, H., Ii, M., Nakano, S., Tatsumi, C., Kubota, K., Takasaki, K., Mishima, K., Fujiwara, M., and Iwasaki, K. (2016). Overexpression of Swedish mutant APP in aged astrocytes attenuates excitatory synaptic transmission. Physiological reports *4*.

Keene, A.C., Stratmann, M., Keller, A., Perrat, P.N., Vosshall, L.B., and Waddell, S. (2004). Diverse odor-conditioned memories require uniquely timed dorsal paired medial neuron output. Neuron *44*, 521-533.

Kelly, B.T., McCoy, A.J., Spate, K., Miller, S.E., Evans, P.R., Honing, S., and Owen, D.J. (2008). A structural explanation for the binding of endocytic dileucine motifs by the AP2 complex. Nature *456*, 976-979.

Keshishian, H., Broadie, K., Chiba, A., and Bate, M. (1996). The drosophila neuromuscular junction: a model system for studying synaptic development and function. Annual review of neuroscience *19*, 545-575.

Kfoury, N., Holmes, B.B., Jiang, H., Holtzman, D.M., and Diamond, M.I. (2012). Trans-cellular

propagation of Tau aggregation by fibrillar species. The Journal of biological chemistry *287*, 19440-19451.

Kim, C.J., Ryu, W.S., Kwak, J.W., Park, C.T., and Ryoo, U.H. (1996). Changes in Lp(a) lipoprotein and lipid levels after cessation of female sex hormone production and estrogen replacement therapy. Archives of internal medicine *156*, 500-504.

Kim, H., Ki, H., Park, H.S., and Kim, K. (2005). Presenilin-1 D257A and D385A mutants fail to cleave Notch in their endoproteolyzed forms, but only presenilin-1 D385A mutant can restore its gamma-secretase activity with the compensatory overexpression of normal C-terminal fragment. The Journal of biological chemistry *280*, 22462-22472.

Kim, H.J., Raphael, A.R., LaDow, E.S., McGurk, L., Weber, R.A., Trojanowski, J.Q., Lee, V.M., Finkbeiner, S., Gitler, A.D., and Bonini, N.M. (2014). Therapeutic modulation of eIF2alpha phosphorylation rescues TDP-43 toxicity in amyotrophic lateral sclerosis disease models. Nature genetics *46*, 152-160.

Kim, J., Onstead, L., Randle, S., Price, R., Smithson, L., Zwizinski, C., Dickson, D.W., Golde, T., and McGowan, E. (2007a). Abeta40 inhibits amyloid deposition in vivo. The Journal of neuroscience : the official journal of the Society for Neuroscience *27*, 627-633.

Kim, S., Sato, Y., Mohan, P.S., Peterhoff, C., Pensalfini, A., Rigoglioso, A., Jiang, Y., and Nixon, R.A. (2016). Evidence that the rab5 effector APPL1 mediates APP-betaCTF-induced dysfunction of endosomes in Down syndrome and Alzheimer's disease. Molecular psychiatry *21*, 707-716.

Kim, S.H., Leem, J.Y., Lah, J.J., Slunt, H.H., Levey, A.I., Thinakaran, G., and Sisodia, S.S. (2001). Multiple effects of aspartate mutant presenilin 1 on the processing and trafficking of amyloid precursor protein. The Journal of biological chemistry *276*, 43343-43350.

Kim, S.M., Kim, M.Y., Ann, E.J., Mo, J.S., Yoon, J.H., and Park, H.S. (2012). Presenilin-2 regulates the degradation of RBP-Jk protein through p38 mitogen-activated protein kinase. Journal of cell science *125*, 1296-1308.

Kim, T., Vidal, G.S., Djurisic, M., William, C.M., Birnbaum, M.E., Garcia, K.C., Hyman, B.T., and Shatz, C.J. (2013a). Human LilrB2 is a beta-amyloid receptor and its murine homolog PirB regulates synaptic plasticity in an Alzheimer's model. Science *341*, 1399-1404.

Kim, T.W., Pettingell, W.H., Hallmark, O.G., Moir, R.D., Wasco, W., and Tanzi, R.E. (1997). Endoproteolytic cleavage and proteasomal degradation of presenilin 2 in transfected cells. The Journal of biological chemistry *272*, 11006-11010.

Kim, W.S., Li, H., Ruberu, K., Chan, S., Elliott, D.A., Low, J.K., Cheng, D., Karl, T., and Garner, B. (2013b). Deletion of Abca7 increases cerebral amyloid-beta accumulation in the J20 mouse model of Alzheimer's disease. The Journal of neuroscience : the official journal of the Society for Neuroscience *33*, 4387-4394.

Kim, Y.C., Lee, H.G., and Han, K.A. (2007b). D1 dopamine receptor dDA1 is required in the mushroom body neurons for aversive and appetitive learning in Drosophila. The Journal of neuroscience : the official journal of the Society for Neuroscience *27*, 7640-7647.

Kimberly, W.T., Zheng, J.B., Guenette, S.Y., and Selkoe, D.J. (2001). The intracellular domain of the beta-amyloid precursor protein is stabilized by Fe65 and translocates to the nucleus in a notch-like manner. The Journal of biological chemistry *276*, 40288-40292.

Kinoshita, A., Fukumoto, H., Shah, T., Whelan, C.M., Irizarry, M.C., and Hyman, B.T. (2003). Demonstration by FRET of BACE interaction with the amyloid precursor protein at the cell surface and in early endosomes. Journal of cell science *116*, 3339-3346.

Kleinberger, G., Yamanishi, Y., Suarez-Calvet, M., Czirr, E., Lohmann, E., Cuyvers, E., Struyfs, H., Pettkus, N., Wenninger-Weinzierl, A., Mazaheri, F.*, et al.* (2014). TREM2 mutations implicated in neurodegeneration impair cell surface transport and phagocytosis. Science translational medicine *6*, 243ra286.

Klockner, U., Storck, T., Conradt, M., and Stoffel, W. (1993). Electrogenic L-glutamate uptake in Xenopus laevis oocytes expressing a cloned rat brain L-glutamate/L-aspartate transporter (GLAST-1). The Journal of biological chemistry *268*, 14594-14596.

Knowles, T.P., Vendruscolo, M., and Dobson, C.M. (2014). The amyloid state and its association with protein misfolding diseases. Nat Rev Mol Cell Biol *15*, 384-396.

Kobayashi, S., Ishiguro, K., Omori, A., Takamatsu, M., Arioka, M., Imahori, K., and Uchida, T. (1993). A cdc2-related kinase PSSALRE/cdk5 is homologous with the 30 kDa subunit of tau protein kinase II, a proline-directed protein kinase associated with microtubule. FEBS letters *335*, 171-175.

Kondo, T., Asai, M., Tsukita, K., Kutoku, Y., Ohsawa, Y., Sunada, Y., Imamura, K., Egawa, N., Yahata, N., Okita, K.*, et al.* (2013). Modeling Alzheimer's disease with iPSCs reveals stress phenotypes associated with intracellular Abeta and differential drug responsiveness. Cell stem cell *12*, 487-496.

Koo, E.H. (2002). The beta-amyloid precursor protein (APP) and Alzheimer's disease: does the tail wag the dog? Traffic *3*, 763-770.

Koo, E.H., and Squazzo, S.L. (1994). Evidence that production and release of amyloid beta-protein involves the endocytic pathway. The Journal of biological chemistry *269*, 17386-17389.

Koo, S.J., Kochlamazashvili, G., Rost, B., Puchkov, D., Gimber, N., Lehmann, M., Tadeus, G., Schmoranzer, J., Rosenmund, C., Haucke, V.*, et al.* (2015). Vesicular Synaptobrevin/VAMP2 Levels Guarded by AP180 Control Efficient Neurotransmission. Neuron *88*, 330-344.

Koo, S.J., Markovic, S., Puchkov, D., Mahrenholz, C.C., Beceren-Braun, F., Maritzen, T., Dernedde, J., Volkmer, R., Oschkinat, H., and Haucke, V. (2011). SNARE motif-mediated sorting of synaptobrevin by the endocytic adaptors clathrin assembly lymphoid myeloid leukemia (CALM) and AP180 at synapses. Proceedings of the National Academy of Sciences of the United States of America *108*, 13540-13545.

Kosaka, T., and Ikeda, K. (1983). Reversible blockage of membrane retrieval and endocytosis in the garland cell of the temperature-sensitive mutant of Drosophila melanogaster, shibirets1. The Journal of cell biology *97*, 499-507.

Kovacs, I., Torok, I., Zombori, J., and Kasa, P. (1996). Neuropathologic changes in the olfactory bulb in Alzheimer's disease. Neurobiology (Bp) *4*, 123-126.

Kowal, R.C., Herz, J., Goldstein, J.L., Esser, V., and Brown, M.S. (1989). Low density lipoprotein receptor-related protein mediates uptake of cholesteryl esters derived from apoprotein E-enriched lipoproteins. Proceedings of the National Academy of Sciences of the United States of America *86*, 5810-5814.

Krashes, M.J., Keene, A.C., Leung, B., Armstrong, J.D., and Waddell, S. (2007). Sequential use of mushroom body neuron subsets during drosophila odor memory processing. Neuron *53*, 103-115.

Kretner, B., Fukumori, A., Gutsmiedl, A., Page, R.M., Luebbers, T., Galley, G., Baumann, K., Haass, C., and Steiner, H. (2011). Attenuated Abeta42 responses to low potency gamma-secretase modulators can be overcome for many pathogenic presenilin mutants by second-generation compounds. The Journal of biological chemistry *286*, 15240-15251.

Kronschlager, M.T., Drdla-Schutting, R., Gassner, M., Honsek, S.D., Teuchmann, H.L., and Sandkuhler, J. (2016). Gliogenic LTP spreads widely in nociceptive pathways. Science *354*, 1144-1148.

Kruglyak, L. (2008). The road to genome-wide association studies. Nature reviews Genetics *9*, 314-318.

Kundu, A., Milosch, N., Antonietti, P., Baumkotter, F., Zymny, A., Muller, U.C., Kins, S., Hajieva, P., Behl, C., and Kogel, D. (2016). Modulation of BAG3 Expression and Proteasomal Activity by sAPPalpha Does Not Require Membrane-Tethered Holo-APP. Molecular neurobiology *53*, 5985-5994.

Lahr, R.M., Fonseca, B.D., Ciotti, G.E., Al-Ashtal, H.A., Jia, J.J., Niklaus, M.R., Blagden, S.P., Alain, T., and Berman, A.J. (2017). La-related protein 1 (LARP1) binds the mRNA cap, blocking eIF4F assembly on TOP mRNAs. eLife *6*.

Lai, S.L., and Lee, T. (2006). Genetic mosaic with dual binary transcriptional systems in Drosophila. Nature neuroscience *9*, 703-709.

Lambert, J.C., Heath, S., Even, G., Campion, D., Sleegers, K., Hiltunen, M., Combarros, O., Zelenika, D., Bullido, M.J., Tavernier, B.*, et al.* (2009). Genome-wide association study identifies variants at CLU and CR1 associated with Alzheimer's disease. Nature genetics *41*, 1094-1099.

Lambert, J.C., Ibrahim-Verbaas, C.A., Harold, D., Naj, A.C., Sims, R., Bellenguez, C., DeStafano, A.L., Bis, J.C., Beecham, G.W., Grenier-Boley, B.*, et al.* (2013). Meta-analysis of 74,046 individuals identifies 11 new susceptibility loci for Alzheimer's disease. Nature genetics *45*, 1452-1458.

Lambert, J.C., Zelenika, D., Hiltunen, M., Chouraki, V., Combarros, O., Bullido, M.J., Tognoni, G., Fievet, N., Boland, A., Arosio, B.*, et al.* (2011). Evidence of the association of BIN1 and PICALM with the AD risk in contrasting European populations. Neurobiology of aging *32*, 756 e711-755.

Lasagna-Reeves, C.A., de Haro, M., Hao, S., Park, J., Rousseaux, M.W., Al-Ramahi, I., Jafar-Nejad, P., Vilanova-Velez, L., See, L., De Maio, A.*, et al.* (2016). Reduction of Nuak1 Decreases Tau and Reverses Phenotypes in a Tauopathy Mouse Model. Neuron *92*, 407-418.

Lauren, J., Gimbel, D.A., Nygaard, H.B., Gilbert, J.W., and Strittmatter, S.M. (2009). Cellular prion protein mediates impairment of synaptic plasticity by amyloid-beta oligomers. Nature *457*, 1128-1132.

Lee, J., Culyba, E.K., Powers, E.T., and Kelly, J.W. (2011). Amyloid-beta forms fibrils by nucleated conformational conversion of oligomers. Nat Chem Biol *7*, 602-609.

Lee, J.H., Yu, W.H., Kumar, A., Lee, S., Mohan, P.S., Peterhoff, C.M., Wolfe, D.M., Martinez-Vicente, M., Massey, A.C., Sovak, G.*, et al.* (2010a). Lysosomal proteolysis and autophagy require presenilin 1 and are disrupted by Alzheimer-related PS1 mutations. Cell *141*, 1146-1158.

Lee, K.J., Moussa, C.E., Lee, Y., Sung, Y., Howell, B.W., Turner, R.S., Pak, D.T., and Hoe, H.S. (2010b). Beta amyloid-independent role of amyloid precursor protein in generation and maintenance of dendritic spines. Neuroscience *169*, 344-356.

Lee, R.C., Feinbaum, R.L., and Ambros, V. (1993). The C. elegans heterochronic gene lin-4 encodes small RNAs with antisense complementarity to lin-14. Cell *75*, 843-854.

Lee, S.J., Liyanage, U., Bickel, P.E., Xia, W., Lansbury, P.T., Jr., and Kosik, K.S. (1998). A detergent-insoluble membrane compartment contains A beta in vivo. Nature medicine *4*, 730-734.

Lee, V.M., Goedert, M., and Trojanowski, J.Q. (2001). Neurodegenerative tauopathies. Annual review of neuroscience *24*, 1121-1159.

Lee, Y., Morrison, B.M., Li, Y., Lengacher, S., Farah, M.H., Hoffman, P.N., Liu, Y., Tsingalia, A., Jin, L., Zhang, P.W.*, et al.* (2012). Oligodendroglia metabolically support axons and contribute to neurodegeneration. Nature *487*, 443-448.

Leiserson, W.M., Harkins, E.W., and Keshishian, H. (2000). Fray, a Drosophila serine/threonine kinase homologous to mammalian PASK, is required for axonal ensheathment. Neuron *28*, 793-806.

Leprince, C., Le Scolan, E., Meunier, B., Fraisier, V., Brandon, N., De Gunzburg, J., and Camonis, J. (2003). Sorting nexin 4 and amphiphysin 2, a new partnership between endocytosis and intracellular trafficking. Journal of cell science *116*, 1937-1948.

Leprince, C., Romero, F., Cussac, D., Vayssiere, B., Berger, R., Tavitian, A., and Camonis, J.H. (1997). A new member of the amphiphysin family connecting endocytosis and signal transduction pathways. The Journal of biological chemistry *272*, 15101-15105.

Leventis, P.A., Chow, B.M., Stewart, B.A., Iyengar, B., Campos, A.R., and Boulianne, G.L. (2001). Drosophila Amphiphysin is a post-synaptic protein required for normal locomotion but not endocytosis. Traffic *2*, 839-850.

Levy-Lahad, E., Wasco, W., Poorkaj, P., Romano, D.M., Oshima, J., Pettingell, W.H., Yu, C.E., Jondro, P.D., Schmidt, S.D., Wang, K.*, et al.* (1995a). Candidate gene for the chromosome 1 familial Alzheimer's disease locus. Science *269*, 973-977.

Levy-Lahad, E., Wijsman, E.M., Nemens, E., Anderson, L., Goddard, K.A., Weber, J.L., Bird, T.D., and Schellenberg, G.D. (1995b). A familial Alzheimer's disease locus on chromosome 1. Science *269*, 970-973.

Levy, E., Carman, M.D., Fernandez-Madrid, I.J., Power, M.D., Lieberburg, I., van Duinen, S.G., Bots, G.T., Luyendijk, W., and Frangione, B. (1990). Mutation of the Alzheimer's disease amyloid gene in hereditary cerebral hemorrhage, Dutch type. Science *248*, 1124-1126.

Levy, L.M., Warr, O., and Attwell, D. (1998). Stoichiometry of the glial glutamate transporter GLT-1 expressed inducibly in a Chinese hamster ovary cell line selected for low endogenous Na+-dependent glutamate uptake. The Journal of neuroscience : the official journal of the Society for Neuroscience *18*, 9620-9628.

Lewis, J., Dickson, D.W., Lin, W.L., Chisholm, L., Corral, A., Jones, G., Yen, S.H., Sahara, N., Skipper, L., Yager, D.*, et al.* (2001). Enhanced neurofibrillary degeneration in transgenic mice expressing mutant tau and APP. Science *293*, 1487-1491.

Li, H., Karl, T., and Garner, B. (2016). Abca7 deletion does not affect adult neurogenesis in the mouse. Bioscience reports *36*.

Li, J., Hart, R.P., Mallimo, E.M., Swerdel, M.R., Kusnecov, A.W., and Herrup, K. (2013). EZH2-mediated H3K27 trimethylation mediates neurodegeneration in ataxia-telangiectasia. Nature neuroscience *16*, 1745-1753.

Li, J., Kanekiyo, T., Shinohara, M., Zhang, Y., LaDu, M.J., Xu, H., and Bu, G. (2012). Differential regulation of amyloid-beta endocytic trafficking and lysosomal degradation by apolipoprotein E isoforms. The Journal of biological chemistry *287*, 44593-44601.

Li, J.L., Fujiyama, F., Kaneko, T., and Mizuno, N. (2003). Expression of vesicular glutamate

transporters, VGluT1 and VGluT2, in axon terminals of nociceptive primary afferent fibers in the superficial layers of the medullary and spinal dorsal horns of the rat. The Journal of comparative neurology *457*, 236-249.

Li, S., Hong, S., Shepardson, N.E., Walsh, D.M., Shankar, G.M., and Selkoe, D. (2009). Soluble oligomers of amyloid Beta protein facilitate hippocampal long-term depression by disrupting neuronal glutamate uptake. Neuron *62*, 788-801.

Li, S., Jin, M., Koeglsperger, T., Shepardson, N.E., Shankar, G.M., and Selkoe, D.J. (2011). Soluble Abeta oligomers inhibit long-term potentiation through a mechanism involving excessive activation of extrasynaptic NR2B-containing NMDA receptors. The Journal of neuroscience : the official journal of the Society for Neuroscience *31*, 6627-6638.

Li, W., Gao, B., Lee, S.M., Bennett, K., and Fang, D. (2007). RLE-1, an E3 ubiquitin ligase, regulates C. elegans aging by catalyzing DAF-16 polyubiquitination. Developmental cell *12*, 235-246.

Li, Y., Xu, W., McBurney, M.W., and Longo, V.D. (2008). SirT1 inhibition reduces IGF-I/IRS-2/Ras/ERK1/2 signaling and protects neurons. Cell metabolism *8*, 38-48.

Li, Z., Burrone, J., Tyler, W.J., Hartman, K.N., Albeanu, D.F., and Murthy, V.N. (2005). Synaptic vesicle recycling studied in transgenic mice expressing synaptopHluorin. Proceedings of the National Academy of Sciences of the United States of America *102*, 6131-6136.

Li, Z.W., Stark, G., Gotz, J., Rulicke, T., Gschwind, M., Huber, G., Muller, U., and Weissmann, C. (1996). Generation of mice with a 200-kb amyloid precursor protein gene deletion by Cre recombinase-mediated site-specific recombination in embryonic stem cells. Proceedings of the National Academy of Sciences of the United States of America *93*, 6158-6162.

Lichtenthaler, S.F., Multhaup, G., Masters, C.L., and Beyreuther, K. (1999). A novel substrate for analyzing Alzheimer's disease gamma-secretase. FEBS letters *453*, 288-292.

Lill, C.M., Rengmark, A., Pihlstrom, L., Fogh, I., Shatunov, A., Sleiman, P.M., Wang, L.S., Liu,

T., Lassen, C.F., Meissner, E.*, et al.* (2015). The role of TREM2 R47H as a risk factor for Alzheimer's disease, frontotemporal lobar degeneration, amyotrophic lateral sclerosis, and Parkinson's disease. Alzheimer's & dementia : the journal of the Alzheimer's Association *11*, 1407-1416.

Lin, A.C., Bygrave, A.M., de Calignon, A., Lee, T., and Miesenbock, G. (2014). Sparse, decorrelated odor coding in the mushroom body enhances learned odor discrimination. Nature neuroscience *17*, 559-568.

Lin, C., Smith, E.R., Takahashi, H., Lai, K.C., Martin-Brown, S., Florens, L., Washburn, M.P., Conaway, J.W., Conaway, R.C., and Shilatifard, A. (2010). AFF4, a component of the ELL/P-TEFb elongation complex and a shared subunit of MLL chimeras, can link transcription elongation to leukemia. Mol Cell *37*, 429-437.

Lin, D.T., and Huganir, R.L. (2007). PICK1 and phosphorylation of the glutamate receptor 2 (GluR2) AMPA receptor subunit regulates GluR2 recycling after NMDA receptor-induced internalization. The Journal of neuroscience : the official journal of the Society for Neuroscience *27*, 13903-13908.

Ling, D., and Salvaterra, P.M. (2011). Robust RT-qPCR data normalization: validation and selection of internal reference genes during post-experimental data analysis. PloS one *6*, e17762.

Lipton, S.A. (2006). Paradigm shift in neuroprotection by NMDA receptor blockade: memantine and beyond. Nature reviews Drug discovery *5*, 160-170.

Liu, F., Iqbal, K., Grundke-Iqbal, I., Hart, G.W., and Gong, C.X. (2004). O-GlcNAcylation regulates phosphorylation of tau: a mechanism involved in Alzheimer's disease. Proceedings of the National Academy of Sciences of the United States of America *101*, 10804-10809.

Liu, G., Rogers, J., Murphy, C.T., and Rongo, C. (2011). EGF signalling activates the ubiquitin proteasome system to modulate C. elegans lifespan. The EMBO journal *30*, 2990-3003.

Liu, L., MacKenzie, K.R., Putluri, N., Maletic-Savatic, M., and Bellen, H.J. (2017). The Glia-Neuron Lactate Shuttle and Elevated ROS Promote Lipid Synthesis in Neurons and Lipid Droplet Accumulation in Glia via APOE/D. Cell metabolism *26*, 719-737 e716.

Liu, S.J., Gasperini, R., Foa, L., and Small, D.H. (2010). Amyloid-beta decreases cell-surface AMPA receptors by increasing intracellular calcium and phosphorylation of GluR2. Journal of Alzheimer's disease : JAD *21*, 655-666.

Liu, W.W., and Wilson, R.I. (2013). Glutamate is an inhibitory neurotransmitter in the Drosophila olfactory system. Proceedings of the National Academy of Sciences of the United States of America *110*, 10294-10299.

Liu, X., and Davis, R.L. (2009). The GABAergic anterior paired lateral neuron suppresses and is suppressed by olfactory learning. Nature neuroscience *12*, 53-59.

Liu, X., Krause, W.C., and Davis, R.L. (2007). GABAA receptor RDL inhibits Drosophila olfactory associative learning. Neuron *56*, 1090-1102.

LoPresti, P., Szuchet, S., Papasozomenos, S.C., Zinkowski, R.P., and Binder, L.I. (1995). Functional implications for the microtubule-associated protein tau: localization in oligodendrocytes. Proceedings of the National Academy of Sciences of the United States of America *92*, 10369-10373.

Lu, B., Al-Ramahi, I., Valencia, A., Wang, Q., Berenshteyn, F., Yang, H., Gallego-Flores, T., Ichcho, S., Lacoste, A., Hild, M.*, et al.* (2013). Identification of NUB1 as a suppressor of mutant Huntington toxicity via enhanced protein clearance. Nature neuroscience *16*, 562-570.

Lu, T.Y., Doherty, J., and Freeman, M.R. (2014). DRK/DOS/SOS converge with Crk/Mbc/dCed-12 to activate Rac1 during glial engulfment of axonal debris. Proceedings of the National Academy of Sciences of the United States of America *111*, 12544-12549.

Lucin, K.M., O'Brien, C.E., Bieri, G., Czirr, E., Mosher, K.I., Abbey, R.J., Mastroeni, D.F., Rogers, J., Spencer, B., Masliah, E.*, et al.* (2013). Microglial beclin 1 regulates retromer

trafficking and phagocytosis and is impaired in Alzheimer's disease. Neuron *79*, 873-886.

Luthi-Carter, R., Taylor, D.M., Pallos, J., Lambert, E., Amore, A., Parker, A., Moffitt, H., Smith, D.L., Runne, H., Gokce, O.*, et al.* (2010). SIRT2 inhibition achieves neuroprotection by decreasing sterol biosynthesis. Proceedings of the National Academy of Sciences of the United States of America *107*, 7927-7932.

Lynch, J.R., Tang, W., Wang, H., Vitek, M.P., Bennett, E.R., Sullivan, P.M., Warner, D.S., and Laskowitz, D.T. (2003). APOE genotype and an ApoE-mimetic peptide modify the systemic and central nervous system inflammatory response. The Journal of biological chemistry *278*, 48529-48533.

Ma, C., Su, L., Seven, A.B., Xu, Y., and Rizo, J. (2013a). Reconstitution of the vital functions of Munc18 and Munc13 in neurotransmitter release. Science *339*, 421-425.

Ma, J., Yee, A., Brewer, H.B., Jr., Das, S., and Potter, H. (1994). Amyloid-associated proteins alpha 1-antichymotrypsin and apolipoprotein E promote assembly of Alzheimer beta-protein into filaments. Nature *372*, 92-94.

Ma, T., Trinh, M.A., Wexler, A.J., Bourbon, C., Gatti, E., Pierre, P., Cavener, D.R., and Klann, E. (2013b). Suppression of eIF2alpha kinases alleviates Alzheimer's disease-related plasticity and memory deficits. Nature neuroscience *16*, 1299-1305.

Maas, T., Eidenmuller, J., and Brandt, R. (2000). Interaction of tau with the neural membrane cortex is regulated by phosphorylation at sites that are modified in paired helical filaments. The Journal of biological chemistry *275*, 15733-15740.

Mac Callum, P.E., Hebert, M., Adamec, R.E., and Blundell, J. (2014). Systemic inhibition of mTOR kinase via rapamycin disrupts consolidation and reconsolidation of auditory fear memory. Neurobiology of learning and memory *112*, 176-185.

MacDonald, J.M., Beach, M.G., Porpiglia, E., Sheehan, A.E., Watts, R.J., and Freeman, M.R. (2006). The Drosophila cell corpse engulfment receptor Draper mediates glial clearance of

severed axons. Neuron *50*, 869-881.

Macdonald, J.M., Doherty, J., Hackett, R., and Freeman, M.R. (2013). The c-Jun kinase signaling cascade promotes glial engulfment activity through activation of draper and phagocytic function. Cell death and differentiation *20*, 1140-1148.

Macia, E., Ehrlich, M., Massol, R., Boucrot, E., Brunner, C., and Kirchhausen, T. (2006). Dynasore, a cell-permeable inhibitor of dynamin. Developmental cell *10*, 839-850.

Madabhushi, R., Gao, F., Pfenning, A.R., Pan, L., Yamakawa, S., Seo, J., Rueda, R., Phan, T.X., Yamakawa, H., Pao, P.C.*, et al.* (2015). Activity-Induced DNA Breaks Govern the Expression of Neuronal Early-Response Genes. Cell *161*, 1592-1605.

Mao, Z., and Davis, R.L. (2009). Eight different types of dopaminergic neurons innervate the Drosophila mushroom body neuropil: anatomical and physiological heterogeneity. Frontiers in neural circuits *3*, 5.

Martin, D., Thompson, M.A., and Nadler, J.V. (1993). The neuroprotective agent riluzole inhibits release of glutamate and aspartate from slices of hippocampal area CA1. European journal of pharmacology *250*, 473-476.

Martin, S.G., Dobi, K.C., and St Johnston, D. (2001). A rapid method to map mutations in Drosophila. Genome biology *2*, RESEARCH0036.

Marvin, J.S., Borghuis, B.G., Tian, L., Cichon, J., Harnett, M.T., Akerboom, J., Gordus, A., Renninger, S.L., Chen, T.W., Bargmann, C.I.*, et al.* (2013). An optimized fluorescent probe for visualizing glutamate neurotransmission. Nature methods *10*, 162-170.

Massol, R.H., Boll, W., Griffin, A.M., and Kirchhausen, T. (2006). A burst of auxilin recruitment determines the onset of clathrin-coated vesicle uncoating. Proceedings of the National Academy of Sciences of the United States of America *103*, 10265-10270.

Matsui, Y., Kikuchi, A., Araki, S., Hata, Y., Kondo, J., Teranishi, Y., and Takai, Y. (1990). Molecular cloning and characterization of a novel type of regulatory protein (GDI) for smg

p25A, a ras p21-like GTP-binding protein. Molecular and cellular biology *10*, 4116-4122.

Matsumoto, K., Akao, Y., Yi, H., Shamoto-Nagai, M., Maruyama, W., and Naoi, M. (2006). Overexpression of amyloid precursor protein induces susceptibility to oxidative stress in human neuroblastoma SH-SY5Y cells. J Neural Transm (Vienna) *113*, 125-135.

Matsumoto, M., Kurihara, S., Kibe, R., Ashida, H., and Benno, Y. (2011). Longevity in mice is promoted by probiotic-induced suppression of colonic senescence dependent on upregulation of gut bacterial polyamine production. PloS one *6*, e23652.

Matta, S., Van Kolen, K., da Cunha, R., van den Bogaart, G., Mandemakers, W., Miskiewicz, K., De Bock, P.J., Morais, V.A., Vilain, S., Haddad, D.*, et al.* (2012). LRRK2 controls an EndoA phosphorylation cycle in synaptic endocytosis. Neuron *75*, 1008-1021.

Mauch, D.H., Nagler, K., Schumacher, S., Goritz, C., Muller, E.C., Otto, A., and Pfrieger, F.W. (2001). CNS synaptogenesis promoted by glia-derived cholesterol. Science *294*, 1354-1357.

Maurer, K., Volk, S., and Gerbaldo, H. (1997). Auguste D and Alzheimer's disease. Lancet *349*, 1546-1549.

Mawal-Dewan, M., Henley, J., Van de Voorde, A., Trojanowski, J.Q., and Lee, V.M. (1994). The phosphorylation state of tau in the developing rat brain is regulated by phosphoprotein phosphatases. The Journal of biological chemistry *269*, 30981-30987.

Mawuenyega, K.G., Sigurdson, W., Ovod, V., Munsell, L., Kasten, T., Morris, J.C., Yarasheski, K.E., and Bateman, R.J. (2010). Decreased clearance of CNS beta-amyloid in Alzheimer's disease. Science *330*, 1774.

McCarthy, M.I., Abecasis, G.R., Cardon, L.R., Goldstein, D.B., Little, J., Ioannidis, J.P., and Hirschhorn, J.N. (2008). Genome-wide association studies for complex traits: consensus, uncertainty and challenges. Nature reviews Genetics *9*, 356-369.

McGuire, S.E., Le, P.T., and Davis, R.L. (2001). The role of Drosophila mushroom body signaling in olfactory memory. Science *293*, 1330-1333.

McKenzie, I.A., Ohayon, D., Li, H., de Faria, J.P., Emery, B., Tohyama, K., and Richardson, W.D. (2014). Motor skill learning requires active central myelination. Science *346*, 318-322.

McLauchlan, H., Newell, J., Morrice, N., Osborne, A., West, M., and Smythe, E. (1998). A novel role for Rab5-GDI in ligand sequestration into clathrin-coated pits. Current biology : CB *8*, 34-45.

McNew, J.A., Parlati, F., Fukuda, R., Johnston, R.J., Paz, K., Paumet, F., Sollner, T.H., and Rothman, J.E. (2000). Compartmental specificity of cellular membrane fusion encoded in SNARE proteins. Nature *407*, 153-159.

Merkwirth, C., Jovaisaite, V., Durieux, J., Matilainen, O., Jordan, S.D., Quiros, P.M., Steffen, K.K., Williams, E.G., Mouchiroud, L., Tronnes, S.U.*, et al.* (2016). Two Conserved Histone Demethylases Regulate Mitochondrial Stress-Induced Longevity. Cell *165*, 1209-1223.

Mhatre, S.D., Satyasi, V., Killen, M., Paddock, B.E., Moir, R.D., Saunders, A.J., and Marenda, D.R. (2014). Synaptic abnormalities in a Drosophila model of Alzheimer's disease. Dis Model Mech *7*, 373-385.

Micheva, K.D., Kay, B.K., and McPherson, P.S. (1997). Synaptojanin forms two separate complexes in the nerve terminal. Interactions with endophilin and amphiphysin. The Journal of biological chemistry *272*, 27239-27245.

Miesenbock, G., De Angelis, D.A., and Rothman, J.E. (1998). Visualizing secretion and synaptic transmission with pH-sensitive green fluorescent proteins. Nature *394*, 192-195.

Miller, S.E., Sahlender, D.A., Graham, S.C., Honing, S., Robinson, M.S., Peden, A.A., and Owen, D.J. (2011). The molecular basis for the endocytosis of small R-SNAREs by the clathrin adaptor CALM. Cell *147*, 1118-1131.

Milnerwood, A.J., Gladding, C.M., Pouladi, M.A., Kaufman, A.M., Hines, R.M., Boyd, J.D., Ko, R.W., Vasuta, O.C., Graham, R.K., Hayden, M.R.*, et al.* (2010). Early increase in extrasynaptic NMDA receptor signaling and expression contributes to phenotype onset in Huntington's

disease mice. Neuron *65*, 178-190.

Minami, S.S., Min, S.W., Krabbe, G., Wang, C., Zhou, Y., Asgarov, R., Li, Y., Martens, L.H., Elia, L.P., Ward, M.E.*, et al.* (2014). Progranulin protects against amyloid beta deposition and toxicity in Alzheimer's disease mouse models. Nature medicine *20*, 1157-1164.

Minnerly, J., Zhang, J., Parker, T., Kaul, T., and Jia, K. (2017). The cell non-autonomous function of ATG-18 is essential for neuroendocrine regulation of Caenorhabditis elegans lifespan. PLoS genetics *13*, e1006764.

Mitri, C., Parmentier, M.L., Pin, J.P., Bockaert, J., and Grau, Y. (2004). Divergent evolution in metabotropic glutamate receptors. A new receptor activated by an endogenous ligand different from glutamate in insects. The Journal of biological chemistry *279*, 9313-9320.

Miyagawa, T., Ebinuma, I., Morohashi, Y., Hori, Y., Young Chang, M., Hattori, H., Maehara, T., Yokoshima, S., Fukuyama, T., Tsuji, S.*, et al.* (2016). BIN1 regulates BACE1 intracellular trafficking and amyloid-beta production. Human molecular genetics *25*, 2948-2958.

Mizushima, N., Noda, T., Yoshimori, T., Tanaka, Y., Ishii, T., George, M.D., Klionsky, D.J., Ohsumi, M., and Ohsumi, Y. (1998). A protein conjugation system essential for autophagy. Nature *395*, 395-398.

Moore, S., Evans, L.D., Andersson, T., Portelius, E., Smith, J., Dias, T.B., Saurat, N., McGlade, A., Kirwan, P., Blennow, K.*, et al.* (2015). APP metabolism regulates tau proteostasis in human cerebral cortex neurons. Cell reports *11*, 689-696.

Moreau, K., Fleming, A., Imarisio, S., Lopez Ramirez, A., Mercer, J.L., Jimenez-Sanchez, M., Bento, C.F., Puri, C., Zavodszky, E., Siddiqi, F.*, et al.* (2014). PICALM modulates autophagy activity and tau accumulation. Nature communications *5*, 4998.

Mori, H., Kondo, J., and Ihara, Y. (1987). Ubiquitin is a component of paired helical filaments in Alzheimer's disease. Science *235*, 1641-1644.

Motley, A., Bright, N.A., Seaman, M.N., and Robinson, M.S. (2003). Clathrin-mediated

endocytosis in AP-2-depleted cells. The Journal of cell biology *162*, 909-918.

Mucke, L., Masliah, E., Yu, G.Q., Mallory, M., Rockenstein, E.M., Tatsuno, G., Hu, K., Kholodenko, D., Johnson-Wood, K., and McConlogue, L. (2000). High-level neuronal expression of abeta 1-42 in wild-type human amyloid protein precursor transgenic mice: synaptotoxicity without plaque formation. The Journal of neuroscience : the official journal of the Society for Neuroscience *20*, 4050-4058.

Muratore, C.R., Rice, H.C., Srikanth, P., Callahan, D.G., Shin, T., Benjamin, L.N., Walsh, D.M., Selkoe, D.J., and Young-Pearse, T.L. (2014). The familial Alzheimer's disease APPV717I mutation alters APP processing and Tau expression in iPSC-derived neurons. Human molecular genetics *23*, 3523-3536.

Muthukumar, A.K., Stork, T., and Freeman, M.R. (2014). Activity-dependent regulation of astrocyte GAT levels during synaptogenesis. Nature neuroscience *17*, 1340-1350.

Nagele, R.G., Wegiel, J., Venkataraman, V., Imaki, H., Wang, K.C., and Wegiel, J. (2004). Contribution of glial cells to the development of amyloid plaques in Alzheimer's disease. Neurobiology of aging *25*, 663-674.

Naj, A.C., Jun, G., Beecham, G.W., Wang, L.S., Vardarajan, B.N., Buros, J., Gallins, P.J., Buxbaum, J.D., Jarvik, G.P., Crane, P.K.*, et al.* (2011). Common variants at MS4A4/MS4A6E, CD2AP, CD33 and EPHA1 are associated with late-onset Alzheimer's disease. Nature genetics *43*, 436-441.

Namba, Y., Tomonaga, M., Kawasaki, H., Otomo, E., and Ikeda, K. (1991). Apolipoprotein E immunoreactivity in cerebral amyloid deposits and neurofibrillary tangles in Alzheimer's disease and kuru plaque amyloid in Creutzfeldt-Jakob disease. Brain Res *541*, 163-166.

Nathan, B.P., Bellosta, S., Sanan, D.A., Weisgraber, K.H., Mahley, R.W., and Pitas, R.E. (1994). Differential effects of apolipoproteins E3 and E4 on neuronal growth in vitro. Science *264*, 850-852.

Nelson, O., Tu, H., Lei, T., Bentahir, M., de Strooper, B., and Bezprozvanny, I. (2007). Familial Alzheimer disease-linked mutations specifically disrupt Ca2+ leak function of presenilin 1. The Journal of clinical investigation *117*, 1230-1239.

Nelson, R., Sawaya, M.R., Balbirnie, M., Madsen, A.O., Riekel, C., Grothe, R., and Eisenberg, D. (2005). Structure of the cross-beta spine of amyloid-like fibrils. Nature *435*, 773-778.

Nelson, R.E., Fessler, L.I., Takagi, Y., Blumberg, B., Keene, D.R., Olson, P.F., Parker, C.G., and Fessler, J.H. (1994). Peroxidasin: a novel enzyme-matrix protein of Drosophila development. The EMBO journal *13*, 3438-3447.

Nett, W.J., Oloff, S.H., and McCarthy, K.D. (2002). Hippocampal astrocytes in situ exhibit calcium oscillations that occur independent of neuronal activity. Journal of neurophysiology *87*, 528-537.

Neve, R.L., Harris, P., Kosik, K.S., Kurnit, D.M., and Donlon, T.A. (1986). Identification of cDNA clones for the human microtubule-associated protein tau and chromosomal localization of the genes for tau and microtubule-associated protein 2. Brain Res *387*, 271-280.

Ng, T.F., Lee, F.K., Song, Z.T., Calcutt, N.A., Lee, A.Y., Chung, S.S., and Chung, S.K. (1998). Effects of sorbitol dehydrogenase deficiency on nerve conduction in experimental diabetic mice. Diabetes *47*, 961-966.

Niccoli, T., Cabecinha, M., Tillmann, A., Kerr, F., Wong, C.T., Cardenes, D., Vincent, A.J., Bettedi, L., Li, L., Gronke, S*., et al.* (2016). Increased Glucose Transport into Neurons Rescues Abeta Toxicity in Drosophila. Current biology : CB *26*, 2550.

Niccoli, T., and Partridge, L. (2012). Ageing as a risk factor for disease. Current biology : CB *22*, R741-752.

Nikolaev, A., McLaughlin, T., O'Leary, D.D., and Tessier-Lavigne, M. (2009). APP binds DR6 to trigger axon pruning and neuron death via distinct caspases. Nature *457*, 981-989.

Nilsberth, C., Westlind-Danielsson, A., Eckman, C.B., Condron, M.M., Axelman, K., Forsell, C.,

Stenh, C., Luthman, J., Teplow, D.B., Younkin, S.G.*, et al.* (2001). The 'Arctic' APP mutation (E693G) causes Alzheimer's disease by enhanced Abeta protofibril formation. Nature neuroscience *4*, 887-893.

Nishimura, M., Yu, G., Levesque, G., Zhang, D.M., Ruel, L., Chen, F., Milman, P., Holmes, E., Liang, Y., Kawarai, T.*, et al.* (1999). Presenilin mutations associated with Alzheimer disease cause defective intracellular trafficking of beta-catenin, a component of the presenilin protein complex. Nature medicine *5*, 164-169.

Nusslein-Volhard, C., and Wieschaus, E. (1980). Mutations affecting segment number and polarity in Drosophila. Nature *287*, 795-801.

Nusslein-Volhard, C., Wieschaus, E., and Kluding, H. (1984). Mutations affecting the pattern of the larval cuticle inDrosophila melanogaster : I. Zygotic loci on the second chromosome. Wilhelm Roux's archives of developmental biology *193*, 267-282.

O'Rourke, E.J., Kuballa, P., Xavier, R., and Ruvkun, G. (2013). omega-6 Polyunsaturated fatty acids extend life span through the activation of autophagy. Genes & development *27*, 429-440.

Oakley, H., Cole, S.L., Logan, S., Maus, E., Shao, P., Craft, J., Guillozet-Bongaarts, A., Ohno, M., Disterhoft, J., Van Eldik, L.*, et al.* (2006). Intraneuronal beta-amyloid aggregates, neurodegeneration, and neuron loss in transgenic mice with five familial Alzheimer's disease mutations: potential factors in amyloid plaque formation. The Journal of neuroscience : the official journal of the Society for Neuroscience *26*, 10129-10140.

Obregon, D., Hou, H., Deng, J., Giunta, B., Tian, J., Darlington, D., Shahaduzzaman, M., Zhu, Y., Mori, T., Mattson, M.P.*, et al.* (2012). Soluble amyloid precursor protein-alpha modulates beta-secretase activity and amyloid-beta generation. Nature communications *3*, 777.

Obrosova, I.G., Fathallah, L., Lang, H.J., and Greene, D.A. (1999). Evaluation of a sorbitol dehydrogenase inhibitor on diabetic peripheral nerve metabolism: a prevention study. Diabetologia *42*, 1187-1194.

Oddo, S., Billings, L., Kesslak, J.P., Cribbs, D.H., and LaFerla, F.M. (2004). Abeta immunotherapy leads to clearance of early, but not late, hyperphosphorylated tau aggregates via the proteasome. Neuron *43*, 321-332.

Ohno, H., Stewart, J., Fournier, M.C., Bosshart, H., Rhee, I., Miyatake, S., Saito, T., Gallusser, A., Kirchhausen, T., and Bonifacino, J.S. (1995). Interaction of tyrosine-based sorting signals with clathrin-associated proteins. Science *269*, 1872-1875.

Okamoto, S., Pouladi, M.A., Talantova, M., Yao, D., Xia, P., Ehrnhoefer, D.E., Zaidi, R., Clemente, A., Kaul, M., Graham, R.K.*, et al.* (2009). Balance between synaptic versus extrasynaptic NMDA receptor activity influences inclusions and neurotoxicity of mutant huntingtin. Nature medicine *15*, 1407-1413.

Okochi, M., Tagami, S., Yanagida, K., Takami, M., Kodama, T.S., Mori, K., Nakayama, T., Ihara, Y., and Takeda, M. (2013). gamma-secretase modulators and presenilin 1 mutants act differently on presenilin/gamma-secretase function to cleave Abeta42 and Abeta43. Cell reports *3*, 42-51.

Oliet, S.H., Malenka, R.C., and Nicoll, R.A. (1997). Two distinct forms of long-term depression coexist in CA1 hippocampal pyramidal cells. Neuron *18*, 969-982.

Olivier, J.P., Raabe, T., Henkemeyer, M., Dickson, B., Mbamalu, G., Margolis, B., Schlessinger, J., Hafen, E., and Pawson, T. (1993). A Drosophila SH2-SH3 adaptor protein implicated in coupling the sevenless tyrosine kinase to an activator of Ras guanine nucleotide exchange, Sos. Cell *73*, 179-191.

Olsen, P.H., and Ambros, V. (1999). The lin-4 regulatory RNA controls developmental timing in Caenorhabditis elegans by blocking LIN-14 protein synthesis after the initiation of translation. Dev Biol *216*, 671-680.

Osorio, C., Sullivan, P.M., He, D.N., Mace, B.E., Ervin, J.F., Strittmatter, W.J., and Alzate, O. (2007). Mortalin is regulated by APOE in hippocampus of AD patients and by human APOE in TR mice. Neurobiology of aging *28*, 1853-1862.

Osterhout, J.A., Stafford, B.K., Nguyen, P.L., Yoshihara, Y., and Huberman, A.D. (2015). Contactin-4 mediates axon-target specificity and functional development of the accessory optic system. Neuron *86*, 985-999.

Osterwalder, T., Yoon, K.S., White, B.H., and Keshishian, H. (2001). A conditional tissue-specific transgene expression system using inducible GAL4. Proceedings of the National Academy of Sciences of the United States of America *98*, 12596-12601.

Owald, D., Felsenberg, J., Talbot, C.B., Das, G., Perisse, E., Huetteroth, W., and Waddell, S. (2015). Activity of defined mushroom body output neurons underlies learned olfactory behavior in Drosophila. Neuron *86*, 417-427.

Owe, S.G., Marcaggi, P., and Attwell, D. (2006). The ionic stoichiometry of the GLAST glutamate transporter in salamander retinal glia. The Journal of physiology *577*, 591-599.

Pai, T.P., Chen, C.C., Lin, H.H., Chin, A.L., Lai, J.S., Lee, P.T., Tully, T., and Chiang, A.S. (2013). Drosophila ORB protein in two mushroom body output neurons is necessary for long-term memory formation. Proceedings of the National Academy of Sciences of the United States of America *110*, 7898-7903.

Palmer, C.L., Lim, W., Hastie, P.G., Toward, M., Korolchuk, V.I., Burbidge, S.A., Banting, G., Collingridge, G.L., Isaac, J.T., and Henley, J.M. (2005). Hippocalcin functions as a calcium sensor in hippocampal LTD. Neuron *47*, 487-494.

Panatier, A., Vallee, J., Haber, M., Murai, K.K., Lacaille, J.C., and Robitaille, R. (2011). Astrocytes are endogenous regulators of basal transmission at central synapses. Cell *146*, 785-798.

Pant, S., Sharma, M., Patel, K., Caplan, S., Carr, C.M., and Grant, B.D. (2009). AMPH-1/Amphiphysin/Bin1 functions with RME-1/Ehd1 in endocytic recycling. Nature cell biology *11*, 1399-1410.

Parcon, P.A., Balasubramaniam, M., Ayyadevara, S., Jones, R.A., Liu, L., Shmookler Reis,

R.J., Barger, S.W., Mrak, R.E., and Griffin, W.S.T. (2017). Apolipoprotein E4 inhibits autophagy gene products through direct, specific binding to CLEAR motifs. Alzheimer's & dementia : the journal of the Alzheimer's Association.

Parikh, I., Fardo, D.W., and Estus, S. (2014). Genetics of PICALM expression and Alzheimer's disease. PloS one *9*, e91242.

Park, J., Al-Ramahi, I., Tan, Q., Mollema, N., Diaz-Garcia, J.R., Gallego-Flores, T., Lu, H.C., Lagalwar, S., Duvick, L., Kang, H.*, et al.* (2013). RAS-MAPK-MSK1 pathway modulates ataxin 1 protein levels and toxicity in SCA1. Nature *498*, 325-331.

Parker, J.A., Arango, M., Abderrahmane, S., Lambert, E., Tourette, C., Catoire, H., and Neri, C. (2005). Resveratrol rescues mutant polyglutamine cytotoxicity in nematode and mammalian neurons. Nature genetics *37*, 349-350.

Parmentier, M.L., Pin, J.P., Bockaert, J., and Grau, Y. (1996). Cloning and functional expression of a Drosophila metabotropic glutamate receptor expressed in the embryonic CNS. The Journal of neuroscience : the official journal of the Society for Neuroscience *16*, 6687-6694.

Parsons, C.G., Danysz, W., and Quack, G. (1999). Memantine is a clinically well tolerated N-methyl-D-aspartate (NMDA) receptor antagonist--a review of preclinical data. Neuropharmacology *38*, 735-767.

Parsons, R.G., Gafford, G.M., and Helmstetter, F.J. (2006). Translational control via the mammalian target of rapamycin pathway is critical for the formation and stability of long-term fear memory in amygdala neurons. The Journal of neuroscience : the official journal of the Society for Neuroscience *26*, 12977-12983.

Partridge, L., and Gems, D. (2007). Benchmarks for ageing studies. Nature *450*, 165-167.

Pascual, A., and Preat, T. (2001). Localization of long-term memory within the Drosophila mushroom body. Science *294*, 1115-1117.

Pasqualato, S., Renault, L., and Cherfils, J. (2002). Arf, Arl, Arp and Sar proteins: a family of GTP-binding proteins with a structural device for 'front-back' communication. EMBO reports *3*, 1035-1041.

Pearce, M.M., Spartz, E.J., Hong, W., Luo, L., and Kopito, R.R. (2015). Prion-like transmission of neuronal huntingtin aggregates to phagocytic glia in the Drosophila brain. Nature communications *6*, 6768.

Peineau, S., Nicolas, C.S., Bortolotto, Z.A., Bhat, R.V., Ryves, W.J., Harwood, A.J., Dournaud, P., Fitzjohn, S.M., and Collingridge, G.L. (2009). A systematic investigation of the protein kinases involved in NMDA receptor-dependent LTD: evidence for a role of GSK-3 but not other serine/threonine kinases. Molecular brain *2*, 22.

Perea, G., and Araque, A. (2005). Properties of synaptically evoked astrocyte calcium signal reveal synaptic information processing by astrocytes. The Journal of neuroscience : the official journal of the Society for Neuroscience *25*, 2192-2203.

Perisse, E., Yin, Y., Lin, A.C., Lin, S., Huetteroth, W., and Waddell, S. (2013). Different kenyon cell populations drive learned approach and avoidance in Drosophila. Neuron *79*, 945-956.

Perrimon, N., Lanjuin, A., Arnold, C., and Noll, E. (1996). Zygotic lethal mutations with maternal effect phenotypes in Drosophila melanogaster. II. Loci on the second and third chromosomes identified by P-element-induced mutations. Genetics *144*, 1681-1692.

Perry, E.K., Gibson, P.H., Blessed, G., Perry, R.H., and Tomlinson, B.E. (1977). Neurotransmitter enzyme abnormalities in senile dementia. Choline acetyltransferase and glutamic acid decarboxylase activities in necropsy brain tissue. J Neurol Sci *34*, 247-265.

Petersen, R.C., Smith, G.E., Ivnik, R.J., Tangalos, E.G., Schaid, D.J., Thibodeau, S.N., Kokmen, E., Waring, S.C., and Kurland, L.T. (1995). Apolipoprotein E status as a predictor of the development of Alzheimer's disease in memory-impaired individuals. Jama *273*, 1274-1278.

Petersen, S.A., Fetter, R.D., Noordermeer, J.N., Goodman, C.S., and DiAntonio, A. (1997). Genetic analysis of glutamate receptors in Drosophila reveals a retrograde signal regulating presynaptic transmitter release. Neuron *19*, 1237-1248.

Petrovski, S., Kury, S., Myers, C.T., Anyane-Yeboa, K., Cogne, B., Bialer, M., Xia, F., Hemati, P., Riviello, J., Mehaffey, M.*, et al.* (2016). Germline De Novo Mutations in GNB1 Cause Severe Neurodevelopmental Disability, Hypotonia, and Seizures. American journal of human genetics *98*, 1001-1010.

Pfrieger, F.W. (2003). Cholesterol homeostasis and function in neurons of the central nervous system. Cellular and molecular life sciences : CMLS *60*, 1158-1171.

Piaceri, I., Bagnoli, S., Lucenteforte, E., Mancuso, M., Tedde, A., Siciliano, G., Piacentini, S., Bracco, L., Sorbi, S., and Nacmias, B. (2011). Implication of a genetic variant at PICALM in Alzheimer's disease patients and centenarians. Journal of Alzheimer's disease : JAD *24*, 409-413.

Piao, X., Zhang, X., Wu, L., and Belasco, J.G. (2010). CCR4-NOT deadenylates mRNA associated with RNA-induced silencing complexes in human cells. Mol Cell Biol *30*, 1486-1494.

Piccini, A., Zanusso, G., Borghi, R., Noviello, C., Monaco, S., Russo, R., Damonte, G., Armirotti, A., Gelati, M., Giordano, R.*, et al.* (2007). Association of a presenilin 1 S170F mutation with a novel Alzheimer disease molecular phenotype. Arch Neurol *64*, 738-745.

Ping, Y., Hahm, E.T., Waro, G., Song, Q., Vo-Ba, D.A., Licursi, A., Bao, H., Ganoe, L., Finch, K., and Tsunoda, S. (2015). Linking abeta42-induced hyperexcitability to neurodegeneration, learning and motor deficits, and a shorter lifespan in an Alzheimer's model. PLoS genetics *11*, e1005025.

Pitman, J.L., Huetteroth, W., Burke, C.J., Krashes, M.J., Lai, S.L., Lee, T., and Waddell, S. (2011). A pair of inhibitory neurons are required to sustain labile memory in the Drosophila mushroom body. Current biology : CB *21*, 855-861.

Placais, P.Y., Trannoy, S., Friedrich, A.B., Tanimoto, H., and Preat, T. (2013). Two pairs of mushroom body efferent neurons are required for appetitive long-term memory retrieval in Drosophila. Cell reports *5*, 769-780.

Plucinska, K., Crouch, B., Koss, D., Robinson, L., Siebrecht, M., Riedel, G., and Platt, B. (2014). Knock-in of human BACE1 cleaves murine APP and reiterates Alzheimer-like phenotypes. The Journal of neuroscience : the official journal of the Society for Neuroscience *34*, 10710-10728.

Poirier, L., Shane, A., Zheng, J., and Seroude, L. (2008). Characterization of the Drosophila gene-switch system in aging studies: a cautionary tale. Aging cell *7*, 758-770.

Ponomareva, N.V., Andreeva, T.V., Protasova, M.S., Shagam, L.I., Malina, D.D., Goltsov, A.Y., Fokin, V.F., Illarioshkin, S.N., and Rogaev, E.I. (2017). Quantitative EEG during normal aging: association with the Alzheimer's disease genetic risk variant in PICALM gene. Neurobiology of aging *51*, 177 e171-177 e178.

Potter, C.J., Tasic, B., Russler, E.V., Liang, L., and Luo, L. (2010). The Q system: a repressible binary system for transgene expression, lineage tracing, and mosaic analysis. Cell *141*, 536-548.

Pryor, P.R., Jackson, L., Gray, S.R., Edeling, M.A., Thompson, A., Sanderson, C.M., Evans, P.R., Owen, D.J., and Luzio, J.P. (2008). Molecular basis for the sorting of the SNARE VAMP7 into endocytic clathrin-coated vesicles by the ArfGAP Hrb. Cell *134*, 817-827.

Qin, H., Cressy, M., Li, W., Coravos, J.S., Izzi, S.A., and Dubnau, J. (2012). Gamma neurons mediate dopaminergic input during aversive olfactory memory formation in Drosophila. Current biology : CB *22*, 608-614.

Raj, T., Shulman, J.M., Keenan, B.T., Chibnik, L.B., Evans, D.A., Bennett, D.A., Stranger, B.E., and De Jager, P.L. (2012). Alzheimer disease susceptibility loci: evidence for a protein network under natural selection. American journal of human genetics *90*, 720-726.

Rall, S.C., Jr., Weisgraber, K.H., Innerarity, T.L., and Mahley, R.W. (1982). Structural basis for receptor binding heterogeneity of apolipoprotein E from type III hyperlipoproteinemic subjects. Proceedings of the National Academy of Sciences of the United States of America *79*, 4696-4700.

Ramaker, J.M., Swanson, T.L., and Copenhaver, P.F. (2013). Amyloid precursor proteins interact with the heterotrimeric G protein Go in the control of neuronal migration. The Journal of neuroscience : the official journal of the Society for Neuroscience *33*, 10165-10181.

Ramakers, I.H., Visser, P.J., Aalten, P., Bekers, O., Sleegers, K., van Broeckhoven, C.L., Jolles, J., and Verhey, F.R. (2008). The association between APOE genotype and memory dysfunction in subjects with mild cognitive impairment is related to age and Alzheimer pathology. Dementia and geriatric cognitive disorders *26*, 101-108.

Ramjaun, A.R., and McPherson, P.S. (1998). Multiple amphiphysin II splice variants display differential clathrin binding: identification of two distinct clathrin-binding sites. Journal of neurochemistry *70*, 2369-2376.

Rapoport, I., Boll, W., Yu, A., Bocking, T., and Kirchhausen, T. (2008). A motif in the clathrin heavy chain required for the Hsc70/auxilin uncoating reaction. Molecular biology of the cell *19*, 405-413.

Rapoport, M., Dawson, H.N., Binder, L.I., Vitek, M.P., and Ferreira, A. (2002). Tau is essential to beta -amyloid-induced neurotoxicity. Proceedings of the National Academy of Sciences of the United States of America *99*, 6364-6369.

Rapp, A., Gmeiner, B., and Huttinger, M. (2006). Implication of apoE isoforms in cholesterol metabolism by primary rat hippocampal neurons and astrocytes. Biochimie *88*, 473-483.

Ravikumar, B., Vacher, C., Berger, Z., Davies, J.E., Luo, S., Oroz, L.G., Scaravilli, F., Easton, D.F., Duden, R., O'Kane, C.J.*, et al.* (2004). Inhibition of mTOR induces autophagy and reduces toxicity of polyglutamine expansions in fly and mouse models of Huntington disease. Nature genetics *36*, 585-595.

Razzaq, A., Robinson, I.M., McMahon, H.T., Skepper, J.N., Su, Y., Zelhof, A.C., Jackson, A.P., Gay, N.J., and O'Kane, C.J. (2001). Amphiphysin is necessary for organization of the excitation-contraction coupling machinery of muscles, but not for synaptic vesicle endocytosis in Drosophila. Genes & development *15*, 2967-2979.

Rea, S.L., Ventura, N., and Johnson, T.E. (2007). Relationship between mitochondrial electron transport chain dysfunction, development, and life extension in Caenorhabditis elegans. PLoS biology *5*, e259.

Rebeck, G.W., Reiter, J.S., Strickland, D.K., and Hyman, B.T. (1993). Apolipoprotein E in sporadic Alzheimer's disease: allelic variation and receptor interactions. Neuron *11*, 575-580.

Rehwinkel, J., Letunic, I., Raes, J., Bork, P., and Izaurralde, E. (2005). Nonsense-mediated mRNA decay factors act in concert to regulate common mRNA targets. RNA *11*, 1530-1544.

Reider, A., Barker, S.L., Mishra, S.K., Im, Y.J., Maldonado-Baez, L., Hurley, J.H., Traub, L.M., and Wendland, B. (2009). Syp1 is a conserved endocytic adaptor that contains domains involved in cargo selection and membrane tubulation. The EMBO journal *28*, 3103-3116.

Reinders, N.R., Pao, Y., Renner, M.C., da Silva-Matos, C.M., Lodder, T.R., Malinow, R., and Kessels, H.W. (2016). Amyloid-beta effects on synapses and memory require AMPA receptor subunit GluA3. Proceedings of the National Academy of Sciences of the United States of America *113*, E6526-E6534.

Reinhart, B.J., Slack, F.J., Basson, M., Pasquinelli, A.E., Bettinger, J.C., Rougvie, A.E., Horvitz, H.R., and Ruvkun, G. (2000). The 21-nucleotide let-7 RNA regulates developmental timing in Caenorhabditis elegans. Nature *403*, 901-906.

Rhein, V., Song, X., Wiesner, A., Ittner, L.M., Baysang, G., Meier, F., Ozmen, L., Bluethmann, H., Drose, S., Brandt, U.*, et al.* (2009). Amyloid-beta and tau synergistically impair the oxidative phosphorylation system in triple transgenic Alzheimer's disease mice. Proceedings of the National Academy of Sciences of the United States of America *106*, 20057-20062.

Riabinina, O., Luginbuhl, D., Marr, E., Liu, S., Wu, M.N., Luo, L., and Potter, C.J. (2015). Improved and expanded Q-system reagents for genetic manipulations. Nature methods *12*, 219-222, 215 p following 222.

Riemensperger, T., Voller, T., Stock, P., Buchner, E., and Fiala, A. (2005). Punishment prediction by dopaminergic neurons in Drosophila. Current biology : CB *15*, 1953-1960.

Rihel, J., Prober, D.A., Arvanites, A., Lam, K., Zimmerman, S., Jang, S., Haggarty, S.J., Kokel, D., Rubin, L.L., Peterson, R.T.*, et al.* (2010). Zebrafish behavioral profiling links drugs to biological targets and rest/wake regulation. Science *327*, 348-351.

Ring, S., Weyer, S.W., Kilian, S.B., Waldron, E., Pietrzik, C.U., Filippov, M.A., Herms, J., Buchholz, C., Eckman, C.B., Korte, M.*, et al.* (2007). The secreted beta-amyloid precursor protein ectodomain APPs alpha is sufficient to rescue the anatomical, behavioral, and electrophysiological abnormalities of APP-deficient mice. The Journal of neuroscience : the official journal of the Society for Neuroscience *27*, 7817-7826.

Rinholm, J.E., Hamilton, N.B., Kessaris, N., Richardson, W.D., Bergersen, L.H., and Attwell, D. (2011). Regulation of oligodendrocyte development and myelination by glucose and lactate. The Journal of neuroscience : the official journal of the Society for Neuroscience *31*, 538-548.

Rink, J., Ghigo, E., Kalaidzidis, Y., and Zerial, M. (2005). Rab conversion as a mechanism of progression from early to late endosomes. Cell *122*, 735-749.

Roberson, E.D., Scearce-Levie, K., Palop, J.J., Yan, F., Cheng, I.H., Wu, T., Gerstein, H., Yu, G.Q., and Mucke, L. (2007). Reducing endogenous tau ameliorates amyloid beta-induced deficits in an Alzheimer's disease mouse model. Science *316*, 750-754.

Rogers, I., Kerr, F., Martinez, P., Hardy, J., Lovestone, S., and Partridge, L. (2012). Ageing increases vulnerability to abeta42 toxicity in Drosophila. PloS one *7*, e40569.

Rogge, R.D., Karlovich, C.A., and Banerjee, U. (1991). Genetic dissection of a neurodevelopmental pathway: Son of sevenless functions downstream of the sevenless and

EGF receptor tyrosine kinases. Cell *64*, 39-48.

Rorth, P., Szabo, K., Bailey, A., Laverty, T., Rehm, J., Rubin, G.M., Weigmann, K., Milan, M., Benes, V., Ansorge, W.*, et al.* (1998). Systematic gain-of-function genetics in Drosophila. Development *125*, 1049-1057.

Rossano, A.J., Kato, A., Minard, K.I., Romero, M.F., and Macleod, G.T. (2017). Na(+) /H(+) exchange via the Drosophila vesicular glutamate transporter mediates activity-induced acid efflux from presynaptic terminals. J Physiol *595*, 805-824.

Rousseaux, M.W., de Haro, M., Lasagna-Reeves, C.A., De Maio, A., Park, J., Jafar-Nejad, P., Al-Ramahi, I., Sharma, A., See, L., Lu, N.*, et al.* (2016). TRIM28 regulates the nuclear accumulation and toxicity of both alpha-synuclein and tau. eLife *5*.

Roux, A., Uyhazi, K., Frost, A., and De Camilli, P. (2006). GTP-dependent twisting of dynamin implicates constriction and tension in membrane fission. Nature *441*, 528-531.

Rubino, M., Miaczynska, M., Lippe, R., and Zerial, M. (2000). Selective membrane recruitment of EEA1 suggests a role in directional transport of clathrin-coated vesicles to early endosomes. The Journal of biological chemistry *275*, 3745-3748.

Ryu, D., Mouchiroud, L., Andreux, P.A., Katsyuba, E., Moullan, N., Nicolet-Dit-Felix, A.A., Williams, E.G., Jha, P., Lo Sasso, G., Huzard, D.*, et al.* (2016). Urolithin A induces mitophagy and prolongs lifespan in C. elegans and increases muscle function in rodents. Nature medicine *22*, 879-888.

Saab, A.S., Tzvetavona, I.D., Trevisiol, A., Baltan, S., Dibaj, P., Kusch, K., Mobius, W., Goetze, B., Jahn, H.M., Huang, W.*, et al.* (2016). Oligodendroglial NMDA Receptors Regulate Glucose Import and Axonal Energy Metabolism. Neuron *91*, 119-132.

Saffarian, S., Cocucci, E., and Kirchhausen, T. (2009). Distinct dynamics of endocytic clathrin-coated pits and coated plaques. PLoS biology *7*, e1000191.

Saito, T., Matsuba, Y., Mihira, N., Takano, J., Nilsson, P., Itohara, S., Iwata, N., and Saido, T.C.

(2014). Single App knock-in mouse models of Alzheimer's disease. Nature neuroscience *17*, 661-663.

Sakae, N., Liu, C.C., Shinohara, M., Frisch-Daiello, J., Ma, L., Yamazaki, Y., Tachibana, M., Younkin, L., Kurti, A., Carrasquillo, M.M.*, et al.* (2016). ABCA7 Deficiency Accelerates Amyloid-beta Generation and Alzheimer's Neuronal Pathology. The Journal of neuroscience : the official journal of the Society for Neuroscience *36*, 3848-3859.

Sankaranarayanan, S., and Ryan, T.A. (2000). Real-time measurements of vesicle-SNARE recycling in synapses of the central nervous system. Nature cell biology *2*, 197-204.

Santacruz, K., Lewis, J., Spires, T., Paulson, J., Kotilinek, L., Ingelsson, M., Guimaraes, A., DeTure, M., Ramsden, M., McGowan, E.*, et al.* (2005). Tau suppression in a neurodegenerative mouse model improves memory function. Science *309*, 476-481.

Satoh, K., Abe-Dohmae, S., Yokoyama, S., St George-Hyslop, P., and Fraser, P.E. (2015). ATP-binding cassette transporter A7 (ABCA7) loss of function alters Alzheimer amyloid processing. The Journal of biological chemistry *290*, 24152-24165.

Saydoff, J.A., Olariu, A., Sheng, J., Hu, Z., Li, Q., Garcia, R., Pei, J., Sun, G.Y., and von Borstel, R. (2013). Uridine prodrug improves memory in Tg2576 and TAPP mice and reduces pathological factors associated with Alzheimer's disease in related models. Journal of Alzheimer's disease : JAD *36*, 637-657.

Sayer, J.A., Otto, E.A., O'Toole, J.F., Nurnberg, G., Kennedy, M.A., Becker, C., Hennies, H.C., Helou, J., Attanasio, M., Fausett, B.V.*, et al.* (2006). The centrosomal protein nephrocystin-6 is mutated in Joubert syndrome and activates transcription factor ATF4. Nature genetics *38*, 674-681.

Schafer, M.K., Varoqui, H., Defamie, N., Weihe, E., and Erickson, J.D. (2002). Molecular cloning and functional identification of mouse vesicular glutamate transporter 3 and its expression in subsets of novel excitatory neurons. The Journal of biological chemistry *277*, 50734-50748.

Scheele, U., Kalthoff, C., and Ungewickell, E. (2001). Multiple interactions of auxilin 1 with clathrin and the AP-2 adaptor complex. The Journal of biological chemistry *276*, 36131-36138.

Schicknick, H., Schott, B.H., Budinger, E., Smalla, K.H., Riedel, A., Seidenbecher, C.I., Scheich, H., Gundelfinger, E.D., and Tischmeyer, W. (2008). Dopaminergic modulation of auditory cortex-dependent memory consolidation through mTOR. Cerebral cortex *18*, 2646-2658.

Schlossman, D.M., Schmid, S.L., Braell, W.A., and Rothman, J.E. (1984). An enzyme that removes clathrin coats: purification of an uncoating ATPase. The Journal of cell biology *99*, 723-733.

Schmechel, D.E., Saunders, A.M., Strittmatter, W.J., Crain, B.J., Hulette, C.M., Joo, S.H., Pericak-Vance, M.A., Goldgaber, D., and Roses, A.D. (1993). Increased amyloid beta-peptide deposition in cerebral cortex as a consequence of apolipoprotein E genotype in late-onset Alzheimer disease. Proceedings of the National Academy of Sciences of the United States of America *90*, 9649-9653.

Schonberger, S.J., Edgar, P.F., Kydd, R., Faull, R.L., and Cooper, G.J. (2001). Proteomic analysis of the brain in Alzheimer's disease: molecular phenotype of a complex disease process. Proteomics *1*, 1519-1528.

Schroll, C., Riemensperger, T., Bucher, D., Ehmer, J., Voller, T., Erbguth, K., Gerber, B., Hendel, T., Nagel, G., Buchner, E.*, et al.* (2006). Light-induced activation of distinct modulatory neurons triggers appetitive or aversive learning in Drosophila larvae. Current biology : CB *16*, 1741-1747.

Schuster, C.M., Ultsch, A., Schloss, P., Cox, J.A., Schmitt, B., and Betz, H. (1991). Molecular cloning of an invertebrate glutamate receptor subunit expressed in Drosophila muscle. Science *254*, 112-114.

Schwabe, T., Bainton, R.J., Fetter, R.D., Heberlein, U., and Gaul, U. (2005). GPCR signaling is required for blood-brain barrier formation in drosophila. Cell *123*, 133-144.

Schwaerzel, M., Monastirioti, M., Scholz, H., Friggi-Grelin, F., Birman, S., and Heisenberg, M. (2003). Dopamine and octopamine differentiate between aversive and appetitive olfactory memories in Drosophila. The Journal of neuroscience : the official journal of the Society for Neuroscience *23*, 10495-10502.

Scotland, P.B., Heath, J.L., Conway, A.E., Porter, N.B., Armstrong, M.B., Walker, J.A., Klebig, M.L., Lavau, C.P., and Wechsler, D.S. (2012). The PICALM protein plays a key role in iron homeostasis and cell proliferation. PloS one *7*, e44252.

Seabrook, G.R., Smith, D.W., Bowery, B.J., Easter, A., Reynolds, T., Fitzjohn, S.M., Morton, R.A., Zheng, H., Dawson, G.R., Sirinathsinghji, D.J.*, et al.* (1999). Mechanisms contributing to the deficits in hippocampal synaptic plasticity in mice lacking amyloid precursor protein. Neuropharmacology *38*, 349-359.

Seggerson, K., Tang, L., and Moss, E.G. (2002). Two genetic circuits repress the Caenorhabditis elegans heterochronic gene lin-28 after translation initiation. Dev Biol *243*, 215-225.

Segovia, G., Del Arco, A., Prieto, L., and Mora, F. (2001). Glutamate-glutamine cycle and aging in striatum of the awake rat: effects of a glutamate transporter blocker. Neurochemical research *26*, 37-41.

Selkoe, D.J. (2002). Alzheimer's disease is a synaptic failure. Science *298*, 789-791.

Selkoe, D.J., and Podlisny, M.B. (2002). Deciphering the genetic basis of Alzheimer's disease. Annu Rev Genomics Hum Genet *3*, 67-99.

Seo, J., Giusti-Rodriguez, P., Zhou, Y., Rudenko, A., Cho, S., Ota, K.T., Park, C., Patzke, H., Madabhushi, R., Pan, L.*, et al.* (2014). Activity-dependent p25 generation regulates synaptic plasticity and Abeta-induced cognitive impairment. Cell *157*, 486-498.

Seshadri, S., Fitzpatrick, A.L., Ikram, M.A., DeStefano, A.L., Gudnason, V., Boada, M., Bis, J.C., Smith, A.V., Carassquillo, M.M., Lambert, J.C.*, et al.* (2010). Genome-wide analysis of

genetic loci associated with Alzheimer disease. Jama *303*, 1832-1840.

Seubert, P., Vigo-Pelfrey, C., Esch, F., Lee, M., Dovey, H., Davis, D., Sinha, S., Schlossmacher, M., Whaley, J., Swindlehurst, C.*, et al.* (1992). Isolation and quantification of soluble Alzheimer's beta-peptide from biological fluids. Nature *359*, 325-327.

Shankar, G.M., Bloodgood, B.L., Townsend, M., Walsh, D.M., Selkoe, D.J., and Sabatini, B.L. (2007). Natural oligomers of the Alzheimer amyloid-beta protein induce reversible synapse loss by modulating an NMDA-type glutamate receptor-dependent signaling pathway. The Journal of neuroscience : the official journal of the Society for Neuroscience *27*, 2866-2875.

Sherrington, R., Rogaev, E.I., Liang, Y., Rogaeva, E.A., Levesque, G., Ikeda, M., Chi, H., Lin, C., Li, G., Holman, K.*, et al.* (1995). Cloning of a gene bearing missense mutations in early-onset familial Alzheimer's disease. Nature *375*, 754-760.

Shi, Y., Kirwan, P., Smith, J., MacLean, G., Orkin, S.H., and Livesey, F.J. (2012). A human stem cell model of early Alzheimer's disease pathology in Down syndrome. Sci Transl Med *4*, 124ra129.

Shi, Y., Yamada, K., Liddelow, S.A., Smith, S.T., Zhao, L., Luo, W., Tsai, R.M., Spina, S., Grinberg, L.T., Rojas, J.C.*, et al.* (2017). ApoE4 markedly exacerbates tau-mediated neurodegeneration in a mouse model of tauopathy. Nature *549*, 523-527.

Shin, R.W., Iwaki, T., Kitamoto, T., and Tateishi, J. (1991a). Hydrated autoclave pretreatment enhances tau immunoreactivity in formalin-fixed normal and Alzheimer's disease brain tissues. Lab Invest *64*, 693-702.

Shin, R.W., Kitamoto, T., and Tateishi, J. (1991b). Modified tau is present in younger nondemented persons: a study of subcortical nuclei in Alzheimer's disease and progressive supranuclear palsy. Acta neuropathologica *81*, 517-523.

Shuai, Y., Lu, B., Hu, Y., Wang, L., Sun, K., and Zhong, Y. (2010). Forgetting is regulated through Rac activity in Drosophila. Cell *140*, 579-589.

Sigrist, S.J., Thiel, P.R., Reiff, D.F., and Schuster, C.M. (2002). The postsynaptic glutamate receptor subunit DGluR-IIA mediates long-term plasticity in Drosophila. The Journal of neuroscience : the official journal of the Society for Neuroscience *22*, 7362-7372.

Simpson, J.E., Ince, P.G., Lace, G., Forster, G., Shaw, P.J., Matthews, F., Savva, G., Brayne, C., Wharton, S.B., Function, M.R.C.C.*, et al.* (2010). Astrocyte phenotype in relation to Alzheimer-type pathology in the ageing brain. Neurobiology of aging *31*, 578-590.

Singleton, A., and Hardy, J. (2016). The Evolution of Genetics: Alzheimer's and Parkinson's Diseases. Neuron *90*, 1154-1163.

Sisodia, S.S. (1992). Beta-amyloid precursor protein cleavage by a membrane-bound protease. Proceedings of the National Academy of Sciences of the United States of America *89*, 6075-6079.

Sizova, D., Charbaut, E., Delalande, F., Poirier, F., High, A.A., Parker, F., Van Dorsselaer, A., Duchesne, M., and Diu-Hercend, A. (2007). Proteomic analysis of brain tissue from an Alzheimer's disease mouse model by two-dimensional difference gel electrophoresis. Neurobiology of aging *28*, 357-370.

Skovronsky, D.M., Doms, R.W., and Lee, V.M. (1998). Detection of a novel intraneuronal pool of insoluble amyloid beta protein that accumulates with time in culture. J Cell Biol *141*, 1031-1039.

Slepnev, V.I., Ochoa, G.C., Butler, M.H., and De Camilli, P. (2000). Tandem arrangement of the clathrin and AP-2 binding domains in amphiphysin 1 and disruption of clathrin coat function by amphiphysin fragments comprising these sites. The Journal of biological chemistry *275*, 17583-17589.

Smith, G.E., Bohac, D.L., Waring, S.C., Kokmen, E., Tangalos, E.G., Ivnik, R.J., and Petersen, R.C. (1998). Apolipoprotein E genotype influences cognitive 'phenotype' in patients with Alzheimer's disease but not in healthy control subjects. Neurology *50*, 355-362.

Snyder, E.M., Nong, Y., Almeida, C.G., Paul, S., Moran, T., Choi, E.Y., Nairn, A.C., Salter, M.W., Lombroso, P.J., Gouras, G.K.*, et al.* (2005). Regulation of NMDA receptor trafficking by amyloid-beta. Nature neuroscience *8*, 1051-1058.

Soda, K., Dobashi, Y., Kano, Y., Tsujinaka, S., and Konishi, F. (2009). Polyamine-rich food decreases age-associated pathology and mortality in aged mice. Experimental gerontology *44*, 727-732.

Sofola, O., Kerr, F., Rogers, I., Killick, R., Augustin, H., Gandy, C., Allen, M.J., Hardy, J., Lovestone, S., and Partridge, L. (2010). Inhibition of GSK-3 ameliorates Abeta pathology in an adult-onset Drosophila model of Alzheimer's disease. PLoS genetics *6*, e1001087.

Sofroniew, M.V. (2015). Astrocyte barriers to neurotoxic inflammation. Nature reviews Neuroscience *16*, 249-263.

Sofroniew, M.V., and Vinters, H.V. (2010). Astrocytes: biology and pathology. Acta neuropathologica *119*, 7-35.

Sollvander, S., Nikitidou, E., Brolin, R., Soderberg, L., Sehlin, D., Lannfelt, L., and Erlandsson, A. (2016). Accumulation of amyloid-beta by astrocytes result in enlarged endosomes and microvesicle-induced apoptosis of neurons. Mol Neurodegener *11*, 38.

Sonnichsen, B., De Renzis, S., Nielsen, E., Rietdorf, J., and Zerial, M. (2000). Distinct membrane domains on endosomes in the recycling pathway visualized by multicolor imaging of Rab4, Rab5, and Rab11. The Journal of cell biology *149*, 901-914.

Spilman, P., Podlutskaya, N., Hart, M.J., Debnath, J., Gorostiza, O., Bredesen, D., Richardson, A., Strong, R., and Galvan, V. (2010). Inhibition of mTOR by rapamycin abolishes cognitive deficits and reduces amyloid-beta levels in a mouse model of Alzheimer's disease. PloS one *5*, e9979.

Spradling, A.C., Stern, D., Beaton, A., Rhem, E.J., Laverty, T., Mozden, N., Misra, S., and Rubin, G.M. (1999). The Berkeley Drosophila Genome Project gene disruption project: Single

P-element insertions mutating 25% of vital Drosophila genes. Genetics *153*, 135-177.

Stallcup, W.B., Bulloch, K., and Baetge, E.E. (1979). Coupled transport of glutamate and sodium in a cerebellar nerve cell line. Journal of neurochemistry *32*, 57-65.

Steinbach, J.P., Muller, U., Leist, M., Li, Z.W., Nicotera, P., and Aguzzi, A. (1998). Hypersensitivity to seizures in beta-amyloid precursor protein deficient mice. Cell death and differentiation *5*, 858-866.

Steiner, H., Duff, K., Capell, A., Romig, H., Grim, M.G., Lincoln, S., Hardy, J., Yu, X., Picciano, M., Fechteler, K.*, et al.* (1999a). A loss of function mutation of presenilin-2 interferes with amyloid beta-peptide production and notch signaling. The Journal of biological chemistry *274*, 28669-28673.

Steiner, H., Romig, H., Grim, M.G., Philipp, U., Pesold, B., Citron, M., Baumeister, R., and Haass, C. (1999b). The biological and pathological function of the presenilin-1 Deltaexon 9 mutation is independent of its defect to undergo proteolytic processing. The Journal of biological chemistry *274*, 7615-7618.

Stenmark, P., Grunler, J., Mattsson, J., Sindelar, P.J., Nordlund, P., and Berthold, D.A. (2001). A new member of the family of di-iron carboxylate proteins. Coq7 (clk-1), a membrane-bound hydroxylase involved in ubiquinone biosynthesis. The Journal of biological chemistry *276*, 33297-33300.

Stimpson, H.E., Toret, C.P., Cheng, A.T., Pauly, B.S., and Drubin, D.G. (2009). Early-arriving Syp1p and Ede1p function in endocytic site placement and formation in budding yeast. Molecular biology of the cell *20*, 4640-4651.

Stork, T., Engelen, D., Krudewig, A., Silies, M., Bainton, R.J., and Klambt, C. (2008). Organization and function of the blood-brain barrier in Drosophila. The Journal of neuroscience : the official journal of the Society for Neuroscience *28*, 587-597.

Stork, T., Sheehan, A., Tasdemir-Yilmaz, O.E., and Freeman, M.R. (2014). Neuron-glia

interactions through the Heartless FGF receptor signaling pathway mediate morphogenesis of Drosophila astrocytes. Neuron *83*, 388-403.

Stowell, M.H., Marks, B., Wigge, P., and McMahon, H.T. (1999). Nucleotide-dependent conformational changes in dynamin: evidence for a mechanochemical molecular spring. Nature cell biology *1*, 27-32.

Strittmatter, W.J., Saunders, A.M., Schmechel, D., Pericak-Vance, M., Enghild, J., Salvesen, G.S., and Roses, A.D. (1993). Apolipoprotein E: high-avidity binding to beta-amyloid and increased frequency of type 4 allele in late-onset familial Alzheimer disease. Proceedings of the National Academy of Sciences of the United States of America *90*, 1977-1981.

Suberbielle, E., Djukic, B., Evans, M., Kim, D.H., Taneja, P., Wang, X., Finucane, M., Knox, J., Ho, K., Devidze, N.*, et al.* (2015). DNA repair factor BRCA1 depletion occurs in Alzheimer brains and impairs cognitive function in mice. Nature communications *6*, 8897.

Suberbielle, E., Sanchez, P.E., Kravitz, A.V., Wang, X., Ho, K., Eilertson, K., Devidze, N., Kreitzer, A.C., and Mucke, L. (2013). Physiologic brain activity causes DNA double-strand breaks in neurons, with exacerbation by amyloid-beta. Nature neuroscience *16*, 613-621.

Suhs, K.W., Fairless, R., Williams, S.K., Heine, K., Cavalie, A., and Diem, R. (2014). N-methyl-D-aspartate receptor blockade is neuroprotective in experimental autoimmune optic neuritis. Journal of neuropathology and experimental neurology *73*, 507-518.

Sundborger, A., Soderblom, C., Vorontsova, O., Evergren, E., Hinshaw, J.E., and Shupliakov, O. (2011). An endophilin-dynamin complex promotes budding of clathrin-coated vesicles during synaptic vesicle recycling. Journal of cell science *124*, 133-143.

Sweitzer, S.M., and Hinshaw, J.E. (1998). Dynamin undergoes a GTP-dependent conformational change causing vesiculation. Cell *93*, 1021-1029.

Sydow, A., Van der Jeugd, A., Zheng, F., Ahmed, T., Balschun, D., Petrova, O., Drexler, D., Zhou, L., Rune, G., Mandelkow, E.*, et al.* (2011). Tau-induced defects in synaptic plasticity,

learning, and memory are reversible in transgenic mice after switching off the toxic Tau mutant. The Journal of neuroscience : the official journal of the Society for Neuroscience *31*, 2511-2525.

Szatkowski, M., Barbour, B., and Attwell, D. (1990). Non-vesicular release of glutamate from glial cells by reversed electrogenic glutamate uptake. Nature *348*, 443-446.

Takasugi, N., Tomita, T., Hayashi, I., Tsuruoka, M., Niimura, M., Takahashi, Y., Thinakaran, G., and Iwatsubo, T. (2003). The role of presenilin cofactors in the gamma-secretase complex. Nature *422*, 438-441.

Takei, K., Slepnev, V.I., Haucke, V., and De Camilli, P. (1999). Functional partnership between amphiphysin and dynamin in clathrin-mediated endocytosis. Nature cell biology *1*, 33-39.

Talantova, M., Sanz-Blasco, S., Zhang, X., Xia, P., Akhtar, M.W., Okamoto, S., Dziewczapolski, G., Nakamura, T., Cao, G., Pratt, A.E.*, et al.* (2013). Abeta induces astrocytic glutamate release, extrasynaptic NMDA receptor activation, and synaptic loss. Proceedings of the National Academy of Sciences of the United States of America *110*, E2518-2527.

Tanzi, R.E., and Bertram, L. (2005). Twenty years of the Alzheimer's disease amyloid hypothesis: a genetic perspective. Cell *120*, 545-555.

Tardiff, D.F., Jui, N.T., Khurana, V., Tambe, M.A., Thompson, M.L., Chung, C.Y., Kamadurai, H.B., Kim, H.T., Lancaster, A.K., Caldwell, K.A.*, et al.* (2013). Yeast reveal a "druggable" Rsp5/Nedd4 network that ameliorates alpha-synuclein toxicity in neurons. Science *342*, 979-983.

Tasdemir-Yilmaz, O.E., and Freeman, M.R. (2014). Astrocytes engage unique molecular programs to engulf pruned neuronal debris from distinct subsets of neurons. Genes & development *28*, 20-33.

Taylor, M.J., Perrais, D., and Merrifield, C.J. (2011). A high precision survey of the molecular dynamics of mammalian clathrin-mediated endocytosis. PLoS biology *9*, e1000604.

Tcherkezian, J., Cargnello, M., Romeo, Y., Huttlin, E.L., Lavoie, G., Gygi, S.P., and Roux, P.P. (2014). Proteomic analysis of cap-dependent translation identifies LARP1 as a key regulator of 5'TOP mRNA translation. Genes & development *28*, 357-371.

Tebar, F., Bohlander, S.K., and Sorkin, A. (1999). Clathrin assembly lymphoid myeloid leukemia (CALM) protein: localization in endocytic-coated pits, interactions with clathrin, and the impact of overexpression on clathrin-mediated traffic. Molecular biology of the cell *10*, 2687-2702.

Tebar, F., Sorkina, T., Sorkin, A., Ericsson, M., and Kirchhausen, T. (1996). Eps15 is a component of clathrin-coated pits and vesicles and is located at the rim of coated pits. The Journal of biological chemistry *271*, 28727-28730.

Terashima, A., Pelkey, K.A., Rah, J.C., Suh, Y.H., Roche, K.W., Collingridge, G.L., McBain, C.J., and Isaac, J.T. (2008). An essential role for PICK1 in NMDA receptor-dependent bidirectional synaptic plasticity. Neuron *57*, 872-882.

Terwel, D., Muyllaert, D., Dewachter, I., Borghgraef, P., Croes, S., Devijver, H., and Van Leuven, F. (2008). Amyloid activates GSK-3beta to aggravate neuronal tauopathy in bigenic mice. Am J Pathol *172*, 786-798.

Thal, D.R., Schultz, C., Dehghani, F., Yamaguchi, H., Braak, H., and Braak, E. (2000). Amyloid beta-protein (Abeta)-containing astrocytes are located preferentially near N-terminal-truncated Abeta deposits in the human entorhinal cortex. Acta neuropathologica *100*, 608-617.

Thinakaran, G., Harris, C.L., Ratovitski, T., Davenport, F., Slunt, H.H., Price, D.L., Borchelt, D.R., and Sisodia, S.S. (1997). Evidence that levels of presenilins (PS1 and PS2) are coordinately regulated by competition for limiting cellular factors. The Journal of biological chemistry *272*, 28415-28422.

Thinakaran, G., Regard, J.B., Bouton, C.M., Harris, C.L., Price, D.L., Borchelt, D.R., and Sisodia, S.S. (1998). Stable association of presenilin derivatives and absence of presenilin interactions with APP. Neurobiol Dis *4*, 438-453.

Tian, H., Davidowitz, E., Lopez, P., Emadi, S., Moe, J., and Sierks, M. (2013a). Trimeric tau is toxic to human neuronal cells at low nanomolar concentrations. Int J Cell Biol *2013*, 260787.

Tian, Y., Chang, J.C., Fan, E.Y., Flajolet, M., and Greengard, P. (2013b). Adaptor complex AP2/PICALM, through interaction with LC3, targets Alzheimer's APP-CTF for terminal degradation via autophagy. Proceedings of the National Academy of Sciences of the United States of America *110*, 17071-17076.

Tien, N.T., Karaca, I., Tamboli, I.Y., and Walter, J. (2016). Trehalose Alters Subcellular Trafficking and the Metabolism of the Alzheimer-associated Amyloid Precursor Protein. The Journal of biological chemistry *291*, 10528-10540.

Tilton, R.G., Chang, K., Nyengaard, J.R., Van den Enden, M., Ido, Y., and Williamson, J.R. (1995). Inhibition of sorbitol dehydrogenase. Effects on vascular and neural dysfunction in streptozocin-induced diabetic rats. Diabetes *44*, 234-242.

Tracy, T.E., Sohn, P.D., Minami, S.S., Wang, C., Min, S.W., Li, Y., Zhou, Y., Le, D., Lo, I., Ponnusamy, R.*, et al.* (2016). Acetylated Tau Obstructs KIBRA-Mediated Signaling in Synaptic Plasticity and Promotes Tauopathy-Related Memory Loss. Neuron *90*, 245-260.

Treusch, S., Hamamichi, S., Goodman, J.L., Matlack, K.E., Chung, C.Y., Baru, V., Shulman, J.M., Parrado, A., Bevis, B.J., Valastyan, J.S.*, et al.* (2011). Functional links between Abeta toxicity, endocytic trafficking, and Alzheimer's disease risk factors in yeast. Science *334*, 1241-1245.

Tsubuki, S., Takaki, Y., and Saido, T.C. (2003). Dutch, Flemish, Italian, and Arctic mutations of APP and resistance of Abeta to physiologically relevant proteolytic degradation. Lancet *361*, 1957-1958.

Tu, H., Nelson, O., Bezprozvanny, A., Wang, Z., Lee, S.F., Hao, Y.H., Serneels, L., De Strooper, B., Yu, G., and Bezprozvanny, I. (2006). Presenilins form ER Ca2+ leak channels, a function disrupted by familial Alzheimer's disease-linked mutations. Cell *126*, 981-993.

Tufi, R., Gandhi, S., de Castro, I.P., Lehmann, S., Angelova, P.R., Dinsdale, D., Deas, E., Plun-Favreau, H., Nicotera, P., Abramov, A.Y.*, et al.* (2014). Enhancing nucleotide metabolism protects against mitochondrial dysfunction and neurodegeneration in a PINK1 model of Parkinson's disease. Nature cell biology *16*, 157-166.

Tully, T., Preat, T., Boynton, S.C., and Del Vecchio, M. (1994). Genetic dissection of consolidated memory in Drosophila. Cell *79*, 35-47.

Turner, G.C., Bazhenov, M., and Laurent, G. (2008). Olfactory representations by Drosophila mushroom body neurons. Journal of neurophysiology *99*, 734-746.

Tzingounis, A.V., and Wadiche, J.I. (2007). Glutamate transporters: confining runaway excitation by shaping synaptic transmission. Nature reviews Neuroscience *8*, 935-947.

Ubelmann, F., Burrinha, T., Salavessa, L., Gomes, R., Ferreira, C., Moreno, N., and Guimas Almeida, C. (2017). Bin1 and CD2AP polarise the endocytic generation of beta-amyloid. EMBO reports *18*, 102-122.

Ulland, T.K., Song, W.M., Huang, S.C., Ulrich, J.D., Sergushichev, A., Beatty, W.L., Loboda, A.A., Zhou, Y., Cairns, N.J., Kambal, A.*, et al.* (2017). TREM2 Maintains Microglial Metabolic Fitness in Alzheimer's Disease. Cell *170*, 649-663 e613.

Ultsch, A., Schuster, C.M., Laube, B., Betz, H., and Schmitt, B. (1993). Glutamate receptors of Drosophila melanogaster. Primary structure of a putative NMDA receptor protein expressed in the head of the adult fly. FEBS letters *324*, 171-177.

Ultsch, A., Schuster, C.M., Laube, B., Schloss, P., Schmitt, B., and Betz, H. (1992). Glutamate receptors of Drosophila melanogaster: cloning of a kainate-selective subunit expressed in the central nervous system. Proceedings of the National Academy of Sciences of the United States of America *89*, 10484-10488.

Um, J.W., Kaufman, A.C., Kostylev, M., Heiss, J.K., Stagi, M., Takahashi, H., Kerrisk, M.E., Vortmeyer, A., Wisniewski, T., Koleske, A.J.*, et al.* (2013). Metabotropic glutamate receptor 5 is

a coreceptor for Alzheimer abeta oligomer bound to cellular prion protein. Neuron *79*, 887-902.

Um, J.W., Nygaard, H.B., Heiss, J.K., Kostylev, M.A., Stagi, M., Vortmeyer, A., Wisniewski, T., Gunther, E.C., and Strittmatter, S.M. (2012). Alzheimer amyloid-beta oligomer bound to postsynaptic prion protein activates Fyn to impair neurons. Nature neuroscience *15*, 1227-1235.

Uttner, I., Kirchheiner, J., Tumani, H., Mottaghy, F.M., Lebedeva, E., Ozer, E., Ludolph, A.C., Huber, R., and von Arnim, C.A. (2010). A novel presenilin1 mutation (Q223R) associated with early onset Alzheimer's disease, dysarthria and spastic paraparesis and decreased Abeta levels in CSF. European journal of neurology *17*, 631-633.

Vajo, Z., King, L.M., Jonassen, T., Wilkin, D.J., Ho, N., Munnich, A., Clarke, C.F., and Francomano, C.A. (1999). Conservation of the Caenorhabditis elegans timing gene clk-1 from yeast to human: a gene required for ubiquinone biosynthesis with potential implications for aging. Mammalian genome : official journal of the International Mammalian Genome Society *10*, 1000-1004.

Valente, E.M., Silhavy, J.L., Brancati, F., Barrano, G., Krishnaswami, S.R., Castori, M., Lancaster, M.A., Boltshauser, E., Boccone, L., Al-Gazali, L.*, et al.* (2006). Mutations in CEP290, which encodes a centrosomal protein, cause pleiotropic forms of Joubert syndrome. Nature genetics *38*, 623-625.

van der Bliek, A.M., Redelmeier, T.E., Damke, H., Tisdale, E.J., Meyerowitz, E.M., and Schmid, S.L. (1993). Mutations in human dynamin block an intermediate stage in coated vesicle formation. The Journal of cell biology *122*, 553-563.

Van der Jeugd, A., Hochgrafe, K., Ahmed, T., Decker, J.M., Sydow, A., Hofmann, A., Wu, D., Messing, L., Balschun, D., D'Hooge, R.*, et al.* (2012). Cognitive defects are reversible in inducible mice expressing pro-aggregant full-length human Tau. Acta Neuropathol *123*, 787-805.

Vanlandingham, P.A., Barmchi, M.P., Royer, S., Green, R., Bao, H., Reist, N., and Zhang, B.

(2014). AP180 couples protein retrieval to clathrin-mediated endocytosis of synaptic vesicles. Traffic *15*, 433-450.

Veinbergs, I., Mallory, M., Mante, M., Rockenstein, E., Gilbert, J.R., and Masliah, E. (1999). Differential neurotrophic effects of apolipoprotein E in aged transgenic mice. Neuroscience letters *265*, 218-222.

Ventimiglia, D., and Bargmann, C.I. (2017). Diverse modes of synaptic signaling, regulation, and plasticity distinguish two classes of C. elegans glutamatergic neurons. eLife *6*.

Verbich, D., Prenosil, G.A., Chang, P.K., Murai, K.K., and McKinney, R.A. (2012). Glial glutamate transport modulates dendritic spine head protrusions in the hippocampus. Glia *60*, 1067-1077.

Verma, P., Augustine, G.J., Ammar, M.R., Tashiro, A., and Cohen, S.M. (2015). A neuroprotective role for microRNA miR-1000 mediated by limiting glutamate excitotoxicity. Nature neuroscience *18*, 379-385.

Vilchez, D., Morantte, I., Liu, Z., Douglas, P.M., Merkwirth, C., Rodrigues, A.P., Manning, G., and Dillin, A. (2012). RPN-6 determines C. elegans longevity under proteotoxic stress conditions. Nature *489*, 263-268.

Vilhjalmsson, B.J., and Nordborg, M. (2013). The nature of confounding in genome-wide association studies. Nature reviews Genetics *14*, 1-2.

Vinatier, J., Herzog, E., Plamont, M.A., Wojcik, S.M., Schmidt, A., Brose, N., Daviet, L., El Mestikawy, S., and Giros, B. (2006). Interaction between the vesicular glutamate transporter type 1 and endophilin A1, a protein essential for endocytosis. Journal of neurochemistry *97*, 1111-1125.

Volkner, M., Lenz-Bohme, B., Betz, H., and Schmitt, B. (2000). Novel CNS glutamate receptor subunit genes of Drosophila melanogaster. Journal of neurochemistry *75*, 1791-1799.

Vossel, K.A., Zhang, K., Brodbeck, J., Daub, A.C., Sharma, P., Finkbeiner, S., Cui, B., and

Mucke, L. (2010). Tau reduction prevents Abeta-induced defects in axonal transport. Science *330*, 198.

Waddell, S., Armstrong, J.D., Kitamoto, T., Kaiser, K., and Quinn, W.G. (2000). The amnesiac gene product is expressed in two neurons in the Drosophila brain that are critical for memory. Cell *103*, 805-813.

Wadiche, J.I., Arriza, J.L., Amara, S.G., and Kavanaugh, M.P. (1995). Kinetics of a human glutamate transporter. Neuron *14*, 1019-1027.

Walsh, D.M., and Selkoe, D.J. (2007). A beta oligomers - a decade of discovery. Journal of neurochemistry *101*, 1172-1184.

Walter, J., Capell, A., Grunberg, J., Pesold, B., Schindzielorz, A., Prior, R., Podlisny, M.B., Fraser, P., Hyslop, P.S., Selkoe, D.J.*, et al.* (1996). The Alzheimer's disease-associated presenilins are differentially phosphorylated proteins located predominantly within the endoplasmic reticulum. Mol Med *2*, 673-691.

Wang, B., Wang, Z., Sun, L., Yang, L., Li, H., Cole, A.L., Rodriguez-Rivera, J., Lu, H.C., and Zheng, H. (2014). The amyloid precursor protein controls adult hippocampal neurogenesis through GABAergic interneurons. The Journal of neuroscience : the official journal of the Society for Neuroscience *34*, 13314-13325.

Wang, H.Y., Lee, D.H., Davis, C.B., and Shank, R.P. (2000). Amyloid peptide Abeta(1-42) binds selectively and with picomolar affinity to alpha7 nicotinic acetylcholine receptors. Journal of neurochemistry *75*, 1155-1161.

Wang, H.Y., Li, W., Benedetti, N.J., and Lee, D.H. (2003). Alpha 7 nicotinic acetylcholine receptors mediate beta-amyloid peptide-induced tau protein phosphorylation. The Journal of biological chemistry *278*, 31547-31553.

Wang, J., Dickson, D.W., Trojanowski, J.Q., and Lee, V.M. (1999). The levels of soluble versus insoluble brain Abeta distinguish Alzheimer's disease from normal and pathologic aging.

Experimental neurology *158*, 328-337.

Wang, L., Chiang, H.C., Wu, W., Liang, B., Xie, Z., Yao, X., Ma, W., Du, S., and Zhong, Y. (2012). Epidermal growth factor receptor is a preferred target for treating amyloid-beta-induced memory loss. Proceedings of the National Academy of Sciences of the United States of America *109*, 16743-16748.

Wang, R., and Zhang, D. (2005). Memantine prolongs survival in an amyotrophic lateral sclerosis mouse model. The European journal of neuroscience *22*, 2376-2380.

Wang, X., Lou, N., Xu, Q., Tian, G.F., Peng, W.G., Han, X., Kang, J., Takano, T., and Nedergaard, M. (2006). Astrocytic Ca2+ signaling evoked by sensory stimulation in vivo. Nature neuroscience *9*, 816-823.

Wang, X., Su, B., Lee, H.G., Li, X., Perry, G., Smith, M.A., and Zhu, X. (2009a). Impaired balance of mitochondrial fission and fusion in Alzheimer's disease. The Journal of neuroscience : the official journal of the Society for Neuroscience *29*, 9090-9103.

Wang, Y., Cella, M., Mallinson, K., Ulrich, J.D., Young, K.L., Robinette, M.L., Gilfillan, S., Krishnan, G.M., Sudhakar, S., Zinselmeyer, B.H.*, et al.* (2015). TREM2 lipid sensing sustains the microglial response in an Alzheimer's disease model. Cell *160*, 1061-1071.

Wang, Y., Mamiya, A., Chiang, A.S., and Zhong, Y. (2008). Imaging of an early memory trace in the Drosophila mushroom body. The Journal of neuroscience : the official journal of the Society for Neuroscience *28*, 4368-4376.

Wang, Y., and Mandelkow, E. (2016). Tau in physiology and pathology. Nature reviews Neuroscience *17*, 5-21.

Wang, Z., Wang, B., Yang, L., Guo, Q., Aithmitti, N., Songyang, Z., and Zheng, H. (2009b). Presynaptic and postsynaptic interaction of the amyloid precursor protein promotes peripheral and central synaptogenesis. The Journal of neuroscience : the official journal of the Society for Neuroscience *29*, 10788-10801.

Watanabe, A., Hasegawa, M., Suzuki, M., Takio, K., Morishima-Kawashima, M., Titani, K., Arai, T., Kosik, K.S., and Ihara, Y. (1993). In vivo phosphorylation sites in fetal and adult rat tau. The Journal of biological chemistry *268*, 25712-25717.

Wechsler-Reya, R., Sakamuro, D., Zhang, J., Duhadaway, J., and Prendergast, G.C. (1997). Structural analysis of the human BIN1 gene. Evidence for tissue-specific transcriptional regulation and alternate RNA splicing. The Journal of biological chemistry *272*, 31453-31458.

Weingarten, M.D., Lockwood, A.H., Hwo, S.Y., and Kirschner, M.W. (1975). A protein factor essential for microtubule assembly. Proceedings of the National Academy of Sciences of the United States of America *72*, 1858-1862.

Weisgraber, K.H., Rall, S.C., Jr., and Mahley, R.W. (1981). Human E apoprotein heterogeneity. Cysteine-arginine interchanges in the amino acid sequence of the apo-E isoforms. The Journal of biological chemistry *256*, 9077-9083.

Wertkin, A.M., Turner, R.S., Pleasure, S.J., Golde, T.E., Younkin, S.G., Trojanowski, J.Q., and Lee, V.M. (1993). Human neurons derived from a teratocarcinoma cell line express solely the 695-amino acid amyloid precursor protein and produce intracellular beta-amyloid or A4 peptides. Proceedings of the National Academy of Sciences of the United States of America *90*, 9513-9517.

Whitcomb, D.J., Hogg, E.L., Regan, P., Piers, T., Narayan, P., Whitehead, G., Winters, B.L., Kim, D.H., Kim, E., St George-Hyslop, P.*, et al.* (2015). Intracellular oligomeric amyloid-beta rapidly regulates GluA1 subunit of AMPA receptor in the hippocampus. Scientific reports *5*, 10934.

Whitehair, D.C., Sherzai, A., Emond, J., Raman, R., Aisen, P.S., Petersen, R.C., Fleisher, A.S., and Alzheimer's Disease Cooperative, S. (2010). Influence of apolipoprotein E varepsilon4 on rates of cognitive and functional decline in mild cognitive impairment. Alzheimer's & dementia : the journal of the Alzheimer's Association *6*, 412-419.

Whitehouse, P.J., Price, D.L., Struble, R.G., Clark, A.W., Coyle, J.T., and Delon, M.R. (1982).

Alzheimer's disease and senile dementia: loss of neurons in the basal forebrain. Science *215*, 1237-1239.

Wigge, P., Kohler, K., Vallis, Y., Doyle, C.A., Owen, D., Hunt, S.P., and McMahon, H.T. (1997). Amphiphysin heterodimers: potential role in clathrin-mediated endocytosis. Molecular biology of the cell *8*, 2003-2015.

Wijsman, E.M., Pankratz, N.D., Choi, Y., Rothstein, J.H., Faber, K.M., Cheng, R., Lee, J.H., Bird, T.D., Bennett, D.A., Diaz-Arrastia, R.*, et al.* (2011). Genome-wide association of familial late-onset Alzheimer's disease replicates BIN1 and CLU and nominates CUGBP2 in interaction with APOE. PLoS genetics *7*, e1001308.

Wild-Bode, C., Yamazaki, T., Capell, A., Leimer, U., Steiner, H., Ihara, Y., and Haass, C. (1997). Intracellular generation and accumulation of amyloid beta-peptide terminating at amino acid 42. The Journal of biological chemistry *272*, 16085-16088.

Willem, M., Tahirovic, S., Busche, M.A., Ovsepian, S.V., Chafai, M., Kootar, S., Hornburg, D., Evans, L.D., Moore, S., Daria, A.*, et al.* (2015). eta-Secretase processing of APP inhibits neuronal activity in the hippocampus. Nature *526*, 443-447.

Williams, R.L., and Urbe, S. (2007). The emerging shape of the ESCRT machinery. Nat Rev Mol Cell Biol *8*, 355-368.

Winkler, E.A., Nishida, Y., Sagare, A.P., Rege, S.V., Bell, R.D., Perlmutter, D., Sengillo, J.D., Hillman, S., Kong, P., Nelson, A.R.*, et al.* (2015). GLUT1 reductions exacerbate Alzheimer's disease vasculo-neuronal dysfunction and degeneration. Nature neuroscience *18*, 521-530.

Wolfe, M.S., Xia, W., Moore, C.L., Leatherwood, D.D., Ostaszewski, B., Rahmati, T., Donkor, I.O., and Selkoe, D.J. (1999a). Peptidomimetic probes and molecular modeling suggest that Alzheimer's gamma-secretase is an intramembrane-cleaving aspartyl protease. Biochemistry *38*, 4720-4727.

Wolfe, M.S., Xia, W., Ostaszewski, B.L., Diehl, T.S., Kimberly, W.T., and Selkoe, D.J. (1999b).

Two transmembrane aspartates in presenilin-1 required for presenilin endoproteolysis and gamma-secretase activity. Nature *398*, 513-517.

Wong, A., Boutis, P., and Hekimi, S. (1995). Mutations in the clk-1 gene of Caenorhabditis elegans affect developmental and behavioral timing. Genetics *139*, 1247-1259.

Wray, N.R., Yang, J., Hayes, B.J., Price, A.L., Goddard, M.E., and Visscher, P.M. (2013). Pitfalls of predicting complex traits from SNPs. Nature reviews Genetics *14*, 507-515.

Wu, C.L., Xia, S., Fu, T.F., Wang, H., Chen, Y.H., Leong, D., Chiang, A.S., and Tully, T. (2007). Specific requirement of NMDA receptors for long-term memory consolidation in Drosophila ellipsoid body. Nature neuroscience *10*, 1578-1586.

Wu, J.W., Herman, M., Liu, L., Simoes, S., Acker, C.M., Figueroa, H., Steinberg, J.I., Margittai, M., Kayed, R., Zurzolo, C.*, et al.* (2013). Small misfolded Tau species are internalized via bulk endocytosis and anterogradely and retrogradely transported in neurons. The Journal of biological chemistry *288*, 1856-1870.

Wu, L., Fan, J., and Belasco, J.G. (2006). MicroRNAs direct rapid deadenylation of mRNA. Proceedings of the National Academy of Sciences of the United States of America *103*, 4034-4039.

Wyss-Coray, T., Loike, J.D., Brionne, T.C., Lu, E., Anankov, R., Yan, F., Silverstein, S.C., and Husemann, J. (2003). Adult mouse astrocytes degrade amyloid-beta in vitro and in situ. Nature medicine *9*, 453-457.

Xia, D., Watanabe, H., Wu, B., Lee, S.H., Li, Y., Tsvetkov, E., Bolshakov, V.Y., Shen, J., and Kelleher, R.J., 3rd (2015). Presenilin-1 knockin mice reveal loss-of-function mechanism for familial Alzheimer's disease. Neuron *85*, 967-981.

Xia, S., Miyashita, T., Fu, T.F., Lin, W.Y., Wu, C.L., Pyzocha, L., Lin, I.R., Saitoe, M., Tully, T., and Chiang, A.S. (2005). NMDA receptors mediate olfactory learning and memory in Drosophila. Current biology : CB *15*, 603-615.

Xia, W., Ray, W.J., Ostaszewski, B.L., Rahmati, T., Kimberly, W.T., Wolfe, M.S., Zhang, J., Goate, A.M., and Selkoe, D.J. (2000). Presenilin complexes with the C-terminal fragments of amyloid precursor protein at the sites of amyloid beta-protein generation. Proceedings of the National Academy of Sciences of the United States of America *97*, 9299-9304.

Xiao, Q., Gil, S.C., Yan, P., Wang, Y., Han, S., Gonzales, E., Perez, R., Cirrito, J.R., and Lee, J.M. (2012). Role of phosphatidylinositol clathrin assembly lymphoid-myeloid leukemia (PICALM) in intracellular amyloid precursor protein (APP) processing and amyloid plaque pathogenesis. The Journal of biological chemistry *287*, 21279-21289.

Xie, Z., Huang, C., Ci, B., Wang, L., and Zhong, Y. (2013). Requirement of the combination of mushroom body gamma lobe and alpha/beta lobes for the retrieval of both aversive and appetitive early memories in Drosophila. Learning & memory *20*, 474-481.

Xing, Y., Bocking, T., Wolf, M., Grigorieff, N., Kirchhausen, T., and Harrison, S.C. (2010). Structure of clathrin coat with bound Hsc70 and auxilin: mechanism of Hsc70-facilitated disassembly. The EMBO journal *29*, 655-665.

Xu, H., Greengard, P., and Gandy, S. (1995a). Regulated formation of Golgi secretory vesicles containing Alzheimer beta-amyloid precursor protein. The Journal of biological chemistry *270*, 23243-23245.

Xu, T., Wang, W., Zhang, S., Stewart, R.A., and Yu, W. (1995b). Identifying tumor suppressors in genetic mosaics: the Drosophila lats gene encodes a putative protein kinase. Development *121*, 1053-1063.

Yamamoto, S., Jaiswal, M., Charng, W.L., Gambin, T., Karaca, E., Mirzaa, G., Wiszniewski, W., Sandoval, H., Haelterman, N.A., Xiong, B.*, et al.* (2014). A drosophila genetic resource of mutants to study mechanisms underlying human genetic diseases. Cell *159*, 200-214.

Yan, S.D., Chen, X., Fu, J., Chen, M., Zhu, H., Roher, A., Slattery, T., Zhao, L., Nagashima, M., Morser, J.*, et al.* (1996). RAGE and amyloid-beta peptide neurotoxicity in Alzheimer's disease. Nature *382*, 685-691.

Yang, Y., Gozen, O., Watkins, A., Lorenzini, I., Lepore, A., Gao, Y., Vidensky, S., Brennan, J., Poulsen, D., Won Park, J.*, et al.* (2009). Presynaptic regulation of astroglial excitatory neurotransmitter transporter GLT1. Neuron *61*, 880-894.

Yao, J., Irwin, R.W., Zhao, L., Nilsen, J., Hamilton, R.T., and Brinton, R.D. (2009). Mitochondrial bioenergetic deficit precedes Alzheimer's pathology in female mouse model of Alzheimer's disease. Proceedings of the National Academy of Sciences of the United States of America *106*, 14670-14675.

Yeh, F.L., Wang, Y., Tom, I., Gonzalez, L.C., and Sheng, M. (2016). TREM2 Binds to Apolipoproteins, Including APOE and CLU/APOJ, and Thereby Facilitates Uptake of Amyloid-Beta by Microglia. Neuron *91*, 328-340.

Yoon, S.O., Park, D.J., Ryu, J.C., Ozer, H.G., Tep, C., Shin, Y.J., Lim, T.H., Pastorino, L., Kunwar, A.J., Walton, J.C.*, et al.* (2012). JNK3 perpetuates metabolic stress induced by Abeta peptides. Neuron *75*, 824-837.

Yoshida, H., and Ihara, Y. (1993). Tau in paired helical filaments is functionally distinct from fetal tau: assembly incompetence of paired helical filament-tau. Journal of neurochemistry *61*, 1183-1186.

Youmans, K.L., Tai, L.M., Nwabuisi-Heath, E., Jungbauer, L., Kanekiyo, T., Gan, M., Kim, J., Eimer, W.A., Estus, S., Rebeck, G.W.*, et al.* (2012). APOE4-specific changes in Abeta accumulation in a new transgenic mouse model of Alzheimer disease. The Journal of biological chemistry *287*, 41774-41786.

Yu, C., Nwabuisi-Heath, E., Laxton, K., and Ladu, M.J. (2010). Endocytic pathways mediating oligomeric Abeta42 neurotoxicity. Molecular neurodegeneration *5*, 19.

Yu, D., Akalal, D.B., and Davis, R.L. (2006). Drosophila alpha/beta mushroom body neurons form a branch-specific, long-term cellular memory trace after spaced olfactory conditioning. Neuron *52*, 845-855.

Yu, D., Keene, A.C., Srivatsan, A., Waddell, S., and Davis, R.L. (2005). Drosophila DPM neurons form a delayed and branch-specific memory trace after olfactory classical conditioning. Cell *123*, 945-957.

Yu, D., Ponomarev, A., and Davis, R.L. (2004). Altered representation of the spatial code for odors after olfactory classical conditioning; memory trace formation by synaptic recruitment. Neuron *42*, 437-449.

Zars, T., Fischer, M., Schulz, R., and Heisenberg, M. (2000). Localization of a short-term memory in Drosophila. Science *288*, 672-675.

Zelhof, A.C., Bao, H., Hardy, R.W., Razzaq, A., Zhang, B., and Doe, C.Q. (2001). Drosophila Amphiphysin is implicated in protein localization and membrane morphogenesis but not in synaptic vesicle endocytosis. Development *128*, 5005-5015.

Zerangue, N., and Kavanaugh, M.P. (1996a). Flux coupling in a neuronal glutamate transporter. Nature *383*, 634-637.

Zerangue, N., and Kavanaugh, M.P. (1996b). Interaction of L-cysteine with a human excitatory amino acid transporter. The Journal of physiology *493 (Pt 2)*, 419-423.

Zhang, H., Ryu, D., Wu, Y., Gariani, K., Wang, X., Luan, P., D'Amico, D., Ropelle, E.R., Lutolf, M.P., Aebersold, R.*, et al.* (2016). NAD(+) repletion improves mitochondrial and stem cell function and enhances life span in mice. Science *352*, 1436-1443.

Zhang, S., and Roman, G. (2013). Presynaptic inhibition of gamma lobe neurons is required for olfactory learning in Drosophila. Current biology : CB *23*, 2519-2527.

Zhang, Z., Wang, D., Sun, T., Xu, J., Chiang, H.C., Shin, W., and Wu, L.G. (2013). The SNARE proteins SNAP25 and synaptobrevin are involved in endocytosis at hippocampal synapses. The Journal of neuroscience : the official journal of the Society for Neuroscience *33*, 9169-9175.

Zhao, J., Davis, M.D., Martens, Y.A., Shinohara, M., Graff-Radford, N.R., Younkin, S.G.,

Wszolek, Z.K., Kanekiyo, T., and Bu, G. (2017). APOE epsilon4/epsilon4 diminishes neurotrophic function of human iPSC-derived astrocytes. Human molecular genetics *26*, 2690-2700.

Zhao, W.Q., Santini, F., Breese, R., Ross, D., Zhang, X.D., Stone, D.J., Ferrer, M., Townsend, M., Wolfe, A.L., Seager, M.A*., et al.* (2010). Inhibition of calcineurin-mediated endocytosis and alpha-amino-3-hydroxy-5-methyl-4-isoxazolepropionic acid (AMPA) receptors prevents amyloid beta oligomer-induced synaptic disruption. The Journal of biological chemistry *285*, 7619-7632.

Zhao, Z., Nelson, A.R., Betsholtz, C., and Zlokovic, B.V. (2015a). Establishment and Dysfunction of the Blood-Brain Barrier. Cell *163*, 1064-1078.

Zhao, Z., Sagare, A.P., Ma, Q., Halliday, M.R., Kong, P., Kisler, K., Winkler, E.A., Ramanathan, A., Kanekiyo, T., Bu, G*., et al.* (2015b). Central role for PICALM in amyloid-beta blood-brain barrier transcytosis and clearance. Nature neuroscience *18*, 978-987.

Zheng, H., Jiang, M., Trumbauer, M.E., Sirinathsinghji, D.J., Hopkins, R., Smith, D.W., Heavens, R.P., Dawson, G.R., Boyce, S., Conner, M.W*., et al.* (1995). beta-Amyloid precursor protein-deficient mice show reactive gliosis and decreased locomotor activity. Cell *81*, 525-531.

Zick, M., and Wickner, W.T. (2014). A distinct tethering step is vital for vacuole membrane fusion. eLife *3*, e03251.

Ziegenfuss, J.S., Biswas, R., Avery, M.A., Hong, K., Sheehan, A.E., Yeung, Y.G., Stanley, E.R., and Freeman, M.R. (2008). Draper-dependent glial phagocytic activity is mediated by Src and Syk family kinase signalling. Nature *453*, 935-939.

Ziegenfuss, J.S., Doherty, J., and Freeman, M.R. (2012). Distinct molecular pathways mediate glial activation and engulfment of axonal debris after axotomy. Nature neuroscience *15*, 979-987.

Zlokovic, B.V. (2008). The blood-brain barrier in health and chronic neurodegenerative disorders. Neuron *57*, 178-201.

Zou, C., Crux, S., Marinesco, S., Montagna, E., Sgobio, C., Shi, Y., Shi, S., Zhu, K., Dorostkar, M.M., Muller, U.C.*, et al.* (2016). Amyloid precursor protein maintains constitutive and adaptive plasticity of dendritic spines in adult brain by regulating D-serine homeostasis. The EMBO journal *35*, 2213-2222.

Appendix

List of abbreviations

Abbreviation	Denotation
α7 nAChR	α7 nicotinic acetylcholine receptor
Aβ	Amyloid beta
$A\beta_{arc}$	Arctic Aβ
AD	Alzheimer's disease
ADAM	Metallopeptidase
ADHD	Attention deficit hyperactivity disorder
AICD	Amyloid intracellular domain
AKT1	Protein kinase B
ALS	Amyotrophic lateral sclerosis
AMPAR	α-amino-3-hydroxy-5-methyl-4-isoxazolepropionic acid-type glutamate receptor
Amph	Amphiphysin
AP2	Adaptor protein 2
APLn	Anterior paired lateral neuron
ApoE	Apolipoprotein E
APP	Amyloid precursor protein
APPL	APP-like protein
APP^{SW}	Swedish APP
ARF	ADP ribosylation factor
ATG	Autophagy related protein
BACE	Beta-amyloid cleaving enzyme
BIN1	Bridging integrator 1
BIP (GRP78)	Glucose-regulated protein 78kDa
C83	83-residue C-terminal fragments
C99	99-residue C-terminal fragments

CaMKII	Calcium/Calmodulin dependent protein kinase
CDK	Cyclin-dependent kinase
CME	Clathrin-mediated endocytosis
CI	Ca^{2+}-impermeable
CLC	Clathrin
CNS	Central nervous system
CP	Ca^{2+}-permeable
cpGFP	circularly permutated GFP
CRISPR	Clustered regularly interspaced short palindromic repeat
CTF	C-terminal fragment
d	day
DALn	Dorsal anterior lateral DAL neurons
DLG	Discs large MAGUK scaffold protein
DLM	Dorsal longitudinal muscle
DPMn	Dorsal paired medial neuron
DR6	Death receptor 6
E	Exon
EAAT	Excitatory amino acid transporter
ECM	Extracellular matrix
eIF1A	eukaryotic translation initiation factor 1A
eIF2α	eukaryotic translation initiation factor 2 subunit alpha
ENDOA	Endophilin
EOAD	Early-onset AD
ELISA	Enzyme-linked immunosorbent assay
EphB2	Ephrin type-B receptor 2
ER	Endoplasmic reticulum
ESCRT	Endosomal sorting complex required for transport
ETC	Electron transport chain
FAD	Familial AD

FTD	Frontotemporal dementia
FTDP-17	Frontotemporal dementia like Parkinsonism linked to chromosome17
FYN	FYN proto-oncogene
GAK	Cyclin G associated kinase
GAP	GTPase-activating protein
GDI	GDP dissociation inhibitor
GEF	Guanidine exchange factor
GEI	Genetically encoded indicator
GETI	Genetically encoded transmitter indicator
GEVI	Genetically encoded voltage indicator
GF	Giant fiber
GFP	Green fluorescence protein
GltI	Glial glutamate transporter I
GluA	AMPAR subunit
GluCl	Glutamate-gated chloride channel
GluR	Glutamate receptor
GMR	Glass multiple reporter
GO	Gene ontology
GS	Gene switch
GSK	Glycogen synthase kinase
GDP	Guanosine diphosphate
GTP	Guanosine triphosphate
GTPase	GTP hydrolase
GWAS	Genome-wide association studies
HD	Huntington's disease
hNPC	human neural progenitor cells
HSC70	Heat shock 70kDa protein
iGluSnFR	intensity-based glutamate-sensing fluorescent reporter
IIS	Insulin-like substrate

iPSC	induced pluripotent stem cells
ITM	Intermediate-term memory
JNK3	C-Jun N-terminal kinase 3
KC	Kenyon cell
lap	Like AP180 protein
LC3	Microtubule associated protein 1 light chain 3
LDLR	Low density lipoprotein receptor
LilrB2	Leukocyte immunoglobulin like receptor B2
LOAD	Late-onset AD
LP-LTM	Late-phase long-term memory
LRP1	LDLR-related protein 1
LTM	Long-term memory
kDa	kilo Dalton
KI	Knock in
MAPT	Microtubule-associated proteins
Mb	Million bp
MB	Mushroom body
MBN	Mushroom body neuron
MBON	Mushroom body output neuron
mGluR5	metabolic glutamate receptor 5
min	minutes
miRNA	MicroRNA
MMP5	Matrix metalloproteinase 5
MT	Microtubule
mTOR	Mechanistic target of rapamycin kinase
MVB	Multivesicular body
N	N-terminal
NAD	Nicotinamide adenine dinucleotide
NFT	Neurofibrillary tangle

NMDAR	N-methyl-D-aspartate receptor
NMJ	Neuromuscular junction
NR	NMDAR subunit
NSF	N-ethylmaleimide-sensitive factor
NTF	N-terminal fragment
p62	Phosphotyrosine-independent ligand for the Lck SH2 domain of 62kDa
PCR	Polymerase chain reaction
PD	Parkinson's disease
PHF	Paired helical filament
PICALM	Phosphatidylinositol binding clathrin assembly protein
piRNA	PIWI-interacting RNA
PKA	Protein kinase A
PNS	Peripheral nervous system
PP2A	Protein phosphatase 2A
PP2B	Protein phosphatase 2B
PrP	Prion protein
PSD-95	Postsynaptic density protein 95
PSEN (PS)	Presenilin
PXN	Peroxiredoxin
QUAS	QF binding UAS
R	Repeat sequence
RAB	Ras-related protein
RAS	RAS proto-oncogene
REP	Rough eye phenotype
RNAi	RNA interference
ROS	Reactive oxygen species
RT-qPCR	Reverse transcription quantitative PCR
RU	Mifepristone
SAD	Sporadic AD

SDH	Sorbitol dehydrogenase
SCA	Spinocerrebellar ataxia
shRNA	short hairpin RNA
siRNA	small interfering RNA
SIRT	Sirtuin
SM	Sec1-Munc18
SNAP25	Synaptosome associated protein 25
SNARE	Soluble NSF attachment protein receptor
SNP	Single nucleotide polymorphism
STM	Short-term memory
SYP	Synaptophysin
SYT1	Synaptotagmin 1
SYX	Syntaxin
TF	Transcriptional factor
TM	Transmembrane
TTM	Tergotrochanteral muscle
UAS	Upstream-activating sequence
UPS	Ubiquitin proteasome system
UPR	Unfolded protein response
VAMP (SYB)	Vesicle associated membrane protein (Synaptobrevin)
VDRC	Vienna *Drosophila* RNAi Center
VGlut	Vesicular glutamate transporter
VNC	Ventral nerve cord
WAVE1	Wiskott-Aldrich syndrome protein 1
XBP1	X-box binding protein 1